RIGA TECHNICAL UNIVERSITY
LATVIA MARITIME ACADEMY

A. Zāģeris

Optimization of technical and efficiency parameters for waste heat recovery system

THESES for DOCTOR of TECHNICAL SCIENCES

2009

RIGA TECHNICAL UNIVERSITY
Engineering Technology, Mechanics and Machine Building
LATVIA MARITIME ACADEMY
Marine Engineering Department

Arnis ZĀĢERIS
Candidate for a doctor's degree according doctoral programme „ Mechanical Engineering"

OPTIMIZATION OF TECHNICAL AND EFFICIENCY PARAMETERS FOR WASTE HEAT RECOVERY SYSTEM

Theses

Research work supervisors:
Dr. habil. sc. ing., professor
V.A.Semeka,
Dr. habil. sc. ing., professor
J.Cimanskis

Rīga 2009

THESES FOR DOCTOR'S SCN.ING DEGREE IS SUBMITTED TO RIGA TECHNICAL UNIVERSITY

Theses "**Optimization of technical and efficiency parameters for waste heat recovery system**" is worked out by Mr.Arnis Zāģeris under the guidance of both professor Dr. habil. sc. ing. Mr.V.A.Semeka at Admiral Makarov State Maritime Academy in St.Petersburg and professor Dr. habil. sc. ing. Mr.J.Cimanskis at Latvian Maritime Academy and submitted for a doctor's sc. ing. degree in Riga Technical University.

Theses is written in English, consisting of Introduction, six chapters, Conclusions, references (151 publication titles), in total 199 pages.

Date: _____ Arnis Zāģeris

ANNOTATION.

The presented studies are devoted for thorough investigations of Waste Heat Recovery System usefulness onboard the ships. The main core is developed original optimization method for exhaust boiler evaluation in dependence on different thermodynamic and geometric factors at the condition, when boiler dimensions, i.e. height or surface, are initially fixed and determined. In a result system of non-linear equations is built up. As an advantage it should be noted that different unified equations are introduced in order to receive final results universal for wide range of power plants with different output. The influence of various hydro-dynamical, heat resistance and other factors are considered in our evaluations.

In order to achieve the highest output per one equipment volume unit thorough optimization of WHRS is carried out based on the proposed analytic method for Heat Recovery Circuit with thermostatic recirculation valve, which is chosen as the base option. By finding and grounding of optimal steam pressure, surface distribution and heat transfer intensification the common regularities are brought out to choose the most beneficial option. As an alternative WHRS with intermediate steam extraction is compared.

WHRS for advanced slow speed diesel power plants is separately highlighted due to significantly lowered flue gas potential that makes heat recovery a quite challenging task. Therefore in order to utilize gas heat as deep as possible another system of non-linear equations is built up based on desired and fixed cooling rate, i.e. gas temperature drop in exhaust boiler. In a result the pressure and other characteristic choice is carried out at different operational and ambient conditions. Here the main task is to get as high output as possible.

In practical part of the Theses the impact and measurement method for pollution coefficient from gas side is explored. Obtained results might be efficiently utilized in WHRS optimization process.

ANOTĀCIJA.

Šajā disertācijā „Dziļās gāzu reģenerācijas sistēmas tehnisko un termodinamisko parametru optimizācija” tiek vispusīgi analizētas gāzu un dzesējamo šķidruma siltuma reģenerācijas iespējas, adaptējot tās kuģu vajadzībām. Pētījumu būtība ir balstīta uz izstrādātu matemātiskās analīzes modeli, ar kura palīdzību tiek atrasti Dziļās Gāzu Utilizācijas Sistēmas (DGUS) termodinamiskās efektivitātes parametri, balstoties uz iepriekš determinēta Utilizācijas Katla ģeometriskajiem parametriem un tā gabarītiem, jo sevišķi no augstuma, kas būtībā ir sildvirsmas raksturlielums. Rezultātā tiek iegūta nelineāru vienādojumu kopums. Dažādi sākotnējie lielumi un vienādojumi ir pārveidoti tā, lai to galarezultātu pielietojums būtu maksimāli universāls neatkarīgi no konkrētā izvēlētā bāzes dzinēja modifikācijas. Sistēmas parametru aprēķinos tiek ņemts vērā iespējamie hidrauliskie, siltuma un gāzu dinamiskie zudumi, kuru iespaids ir ievērojams.

Par bāzes opciju tiek izvēlēts Siltuma Reģenerācijas Kontūrs (SRK) ar termostatisko samaisītāj-vārstu, kura vispusīga optimizācija tiek veikta ar mērķi nodrošināt maksimālo jaudas pieaugumu vienā iekārtas (katla) apjoma vienībā. Pamatojot gan optimāla tvaika spiediena izvēli, gan sildvirsmu sadalījumu, tiek atrasta iespējami efektīvākā opcija, ņemot vērā arī glodeņu ribošanu. Siltuma Reģenerācijas Kontūrs ar reģeneratīvo pakāpi katla ūdens apsildei tiek salīdzināts kā potenciāla alternatīva.

Atsevišķi tiek pētīta un pamatota DGUS pielietojums kuģa spēka iekārtai, kuras sastāvā ietilpst moderns zemu apgrieziena divtaktu dīzeļa dzinējs ar minimālu gāzu siltuma potenciālu. Rezultātā tiek izstrādāts un piedāvāts modificēts sistēmas matemātiskās analīzes modelis, kas balstīts uz fiksētu gāzu atdzesēšanas dziļumu, tas ir noteikts gāzu temperatūras kritums utilizācijas katlā. Galarezultātā tiek pamatota gan tvaika spiediena izvēle, gan sildvirsmu sadalījums, kā arī turbo-ģeneratora spēja nodrošināt elektrostacijas jaudas apgādi atkarībā no iespējamiem ekspluatācijas nosacījumiem.

Disertācijas praktiskajā sadaļā tiek pētīts virsmas aizsērējuma koeficienta no izplūdes gāzu puses ietekme un izmaiņas reāli darbojošajā kuģa propulsīvā spēka iekārtā. Iegūtie rezultāti ir interesanti, kuru kopējās likumsakarības būtu vēlams ņemt vērā veicot iekārtas aprēķinus, kas palielina rezultātu ticamību.

CONTENTS.

ABBREVIATIONS.

AB – Auxiliary Boiler

a/a – ambient air

BCS - Boiler Control System;

CWHRS – Complex Waste Heat Recovery System;

DG – Diesel generator;

EB – Exhaust Boiler;

(S)EPP – (Ship's) Electrical Power Plant

f/w – feed water;

GT – Gas Turbine;

HFO - Heavy Fuel Oil;

HRC – Heat Recovery Circuit;

HRSG - Heat Recovery Steam Generator;

HTS - High temperature stage as a part of main engine (diesel) air cooler;

MCR – Maximum continuous rating, i.e. load level of main engine, %;

ME – Main Engine (of Ship's Propulsion System);

MSDE - Medium Speed (four stroke type) Diesel Engine;

PE – Peak Engine;

PZRR - Performance Zone of Reduced Reliability;

RMSD - Root Mean Square Deviation;

SFOC - Specific fuel oil consumption, $kg/(kW \times hr)$;

SSDE - Slow Speed (two stroke type) Diesel Engine;

ST – Steam Turbine;

STG – Steam Turbo-Generator;

s/w – sea water;

t/c – Turbocharger;

TG – Turbo Generator

VLBC – Very Large Bulk Carriers;

VLCC – Very Large Crude Oil Carriers;

WHRS - Waste Heat Recovery System;

MAIN ABBREVIATIONS IN EQUATIONS.

$\overline{c_g}$ - average specific flue/exhaust gas heat, $kJ/^oC$;

G_g - Gas flue amount per second, kg/s;

G_{st} - Exhaust boiler steam capacity, kg/s;

G_{sat} - Saturated steam consumption, kg/s;

h_{g_i} - Gas enthalpy in respective boiler cross section, kJ/kg;

$h_j^{|}$ - Respective (-*j*) boiler water enthalpy, kJ/kg;

h_{sj_i} - Respective (-*i*) steam enthalpy in various cycle points (-*j*), kJ/kg;

Ha - Iso-entropic enthalpy difference, that usefully work-out in steam turbine, kJ/kg;

ΔHe_g - Relative net power loss in main engine due to adverse influence of EB aerodynamic resistance, $kJ/1kg \quad flue \quad gases$;

k - Convective heat transfer coefficient, $W/(m^2 \times K)$;

k_{circ} - Forced circulation coefficient;

k_{rec} - The coefficient of boiler water re-circulation for feed water temperature rise by mixing via thermostatic valve;

$K_{\Delta\eta}$ - additional relative efficiency growth due to ME cooling media heat recovery;

L_{SLel} - Lower Safety Limit of required Electrical energy

Ne_{el} - Ship's electro-station consumption, kW;

Ne_{ST} - Steam turbine output, kW;

Ne_{TG} - Steam turbo-generator output, kW;

ΔP_{g_i} - Aerodynamically resistance of respective boiler surface, kg/m^2;

p_j - Relevant either steam or boiler water pressure, bar;

Δp_{j_i} - Various (-*j*) hydraulic pressure losses on the way of water-steam path (-*i*), bar;

p_s - Exhaust boiler steam pressure in a drum, bar;

Q_i - Either transferred or dissipated heat amount either by flue gases or steam/water, kJ;

S_j^i - Respective (-*j*) entropy at certain steam cycle point (-*i*), $kJ/(kg \times K)$;

t_a - Ambient air temperature, ^oC;

t_{g_0} - Exhaust gas temperature at boiler inlet/after main engine, ^oC;

$t_{g_{exh}}$ - Exhaust gas temperature at boiler outlet, ^oC;

t_{g_i} - Exhaust gas temperature in specific section of EB, ^oC;

t_{fw} - Feed water temperature at boiler inlet, ^oC;

t_{fwp} - Feed water temperature in hot well, ^oC;

t_g^{Σ} - Flue gas temperature gradient usefully recovered by EB, ^oC;

$t_{s/w}$ - Sea water temperature, ^oC;

Δt_{LOG_i} - Mean log temperature difference in respective surface, ^oC;

t_s - Saturation temperature corresponding to steam pressure p_s, ^oC;

w_g - Linear gas velocity, m/s;

W_{C_i} - Gas mass velocity in steam boiler cross section, $kg/(m^2 \times s)$;

U_{SLel} - Upper Safety Limit of required Electrical energy;

x_1 - *Pinch-poin*t or temperature difference between flue gases at an evaporator outlet t_{g_s} and the saturation one t_s, ^oC;

x_2 - Temperature difference between flue gases at a boiler inlet t_{g_0} and superheated steam one t_{st}, ^oC;

x_3 - *Approach temperature* - the difference of temperatures between the saturation and water outlet from an economizer, ^oC;

α - Air excess coefficient;

α_1 - Heat conductivity from gases to steel tube wall, $W/(m^2 \times K)$;

α_2 - Heat conductivity from tube wall to heating-up media (steam-water), $W/(m^2 \times K)$;

ε - Pollution coefficient of EB convective surfaces from gas side, $W/(m^2 \times K)$;

η_{i_j} - Relative efficiency coefficient;

Π - Relative net power/efficiency growth provided solely by WHRS, $\frac{kJ}{1kg\ flue\ \ gases}$;

Π_o - Relative net power/efficiency growth of the power-propulsion system in the whole due to WHRS introduction, $kJ/1kg\ \ flue\ \ gases$;

ξ - Relative steam capacity produced by EB, $kg\ \ steam/1kg\ \ flue\ \ gases$;

ξ_{st} - Relative overheated steam capacity produced by EB, $\frac{kg\ \ saturated\ \ steam}{1kg\ \ flue\ \ gases}$;

ξ_{sat} - relative saturated steam consumption, $kg\ \ saturated\ \ steam/1kg\ \ flue\ \ gases$;

Y_i - Coordinate of relevant extraction point;

χ - Relative steam over-heat rate;

Ψ - Flue gas heat recovery rate;

MAIN GEOMETRICAL CHARACTERISTICS OF TUBE BUNDLE AND EXHAUST BOILER

L, B, H - Exhaust boiler dimensional characteristics, i.e. length, width and height, required for allocation of tube bundles, m;

$L \times B$ - Exhaust boiler (inner) cross section available for gas outflow, m;

d - Tube outside diameter in EB bundle, m;

d_i - Tube inner diameter in EB bundle, m;

S_1 - Cross-head step in tube nest of EB bundle, m;

S_2 - Longitudinal step in tube nest of EB bundle, m;

$S_2^{|}$ - Diagonal step of tubes in the bundle, m;

z_i - Heating coil amount of respective surface;

z_1 - Heating coil amount of an evaporator;

z_2 - Heating coil amount of a super-heater;

z_3 - Heating coil amount of an economizer;

S_r - Fining step on boiler tube, m;

h_r - The height of ribs, m;

δ_r - The thickness of ribs, m;

D - Finned tube outer diameter, m;

INTRODUCTION

Due to world economic globalization merchant trade is becoming more developed and specialized that directly influences ships size, design and technical characteristics. On another hand fossil fuel oil reserves are limited, already causing some shortage and relevant continuous price increase, thus coming to the growth in trade costs. In addition World's Society is becoming more concerned regarding environmental pollution safety, including continuous reduction in gas emission, being supported by different International and local government legislative requirements and norms. So based on it there are two contradictory inputs on shipping development – demands in faster and more cargo supply at so called *fuel oil factor* limitations. Therefore just ship's propulsion plant is the object of our interests, which should be efficient and environmentally friendly. Besides main engine development, good results could be also achieved by comprehensive unused heat recovery, the main constituent of which is effluent gases after either diesel or gas turbine, being recovered in way of produced either power or heat. Then just these so-called Waste Heat Recovery Systems (WHRS) will be the object of our investigations, the highest output of which should be ensured within possibly reduced dimension, otherwise uncontrolled equipment size increase will lead into cargo capacity reduction. Since an exhaust boiler is the main constituent of the WHRS then special thorough attention is to be paid on this equipment in our studies. For some specialized fast ships chosen power plant dimensions are essentially important to be as small as possible, especially their heights, so that efficient cargo operation is ensured as well, therefore any big exhaust boiler installation on top of main engine might be critical. Despite the fact that slow speed diesel engine is dominantly used as ship's main engine, still another options are becoming more attractive due to their high compactness at high output rates. First of all aero-derivative gas turbines are being proven as perspective alternative for specialized cargo and high comfort cruise ships, where still increased costs due to higher fuel consumption are compensated by higher either cargo or passenger capacity at significantly lowered maintenance costs in addition. Achievements in materials science, wide ceramic based metal use in turbine production including different means for blade and vane cooling allows industry to ensure further cycle temperature growth thus adequately reducing fuel consumption. At the same time without efficient flue gas heat recovery it would be difficult to make gas turbine power plant competitive enough. Based on these considerations following tasks could be classified as below:

1. Waste (gas) Heat Recovery System is the object of our investigations;

2. The system should be highly efficient at possibly reduced dimensions, i.e. initial costs;
3. And the height of it could especially important for some type of ships;
4. However the output for such type of vessels should be high enough at the same time;
5. Since an exhaust boiler is the main constituent of WHRS its optimization method is to be elaborated at conditions, where boiler dimensions (height) are fixed;
6. Based on this method thorough investigations of different parameter influence is to be considered in order to obtain the highest power plant efficiency;
7. For slow speed diesel engine power plants, where gas potential is considerably lowered, besides its ultimate recovery also cooling media heat is to be considered for further WHRS efficiency increase.

BRIEF DESCRIPTION OF STUDIES

Presented studies consist of introduction, six chapters, conclusion and references.

In the first chapter **"WHY WASTE HEAT RECOVERY?"** the necessity to investigate WHRS efficiency is fortified by the present situation in fuel oil market at the very first. Tendencies in Worlds development towards to ships specialization, tonnage and particular ship size growth with highly rated power plants is contributory factor to find ways how efficiently to cut down fuel costs. Gas turbine *renaissance* in shipping and stricter International environmental legislation is another input, why Waste Heat Recovery Systems are to be seriously considered during new-building stage.

Second chapter **"THE CHOICE AND JUSTIFICATION OF MAIN THERMODYNAMIC AND GEOMETRICAL CHARACTERISTICS OF WASTE HEAT RECOVERY SYSTEM"** is devoted to substantiate the choice of investigated type of Heat Recovery Circuit. First of all modification of boiler is chosen with the consideration of service experience, as well as design expectations are taken into account. Different surface engagement is being revised from the view point of highest efficiency gain at reasonable dimensions, with the consideration of eventual service reliability and durability. The choice of geometrical characteristics of tube and its nest is another quite complicated task. Firstly, any surface intensifying towards efficiency raise per one volume unit is self evident; but on another hand numerous hidden adverse effects are followed correspondingly. Therefore optimal balance between desired net gain and eventual risks is to be found. Chosen figures in our researches are necessary to carry out further studies in order to bring out common regularities from single results; however these dates could not be considered as something frozen ones. At some other different conditions either service or construction ones, e.g. consumed fuel oil type, applied materials, special service routines, etc.,

other geometrical, thermodynamic characteristics may found appropriate for our designed power plant. The value of this chapter is enclosed in the principle, methodology of the approach, how to chose the main input dates for WHRS.

In the third chapter **"OPTIMIZATION METHOD OF THERMODYNAMIC ANALYZES OF WASTE HEAT RECOVERY CIRCUIT AT FIXED DIMENSIONS (HEIGHT) OF EXHAUST BOILER"** the original method is presented to find efficiency characteristics at pre-determined boiler dimensions. As the boiler cross dimensions, i.e. length and width, are mainly determined by main engine type and rating, i.e. on produced gas amount, and limited by linear gas velocity margins, then just the boiler height, which is quite an essential parameter for some specialized ship, is the measure value of heat exchange surface amount. In addition both gas parameters and engine room sizes are already determined during new building stage for specific ship; and WHRS is deemed as something supplementary, which should be located within designed space at highest possible recovery rate. Presented method could be divided in five main blocks followed by each other –

1. The choice of main input dates,
2. Boiler steam capacity determination,
3. Boiler surface evaluation against obtained efficiency,
4. Aerodynamic resistance determination,
5. Steam turbine cycle efficiency and power plant in the whole.

Additionally *the choice of main input dates*, either geometrical or thermodynamic ones, is divided in sub-blocks corresponding to specific part of efficiency evaluations, so that it becomes possible to find the optimum of one specific WHRS parameter by repeated evaluations. Surface is presented via relevant heating coil amount, which is also very practical figure to start immediate production as specific amount of tube size, length, quantity of elbows is stated. At the same time boiler efficiency parameters are evaluated based on thermodynamic dates, i.e. temperature differences, that are measure values of relevant boiler surfaces. In a result calculated boiler surfaces will differ from our accepted ones, therefore this system of transcendental equations is being solved by means of different mathematic methods of non-linear system solution, i.e. iterative methods. Achieved final results are not specific for one designed power plant; but their relative values are applicable for certain range of main engines. Based on elaborated mathematic model flowchart, it is also possible to re adjust it for other more sophisticated thermodynamic heat recovery circuits as well.

"**HEAT RECOVERY CIRCUIT OPTIMIZATION**" is the fourth and the biggest chapter of Theses. Based on presented method in the third chapter far and wide mathematic modeling

was carried out. Obtained results due to these evaluations were thoroughly analyzed and classified; and in a result this part of theses are being split in following five subchapters. The main task is to find out, how the highest output of WHRS could be achieved within one exhaust boiler volume; but then the impact of each convective surface is to be explored, being reflected in subchapter 4.1 "**Exhaust Boiler Convective Surface Influence on WHRS Thermo-Dynamic Efficiency Indices**". Common regularities brought out at conditions, when one particular surface is being altered, while other two constituents remain invariable. Due to the fact that gas heat recovery possibilities are restricted by relevant gas and steam cycle temperatures, then unlimited surface enlargement cannot ensure steam turbine efficiency growth in the same rate, while adverse diminution impact of boiler gas resistance on main engine (gas turbine) output comes to relevant and dominant power plant efficiency decrease in the whole. Base on these two contradictory factors the highest exhaust boiler surface amount is found and well grounded. Steam pressure is another important thermodynamic characteristic of the cycle, the choice of which is substantiated in subchapter 4.2 "**The Steam Pressure Optimization for Exhaust Gas Boiler at Fixed Dimensions**". Any steam pressure growth favorably affects changes in Rankine cycle efficiency indices, however effluent gas heat recovery rate, the present value of which is steam output, has a tendency to decrease almost in direct ratio at specified exhaust boiler dimensions. Therefore their summary effect is to be taken into account; and in a result at certain steam pressure level the highest steam turbine output is achieved, that corresponds to its first optimum. The second optimum encounters adverse boiler aero-resistance, being dependent on steam pressure almost in direct ratio, impact on main engine (gas turbine) rating. Based on carried out investigations, the level of second pressure optimum is found lower than the first one. Both optimums are directly influenced either by inlet gas temperature alterations or boiler surface sizes. With the consideration of brought out regularities in studies as above further WHRS optimization is carried out by finding the favorable boiler surface internal distribution between each constituent at fixed sizes of its total one, the elaborations of which are presented in subchapter 4.3 "**Fine Optimization of Heat-Exchange Surfaces of Exhaust Boiler within Fixed its Dimensions**". The mutual influence of all boiler constituents, i.e. an economizer, an evaporator and a super-heater, are complicated ones, as any enlargement of one of them is carried out at the expense of remaining two. Finally, the optimal internal surface redistribution is found, which is not something fixed, but being also affected by both inlet gas temperature and total boiler dimensions. In subchapter 4.4 "**Intermediate Steam Extraction Possibilities to Increase WHRS Efficiency**" WHRS with intermediate steam extraction is considered as

an alternative versus *with re-circulation* one. Despite of more efficient way of utilization of recovered heat in steam turbine the additional gain by extraction stage is almost nothing due to pre-determined gas recovery rate at equal boiler dimensions for chosen heat recovery circuits. At the same time it is *less required* gas heat due to cycle *better arrangement* and in a result outlet gas temperature is slightly higher for HRC with regenerative stage. On another hand due to feed water warm up by latent condensation heat, whereas additional gas heat is needed for *re-circulation*, there is some surface internal re-distribution towards evaporator enlargement at the expense of economizer. In order to minimize power plant dimensions boiler convective surface fining is considered as possible and well proven option, being thoroughly investigated in subchapter 4.5 "**Exhaust Boiler Tube Finning Impact on WHRS Thermo-Dynamic Efficiency and Dimensional Indices**". Firstly, fining efficiency was explored at condition, when plain and ribbed tube boiler dimensions are equal. The gain is higher power plant output, which has a tendency to grow down with boiler height enlargement. Still within investigated limits of boiler sizes the relative power plant increment is ensured around 30%. At condition of equal outputs the gain is actual and possible reduction in EB height, which might be important at rather high recovery rates. In a result savings in height might be around 25% with a tendency to grow up at higher WHRS outputs.

"**HEAT RECOVERY PECULIARITIES FOR ADVANCED SLOW SPEED DIESEL ENGINES**" is the fifth chapter of Theses, consisting of three subchapters. Why is there special part dedicated for slow speed diesel engine and its eventual heat recovery? Because just this type of engine is dominant one for ships propulsion; and due to engine development towards ultimate reduction of all possible heat losses it would be a challenge to find something else, what could be efficiently recovered. Therefore in subchapter 5.1 "**Some Aspects of Heat Recovery Possibilities at Low Gas Temperature Potential**" it is presented another approach, mathematic model, how to explore WHRS efficiency at fixed gas cooling rate by exhaust boiler. Only the main equations are presented, while remaining ones are the same as in third chapter. At these conditions evaluated boiler surface sizes could not be of final practical use, as obtained heating coil numbers are not those, which could be applied for boiler production, i.e. do not correspond to integer number divisible on 2 or 4. At the same time based on presented data boiler construction, i.e. surface internal distribution, could be found out in order to reach the highest steam turbine output. Then based on these results real digit numbers closest to evaluated ones could be taken as input data for exact boiler characteristic evaluation as per chapter three. The optimal steam pressure choice is not task for this power plant application, but its possible practical level could be a problematic issue in

order to achieve desired gas cooling rate. Designed boiler steam pressure should be high enough to ensure its applicability to drive steam turbines available in the market as well as to provide required heating capabilities. Therefore achievable steam pressure level is being explored at these different limitative conditions in subchapter 5.2 "**Some Matters Regarding Steam Pressure Choice**". Desired gas cooling rate, convective surface sizes and steam pressure level are interdependent. At determined inlet gas temperature further gas cooling might be impossible without subsequent steam level diminution, what might be unacceptable in some cases. Then more sophisticated double pressure WHRS might be introduced to reach desired recovery rate. Also the impact of other thermodynamic factors is explored in this subchapter. When steam pressure is chosen and boiler design is substantiated, then ultimate possibilities to define, what could be recovered from real ships' power plant with slow speed diesel, are explored in subchapter 5.3 "**Heat Recovery Possibilities for Advanced Slow Speed Diesel Engine Power Plants**". As besides flue gas recovery also cooling water heat is assumed and proposed for utilization, then different options were explored in dependence on required upgrading complexity. That sort of approach is beneficial not only for new-buildings, but also and mainly for ships in operation however still in dependence on their age. Due to low potential of available both jacket and turbocharged air cooling heat power plant efficiency further raise is possible by both substitution of saturated steam consumption and feed water warm up before thermostatic mixing valve. In a result the raise in exhaust boiler steam and turbine output is obtained, however efficiency gain generating could be carried out gradually in dependence of low potential heat consumers. In a result so-called Complex Waste Heat Recovery System (CWHRS) is build up. Besides obtained efficiency dates, their utilization extent is greatly important either, especially, when any shortage in either electricity or heat might lead to WHRS disengagement and unjustified loss of still available steam turbine output in a result. Therefore the efficient ways, how to cover the appearing shortage, are to be thoroughly considered. Ambient temperatures and main engine work load has direct and considerable impact on CWHRS efficiency parameters; hence three main ambient conditions were taken into account in our studies, that practically covers the whole trading area. But at the same time the ship is moving object; and within one voyage sea water and ambient air temperatures might significantly fluctuate. Therefore some main trade lines with highest ambient condition fluctuations were explored. Based on obtained results it becomes possible to estimate, how ships' power plant is to be arranged in dependence on ME rating, sailing region and other factors.

Pollution coefficient from gas side is an important value that determines not only heat transfer efficiency, but also it has a significant impact on convective surface reliability and durability. Therefore in the sixth chapter "**POLLUTION COEFFICIENT DETERMINATION POSSIBILITIES AND OBTAINED RESULT TRUSTWORTHINESS FOR POWER PLANTS IN OPERATION**" we will try to explore more in details the origins of pollution coefficient and to evaluate trustworthiness of proposed practical method for existing value determination onboard the ship in operation. In the first part the nature of pollution coefficient is being explored, based on thorough examination of different available studies. There are a lot of researches applicable for main and oil/coal fired auxiliary boilers, while quite limited amount of technical papers are found for exhaust boilers. Therefore explored available information was critically revised and presented as relevant extractions, which would be practical interest for WHRS installed onboard of modern merchant vessels. This information would be also valuable, when boiler design is being chosen. In the second part of the sixth chapter real level of pollution coefficient for existing power plant in the whole is estimated on board the ship in voyage. Since it is impossible to find directly pollution coefficient for installed exhaust boiler, then it is elaborated via convective transfer equation by conducting extensive calorific measurements of WHRS. Obtained result trustworthiness is evaluated via carried out measurement error, i.e. occasional and instrumental one, and summary error of indirectly measured pollution coefficient was found quite acceptable low. During the processing of experiment results it was concluded that at acquired error of the coefficient the presented method is promising; and by further improvements in conducting measurements, gas temperature in particular, it becomes possible to increase result trustworthiness even more. Another important outcome is the fact that there is quite explicit difference amongst pollution coefficients of each boiler constituent, i.e. a super-heater, an evaporator and an economizer.

In conclusions not only the main outcomes are presented, but based on carried out studies also eventual plans for further studies are substantiated.

THE OBJECTIVE OF THESES

The subject of our investigations is Waste Heat Recovery System designated as further development of ships' power plants, where main engine is either diesel or advanced gas turbine. Since the exhaust boiler is the main constituent, then the new mathematic model is elaborated at fixed boiler dimensions. In order to achieve the highest output per one volume unit thorough optimization of WHRS is carried out based on presented method, where influence of different thermo-dynamic, geometrical characteristics and layouts are being

considered. Separately advanced slow speed diesel power plants are considered in our studies due to ultimately reduced heat recovery possibilities. Pollution coefficient determination is an important task of the studies because of its significant impact on convective heat exchange.

THE NOVELTY OF THESES

Following main unique results, conclusions are brought out during the studies:

1. Mathematic model on non linear equations is brought out for exhaust boiler, WHRS evaluation at accepted boiler dimensions, particularly its height, i.e. fixed amount of heating coils or convective surface.
2. Based on this method thorough investigations were carried out in order to substantiate the optimal boiler dimensional and WHRS thermodynamic parameters with the aim to get the highest output per one surface, per one equipment volume unit. Therefore this task was presented in following steps:
   a. The influence of each boiler constituent was thoroughly explored at unlimited dimensions, and in a result the ultimate boiler surface was found at which the highest output of the power plant in the whole is ensured;
   b. At fixed boiler dimensions steam pressure contradictory influence on WHRS parameters was explored. In a result one optimal meaning of it was brought out, that ensures the highest steam turbine output in dependence on convective surface sizes and inlet gas temperature level. At the same time, when adverse impact of exhaust boiler gas resistance is taken into consideration, then another optimal meaning of steam pressure is stated, which is lower than the first one;
   c. At fixed, constant boiler dimensions, i.e. its height, the interactive influence of each boiler constituent was investigated; and in a result it was found optimal convective surface mutual distribution, which should provide that the highest power plant output is obtained by observing maintenance safety aspects;
   d. Intermediate steam extraction possibilities were explored versus WHRS with feed water *re-circulation* at fixed boiler dimensions. In a result due to higher Rankine cycle efficiency less heat extracted from exhaust gasses is needed, i.e. gas temperature at boiler outlet is evidently higher thus reducing the risk of sulfur- acid corrosion occurrence in tail surfaces, however the additional efficiency gain is doubtful. Boiler surface internal redistribution is shifted towards to evaporator part enlargement at the expense of economizer one;

e. Tube fining is an effective alternative, how to intensify convective surface sizes per one boiler volume unit. In a result, significant boiler reduction in its height is ensured - till ≈25%, what might be essential factor for some specialized ships.

3. For advanced slow speed diesel power plants due to reduced potential of recovered heat different approach is applied to find the way, how to make WHRS attractive:
   a. Another method based on conditions of fixed gas cooling rate is brought out, as the main target is to ensure highest steam turbine output;
   b. The any of listed above optimal pressures is impracticable for this type of ships' power plants due to their low meaning firstly, therefore some other value is to be chosen high enough in dependence on by both thermal and dimensional factors;
   c. Different options how to recover cooling water heat is considered, what results into Complex Waste Heat Recovery System. Its efficiency is explored at different ambient, load and trade conditions.
4. During practical part of studies the method how to find pollution coefficient for the power plant is presented. It was found that at certain conditions our approach is effective enough. The obtained different meanings of pollution coefficient for each boiler constituents are un-weighted factor for future boiler efficiency evaluations.

PRACTICAL VALUE OF STUDIES

Existing results and method are being introduced in development of normative guidance document by CNII MF, as well as during new-building stage of tankers for Latvian Shipping Company.

PUBLICATIONS

There are eight (8) publications.

APPROBATION OF THESES

Approbation of theses was carried out on different International Conferences at Riga Technical University, Kaunas University of Technology, Latvia Maritime Academy, International Conference of Traffic Science in Portorož, Slovenia during the years 2005 till 2008.

IN GRATITUDE

I want to express the gratefulness to my research supervisor professor V.A.Semeka, whose generated idea was given to me to develop it. With the consideration of his enormous background, experience as engineer and scientist a lot of ideas were added, corrected during theses work out, and many of them as guidance for further development.

Professor Juris Cimanskis is my next one research supervisor guiding to finalize the job. Valuable remarks were given with regards of that part, where system was considered for slow speed diesel engine application especially.

I want to express my thankfulness to professor Jānis Vība, who did accept the theses for examination. At the preliminary hearing of the draft numerous remarks were given by members of Institute of Mechanics, which were highlighted in the theses.

My gratefulness to professor Jānis Auziņš, who did thorough examination of theses. There were given valuable remarks how to make a point of the main idea of the job, i.e. multi-parameter optimization, which should be more developed in further researches.

Also professor Jānis Brūnavs and professor Viktoras Sencila did make a valuable contribution to finalize the theses.

CHAPTER 1 THE NECESSITY IN FURTHER DEVELOPMENT OF WASTE HEAT RECOVERY SYSTEM.

The object of our investigation is Waste Heat Recovery System (WHRS) being a part of ship's propulsion unit, where main engine could be either diesel or gas turbine. Waste Heat is that one, which is proposed to be usefully converted into either ship movement or electricity or other power instead of fuel burning. Effluent gases after main engine is the main constituent, which recovery has to be considered at the very first as specific part of it from totally generated heat during combustion will be around 26% [70, 110] for advanced slow speed diesel engines till 35-50% for modern gas turbine power plants [81, 93, 101, 113]. Another quite considerable part is enclosed in different cooling media as water, oil, especially for diesel engines. Despite that potential of this heat is rather low, still useful recovery of it might be of economical interest. Still the main subject of our studies is efficient flue gas heat recovery, where the main constituent of WHRS is Exhaust steam Boiler (EB); and as most advanced system it is assumed, when gas heat is recovered in way of additionally produced power transferred either for ship's propulsion or into electrical supply (See Fig.1.1.) [1, 7, 13, 27, 118, 147]. Sometimes it might be more attractive that saturated steam only is produced, especially it would be of high economical benefit for specialized ships, e.g. chemical tankers trading with high viscosity cargoes, where necessity to run auxiliary boiler could be substituted by exhaust boiler to provide cargo heating.

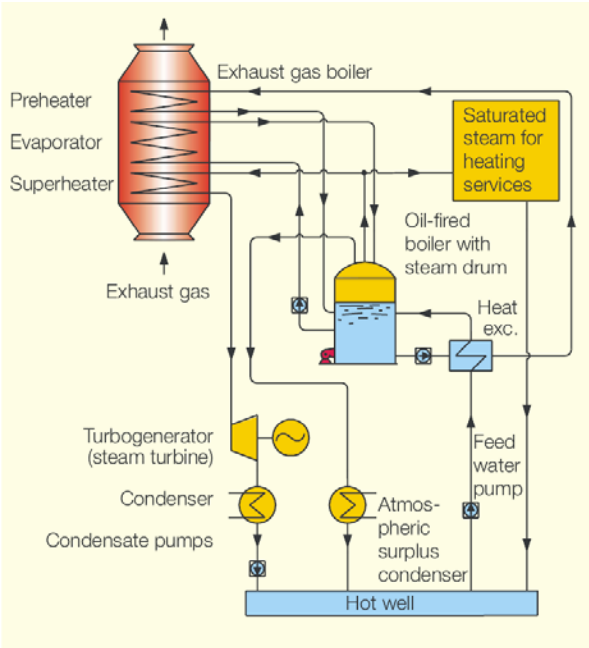

Fig.1.1. Waste (Gas) Heat Recovery System.

<u>Why should we return back and explore again heat recovery systems?</u> There are a lot of carried out studies regarding this issue; and however in different extent still WHRS are being successfully introduced and maintained in shipping trade. There might be several aspects, but still the main one is economical issue, however also environmental safety is

another very important topic, being supported via different international and national legislations [38].

1.1. FUEL PRICE IMPACT.

So the first one and the main core is still **fuel saving, the cost** of which could constitute up to 50÷55% of all related ship's trade expenses. Since seventieth, when high quality motor oil price was below $< 20 \ USD/m.t$, it has climbed up till $>= 615 \ USD/m.t$ (July of 2008) for much lower grade heavy residue fuel oil, what highlights energy saving matters. So for the average size ($DWT \approx 20 \ 000 \ m.t$) of cargo ship at fuel consumption equal to $\approx 20 \ m.t/day$ the total cost of consumed the lowest grade HFO IFO380 will constitute around - $\approx 20 \ m.t/day \times 300 \frac{ME \ \ service \ \ days}{year} \times 615 \frac{\$}{m.t} \Rightarrow= 3'690'000 \frac{USD}{Year}$, for IFO380 Rotterdam price $615 \$/m.t$ on July, 2008. Efficient tanker ship age is till 25 years, what means that total fuel costs might reach as high level as equal to $\approx 3'690'000 \frac{USD}{Year} \times 25 years \Rightarrow= 92'250'000 USD$, while similar vessels new-building price is around $\approx 42'000'000 USD$. At the moment the price is more than double down, but anyway there is an objective tendency for average fuel impact growth. Consequently it is self-evident that any savings in fuel consumption is beneficial, e.g. by introducing advanced WHRS at lowest efficiency equally to $\approx 3.5\%$, the gain during the one year would reach around $\approx 129'000 \ USD$, while during the lifetime it might be not less than $\approx 3'230'000 \ USD$. So based on even these quite modest input dates eventual output results are self-explanatory, why further investigations regarding WHRS usefulness should be explored.

1.2. WORLD'S FLEET DEVELOPMENT FACTOR.

Next one important starting-point is World's Fleet development, being very much dependent on global economical trends. Due to World's economy growth either, the shipping industry has begun quite fast development, what especially makes influence over containership fleet growth (see Fig.1.2) [56, 64, 77]. Container cargo expenses are the highest ones, therefore to reduce transport costs the amount of containers and speed has to be preferably increased, what comes to size enlargement of delivered vessels. The largest container ships ordered today are of 9,600 TEU at 115,000 DWT (see Fig.1.3) [35], however

sizes of 10,000-12,000 TEU, or even 18,000 TEU, may be expected within the next decade. For these very large vessels of the future, the propulsion power requirement may be up to about 100’000 kW/136’000 BHP [78], as required speed amongst merchant ship types is the highest one around 18÷22 knots. In a result specific hard achievable requirements for propulsion system are being put forward, when the highest efficiency and output is to be achieved at lowest possible power plant dimensions to save cargo capacity as much as possible. In fact over the years required containership speed has been increasing constantly, even over 22÷26 knots for post-PANAMAX ships especially.

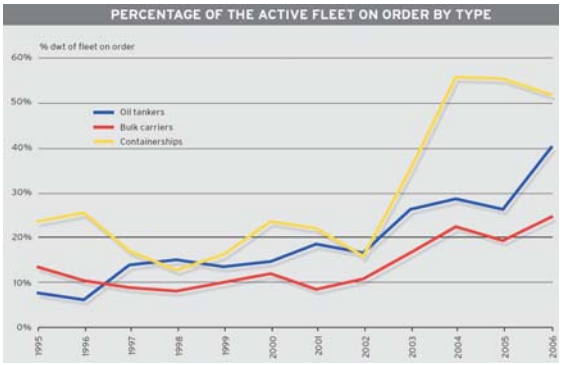

Fig.1.2. World’s Fleet development.

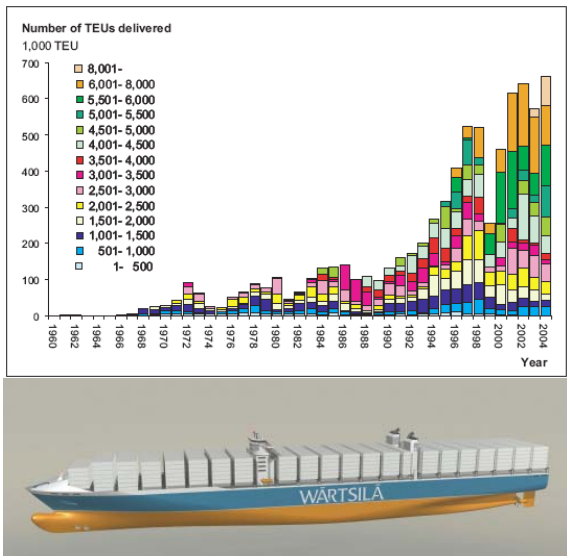

Fig.1.3. Containership type development.

For tankers speed is almost constant within range of 13÷16 knots, meantime their sizes have a tendency to become larger (see Fig.1.4a) [31, 77], accompanied with relevant power increase almost in direct ratio [55, 64]. Chemical tankers are to be specially considered due to their complicated trade. Despite the ship dimensions are below HANDYMAX size as a rule, still the power plant arrangement could be quite sophisticated at even increased power output due to developed cargo unit arrangements. Electro-driven propulsion plants with medium speed engines are found economically attractive solution for these types of ships; and consequently installation of gas heat recovery might be very promising. Growing trade with high viscosity cargoes (see Fig.1.4b) [31], e.g. different vegetable and animal oils, fatty acids, etc., comes to increased demands in saturated steam for heating purposes. Therefore more simple WHRS aimed to substitute auxiliary boiler performance during cargo voyage might be extremely beneficial and achievable innovation. With the

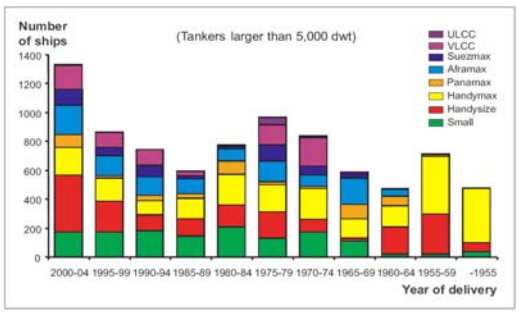

Fig.1.4a. Tanker Fleet development.

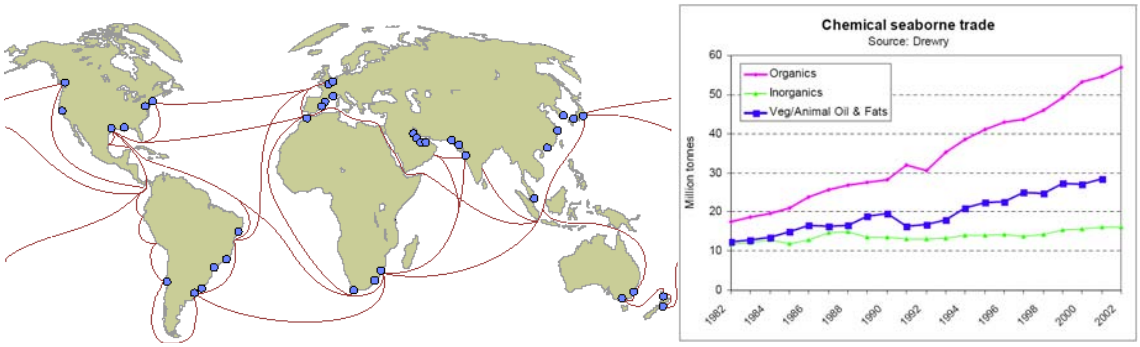

Fig.1.4b. Chemical Tanker Trade

consideration of this trade geography, which is mainly located in low-latitude climate zones with increased ambient temperatures, it might be possible to fully cover demands for cargo heating by exhaust boiler only, especially for new generation double hull tankers.

Similar tendencies of fleet development towards to ship size enlargement are found also for bulk carriers, except that the average size is slightly reduced versus tankers; and biggest part of ordered and available fleet is within range of HANDYMAX and PANAMAX class, followed by still considerable part of CAPESIZE vessels as well [54].

Significantly smaller (around 2.5% of the total world fleet), however due to rapid gas consumption worldwide and consequently with fast development trends, it is LNG Tanker fleet, which is challenging area for our studies in order to introduce WHRS in different extent. Average ship size of gas tankers is considerably high; and the largest vessel now being built can hold 145,000 cubic meters of LNG. However ships with capacities from 200,000 to 240,000 cubic meters are under study, but an increase in ship length and draft however could cause compatibility problems with existing terminals that were designed for smaller vessels. During the sea voyage some gas has a tendency to boil-off, the rates of which constitute around 0.15%, when loaded and 0.10%, when in ballast. In order to re-use this boil-off gas, which otherwise would be lost in atmosphere, steam turbine power plants is the main alternative so far. At significantly higher thermal efficiency diesel engines are proposed by different manufacturers as an alternative, meantime only some part of boil-off gas is possibly to utilize, thus reducing final gain. Therefore another alternative is proposed as well, when fully gas could be used instead of any bunker. The solution is

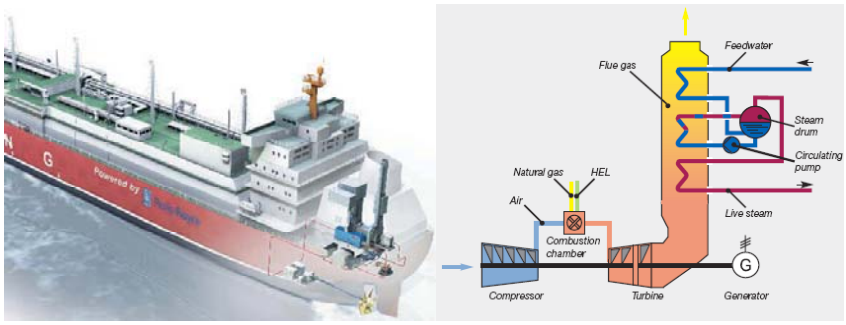

Fig.1.5 LNG Tankers+COGAS type power unit.

advanced gas turbine with high efficiency including WHRS installation, i.e. so-called COGES system (see Fig.1.5) [61]; thermal efficiency of which could reach up to 45-50% [57].

Different Ro-Ro type ships for combine carriage either vehicle or/and containers including passengers are found attractive and economically beneficial way of rather expensive goods transportation. In Europe it is even supported by forthcoming regulations. In a result another nearby segment so called *RO-PAX* ships ensuring the carriage of cars and passengers on comparatively short sea passages (1÷3; 5 days) becomes more and more attractive way of traveling, where high speed is wheel drive for market competitiveness. Therefore as a rule high rated medium speed engines are found as the best solution for power plant set up within limited engine room sizes (see Fig.1.6) [36, 63]. Diesel-electric machinery is another attractive solution for these types of vessels with following characteristics [37, 49]:

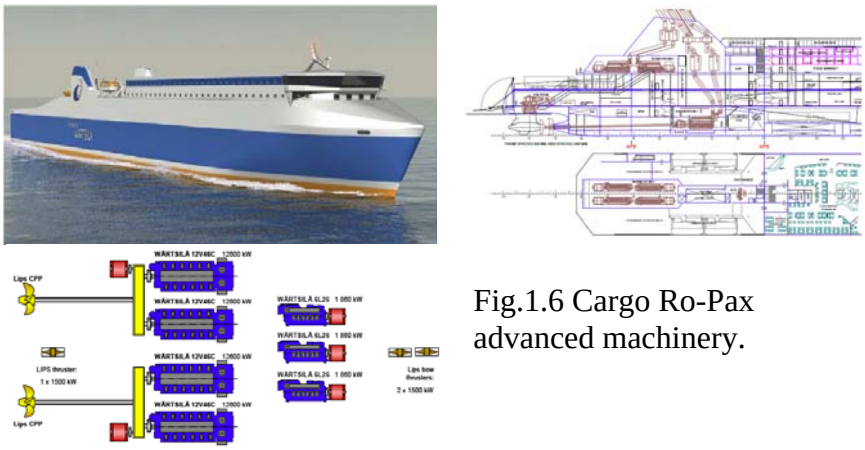

Fig.1.6 Cargo Ro-Pax advanced machinery.

- Offers flexibility in engine room location;
- The installed power can be used for different consumers in different situations;
- It is possible to optimize the engine load by varying the number of gen-sets in use;
- Permits running engines at constant speed;
- Optimum specific fuel consumption and emissions;
- The high torque capability of electric motors allows the use of a fixed pitch propeller with high propulsion efficiency and reduced risk of pressure side cavitation;
- High investment costs;
- Higher transmission losses.

The biggest advantage is the fact that various choices in ship's speed could be obtained without any considerable increase in specific fuel consumption, just by selective engagement of appropriate diesel in circuit. High power-intensity of the plant at limited dimensions comes to specific requirement for WHRS installation, which at the same time should be quite beneficial either.

Despite of the total fleet tonnage growth it is not always that the delivered ship amount has the same rate of development, however released for market sea-born engine output has been increasing constantly [75]. It means that ship's power-intensity per one unit of GRT has grown up considerably. It is another contributing factor towards to heat recovery thorough studies.

1.3. TRADE FACTOR.

Ship trade area is another important factor influencing WHRS efficiency, being highly dependent on ambient and weather conditions. When vessels are trading in climate zones with higher ambient temperatures available heat by effluent gases after main engine is with increased potential as well, therefore possible recovery gain would be more beneficial due to lower consumption in potential heat either. World's Economy driving force is energy resources, i.e. crude oil and products in the very first; therefore tanker fleet shipping routes are generally predetermined, being located in high temperature zones (see Fig.1.7a) [55]. Average yearly both ambient air and sea water temperatures during the voyage will be quite equal at level of around 22/25°C. These conditions are favorable for WHRS installation and efficient use; however tankers are only one part of the whole fleet. Total sea-borne traffic density is dependent on particular country economy development mainly. East coast of China, Indochina is fast developing economical areas, where besides heavy cargo trade (see Fig.1.7b) a lot of shipbuilding and ship-repairing facilities are either located or under construction. On another hand produced good transportation is carried out in way of old economically developed regions like as USA and Europe, being accompanied by long sea passage time (up to 30÷40 days) at considerably high ambient temperatures. Both factors are contributory for efficient heat recovery system performance, as at invariable long term main engine load level also produced power by steam turbine will be unaffected and constant, what makes its utilization process simple both during ship construction and in operation by crew, i.e. lack of different operations, what could result in either some malfunction or significant loss of eventual benefit.

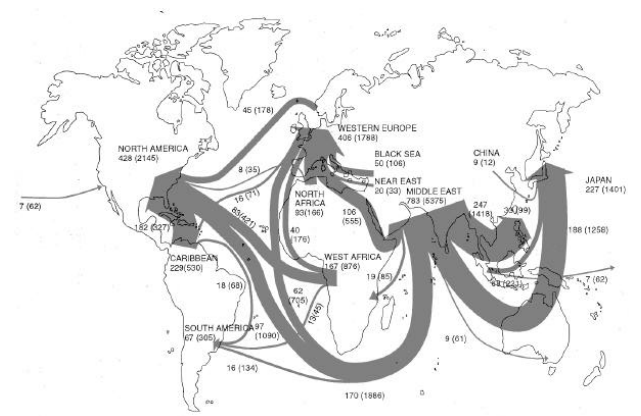

Fig.1.7a. Seaborne Crude oil and product trade.

Separately both traffic density and shipping routes within old economy areas, i.e. Europe (North part of it) and both coast of USA including Great Lake area (see Fig.1.7b), shall be considered specially. Despite of lower ambient temperatures and unstable weather conditions, particularly in North Sea area, energy saving and gas heat recovery might be especially interesting due to more strict Regulations for environment safety and cleanliness, what in its turn results in either different additional equipment or and in required consuming of higher grade (also price wise) fuel oils. Consequently the eventual economical gain is increasing adequately.

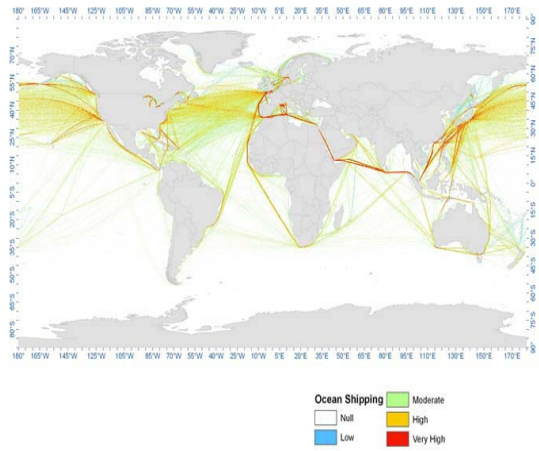

Fig.1.7b. Estimated Shipping Routes.

1.4. ENVIRONMENTAL REQUIREMENT INFLUENCE.

Another key issue is more stringent **environmental requirements** regarding flue **gas emission control and sulfur reduction** in consumed fuel oils (MARPOL Annex VI), already just mentioned. In order to control and reduce air pollution it is established designated SOx Emission Control Areas (SECA's) by IMO conferences, where sulfur content in marine fuel oil is limited till 1.5%. The first designated SECA is the Baltic Sea already since May 19 2006; and the North Sea Area till the English Channel is the next one since November 19 2007 (see Fig.1.8) [38]. Further reduction till 0.1% sulfur limit on fuel used by inland vessels and by seagoing ships at berth in EU ports is agreed by the Council and followed by attending ships. These regulations result into even higher operational costs that are connected with fuel oil consumption; and then economical benefit from any of this type of saving is becoming even more attractive. In addition, by introducing WHRS onboard the ships total gas emission is reduced accordingly.

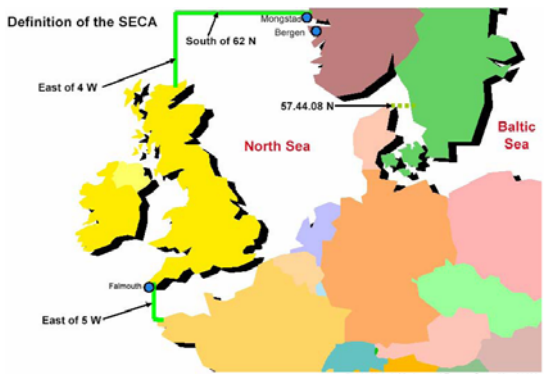

Fig.1.8. Designated SECAs areas.

Another aspect of MARPOL Annex VI is NOx emission control , being applicable for shipboard engines, that are installed on either new-buildings or major conversions already after January 1, 2000. In order to meet this requirement (see Fig.1.9), quite extensive diesel

retrofit and upgrading is required, what includes timing and pressure re-adjustments and application of specially designed injection system components (nozzle, injector, fuel pump), camshaft, combustion chamber (piston, cylinder head, cylinder liner), etc. In a result for advanced medium speed diesel MAN B&W type V 48/60 (400÷450rpm) optimal NOx emission is reduced till around 12 (see Fig. 1.10). By means of supplementary technologies, e.g. water injection, selective catalytic reduction, it becomes possible to reduce NOx level even more. Meantime, without any adjustments considerably lower emission is achieved, when marine gas turbines are used as main engine (see Fig. 1.10).

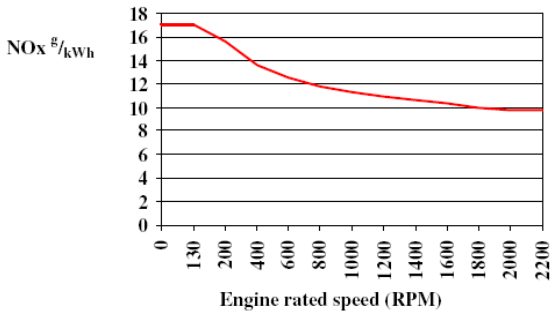

Fig.1.9. Allowable NOx emissions from diesel engines.

NOx emission of marine prime movers in g/kWh

IMO's NO_x limit value for diesels (400-450 rpm)	13
MAN B&W V 48/60, NO_x-opt.	12
V 48/60, NO_x-opt. + fuel-water emulsion (15-20 %)	8 - 9
Engines with direct water injection (50-60 %)	6
Engines with HAM technology	3 - 4
Engines with SCR (Selective Catalytic Reduction)	2
Marine gas turbines without water injection	5
Gas turbines with water injection	2 - 3

Fig.1.10. NOx emission for marine prime movers.

Despite of higher service costs on fuel oil still ***gas turbines start to be more attractive*** as main engine for ship power plants due to their unequivocal advantages and rapid technical development, especially for some specialized ships with high speed and *expensive* cargo. Special case is passenger/cruise ships, where dedicated class notation *COMFORT* gives additional added value for marketing purposes especially, however vibration reduction is essential from the view point of ship's service durability and technical safety either. So, MILLENNIUM is the first large cruises ship that use new propulsion's system: electric motors are fed by alternators driven by combined gas and steam turbine. This system could interest few ones since it will be more and more used in the next buildings. This is an innovative technical feature and, besides marketing, economy of scale, new activities available, etc..., propulsion's technique represents an important element of the product cruise and of course cruise ship design, the main purpose of this site.

The principal advantages of this system are:

- lower costs of exploitation (lower and easier maintenance)
- reduction of nocive emissions (partially because gas oil instead of fuel; -80% oxide of azotes and -90% oxide of sulfur).

- gain in volume and weight considerable (especially combined with Azipods; about 900 tons, that is equivalent to ≈7.2÷9.0 mln. EUR savings, and 50 pas. cabins + 20 crew's cabins have been added).
- lower noise and vibrations level, so better comfort and lower probability of failure for several equipments).

Here's a brief working of the system:

Electric power, for propulsion and other needs of the board, is produced by combined cycle (COGES type): gas turbines and steam turbines. The two main alternators (25 MW, 3’600 rpm) are driven by two gas turbines type LM2500+ built by General Electric. They are stem from large aircraft ones. Each gas turbine is equipped with a recuperative boiler (recuperation of the heat issuing of the combustion of gas in the turbine) which produces the necessary steam to drive a steam turbine (one for the 2 gas turbines) used to drive 9MW alternator. The thermic output is then 43% instead of 39% with gas turbine only. The previous version of this gas turbine model, the General Electric LM2500 is available for a long time onboard US Navy ships and other Navies (the LM2500+ has a higher power of 25%). They are very reliable turbines, only one serious breakdown for 48,800 hours functioning according statistics. For Celebrity, these 48,800 hours would represent 10 years of commercial exploitation of the MILLENNIUM. More, in case of failure, a gas turbine could be able to be replaced in 8 hours only. (a spare one is stored onboard) [16, 39, 40, 44]. To obtain the same final power, lot of heavier and bigger Diesel Engines would be necessary, with higher maintenance costs and higher noise and vibrations (see Fig.1.11).

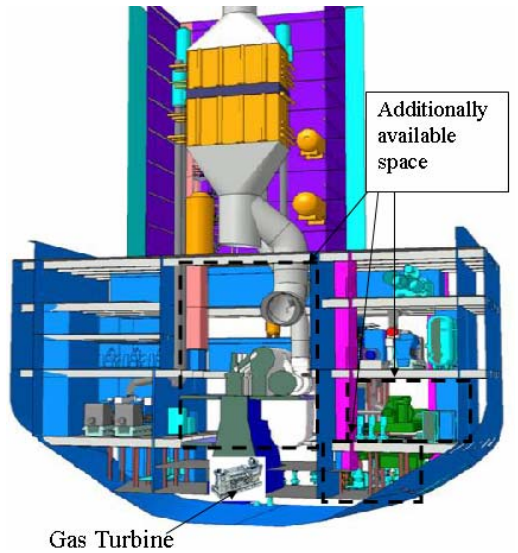

Fig.1.11. Engine room arrangement with slow speed diesel versus Gas turbine.

The specific lube oil consumption of modern gas turbines is typically only 1% of the Diesel engines' figure, but high-priced synthetic lubes have to be used in comparison to the low-priced mineral oils for the Diesel engines. The annual L.O. costs of gas turbines are only about 6% of that of Diesel engines. It has to be pointed out that this merit is of minor importance, since L.O. costs hardly affect the total operating costs.

The return of gas turbines in merchant marine industry is promising, however without WHRS application their competitiveness would be significantly reduced against

diesel power plants. Despite of these technical innovations still advanced slow speed diesel has a big share in the market as ship's main engine.

Based on these considerations further close up studies should be divided in two main groups with the consideration of main engine type.

1.5. THERMAL EFFICIENCY INCREASE FOR SHIP POWER PLANTS WITH ADVANCED SLOW SPEED DIESELS AS MAIN ENGINE.

During the years Slow Speed Diesel Engine has been considerably enhanced, so that specific fuel consumption is reduced as low as possible till $165 \div 163$ g/kWh due to following innovations:

- previously widely used loop-scavenged air exchange system was replaced by piston-uniflow-scavenged one for all two-stroke diesel engines, thus significantly reducing remaining gases in the cycle;
- the growth in relation between piston stroke and diameter S/d ensures increase in thermal efficiency of the cycle due to better scavenging either, while dimensions become bigger at the same time;
- reduction in engine speed till $84 \div 80 rpm$ provides propulsive efficiency rise, however accompanied by relevant engine weight increase as well
- fuel injection system upgrading introducing so-called electronically-controlled common-rail one ensures efficient timing during the whole range of operational loads;
- By increasing jacket cooling water temperature from $\approx 60 \div 65^o C$ till $\approx 80 \div 85^o C$ the efficiency gain is evident due to reduced heat losses, however main engine is being affected by increased thermal stresses

Finally, the total engine efficiency is achieved as high as $\approx 50\%$ (see Fig.1.12a), while remaining part of $\approx 50\%$ are heat losses Q_{hl}, being dissipated in environment [33, 121].

Further consumed fuel efficient utilization could be ensured by recovery of them Q_{hl} as deep as possible. **How to recover wasted energy?**

- By utilizing exhaust gas energy, which constitutes till around $\approx 25 \div 27\%$, in way of both additional power and consumable heat by means of generated steam;
- The special engine tuning in combination with direct ambient scavenge air suction allows to achieve an elevated exhaust gas temperature;
- By using jacket cooling energy and scavenge air cooling energy to heat up feed water;

- By exploiting exhaust gas dynamic energy after cylinders to operate a gas power turbine, especially and mainly for high rated diesel engines. Today's modern high efficiency turbochargers have a surplus in efficiency in the upper load range. It allows to branch-off exhaust gas before turbocharger in order to operate gas turbine.

Finally it becomes possible to return this heat in way of produced electrical energy by steam turbo-generator and relevant power gas turbine engagement (see Fig.1.12b) [72, 110]. At the same time turbo-compound system installation is accompanied by some efficiency loss in main engine either. In our investigations such advanced WHRS with power turbine are not proposed for investigations, as these are some exceptional solutions for high rated engines only [70], but it could be as a good option for extensive heat recovery possibilities either. To ensure further recovery of heat losses, it is proposed to substitute saturated steam consumption for low potential heat consumers by cooling water of both jacket one and scavenging air. Of course, that sort of advanced system introduction should be thoroughly evaluated for each case as size of heat exchangers will grow up considerably; however suchlike modernizations in different extent had been already taken place with positive service experience [74, 78, 88, 148, 149, 151]. As mentioned above, due to more strict environmental regulations certain low NOx emission level is to be achieved in effluent gasses after main engine; but this technical condition is not corresponding to the highest thermic efficiency point of a diesel. Therefore relevant fuel timing is to be carried out in order to meet Requirements; but extended low NOx tuning incurs a fuel penalty of some 2 g/kWh in specific fuel consumption. However, sometimes it is not enough; and then another technique as direct water injection

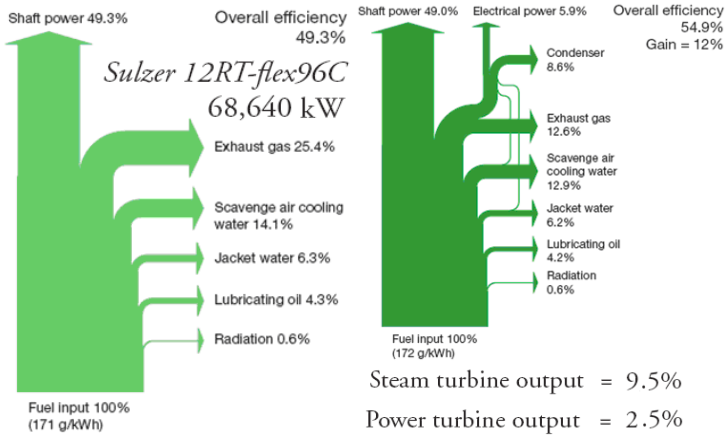

Fig.1.12a. Heat balance of Sulzer 12RTA96C large, low speed marine engines.

Fig.1.12b The effect of WHRS.

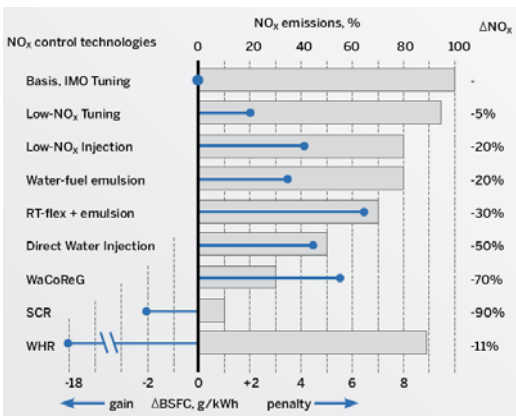

Fig.1.13. Typical changes in NOX emissions & specific fuel consumption for various emissions control technologies.

into the combustion process is proposed for lowering NOx emissions. Under development for Wärtsilä low-speed engines since 1993, this direct water injection (DWI) technique directly reduces cycle temperatures and thus NOx formation. It enables the water to be injected at the right time and place to obtain the greatest NOx reduction. With about 70% water, DWI has been shown to be capable of reducing NOx emissions down to around 8 g/kWh, or to some 50% below the IMO Tier 1 limit. The associated fuel consumption penalty was in the range of 5g/kWh or less [37, 80, 101, 110]. That kind of requirement observation is leading in additional efficiency drop down of the diesel; and as a rule exhaust gases leave the engine with higher potential. Then installed WHRS is capable to compensate this loss at likely invariable overall efficiency of the power plant in the whole. Based on already carried out investigations re different NOx emission reduction systems it was discovered, that any improvement is accompanied by fuel oil consumption increment; while WHRS is ensuring the highest efficiency growth at NOx and CO2 decrease (see Fig.1.13).

1.6. GAS TURBINES AND THEIR CAPABILITIES.

Gas turbines are comparatively new type of engine in marine industry especially. Due to continuity principle of combustion energy transformation into mechanical one of torsional moment it becomes possible to accumulate high power in one volume of equipment, while for diesel engines due to their cyclic mode of power transmission the adjoined mass is much higher. At the present time gas turbines are widely used in shore-based industry, aviation, gas-pipeline industry, navy and others. Meantime, more and more this type of engine is found as attractive solution for merchant shipping industry as well due to their high compactness. There are two type of gas turbines – industrial and aero-derivate type ones. **Industrial type turbines** as a rule are regenerative cycle ones, thermic efficiency of which could reach up to $\eta_T \approx 38\ \%$ and more, while for simple gas turbine cycle it is around $\eta_T \approx 32\% \div 34$ [9, 11, 25] (see Fig.1.14). Efficiency of gas turbine could be further increased by intermediate air cooling between compressor stages, heat of which could be recovered either; and at inlet gas temperature $t_{g_I} \approx 1150^{\circ}C$ the effectiveness could be obtained as high as around $\eta_T \approx 42\ \%$ (see Fig.1.14) [6, 32, 59, 90].

The main advantage of simple cycle aero-derivative gas turbine is its extremely high specific output per one equipment unit weight. So for GEC produced marine gas turbine type LM2500 the average specific weight is around $\approx 0.925\, kg/kW$, which has a tendency to grow down with the inlet gas temperature increase till $\approx 0.210 \div 0.315\, kg/kW$ [40, 46, 67].

Another important advantage is possibility to carry out assembly (aggregate) exchange type of repair, which could be done within cargo operation time in harbor ($\approx 18 hrs$). Due to ancillary equipment and associated ship's systems total specific weight of COGAS type marine power plant together with reduction gear, steam turbine and exhaust boilers will be within range of around $\approx 7.50\, kg/kW$, while similar industrial gas turbine marine power plant with regenerator it is around $\approx 20 \div 25\, kg/kW$. Considerably higher figures will be for power plants, where advanced slow speed diesel engine is used as a main engine, i.e. $\approx 50 \div 65\, kg/kW$. Therefore just aero-derivative type gas turbines are found as an attractive and promising alternative for marine propulsion; however it is not so widely introduced in marine industry so far due to following reasons. Efficiency of simple cycle turbine considerably lower than it is for SSDE, i.e. $\eta_{T_{GT}} \approx 32\% \div 34\%$ for GT versus diesel one $\eta_{T_D} \approx 48\% \div 50\%$ (see Fig.1.14) [16, 49, 59, 130]. The main way how to increase turbine efficiency is to ensure inlet gas temperature growth on the first turbine stages, which is limited due to steel mechanical properties. Nevertheless during the years due to metal theory, industry development **new material** ceramic based are found suitable for turbine blade successful production and operation, thus ensuring to increase inlet gas temperature t_{g_I} on $\Delta t_{g_I} \approx 10 \div 15\, ^\circ C/year$ in average [46, 67]. While for the first generation of marine gas turbine inlet gas temperature was around $t_{g_I} \approx 850 \div 950^\circ C$, then for the next generation of marine engines it has reached the level of $t_{g_I} \approx 1150 \div 1200^\circ C$ at service lifetime up to 50'000 hrs with consequent efficiency growth as well. At the moment there are turbines already in operation with inlet gas temperature up to $t_{g_I} \approx 1260 \div 1350^\circ C$ due to new technologies. Besides material development internal blade cooling is being also proposed [65, 85, 90] as effective alternative to protect its material against adverse exposure to high temperatures, being already efficiently applied in industry [69, 71, 105].

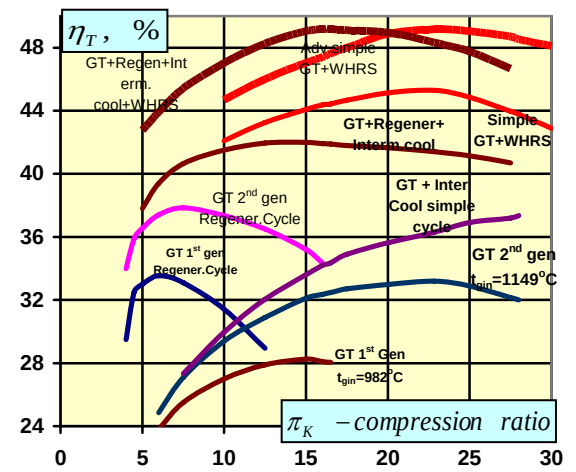

Fig.1.14. Gas Turbine Cycle efficiencies.

Another weak point of aero-derivative turbines is their sensitiveness to consumed fuel oil grade. High vanadium and natrium content in available marine Heavy Fuel Oils

(HFO) IFO180/380 grade is adversely influencing the lifetime of first stage blades especially due to occurring high temperature corrosion. In addition extensive abrasive impact on turbine blades by hard chemical particles is observed in the first stages especially due to high gas velocities. The fuel oil grade substitution by higher one is an extremely expensive solution, as the price difference is almost double between regular marine HFO IFO380/180 and MGO type one; therefore another technical proposal are to be considered for practical use [41, 47, 48, 58, 71, 130]:

- Fuel oil filtering equipment consisting of low and high pressure stages allowing to *catch* particles with size less than 10/5 microns;
- Preparation in storage tanks by observing of regular tank bottom draining and by adding magnesium additives, that precipitate vanadium deposition;
- Fuel washing, the principle of which is to mix into the fuel "clean water" and then remove the water. The water-soluble sodium and potassium are removed with the water. Fuel washing procedures could be quite extensive by adding different de-emulsifiers either;
- Fuel oil treatment by means of either electrostatic or centrifuge method;
- Before fuel oil consuming various additives are added mainly on magnesium base, which shifts V_2O_5 melting point from 675°C till above 1200°C and higher.

The molecule HFO is high developed polymer chain, for burning of which limited sizes of combustion chamber of aero-derivative turbine could be an obstacle, therefore special designs of it are elaborated. At the same time anti-vanadium additives make better conditions also for fuel burning. By making fuel oil and water (10÷20%) emulsion [41, 101] it is also achieved better gas emission parameters from the view point of environmental safety as well. To protect blades from erosion wear out different ceramic base coatings are proposed either.

Based on presented dates as above following advantages, why aero-derivative gas turbine is to be included in our researches, could be brought out as below:

1. Considerably lower and the lowest specific weight of power plant in the whole;
2. In a result the lowest specific volume for engine room arrangement (see Fig.1.11);
3. The lowest initial costs;
4. Ultimately minimized amount of ancillary equipment and systems;
5. The reduced NOx and other gas emission, i.e. the most environmental friendly engine;
6. Lack of vibration, the adverse and considerable post-effects of which is not always duly considered from the economical point either;

7. Practically, lack of lubricating oil consumption;
8. Low installation costs, as there is no necessity for solid basement to fix gas turbine;
9. Ultimately reduced maintenance costs and labor hours;
10. High suitability for automatization;
11. Possibility to carry out unit replacement type repair.

Meantime simple gas turbine cycle is neither efficient enough nor stable against ambient condition fluctuations. Turbine cycle with recuperation has some certain advantages as mentioned above including big combustion chamber suitable for HFO burning, but still outlet gas temperature will be high enough $t_{g_I} \approx 230 \div 300\ ^{\circ}C$ to ensure either high efficiency or effective gas heat recovery (see Fig.1.14) [8, 99]. Additional WHRS installation will make the power plant more robust and complicated. Therefore aero-derivative gas turbine cycle with WHRS is to be chosen as the best alternative. Then by recovering exhaust gas heat in steam boiler and subsequent its steam potential converting into additional energy (see Fig.1.15), the power plant type COGAS efficiency is competitive with similar advanced SSDE power plants. In addition WHRS smooth down the impact due changes in ambient conditions during sea trade. Besides steam turbine adding in power plant, in some researches [22, 50, 101] it s proposed to inject over-heated steam in combustion chamber of gas turbine. The achieved efficiency is slightly below COGAS type power plant, however with possibilities of further development. Meantime, the proposed technical solution is know-how practice, as stable combustion and water recovery technologies are not fully developed and studied out, where increased steam amount impact should bet taken into consideration on turbine wheel calculations, including erosion/corrosion impact on boiler tail surfaces especially. Therefore traditional COGAS system with WHRS (see Fig.1.16) is assumed as the best option for our thorough studies [8, 29, 113, 130].

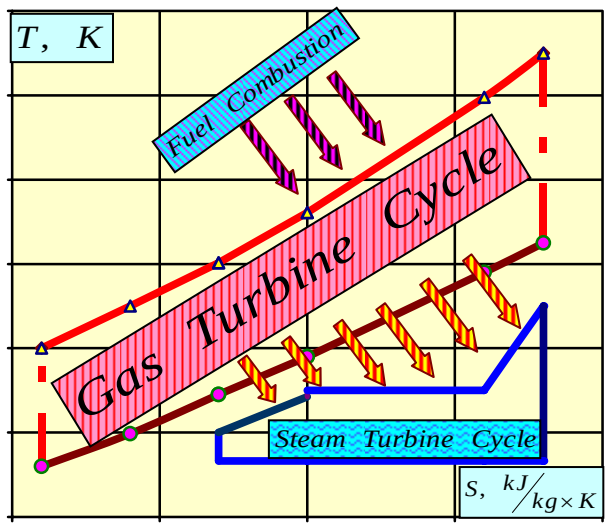

Fig.1.16.Combined Gas-Steam Turbine Cycles.

1.7. PRESENT STATUS OF THE EXPLORATIONS.

Based presented above considerations it comes out quite obvious question, whether the proposed for investigations issue was previously explored not enough. Of course, the problem

was thoroughly studied out by different scientists, institutes and engineering technological centers. First of all, different engine manufacturers, such as M.A.N./B&W, SULZER and others are presenting detailed information of initial dates for heat recovery in dependence on both engine types, rating and possible operating factors. In addition, various options for waste heat recovery are investigated and proposed, however at the same time this information serves as supplementary information. Also such well known marine boiler manufacturers as Aalborg Industries has different boiler types in their range manufacture including heat recovery steam generators (HRSG) for different ranges. One of the most interesting and last achievements in this field was carried out by the well known engineering center Peter Brotherhood Ltd, which has developed combined steam and power exhaust gas turbine, being introduced in ship's electrical power plant for high rated SSDE, and installed on PANAMAX type container ship. Dr.hab.techn. sc., profesor Enin V.I., scientists Flanagan G.T.H., Brucker B. have developed analytic models for different boilers including for WHRS as well, being based on scientific explorations for shore based power plants, where boiler dimensions are found out on pre-determined steam dates that should be achieved. Scientists such as Mr.Kurzon A.G., Mr.Judovin B.S., Mr. Horst W. Koehler, Mr.Brooks F.J, Mr.J.Woodward and others have been investigating heat recovery possibilities by introducing and comparing of different thermodynamic layouts, where also combined gas turbine and diesel cycles are being considered. Further thermic efficiency increment possibilities of gas turbine cycle are considered by different arrangement of blade and other intermediate cooling/recovery possibilities, being introduced in heat recovery cycle and reflected in researches conducted by scientists-engineers Mr.Baily, F.G., Mr.David L., Mr. Masashi ARAI, Mr. Takao SUGIMOTO, Mr.ISHIDA Katsuhiko, Mr.Tetsuji Hoshino, Mr.Dikij N.A., Mr.Zharov G.G., Mr.Vencjulis L.S., Mr.Artemov G.A. and others. Some specific effects of exhaust boiler surface intensification on efficiency outcome were explored by scientists such as Mr.Lazarev V.V., Landa L.S., Mr.Litavrin O.G., Mr.Levchenko G.I., Mr.Bistrov P.G., Mr.K.S.Chana and others, however main analytic equations are presented in handbooks developed by A.S.M.E., C.K.T.I. and other research institutes.

Also for diesel power plants heat recovery possibilities are being explored quite enough, different options for waste heat recovery, including aspects of gas emission reduction, are considered by scientists-engineers Mr.Heinrich Schmid and Mr.German Weisser (Wärtsilä Corporation), Mr.S. Bludszuweit, Mr.H. Jungmichel, Mr.Agafonov V.G., Mr.Kamkin S.V., Mr.Voznitskij I.V., Mr.Maslov V.V. and others.

So it looks like, that there should be almost nothing left for further investigations, but that is not truth; and following considerations should be taken into account in our deeper researches. The thermodynamic efficiency comparison is not an issue of our investigations, as it is quite thoroughly investigated before, but power system optimal build up is the key point. As mentioned previously, ships' spaces are limited in sizes also due to both commercial and quite often design principle reasons. Therefore WHRS build up should be carried out under conditions of dimensional restrictions, especially exhaust boiler, which is the main and biggest constituent of the system. Based on installation possibilities and technical conditions (i.e. acceptable the lowest limit of linear gas velocity in narrow section of tube bundle) just the boiler height is that measure value of convective surfaces and being the main restrictive factor at accepted ship's design. In addition dimensions are the measure value of both boiler price and future maintenance expenses either, therefore gained efficiency should be adequate to investments. How to do it? The answer is quite self evident analytic model for WHRS evaluation should be elaborated at conditions of fixed boiler dimensions, its height. Based on this system the most favorable boiler surface interrelation is to be found out and substantiated at different operational conditions. Also steam pressure is the matter of optimization. Finally, results, regularities would be obtained, based on which the optimal choice of the system and exhaust boiler could be made at fixed costs or dimensions, what is the same.

For ships with SSDE simple exhaust boiler installation is the standard choice, while advanced WHRS installation is an uncommon event also due to unclear final effect. Therefore it is not a standard choice for marine boiler manufacturers to present so sophisticated product as HRSG. A serious obstacle it is limited both new-building and operational experience, when recovered both heat and electrical power should be efficiently utilized, especially during any shortage appearance. At unprepared conditions it results in both considerable efficiency loss and system reliability decrease, what is hardly acceptable. Therefore in order to make the system attractive for ship owners the optimal boiler choice, i.e. mutual convective surface re-distribution, is to be carried out at conditions of fixed gas cooling rate. Further, eventual other heat recovery possibilities are to be optionally considered; and heat/electrical provision rate is to be found out based on various shipping and operational conditions. As soon as mentioned dates are acquired, then they could serve as bases for optimal electrical plant build up, when both highest safety and efficiency are met. This might serve as valuable technical information for ship owners to start build up specific ship for specific trade together with shipbuilding yards and marine equipment manufacturers.

1.8. CONCLUSIONS.

1. The main driving force for further energy saving is on-going fuel price growth; therefore the main way, how to increase power plant efficiency, is to reduce disappearing heat losses in environment.
2. The main constituent of heat losses, which could be recovered irrespectively of main engine type, is enclosed in effluent gasses after main engine.
3. Therefore Waste Heat Recovery System of exhaust gasses is deemed as the best solution for main ship engines (see Fig.1.1, 1.5).
4. Slow speed diesel engines are chosen as the *lowest* alternative for efficient WHRS introduction, where recovery of cooling water heat is to be considered as well.
5. Simple aero-derivative gas turbines are most interesting for WHRS introduction due to the highest both temperatures and gas flow.
6. World's Fleet tendency towards to greater ships with higher speed and subsequent output is a contributory effect for efficient WHRS introduction.
7. Requirements to follow environmental safety, as SECA's area (see Fig.1.8) are another favorable factor to consider more deep energy saving.
8. Global economy development tendencies, towards to hotter ambient temperatures, comes to reduction in main engine efficiency, while the availability of steam turbine cycle in ship's power plant favourably smoothes down efficiency curve of it.
9. The *Renaissance* of gas turbine application as ship's main engine (see Fig.1.11, 1.14) is contributory effect for Heat recovery Circuit (HRC) successful installation.
10. Further investigations for efficient WHRS introduction at low installation and maintenance costs are essential important for any type of ship's power plant.
11. The way how suitability of WHRS installation is presented in this chapter might be applied for real ships with good results as:
    a. Ship type, size, speed has a direct impact on ME and performance dates;
    b. Trade area is important due to ambient temperature level, which has direct impact on ME effluent gas parameters;
    c. Cargo type, e.g. either high viscosity liquids or natural, has direct impact on the choice on WHRS type and/or even on the power plant in the whole;
    d. The choice of engine type and rating is essential factor in our studies.

CHAPTER 2 | THE CHOICE OF MAIN CHARACTERISTICS FOR WASTE HEAT RECOVERY SYSTEM.

2.1. THE CHOICE OF EXHAUST BOILER TYPE.

The main constituent of Waste Heat Recovery System is an exhaust boiler, occupying rather considerable space, and costs of which are the highest ones. Therefore following main technical requirements would be applicable during EB choice for particular case:

1) Suitability to automatization;
2) High specific steam output by one boiler surface unit;
3) High exhaust gas recovery rate;
4) Acceptable long term reliability, i.e. durability, maintainability;
5) Simplicity of boiler arrangement including geometrical construction, which allows us to carry out easy maintenance and eventual repairs (re-tubing, ash deposit cleaning);
6) High enough accumulating capabilities, being defined by boiler water amount, which are important in order to counteract during main engine load level fluctuations;
7) As possible low demands to boiler and feed water quality;
8) Reduced specific boiler costs;
9) As possible minimized weight and dimensions.

To meet conditions above the right choice of boiler type, geometrical characteristics with the consideration of cycle steam thermic characteristics should be thoughtfully carried out.

Boiler with natural circulation [7, 88, 102, 146] is an attractive option due to both simple construction (see Fig.2.1) and high operational capabilities. Comparatively high water content determines good boiler accumulating capabilities, thus resulting in smooth transition line during main engines load changes, and in a result Boiler Control System (BCS) is becoming less complicate. In addition lowered requirements to feed and boiler water quality reduces both maintenance costs and service time by attending crew. On another hand these boilers are less efficient with significantly reduced specific steam generating capabilities, thus achievable flue gas heat recovery rate Ψ will be far from desired one, i.e. $\Psi = (t_{g_0} - t_{g_{exh}})/(t_{g_0} - t_a)$. Refusal to introduce this type of boiler is being related with considerably bigger dimensions required for allocation in engine room due

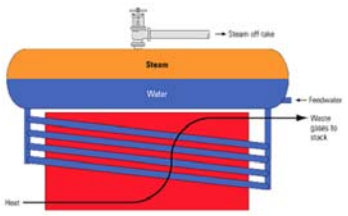

Fig.2.1 The longitudinal drum type of water-tube boiler that operated on the thermo-siphon principle.

to necessity to arrange gas flow turn-off (see Fig.2.1), which results in additional and high growth of boiler aerodynamic resistance either.

Composite marine steam boiler based on natural circulation principle could be considered as good technical solution for ship power plants being a combination of an oil-fired steam boiler and an exhaust gas economizer (see Fig. 2.2.). When the diesel engine is in running mode, fuel oil burner starts only, if demands in steam exceed boiler capacity achieved from main engine exhaust gases. Most common composite boilers nowadays have separated sections for diesel engine exhaust gases and flue gases from the fuel oil burners. The economizer part also works as a silencer for the diesel engine, however quite often an additional silencer is required. Using diesel engine exhaust gases as combustion air for fuel oil burning is quite economically although it makes a unit rather complicated. The proposed option could be an attractive solution for power plants with slow speed diesel as a main engine, when steam shortage could be efficiently and quickly restored. Meantime, the same deficiencies as described for the boilers with natural circulation are those, why this type is used for saturated steam production only being directed for low potential heat consumers, i.e. for heating purposes.

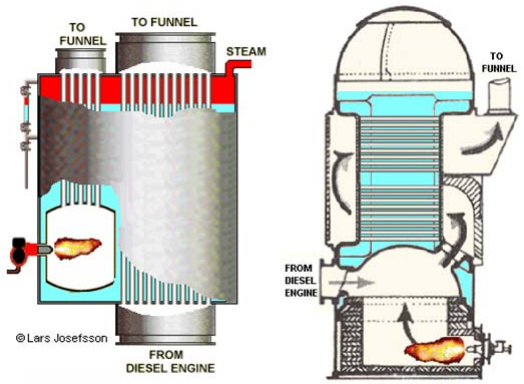

Fig.2.2. Composite marine steam boilers.

Another alternative a forced-through-flow boiler is proposed for installation onboard the ships [27, 98], allowing to reduce boiler dimensions, particularly its height, to a rather great extent also due to distance elimination between heat exchange surfaces. However this type of boiler is practically unknown in marine industry at the moment due to high demands for water treatment, thus extremely reducing equipment reliability. Any eventual tube damage might lead to complete boiler surface and WHRS disabling.


Fig.2.3 Rectangular type exhaust water tube boiler with forced circulation.

With the consideration of concluded above EB is accepted water-tube type with forced circulation of rectangular construction (see Fig.2.3) due to its high reliability and effectiveness [10, 23, 91, 103, 113]. In order to avoid significant increment in boiler height chess type tube disposition in the bundle is

preferred against corridor one, as considerable surface intensification per one boiler volume is achieved for the first option. At gas flow above $80\,kg/s$ coils are accepted doubled, i.e. at collector inlet tube coil is divided on two, otherwise boiler cross section shall be enlarged to a rather great extent In a result coil length is reduced as well, thus significantly minimizing hydraulic resistance also. On another hand boiler both construction and manufacturing is becoming more complicated, resulting in diminution of maintenance reliability. Despite of contradictory outcomes doubled tube surfaces is a solution for high capacity boilers; otherwise it might be necessary to accept multiple dimensions of coil amount equal to 8 in the bundle, what pre-determines their big height, or reduction in surface washing coefficient ω by flue gases, thus coming to relevant heat efficiency diminution. Accumulated service experience of this type of boilers is evidence of their high reliability, however from time to time equipment failure is observed because of coil, casing foundation damages [14, 27, 99, 104, 108].

2.2. BOILER CORROSION IMPACT.

Another threat during operation is internal boiler surface corrosion. For chosen water-tube type boiler areas in way of economizer and evaporator inlet, and tube elbows are most affected by this corrosion. The presence of oxygen is needed to let corrosion happen, however following factors as tube vibration, slow media speed at partial loads, irregular steel structure in way of tube welding, are contributing the development rate of this adverse phenomenon. When either feed water supply is not arranged properly, i.e. lack of proper tightness of the system, or water treatment schedule is not followed as prescribed, or both, then high oxygen O_2 content in boiler water is the main cause of often tube leaks due to their internal corrosion. Based on these threats it might be necessary to consider possible de-aerator installation for oxygen evacuation [95, 142] out of supplied feed water. By setting the lowest acceptable steam/water speed the choice of geometrical characteristics of tube and bundle is to be verified and adjusted correspondingly, especially for the economizer part of the boiler.

Besides internal one, also external corrosion will affect the choice of both boiler geometrical and thermo-dynamical characteristics. In the point of fact the nature of this corrosion type is chemical (sulfur) based one called also as low-temperature corrosion, as being highly expressed at reduced temperatures of gas/heating-up media. The most affected by corrosion areas are tube connections with collectors, where sulfur-anhydrite containing gasses are penetrating internal casings inside boiler dead zones and cooling down till heating-

up media temperature. Also boiler tail surfaces, e.g. economizers, are those, which very often are suffered from sulfur corrosion resulting even in total boiler shut-down (see Fig.2.4). Therefore feed water temperature at boiler inlet t_{fw} is to be chosen high enough to minimize adverse corrosion impact [129]; however at the same time equipment is becoming less thermo-dynamically efficient. In addition boiler tube weld seams are the weakest areas against corrosion due to irregular steal structure with porosities, different inclusions and other defects. By burning high residue fuels with sulfur amount up to 5% external pollution of boiler surfaces might become critical if proper maintenance and construction precautions would be not taken into consideration. Besides the substantiation of feed water temperature, geometry of tube bundle, especially boiler tail surfaces are to be chosen with the consideration of gas velocity, that ensures efficient self-cleaning during operation. Also the use of some higher grade alloy steels more resistant to sulfur acid corrosion might be economically substantiated choice for economizers particularly.

Fig.2.4. Boiler tube sulfur-acid corrosion.

Vibration is another factor adversely influencing boiler safety; and negligence of the root causes will result in relevant corrosion fast development also. Therefore proper boiler installation in a gas path without any sharp turns is utmost important; in case if that is not impossible special guide sheets are recommended to be added in the path to minimize both gas current fluctuations and intensification of ash deposition formation in these zones.

2.3. THE CHOICE OF THERMO-CONNECTION LAYOUT FOR WHRS.

The choice is based on summary overview of maintenance experience and different technical solutions, innovations and proposals [7, 15, 21, 26, 27, 32, 45, 95, 104]. However such an extensive comparison might be rather developed studies not being a task for our researches, therefore we will limit them by the overview of main layouts of WHRS. The right choice of HRC type is important to ensure both high power output and safe, durable, cheap and simple (as low as possible man-power hours during operation) service. For older ship power units it was quite common to use saturated steam to run turbine, thus considerably reducing exhaust boiler dimensions, i.e. its height. But having the boiler, that consists of evaporator only, it becomes impossible to ensure high flue gas recovery rate, as exhaust

temperature t_{g_0} will be always higher than saturation one, corresponding to steam pressure, i.e. $t_{g_0} > t_s$. Lack of super-heater part in EB does not ensure steam overheating and *drying*, what results in considerable losses due to low efficiency of both Rankine (steam turbine) cycle and turbine itself,. Besides, due to high moisture content in produced steam at turbine inlet both blades and nozzles will be highly affected by condensate droplet erosion, what deteriorate both reliability and efficiency during service time. Therefore exhaust boiler consisting of economizer, evaporator and super-heater is the minimum *must* choice for such WHRS.

In order to avoid sulfur acid corrosion destructive effect it was a common practice to introduce HRC with economizer and evaporator engagement in consecutive order onboard the ships (see Fig.2.5). However, at such a surface layout arrangement it is impossible to maintain feed water temperature invariable at economizer inlet, as at partial main engine loads it t_{fw} will grow down as well as boiler steam pressure p_s. Therefore it is recommended to keep feed water temperature as high as around not less than $t_{fw} \geq 130 \div 135^o C$, what considerably either reduces WHRS efficiency or increases EB dimensions, particularly economizer surface sizes. Despite of quite positive operational experience, nevertheless time to time it was discovered serious damages due to internal heating coil corrosion, caused by oxygen presence. Hence HRC with intermediate steam extraction for feed water de-aeration might be proposed as a possible alternative and being investigated further. Meantime in order to maintain temperature t_{fw} at constant safe level the extraction point is to be chosen with the consideration of ME service load range, what reduces steam cycle efficiency pretty much. Therefore other means how to reduce oxygen content in feed water shall be considered, e.g.:

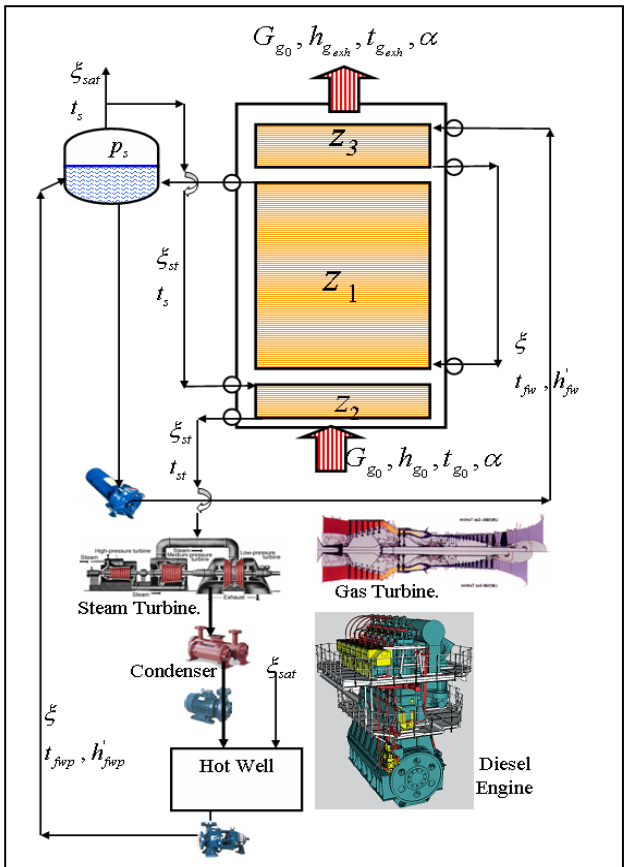

Fig.2.5 WHRS with economizer and evaporator engagement in consecutive order.

- Good sealing of vacuum side mechanisms;
- as much as possible utilize de-aeration capabilities of a condenser;
- arrangements for steam separation;
- boiler water chemical treatment;
- others.

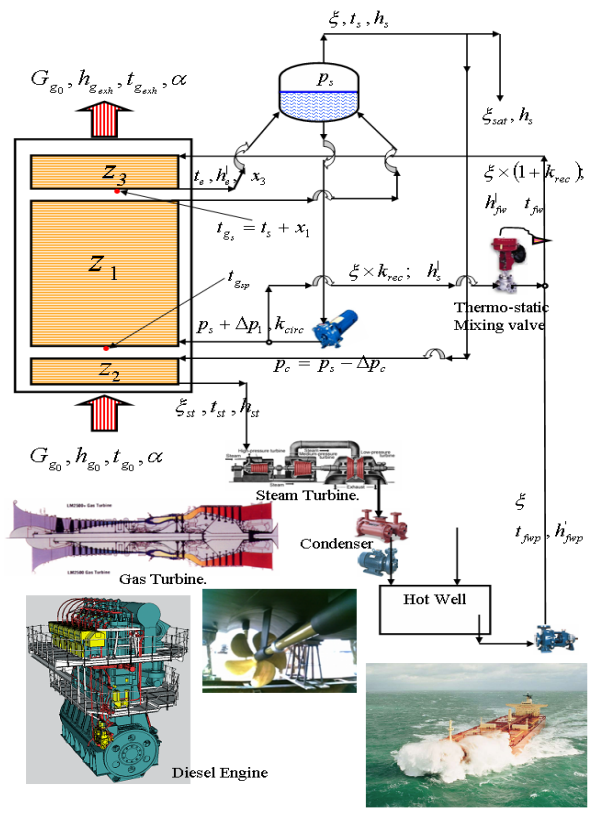

Fig.2.6a HRC with Thermostatic Mixing Valve & Feed Water heat up by Recirculation.

Based on considerations above the most favorable WHRS is considered with thermostatic re-circulation valve for feed water pre-heat, where exhaust boiler consists of economizer, evaporator and super-heater only (see Fig.2.6a) [10, 40, 118, 147]. This HRC is deemed as both reliable and efficient at possibly reduced sizes. Feed water temperature could be adjusted till desired value irrespectively of main engine load level, what especially is important at partial loads. For higher temperatures it becomes possible to lower feed water temperature t_{fw} at economizer inlet thus achieving maximum output without both any tail surface enlargement and sulfur acid corrosion occurrence. However, at the same time gas cooling rate for single-stage pressure boiler is limited by chosen steam pressure p_s, i.e. its saturation temperature t_s; and at higher inlet gas temperatures t_{g_0} there is the tendency for steam pressure to grow up as it is presented in next chapter of the theses. Subsequently, it becomes difficult to cool down flue gasses till the same temperature $t_{g_{exh}}$, without extensive boiler surface enlargement (see Fig.2.6b). Therefore different options for multi-stage steam pressure WHRS are proposed by industry and engineering companies. The simplest option,

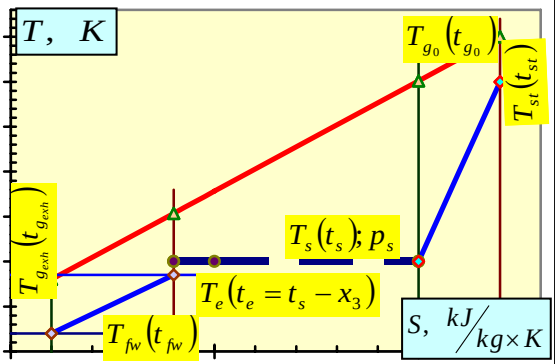

Fig.2.6b Single steam pressure WHRS: temperature-entropy diagram.

when low pressure boiler part consists of an evaporator (see Fig.2.7a) only would be offered either for power units with moderate higher inlet gas temperature t_{g_0} or at increased saturated steam consumption, e.g. passenger ships or ferries. Feed water warm-up is carried out by means of boiler water recirculation from high pressure side, as by providing it from low-pressure stage it will be necessary to install additional booster pump at economizer either outlet or inlet. However by re-circulation arrangement from second stage evaporator it will lead to increased water amount flow $k_{rec}^{II} > k_{rec}^{I}$, thus ensuring deeper gas cooling at the same surface dimensions. Also it is possible to arrange boiler water feed up of low pressure drum either directly after re-circulation valve or after economizer by installing additional pressure reduction and governing valve. In the second option through-flow boiler water amount via economizer is higher by saturated steam consumption $+\xi_{sat}^{II}$ required for low potential heat consumers. At condition, when boiler water temperature at economizer outlet is invariable $t_e^I = const.$, it becomes possible to cool down flue gases to a rather great extent (see Fig.2.7b). Meantime, the location of low pressure boiler part could be different and will be dependent on required saturated steam characteristics. Besides *re-circulation* it is also possible to arrange feed water warm-up by means of de-aeration.

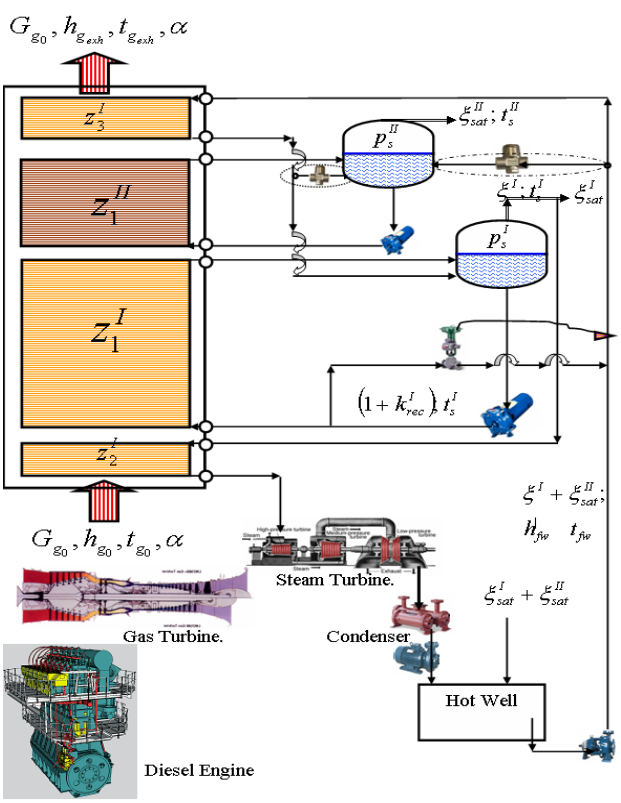

Fig.2.7a Simple double steam pressure WHRS.

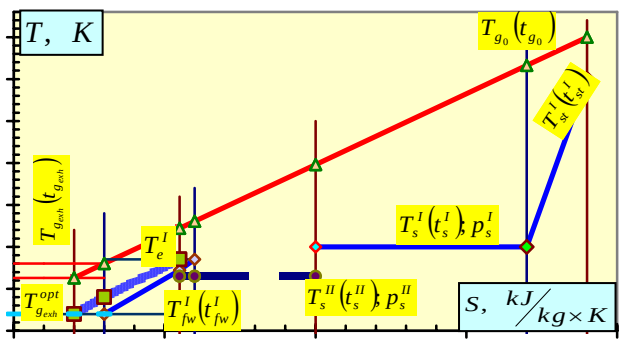

Fig.2.7b Simple double pressure WHRS – temperature-entropy diagram.

Another more advanced option is double pressure WHRS with intermediate steam supply either into steam turbine or in its low pressure stage (see Fig.2.8a) [1, 13, 18, 27, 59],

where also different options could be considered, e.g. feed water warm-up by means of either low or high pressure stage, various boiler surface engagement, etc. Certainly, boiler dimensional height will grow tremendously mainly due to additional distances between surfaces. Power plant installation costs will be considerably higher than in case of single stage WHRS. At the same time daily maintenance of the equipment will be more sophisticated either, that requires higher professionalism by attending crew. Based on these considerations the proposed WHRS (see Fig.2.8a) might be attractive for power plants with high rated either medium speed diesel engines or advanced GT as a ME. For low speed diesel units this option has to be thoroughly re-considered, however it might be quite attractive for high rated engine [33, 72]. Nevertheless, additional gain in efficiency is ensured anyway due to such innovations (see Fig.2.8b). An evaporator is the main constituent of a boiler, which finally determines both dimensions of other related constituents and gas cooling rate at accepted pressure. So called *pinch-point* temperature x_1 is the measure value of evaporator surface sizes z_1, being found as a difference between gas temperature at evaporator outlet t_{g_s} and saturation one t_s, that corresponds to chosen steam pressure p_s, i.e. following equation is valid - $x_1 = t_{g_s} - t_s$. Based on concluded above, recovered by evaporator gas heat t_{g_s} is the measure value of boiler dimensions and recovery efficiency,

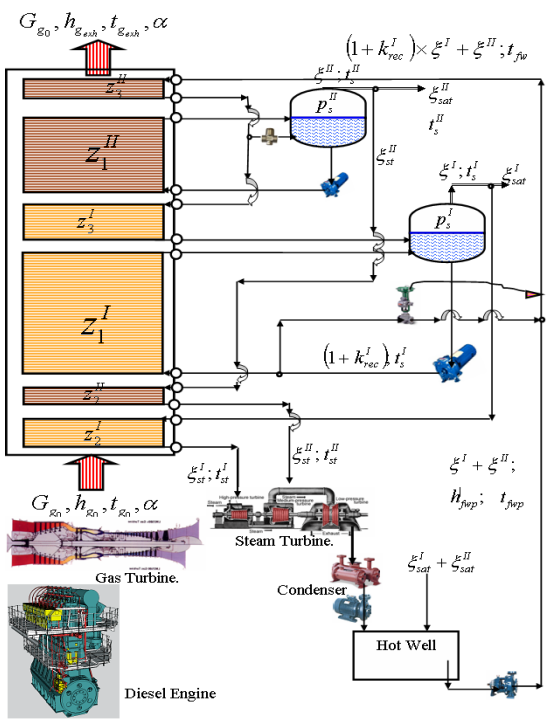

Fig.2.8a Advanced double pressure WHRS with intermediate steam supply.

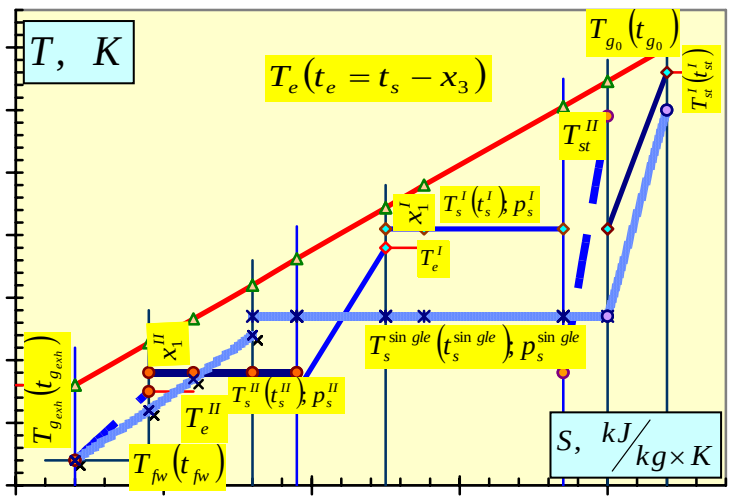

Fig.2.8b Multi-stage pressure WHRS–temperature-entropy diagram.

being contradictory influenced by both surface sizes and steam pressure. As it was mentioned, second boiler stage should be introduced at rather high inlet gas temperatures t_{g_0}. Steam pressure choice is to be chosen so, that available gas heat under *red-gas line* (see Fig.2.8b) is being recovered both as deep as possible $t_{g_{exh}}$ and utilized highly efficient, what means that steam-water lines should be situated as close as possible to gas line, i.e. $Q_{exh} = \int Sdt = \max$. Let's compare, what will happen if one pressure stage is missing. When boiler is consisting of high pressure part only then to achieve the same cooling rate *pinch-point* temperature x_1 should be reduced till possible minimum by increasingly evaporator surface enlargement. Recovered heat will be efficiently used by ST; however at certain pressure level p_s^I it becomes impossible to ensure the same cooling rate. By choosing low pressure stage only desired cooling rate is obtained without any significant additional surface enlargement, but at quite reduced pressure p_s^{II} recovered heat utilization efficiency will be considerably lowered either. Therefore total WHRS efficiency will be definitely higher for multi-stage exhaust boiler than in case of single one, i.e. $\left(\int Sdt\right)^{2-StageEB} > \left(\int Sdt\right)^{1-StageEB}$. The advantage of multi stage WHRS is, that in the part of increased gas temperatures high steam pressure allows us to utilize recovered gas heat with the highest efficiency, while by reducing steam pressure in the second stage much deeper gas cooling rate is obtained. However, in our studies these complicated systems will be not explored due to our stated task over-fulfillment.

Finally, as the base option WHRS with boiler water recirculation for feed one warm-up is chosen (see Fig.2.6a) due to its high efficiency at various main engine load levels and at possibly reduced EB dimensions, particularly its height. The possibility to govern feed water temperature makes the system more reliable as well. HRC with intermediate steam extraction is considered as an alternative being explored in next following chapters.

2.4. SELECTION OF GEOMETRICAL CHARACTERISTICS FOR EXHAUST BOILER.

Boiler surface tube chessboard-type (see Fig.2.9) disposal in the bundle is more preferable than corridor one due to high both compactness and heat transfer efficiency; however, boiler gas resistance is higher either. At equal operational conditions corridor-type bundle is more affected by ash deposit formation on surfaces, being caused by the effect of appearing turbulence after gases passed first tube row. Conditions of gas washing against front part of second row tubes are deteriorating; and in a result it comes not only to grow

down in heat transfer rate, but also to surface pollution intensification from gas side, i.e. suspended particle deposition. At same time the effect from soot blowing is higher for corridor-type tube bundle [21, 23, 26, 27, 100, 133, 134].

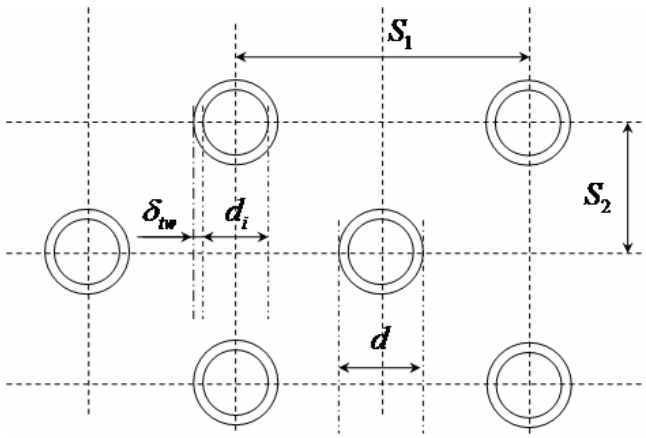

Fig.2.9.Tube chessboard-type disposal in the bundle.

As base option plain tube is considered due to its good service records, the main advantage of which is the minimized pre-disposition to pollution from gas side; therefore surface heat transfer efficiency is being more stable during the service time. In a result the rate of acid-corrosion in tail surface is minimized either, that makes this type of boiler more reliable. Both manufacturing and eventual repair costs also will be the lowest ones possibly to be carried out by ordinary shipyard, while any corrugated tube surfaces would be manufactured by specialized companies at much higher costs and delivery terms.

Recommended tube wall thickness δ_{tw} is chosen in dependence on tube sizes, steam pressure value; and based on different safety requirements, manufacturer recommendation it is accepted equal to $\delta_{tw} \geq 0.0025m$ [17, 20]. Excessive tube outside diameter d reduction is not acceptable either due to relevant and considerable hydo-dynamic resistance growth [87, 114], despite of heat transfer efficiency rise; therefore in our case it is accepted equal to $d = 0.022m$; and in a result inner tube diameter d_i is found equal to $d_i = d - \delta_{tw}$. The right choice of optimal values for cross-head S_1 and longitudinal S_2 steps in tube nest (see Fig.2.9) has a direct impact on both ash deposit formation rate and heat exchange efficiency. At the same time an excessive reduction in the relation between tube step and outside diameter, S_1/d in particular, advances sharp erosion wear out rate of boiler surfaces. Based on above cross-head step S_1 is accepted as small as possible, but with the consideration of service experience the size of step should be enough to provide free tube hollow off, when repairs are needed. Hence, for plain tube surfaces cross-head step is equal to following - $S_1 = 2 \times d + \delta$, where value δ is spacing required for tube installation and hollow off. For evaporator and super-heater surfaces spacing is accepted equal to $\delta = 0.003m$ and

subsequently cross-head step is - $S_1 = 0.047m$. In order to minimize the rate of both scaling and internal oxygen corrosion boiler water speed in a tube is to be ensured high enough; therefore economizer bundle construction is chosen with additionally combined horizontal and vertical bundles. Whereby due to increased tube crook cross-head step is accepted higher and it is equal to $S_1 = 0.050m$. With the consideration to reduce ash deposit formation rate longitudinal step is accepted as small as possible equally to - $S_2 = 0.025m$

2.5. SELECTION OF GEOMETRICAL CHARACTERISTICS FOR FINED SURFACES.

Aspirations to maximize heat recovery rate at limited boiler dimensions different technical solutions towards to heat efficiency intensification are to be introduced during designing and manufacturing. Therefore tube ribbing is considered as one of the main and efficient innovation, how to increase boiler surface density per one volume unit several times, being already successfully implemented in marine industry with good service records [23, 68, 89, 99, 104, 109, 117, 145]. For convective surfaces cross-ribs (see Fig.2.10) are mainly applied due to:

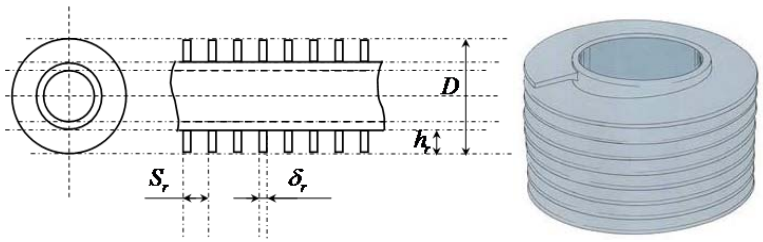

Fig.2.10. Finned tube geometrical characteristics.

- More efficient thermal conductivity up to $30 \div 70\%$ more;
- higher surface density at almost fixed total weight of the boiler;
- both collar and spiral type fins increase tube strength;
- ribbon type tube cross-fining production is well established at decent price.

Taking into consideration available products in the market to manufacture ribbed tubes and service experience following geometrical characteristics found feasible as follows - $S_1/d \approx 2.2 \div 5.0$; $S_2/d \approx 0.7 \div 3.0$; $h_r/d \approx 0.2 \div 1.2$; $\delta_r/d \approx 0.02 \div 0.10$; $S_r/d \approx 0.2 \div 1.0$, where

- S_r - fining step, m;
- h_r - the height of ribs, m;
- δ_r - the thickness of ribs, m but
- D - fined tube outer diameter, m (see Fig.2.10).

Characteristics of ribs. In order to keep boiler weight as low as possible thickness of ribs is to be minimized, but with the consideration of corrosion-erosion impact by flue gases this thickness δ_r is to be sufficient, i.e. $\delta_r \geq 1.0mm$. In our case it is accepted equal to $\delta_r = 1.5mm$ due to low grade heavy fuel oil being consumed by main ship's engine. Fined tube bundle with ribs of considerable height h_r is building up surface characterized by high coefficient of compactness together with increased weight. Excessive height will lead to relevant decrease in thermal conductivity of the fin surface, i.e. average meaning of temperature drop is reducing and efficiency of ribs as well. Thus, the rise of fining coefficient on around 40% is accompanied by thermal conductivity grow down till $\approx 12\%$, which is still beneficial to choose boiler surface of this type. However unlimited growth in fining intensity will be ineffective, therefore with the consideration of service experience the relation δ_r / d is narrowed till following limits - $\delta_r / d \approx 0.35 \div 0.40$, and the height is accepted equal to $h_r = 8mm$. The reduction in fining step comes to relevant decrease in thermal conductivity, as nearby rib roots gas flue becomes weak just on tube base surface, correspondingly laminar border layer is becoming more thick, being characterized by higher both thermal and aerodynamic resistance. On another hand relatively high fining step ensures both low deposit formation rate and good fitness for surface cleaning, soot blowing; however, EB compactness is less. Therefore the optimal fining step is limited within following values - $S_r / d \approx 0.20 \div 0.40$; and in our case it is accepted equal to $S_r = 8mm$. At theses accepted meanings of fining rate, being relation of surfaces between the summary one and that part of tube not occupied by ribs, will constitute around $\varphi \cong 3.58$.

However, good results were achieved by experimental introducing of some boiler surface with reduced fining step till $S_r = 4mm$ without any evidence of increased pollution from gas side [116]. At the same time it is important to consider the fact that particularly these gas turbines (2 units) were operated on considerably better quality MGO fuel type with reduced sulfur content. When lower grade HFO IFO180/380 would be consumed, then such a reduction in S_r might be critical. Also main engine type should be taken into account, when fining characteristics are chosen, as air excess coefficients α are different either for slow speed diesel or gas turbine. So for gas turbine it constitutes around $\alpha_{GT} \approx 5.5 \div 6.5$, while for advanced diesel engine it is $\alpha_{SSD} \approx 3.0 \div 3.5$, subsequently suspended ash particle

concentration per one gas volume unit will be lower, when gas turbine is being used as ship's main engine.

Tube cross-head step in the bundle will be higher for fined surfaces than for plain ones; and in order to ensure free ribbed tube hollow off it is accepted equal to three base tube diameters, i.e. $S_1^r = 3 \times d$, based on previous good maintenance experience as well. In addition with the consideration of ash deposition nature on tube surfaces tube longitudinal step in the bundle is chosen slightly higher than tube base diameter, i.e. $S_2^r = 1.2 \times d$.

By choosing EB with fined tube surfaces it is important to remember about adverse vibration impact on surface reliability in long term, as durability in way of rib and tube connection is becoming broken down; and in a result this part of surface might be partly disengaged. The hazardous source of high vibrations in exhaust boilers is pulsations of effluent gases from main engine, especially from low speed and medium speed diesels, which might be intensified in the tube bundle due to vortex flow formation, flow abruption from rear side of the tube, as well as other factors originating vibrations [53, 133, 134]. The main way, how to escape vibration adverse and fatal post-effects, is correct choice of tube coil length, which is being dependent on all vibration spectrum impact, i.e. frequency and amplitude of imposed and own vibrations of different length of tube due to clamping frequency and end fixation. Meantime surface fining is making tube more robust against any vibrations.

2.6. THE CHOICE OF MAIN THERMO-DYNAMIC CHARACTERISTICS.

Feed water temperature at boiler/economizer inlet t_{fw} is an important efficiency index, which determines possible gas cooling rate $t_{g_{exh}}$ and final efficiency in a result at fixed boiler dimensions. At the same time excessive reduction in it t_{fw} shall not be allowed due to high risk of sulfur-acid corrosion occurrence in tail surfaces as already partly described above. Corrosion rate is directly dependent on both sulfur content in fuel oil consumed by ME and dew-point t_{d-p}, which in its terms is influenced by moisture content in flue gases and air excess coefficient [23, 30, 34, 143, 147, 148]. In order to ensure safe and durable surface lifetime steel tube wall temperature t_{TM}, being defined by both feed water and outlet gas temperature, is to be higher than determined dew-point, i.e. $t_{TM} > t_{d-p}$. For our considered Combined Gas-Steam power plant (COGAS) feed water temperature is recommended to be maintained not less than $t_{fw} \geq 100^o C$. For power plants with advanced slow speed diesel

engines as ship's main propulsion unit dew-point temperature will be higher due to reduced air excess coefficient, subsequently feed water temperature to be increased as well. Based on service experience, different technical norms and recommendations it should be not less than $t_{fw} \geq 120^o C$; however its considerable t_{fw} increase will lead to boiler, economizer particularly, efficiency drop down.

Also gas temperature at exhaust boiler (economizer) outlet $t_{g_{exh}}$ has direct impact on sulfur corrosion rate, therefore based on technical recommendation it should be not less than $t_{g_{exh}} \geq 160^o C$ both for gas turbine and diesel power plants. Actually sharp increase in sulfur acid corrosion rate appears at dew-point temperature equally and less than $t_{d-p} \leq 90 \div 80^o C$ [76, 120]; at temperature higher than $t_{g_{exh}} \geq 90^o C$ corrosion impact is minor; and at high enough tube wall thickness (with increased corrosion allowance $\Delta\delta_{tw}^c$ for tubes of economizer part - $\delta_{tw} + \Delta\delta_{tw}^c$) tail surface performance safety factor might be ensured high enough. In order to reduce corrosion impact different additives for fuel oil burning in main engine are developed and proposed by market allowing us to decrease dew-point temperature. The installation and the usage of different and effective means for soot blowing, tail surface manufacturing of higher grade alloyed steels more resistant to sulfur corrosion will also contribute to safety growth at probably profitable investments. At the fulfillment of these pre-conditions it might be possible to ensure even deeper gas cooling down, up to $t_{g_{exh}} \approx 140^o C$.

Pollution coefficient ε of an EB from gas side is another important characteristic in the determination of heat transfer efficiency. Its influence is under way of the aggravation of convective heat transfer coefficient k expressed as below [43, 51, 108] –

$$k = \left(\frac{1}{\omega \times \alpha_1} + \varepsilon + \frac{d}{d_i} \times \frac{1}{\alpha_2} \right)^{-1}, \tag{2.1}$$

where coefficients α_1, α_2 are heat conductivity ones from gas to wall and wall to warming-up media (boiler water, steam) correspondingly.

According maintenance experience heat transfer coefficient is reduced on **20%** at both scale and soot thickness of **1mm** each, but at soot thickness of **1mm** only the reduction of k constitutes till **17%** [87, 92, 103, 110, 112]. As it can be seen there is dominant and considerable influence of soot deposition on convective heat transfer efficiency; further ash thickness increase till **2mm** will result in respective k reduction on **≈31%** for plain tube

surfaces. Therefore it is utmost important to understand nature of ash deposit formation in order to choose boiler characteristics. More in details the origins of pollution coefficient ε will be presented in following chapters; however main influencing constituents are briefly considered hereinafter. In accordance with experimental works practically both all factors of power unit performance and chosen design characteristics of exhaust boiler have certain and direct impact on pollution rate from gas side, e.g. linear gas speed in boiler cross section w_{g_i}, geometry of the tube and the bundle; fuel oil grade consumed by main engine, heat exchange surface temperature. Chemical elements as Na, Ca, V present in fuel oil have unequivocal impact on ash deposition rate. When ME is running at partial loads, pollution intensity is increasing considerably due to both lowered gas amount and temperatures, and in a result gas linear velocity $w_{g_i} \downarrow$. At flue speed equal to $w_{g_i} \le 9 \div 12\, m/s$ pollution rate in cross-chess type tube bundle is becoming equal to corridor type one. Tube fining rate increase has a direct impact on value ε, and in any case ribbed tubes are more affected to ash deposition than smooth one at similar other conditions. Tube diameter increase, as well as relative tube step and tubes with angle-twist fins have the same adverse impact. At twist angle equal or more than $\gamma_r > 5.7^o$ [60, 62, 73, 92, 137, 138, 143] increased pollution rate is due to gas flow tearing off rib rear side, thus creating dead zones favorable for ash formation and accumulation (see Fig.2.11). All considered factors above that influence pollution rate, either geometrical or thermo-dynamic ones, as gas temperatures and flow G_{g_0} have a direct impact on linear gas velocity; then on another hand it can be concluded, that there is some lowest meaning of linear gas velocity $w_g^{\min}$ in boiler cross section by diminishing of which soot deposit formation will start grow up with accelerated rate. Besides mentioned factors also both linear speed uneven distribution in boiler cross section, ash particle concentration, expected tube lifetime with the consideration of its wear out time and relation of $S_1/(S_1 - d)$, as well as tube steel properties have evident and rather considerable impact on value $w_g^{\min}$. For transversally gas washed tube bundles it is found that the lowest linear gas velocity should not be less as follows - $w_g^{\min} > 6\, m/s$ [21, 94, 102, 108, 109, 135, 136]; therefore

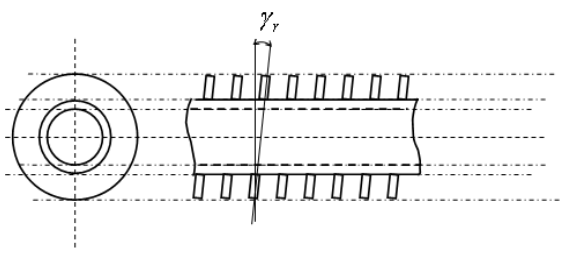

Fig.2.11. Tube with angle-twist fins.

when design of exhaust boiler is chosen the geometry of it should be so that in any case and in all sections actual linear gas velocity is above the minimum, i.e. $w_{g_i} > w_g^{\min}$.

By summarizing results of service experience pollution coefficient is found equal around to $\varepsilon \approx 0.0038 \div 0.0055\ m^2 \times K/W$ for boilers with fined tube surfaces, while for plain tube surfaces it ε is slightly less on around $30 \div 40\%$. At the same time these dates are obtained for either main or auxiliary boilers, mainly operated by burning coal fuel, while exhaust boilers are subject of gas flow impact generated by internal combustion engines running on liquid fuel at several times higher air excess coefficient. Evidently, structure of soot deposits will differ from that mealy one originated from coal burning. Nevertheless, based on maintenance experience of gas tube type boiler for accommodation heating during winter time it was registered notable pollution, when running on coal fuel. Practically every 4÷6 days it was necessary to open it for internal cleaning, while by changing boiler performance on liquid fuel only after 60÷75 days soot removal was needed, at the same time ash deposit fracture is finer during visual inspection. Cleaning periodicity is increasing up to 12÷19 times; and despite that it is very approximate comparison still some ideas, conclusions might be brought out regarding pollution coefficient when different grades of fuels are consuming.

Finally by summing up of all considered factors during design stage of exhaust boilers following meanings of pollution coefficient are accepted [66, 100, 138]:

- For smooth tube Exhaust boiler - $\varepsilon \approx 0.0030\ m^2 \times K/W$;
- For fined tube Exhaust boiler - $\varepsilon \approx 0.0040\ m^2 \times K/W$.

Gas washing coefficient ω, being geometrical uniformity factor of boiler and tube bundle, is accepted equal to $\omega = 0.92$.

2.7. CONCLUSIONS.

1. The main constituent of WHRS is an exhaust boiler, the correct choice of which is extremely important to run power plant both efficient and safe at possibly low manufacturing, installation and maintenance costs.
2. Therefore the boiler is accepted rectangular type, water tube with forced circulation at tube chessboard-type disposal in the bundle, allowing us to obtain the highest output per one boiler volume unit.
3. In order to increase boiler surface steam capacity rate finned tube surfaces are proposed as possible and effective alternative against plain tubes. Geometrical characteristics of ribbed surface are chosen with thorough consideration of manufacturing availability, efficiency outcome and possible adverse post-effects.
4. Heat recovery circuit type is chosen single pressure stage boiler with thermostatic recirculation valve for feed water warm up at economizer inlet due to its simple and solid construction and high operational reliability (see Fig.2.6a).
5. Other thermo-dynamical characteristics of the WHRS, like as feed water temperature t_{fw} and the lowest possible gas temperature $t_{g_{exh}}$ at boiler outlet, are chosen with the consideration of mutual assessment of both efficiency gain and maintenance reliability loss.
6. In order to get truthful results during design stage pollution coefficient meaning is to be chosen as close as possible to actual one that in operation, being influenced by both geometrical characteristics of tube and bundle and gas flow nature.
7. Accepted final dates for chosen WHRS and EB is not something stiff, as by changing some inlet parameters the final characteristics of power plant could differ from already proved. Nevertheless the methodology of approving these dates is important, when system is being installed, to understand mutual interrelation between different indices.

CHAPTER 3. THERMODYNAMIC ANALYZE AND OPTIMIZATION METHOD FOR HEAT RECOVERY CIRCUIT AT FIXED EXHAUST BOILER DIMENSIONS (HEIGHT).

3.1. INTRODUCTION.

The object of the investigations is waste heat recovery system (WHRS) and its main constituent – an exhaust boiler (EB), where flue gas heat after main (base) engine is recovered by steam generating, which is directed for both turbine drive and different demands of low potential heat consumers (see Fig.1.1, 2.6).

The main idea and the novelty of this chapter is to come out with the analytic method for thermodynamically analyses of the WHRS, where all thermal and efficiency parameters of the power plant are evaluated based on initially accepted constant EB dimensions, particularly its height, at chosen tube bundle geometry and other thermodynamically constants. This approach is logical, so as available overall gas heat amount is already predetermined by main engine technical and performance characteristics [11, 67, 70, 74], while previously, on required and initially stated steam output and quality indices, boiler dimensions were those, which had been evaluated, similarly as for main steam cycle units [21, 26, 91, 100, 150]. At the same time compact and advanced power plants with high output are beneficial to make room for additional cargo. So by installing azimuth thrusters and high rated medium speed diesels instead of conventional power plant arrangement, consisting of main SSDE and propeller, it becomes possible to obtain additional cargo capacity up to 10÷12% in dependence on ship's size, what especially is important for high speed containerships providing delivery of expensive cargoes. For some type of ships like Ro-Ro, car ferries and similar, power plant design and its arrangement is especially to be well thought-out as cargo operations should be provided via aft ramp (see Fig.3.1a), as bow ramp arrangement is not deemed enough safe in operation, causing also a lot of additional installations and increased service during operations. Considering these aspects power plant is to be compact, especially

Fig.3.1a. Ro-Ro/Ro-Pax type ships.

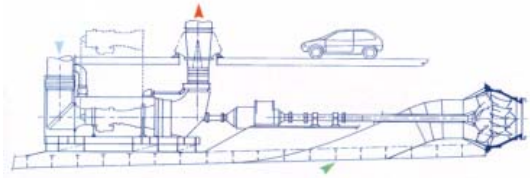
Fig.3.1b. New design concept for car-carriers, ferries, other ships.

in height to ensure free cargo passage. In new concepts for car carriers gas turbine driving water jet is find out as an effective and attractive alternative (see Fig.3.1b), subsequently any additionally installed equipment, including WHRS, should be with similar technical characteristics. Also medium speed diesel is considered as possible prime drive, being widely installed and effectively operated on similar ships till now. At the same time eventual exhaust boiler installation might occupy rather considerable space of engine room, coming even to its dimensional enlargement. For all that engine room spacing growth is not as important and critical as needed height rise due to required EB mounting (see Fig.3.2), what makes cargo (car) loading arrangements more difficult. Boiler installation in some confined corner places is not the best solution either as restricted access might result in lack of proper maintenance during ship's operation time; and in a result indirect cost for eventual repairs like access works, when needed and may be more frequent, might generate a considerable part of the whole repair lump-sum. For GT power plants boiler dimensions, particularly its height, are especially important to have them as low as possible, but high output rate is to be obtained either. Therefore it is very often for such type of ships, that within available and quite limited space, i.e. engine room height, exhaust boiler is to be placed; and in order to get the highest output within this space a comprehensive optimization of the WHRS in the whole is to be carried out with the consideration of various geometrical, thermal and other characteristics. If by force of circumstances for similar, but still another project the appropriate growth in the boiler height becomes possible additional highest output could be obtained by thoughtful investigations considering all aspects above (see Fig.3.2). In general the way how WHRS geometrical and thermal characteristics should be chosen was substantiated in previous second chapter, but at the same time the ideas were presented as general guidelines mainly. In following sub-chapters the choice of characteristics will be more specific related to our object of studies; and also main input dates will be grouped in dependence on either their purpose or origin so that any further and easy optimization by their altering could be carried out.

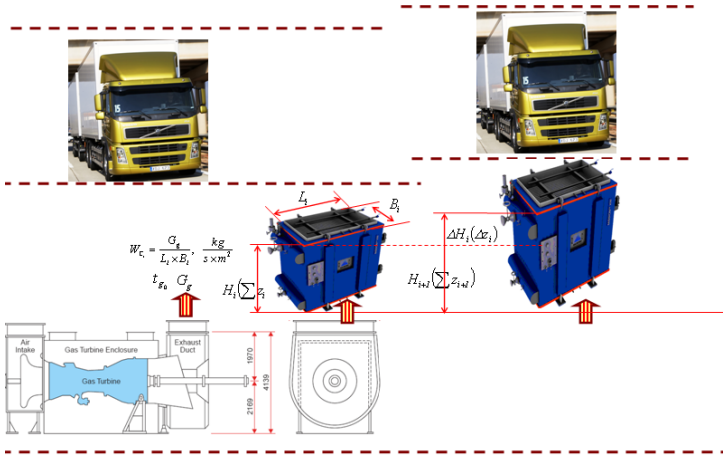

Fig.3.2. Ship's dimensional impact on EB choice.

3.2. SUBSTANTIATION AND MAIN DATA CHOICE.

As the base option in our studies thermodynamic circuit with re-circulated feed water preheat is found more preferable (see Fig.2.6a). Thermal power plant with intermediate steam extraction is proposed as possible choice either as effective alternative to minimize oxygen corrosion in boiler tail surfaces. At the same time, based on below proposed approach, analytic algorithm of thermodynamically analyses for other type of HRC and boilers are and could be elaborated. The boiler is chosen water tube type with rectangular construction as per conclusions previously (see Chapter II). Convective surfaces are considered either plain or finned due to the high efficiency of the last ones, but their amount distribution is to be arranged so, that the number of heating coils could be divisible on integer digit number, which is an advantage, when the real system is designed and manufactured, thus creating conditions for uniform gas stream distribution. For that reason the number of coils has to be divisible on either two or four for an evaporator, which ensures reliable and efficient performance of the boiler. As a considerable advantage of proposed method it should be pointed out that relative values of input, intermediate and final figures are used, what makes the results of explorations universal for different types of main (base) engines at various designed either nominal output or load and ambient conditions including.

When main conditions are finally accepted, the choice of other dates and subsequent evaluations could be carried out. Despite the fact that reasons for eventual choice of main boiler characteristics are well grounded in previous chapter, nevertheless to present the proposed method in the correct sequence of the algorithm some recurrence of already studied items will be presented. We will try to arrange interrelated matters and common substantiations in separate blocks, so that each of chosen characteristics might be varied in order to explore its particular influence on WHRS and the power plant in the whole.

3.3. THE CHOICE OF GENERAL CONSTANT INPUT VALUES.

As noticed above the boiler dimensions, actually the internal one required for allocation of tube bundles, $(L,\ B,\ H)$ are those, which are the main input values, but the choice of them should be somehow grounded. Cross section dimensions $L \times B$ are rather considered from the viewpoint of maintenance safety and efficiency, while the total boiler height is H determined by available installation conditions. When the main dimensions of

the boiler are stated, then the total height Hz_i of tube bundles, which is the characteristic of convection surface amount, is evaluated as a difference between total and summary heights ΔHx, which consist of tail clearances and those between heat exchange surfaces required for free hollow of tube bundles. Only then it is possible to determine the allowable amount of tube bundles in the direction of flue gas outlet as $\Sigma z_n = (H_i - \Delta Hx)/S_2$. This total amount of heating coils should be divided in-between each constituent (1- an evaporator, 2- a super-heater, 3- an economizer) with the aim to ensure the highest output, which finally will be represented as following inequality: $z_1 + z_2 + z_3 \le \Sigma z_n$.

In dependence on technical parameters or heat balance evaluations of ME (diesel, gas turbine) input data for boiler calculations are determined:

- G_g - gas flue amount per second, kg/s;
- t_{g_o} - gas temperature at main engine outlet and EB inlet, °C;
- α - air excess coefficient.

Then for corresponding gas temperature in each section the enthalpy is evaluated as follows - $h_g = f(t_{g_O}, \alpha), \ kJ/kg$, which is dependent on the burnt fuel oil grade [127, 128, 138] either. In our case for used type marine fuels following dependence of flue gas enthalpy in respective boiler cross section h_{g_i} is brought out –

$$h_{g_i} = 0.9879 + 100.7304 \times (t_{g_i}/100) + 0.9059 \times (t_{g_i}/100)^2 + 0.0335 \times (t_{g_i}/100)^3 + c_\alpha \times \left(0.4211 \times (t_{g_i}/100)^2 + 5.7376 \times (t_{g_i}/100) - 1.1998\right), \ kJ/kg \quad (3.1)$$

where $c_\alpha = 1.0704/(0.704 + \alpha) - 0.2$, but temperature t_{g_i} corresponds to that one measured in relevant EB cross section, e.g. either before boiler t_{g_o}, evaporator $t_{g_{sp}}$ and economizer t_{g_s} or after super-heater $t_{g_{sp}}$, evaporator t_{g_s} and at boiler outlet $t_{g_{exh}}$.

The usage of gas mass velocity $W_{C_i} = G_g/(L_i \times B_i), \ kg/(s \times m^2)$ in steam boiler internal cross section instead of linear one is a novelty, which simplifies below acquired equations; and at $W_{C_i} = const.$ via G_g *and* $(L_i \times B_i) = \text{var}$. achieved final results are universal for the wide range of ME types/outputs at various load levels.

3.4. THE CHOICE OF THERMODYNAMICALLY CONSTANT INPUT VALUES.

Prior evaluations of heat transfer efficiency it is important to determine some thermodynamic characteristics of flue gas current, which depend on burnt fuel type, as

coefficients of thermal conductivity λ_0, specific weight γ_0 and kinematics viscosity ν_0 at the temperature of **0°C**. The derivative characteristic of flue gases is equal to $k_{T\Phi} = \lambda_0 \times \gamma_0^{-0.65} \times \nu_0^{-0.05}$, and for our considered case it is - $k_{T\Phi} \approx 26.34$

Another important characteristic in the determination of heat transfer efficiency is pollution coefficient ε of an EB from gas side. Its influence is under way of the aggravation of heat transfer coefficient expressed as below [24, 42, 52, 73]:

$$k = \left(1/\omega \times \alpha_1 + \varepsilon + d/d_i \times 1/\alpha_2 \right)^{-1}, \; W/m^2 \times K \tag{3.2}$$

The level of pollution for each surface is already chosen; however for each project it will vary in dependence on both burnt fuel grade and type of heat exchange surface, i.e. its geometrical parameters, other environmental and service factors. So, at higher meanings of flue gas velocity there is a tendency in the reduction of the average maintenance value of the pollution coefficient due to the effect of self cleaning. Meantime, unreasonable high value of gas velocity leads to excessive growth in EB aerodynamically resistance and in a result to respective power losses in a main engine. In a consequence, the possible lowest meaning of gas linear velocity is recommended as high as $w_c^{\min} > 6 m/s$ (see Chapter 2), affecting boiler internal cross section $(L \times B)$ choice. By observing appropriate chemical treatment routines for boiler water, the adverse influence of scale is reduced till the negligible level so that there is no need of it to be considered in.

Based on different norms for boiler manufacturing the washing coefficient ω is found equal to **0.92,** being dependent on flue gas current distribution, which in its turn is determined by geometrical irregularity of tube bundles. The heat dissipation coefficient η_{al}, that encounters heat losses of EB via insulation, is chosen equal to **0.99** [43, 97, 114].

3.5. THE CHOICE OF CONSTANT GEOMETRICAL PARAMETERS OF TUBE BUNDLE FOR HEAT EXCHANGE AND AERO RESISTANCE CALCULATIONS.

When the general constant values are fixed, then geometrical parameters of tubes and the bundle could be chosen or later varied when the first option is found. In dependence on results of scientific explorations, manufacturing possibilities, and maintenance experience (see chapter 2) following characteristics are accepted for both types of surfaces, smooth and finned ones, as below (see Fig.2.10, 2.11 in Ch.2):

- S_1 - cross head step in tube nest to be sufficient to provide free hollow off, m;

- S_2 - longitudinal step, m;
- d - tube outside diameter, m;
- d_{in} - tube inner diameter, m ;
- δ_{tw} - tube wall thickness, which depends on tube sizes, steam pressure, m.

For finned surface following additional characteristics are necessary to be stated, as below:

- S_r - fining step on boiler tube, m;
- h_r - the height of ribs, m;
- δ_r - the thickness of ribs, m;
- D - finned tube outer diameter, m;

Based on production features, material grade and other ribbing characteristics are to be considered [62, 91, 100, 109, 135, 136], being presented by pre-determined indices as follows:

- thermal conductivity λ_M for steel (metal) ribs, $W/(m \times K)$;
- the coefficient of rib widening in way of base tube surface $\mu_r = f\left(\beta \times h_r; \sqrt{(\delta_{r_2}/\delta_{r_1})}\right)$, where δ_{r_2}, δ_{r_1} thicknesses of ribs on top and in way of base; and the coefficient is equal to $\mu_r = 1$, when thickness of ribs is invariable on the whole its height;
- the coefficient that encounters uneven heat transfer ψ_r in way of connection with the base tube; and it is equal to $\psi_r = 0.9$ for ribs with straight foot, while for cylindrical type one the coefficient is less, i.e. $\psi_r = 0.85$

Finally, the geometrical parameters could be evaluated in advance for thermodynamically analyze of the system, as below:

- $S_2^{|} = \sqrt{\left((S_1/2)^2 + S_2^2\right)}$ - a diagonal step of tubes in the bundle, m;
- $k_w = 0.98 \times S_1/(S_1 - d_{ekv})$ - the relation of steam boiler cross section areas of total and that one available for gas passage;
- d_{ekv} - equivalent tube diameter, determining free space for gas passage. For smooth surfaces it is to $d_{ekv} = d$, while for ribbed surface it is - $d_{ekv} = [2 \times (S_r \times (S_1 - d) - 2 \times \delta_r \times h_r)]/(2 \times h_r + S_r)$;

- D_{ekv} - tube equivalent diameter, determining summary surface from gas side. For smooth surface it is equal to outside one $D_{ekv} = d$, while for finned surface it will be found as - $D_{ekv} = d \times \left(H_{sm} / H_g^{\Sigma}\right)^{-1}$, then
- Surface coefficient for tube bundle is found as - $k_F = 36 \times S_1 / \left(\pi \times D_{ekv}\right)$.

Following coefficients, derivatives are constant at accepted geometrical and surface dimensional characteristics; therefore they are found in advance to evaluate heat conductivity from gases to steel tube wall α_{1_i} as further -

- Derivative, which considers coil amount of respective surface z_1; z_2; z_3 and it is equal to - $c_{z_i} = 1.03 \times \left(1 - 0.5573 / z_i\right), \ i = 1, \ 2, \ 3$;
- Smooth tube disposal coefficient in the bundle - $c_s = 1.0926 \times \left(\dfrac{S_1 - d}{S_2^{|} - d}\right)^{0.25}$;
- Flue gas density impact value at both zero temperature $0^o C$ and atmospheric pressure - $c_\gamma = \left(1.285 / \gamma_0\right)^{0.6}$;
- Tube diameter factor - $c_d = \left(0.022 / d\right)^{0.4}$, which at already accepted diameter is equal to $c_d = 1$;
- Relation of boiler cross sections of that free for gas passage and the dimensional one $\left(L_i \times B_i\right)$ - $k_w = 0.98 \times S_1 / \left(S_1 - d_{ekv}\right)$; and for plain tube surface equivalent diameter is the same outside one $d_{ekv} = d$;
- Summary geometric complex - $A_{1_i} = \left(1.03 \times 17.85 \times \omega \times c_s \times c_d \times c_\gamma \times k_w^{0.6}\right)^{-1} \times k_F \times 100$.

Similar constant geometric complex A_{ε_i} at accepted design characteristics is found to consider gas pollution impact ε on thermal conductivity - $A_{\varepsilon_i} = 0.859968 \times \varepsilon \times k_F \times 100$. There are also some dedicated geometrical constant complexes used for heat conductivity evaluations from steel tube wall to warming-up media α_{2_i}, i.e. either steam or boiler water. In order to simplify our evaluations following constants are to be found in advance –

- Coefficient of tube internal diameter impact - $c_{d_{in}} = \left(0.017 / d_{in}\right)^{0.27}$;
- Relation k_{S_i} of tube internal cross section against boiler the dimensional one $\left(L_i \times B_i\right)$, which is found equal for relevant surface as follows -

- Super-heater - $k_{S_2} = 0.99 \times \pi \times (d_i)^2 / (L_2 \times S_1)$;
- Economizer - $k_{S_3} = 0.99 \times \pi \times (d_i)^2 / (L_3 \times S_1 \times n_g)$, where n_g is coefficient reflecting economizer design peculiarities as in order to achieve high enough boiler water speed by combining horizontal and vertical bundles (see Chapter 1) and in our case it is equal to $n_g = 7$.

- In a result summary geometric complex at accepted boiler design for α_{2_i} evaluation is brought out - $A_{2_i} = 4.1862 \times (d/d_i) \times \left((k_{S_i})^{0.8} / c_{d_{in}} \right) \times k_F \times 100$, which for evaporator surface is equal to - $A_{2_1} = 0$.

Separate derivative values could be evaluated for **finned** surfaces, which are as follows:

- Relation of surfaces of ribs against summary one from gas side $H_{fin} / H_g^{\Sigma} = \left((D/d)^2 - 1 \right) \times \left((D/d)^2 - 1 + 2 \times (S_r - \delta_r)/d \right)^{-1}$; and
- Relation of surfaces of carrier tubes against summary one from gas side - $H_{sm} / H_g^{\Sigma} = 1 - H_{fin} / H_g^{\Sigma}$;
- Relation of surfaces geometrical summary one from gas side against internal one - $H_g^{\Sigma} / H_{in} = \left(H_{sm} / H_g^{\Sigma} \right)^{-1} \times d / d_{in}$
- Relative diagonal and crosshead steps are found as follows - $\sigma_2^{|} = S_2^{|} / d$; $\sigma_1 = S_1 / d$;
- and subsequently characteristics encountering tube disposal is equal to - $\varphi_\sigma = (\sigma_1 - 1) / (\sigma_2^{|} - 1)$;
- geometrical disposition of finned tube in the bundle is found dependable on following - $k_f = 0.23 \times \varphi_\sigma^2 \times (d/S_r)^{-0.54} \times (h_r/S_r)^{-0.14} \times S_r^{-0.35}$;
- coefficient encountering coil amount for particular surface and is found accordingly - $c_{z_i} = 1.01 - e^{-n_i}$, where $n_i = 1.61643 + (z_i/100) \times (1.47244 + (z_i/100) \times 1.48179)$.

When ribbed surface derivative indices, that characterize whether specific surface sizes, tube disposal or some present diameters, are evaluated, it becomes possible to gather all geometrical and flue gas physical influence under some constant complexes as follows:

- complex that considers ribbed tube geometry and flue gas physical condition in narrow section for determination of the coefficient of convective thermal conductivity - $A_{gk_i} = k_f \times k_w^{0.65} \times c_{z_i} \times c_{\text{ТФ}}$;
- due to boiler surface pollution from gas side with the rib diminution factor consideration another complex is brought out - $A_{\varepsilon_i} = 0.86 \times \varepsilon \times \psi_r \times A_{gk_i}$;

Separate geometrical complexes being characteristic of gas flow via narrow section could be found in advance, being required for boiler aero-resistance determination as below [86, 117] –

- for **smooth** tube boiler - $k_h = 0.00277 \times \left(\frac{S_1 - d}{S_2^{|} - d} + 1 \right)^2 \times \left(\frac{0.022}{d} \right)^{0.27} \times k_w^{1.73}$;
- while for **finned** surfaces several additional both geometrical and gas condition complexes shall be evaluated –
  - the factor of narrow free space geometry - $F = 5.4 \times l^{0.05} \times d_{ekv}^{\ -0.3} \times k_w^{1.75}$;
  - and relevant ribbed tube present dimension is equal to –

$$l = \frac{1}{\beta_{Hr} \times S_r} \times \left((S_r - \delta_r) \times d + \frac{0.5 \times (D^2 - d^2) + D \times \delta_r}{d} \times \sqrt{0.785 \times (D^2 - d^2)} \right),$$

  - but characteristic β_{Hr} is measure value of tube ribbing density, expressed as surface relation between total summary against plain tube one - $\beta_{Hr} = H_g^{\Sigma} / H_{sm} = \left(1 - H_{fin} / H_g^{\Sigma}\right)^{-1}$;
  - flue gas physical effluence property complex - $\Gamma = \gamma_0^{0.75} \times \nu_0^{0.25}$;
  - then concluding constant complex of bundle geometrical characteristics and gas physical properties will be equal to - $k_{\text{ТГ}} = 0.6 \times F \times \Gamma / g$.

3.6. THE DETERMINATION OF GEOMETRICAL CONSTANT PARAMETERS OF TUBE BUNDLE FOR THE HYDRAULIC RESISTANCE EVALUATION.

The steam pressure level before turbine nozzles is an important efficiency characteristic of the cycle being greatly dependent on pressure losses on the way of the steam path, which in its turn are possible to be grouped in several constituents. Firstly, hydraulic losses appear in a down tube, which consists of one, installed shut-off valve and one U-turn, from separator until inlet collector of a super-heater, being characterized by resistance coefficient $\varsigma_c (= 7.5)$. The inner diameter of down tube d_{dt} is chosen with respect of

ultimate feasible constraint in steam velocity w_{st}, in order to minimize both hydraulic losses and possible significant tube wear and tear internally. It is recommended to keep not higher than $w_{st} \le 35\, m/s$ [62, 96, 144], however the speed could be also evaluated at initially accepted down tube diameter d_{dt} as per equation - $w_{st} = \xi_{st} \times G_g \times v_s / F_{dt}$ and $F_{dt} = \pi \times (d_{dt}/2)^2$, where values ξ_{st} ; v_s are relative amount of superheated steam and specific volume of saturated steam respectively. Further, hydraulic losses in respective heating coils are to be evaluated, being built up by friction λ and U-turn ζ_{surf} resistance; and in a result their relative values are estimated as: $\lambda = \left(3.33 + 0.87 \times \ln\left(d_i \times 10^3\right)\right)^{-2}$ and $\zeta_{surf} = 0.186 + 0.463/(S_2/d + 0.12)$ [27, 51, 114].

Afterwards summary hydraulic resistance coefficients found equal to:

- $\zeta_2^{\Sigma} = \lambda \times z_2 \times L/(4 \times d_i) + \zeta_{surf} \times (z_2/2+1) + 1$ - for a super-heater;
- $\zeta_1^{\Sigma} = \lambda \times z_1 \times L \times \psi/(4 \times d_i) + \zeta_{surf} \times (z_1/2+1)$ - for an evaporator, where

$\psi = 1.5$ (for EB) is the coefficient of structural features of heating-up media (water/steam), which in its turn depends on evaporation rate, steam pressure and other [42, 120] parameters.

3.7. THE CHOICE OF SOME CONSTANT THERMIC PARAMETERS OF THE CYCLE.

The well-grounded choice of some constant values of thermodynamically cycle is important in order to ensure both the efficiency and the safety of the system. Based on the maintenance experience feed water temperature in hot well t_{fwp} is either accepted equally to 40÷50°C or evaluated in dependence on service conditions [30, 70, 74, 95, 97, 147]. Feed water temperature at economizer inlet t_{fw} is chosen as high as the adverse effect of sulfuric acid corrosion in tail surfaces from gas side is reduced to acceptable minimum (see Chapter 2). However, at the same time it should be as low as possible to ensure the most effective gas cooling at definite boiler (economizer) sizes.

The right choice of steam pressure p_s is important so, that the highest output of the system is ensured. However, its numerical value depends on both inlet and outlet gas temperature level t_{g_0}, on the type of heat recovery circuit and other factors, being more thoroughly investigated in next coming chapters. In fact, during repeated evaluations it is possible to vary the value p_s with the aim to optimize cycle efficiency parameters. When the

pressure level is stated other saturation characteristics could be found according water/steam thermodynamically tables [16] or analytic formulae [5, 28, 126, 132] as below:

- t_s - saturation temperature, °C or $t_s = f_1(p_s)$;
- h_s - enthalpy of saturated steam, kJ/kg or $h_s = f_2(p_s)$;
- $h_s^{'}$ - enthalpy of boiling water, kJ/kg or $h_s^{'} = f_3(p_s)$;
- r_s - specific heat of evaporation, kJ/kg or $r_s = h_s - h_s^{'}$;
- v_s - specific volume of saturated steam, m^3/kg or $v_s = f_4(p_s)$;

Then respective enthalpies of feed water at the economizer inlet $h_{fw}^{'}$ and in a hot well $h_{fwp}^{'}$ are estimated for corresponding accepted temperatures –

$$h_i^{|} = 421.88 \times (t_i/100) - 5.23 \times (t_i/100)^2 + 1.67 \times y - 0.54 \quad ; \quad y = t_s/100 \tag{3.3}$$

Afterwards, the relative necessary amount of boiling water, which is directed from steam drum to heat up feed water from temperature t_{fwp} until t_{fw} by mixing via thermostatic valve, (Fig.2.1) could be evaluated as follows - $k_{rec} = (h_{fw}^{|} - h_{fwp}^{|})/(h_s^{|} - h_{fw}^{|})$. For the system with intermediate steam extraction this amount is equal to $k_{rec} = 0$.

The correct estimation of saturated steam consumption G_{sat}, kg/s, is important because of its direct diminution impact on the net output of a steam turbine, and the consumption of which depends on both ME and ship's type, boiler steam capacity, ambient and other conditions [14, 30, 97, 118, 148, 149]. In our analyses the relative amount of it $\xi_{sat} = G_{sat}/G_g$ (kg saturated steam/ kg flue gases) is introduced, which is found either by means of analytic curves or empirical formulae obtained on results of durable observations and explorations. However pressure losses Δp_{st} in super-heater, being preliminary chosen for later update, have some influence on the total boiler output and saturated either.

To ensure safe maintenance of an evaporator, it is important to choose the correct value of forced circulation coefficient k_{circ} of evaporated media (steam-water), being accepted equal to 2.5÷3.0 [10, 96, 102, 134, 138, 147].

To evaluate steam pressure before turbine nozzles p_{0_T}, hydraulic losses on the way of the steam path from the super-heater outlet collector till the turbine inlet are to be considered, being dependant on installed fixtures as follows - 1) one shut off valve after super-heater, 2) collector with angle output from one side, 3) one collecting triple and 4) one

stop valves [19, 96]. The condenser choice is important as deep vacuum in it will ensure high thermal efficiency of Clausius-Rankin cycle efficiency, i.e. high value of iso-entropic enthalpy difference Ha that usefully works out in steam turbine. Therefore vacuum level in main steam condenser p_x [12, 106], to which relevant saturation temperature T_x, K corresponds, is chosen with the consideration of sea water temperature. Afterwards other relevant thermo-physical characteristics, as enthalpy $h_x^{||}$ and entropy $S_x^{||}$ of dry saturated steam at condenser inlet, could be determined, to calculate adiabatic enthalpy drop Ha.

For the combined gas-steam turbine cycle it is also necessary to consider the coefficients of mechanical efficiency of steam turbine reduction gear η_{m_T}, the indicator efficiency of gas turbine η_{i_g} and its reduction gear η_{m_g}, which are found based on either technical dates or calculations. For the circuit with intermediate steam extraction the value of the approach point is to be stated in the heating stage, being equal to - $\delta h_x^{|} \cong 37\, kJ/kg$ [131].

3.8. THE PRELIMINARY CHOICE OF MAIN INPUT VALUES.

According the technical task sizes of respective heating surfaces (number of heating coils) are determined as follows - $z_1 + z_2 + z_3 \le \Sigma z_n^{\max}$ in dependence on available height for boiler installation; and they are constant values during the calculations. At the same time, the system (mathematical analytic method) is built up so, that the number of heating coils is that value, which is finally evaluated in dependence on accepted above geometrical and thermodynamically parameters. Accordingly, this surface amount is characterized by respective temperature differences preliminary chosen as below:

- $x_1 = t_{gs} - t_S$ - so called *pinch-poin*t or temperature difference between flue gases at an evaporator outlet t_{g_s} and the saturation one t_s;
- $x_2 = t_{g_0} - t_{st}$ - temperature difference between flue gases at a boiler inlet t_{g_0} and superheated steam one t_{st};
- $x_3 = t_s - t_e$ - feed water “non heating“ in an economizer or so called the *approach temperature*, which is the difference between the saturation and water outlet from an economizer; and in order to prevent water boiling in an economizer it must be positive within all operating range.

In reality, to these preliminary accepted temperature differences it will correspond different final evaluated numbers of heating coils $\left(z_i^{calc}\right)$ from initially stated, so that following inequality is valid: $\left|\Delta z_i\right| = \left|z_i^{calc} - z_i\right| > 0$. Subsequently, further adjustment extent to be made in respective temperature differences x_1, x_2, x_3 will depend on this inaccuracy rate of all boiler constituents. As soon as required exact accuracy of respective heating surfaces will be obtained by means of different methods of non-linear equation solution [83, 141] as follows $\left|\Delta z_i\right| = \left|z_i^{calc} - z_i\right| < accuracy\left(10^{-4}\right)$, then the evaluation task could be considered as accomplished one, but already at different from preliminary accepted above temperature differences, which should correspond to initially chosen heating coil amount.

3.9. THERMODYNAMIC EFFICIENCY ANALYSES OF EXHAUST BOILER.

As soon as geometrical and thermodynamically constants of EB and HRC are chosen, the analyses could be performed until the final results will be obtained. Thereupon, by varying either geometrical characteristics of the boiler tube bundle or thermodynamically parameters it becomes possible to compare different options with the aim to obtain the best one.

3.9.1. DETERMINATION OF BOILER STEAM CAPACITY.

Boiler steam capacity is quantity characteristic of the steam cycle, which is determined for specific power unit with concrete main engine type at a specified load level. To make final results more universal irrespective of above mentioned conditions the relative EB steam capacity $\xi = G_{st}/G_g$, $kg\ steam/1kg\ \ flue\ gasses$ is being introduced; and based on heat balance equation it is found as per equation:

$$\xi = \left(\eta_{al} \times \Delta h_{g_{sp}} + \xi_{sat} \times \Delta h_{st}\right) / \left(\Delta h_{st} + \Delta h_s\right), \tag{3.4}$$

where value $\Delta h_{g_{sp}}$ is recovered heat from flue gasses in both super-heater Δh_{g_2} and evaporator Δh_{g_1}, i.e. $\Delta h_{g_{sp}} = \Delta h_{g_1} + \Delta h_{g_2}$. This heat amount $\Delta h_{g_{sp}}$ is also found as a enthalpy difference of following - $\Delta h_{g_{sp}} = h_{g_0} - h_{g_s}$, where enthalpy $h_{g_{sp}}$ after evaporator is the main constituent, that determines boiler output and is dependant on respective temperatures, i.e. surface sizes, as follows: $h_{g_s} = f\left(t_{g_s},\ \alpha\right)$ (see formula #3.1) and $t_{g_s} = f\left(z_1, z_2, z_3, p_s, ...\right) = t_s + x_1$. For generating one kg saturated steam in an

evaporator required heat amount is found as $\Delta h_s = h_s - h_e^{|} + k_{rec} \times \left(h_s^{|} - h_e^{|}\right)$, but to overheat one kg saturated steam up to temperature $t_{st} = t_{g_0} - x_2$ it is equal to the value $\Delta h_{st} = h_{st} - h_s$, kJ/kg. Feed water enthalpy $h_e^{|}$ at the economizer outlet is dependant on both its temperature $t_e = t_s - x_3$ and steam pressure; however within temperature range of $t_e = 130 \div 230^o C$, what is practically acceptable and applicable for existing and eventual ship WHRS, simplified equation is brought out - $h_e^{|} = 25.28 + 378.01 \times \left(t_e/100\right) + 17.75 \times \left(t_e/100\right)^2$. For superheated steam pressure losses in both down tube Δp_c and heating coils Δp_{st} have some certain additional diminishing impact on its enthalpy value $h_{st} = f\left(t_{st}, p_s, \Delta p_{st}, \Delta p_c\right)$ [63]. When both steam temperature $t_{st} = t_s - x_2$ and pressure $p_{st} = p_s - \Delta p_{st} - \Delta p_c$ at super-heater outlet are determined, then its enthalpy is evaluated accordingly –

$$h_{st} = 2143.92 + 301.66 \times \left(t_{st}/100\right) - 8.37 \times \left(t_{st}/100\right)^2 + a_1 \times y_{st} - a_2 \times y_{st}^2, \quad kJ/kg \qquad (3.5),$$

where

$$a_1 = 518.59 - 172.3 \times \left(t_{st}/100\right) + 16.41 \times \left(t_{st}/100\right)^2, a_2 = 210.98 - 70.33 \times \left(t_{st}/100\right) + 6.7 \times \left(t_{st}/100\right)^2$$

but value $y_{st} = t_{s_{ST}}/100$ is saturation temperature factor, which corresponds to pressure p_{st}.

As mentioned before saturated steam consumption ξ_{sat} could be either determined as per different norms and technical standards or evaluated via empirical formula in dependence on various factors, which encounter saturated steam consumption on 1) ejectors of a main condenser and a fresh water evaporator, 2) an evaporator of dirty condensate for bunker, oil heating, 3) steam leakage; then the following equation is obtained:

$$\left(\xi_{sat_{i+1}}\right) \quad \xi_{sat} = 0.00141 + \frac{\left(0.072 + 0.056/n_{shaft}\right)}{G_g} + 0.007 \times \xi, \quad \frac{kg \quad steam}{1 \quad kg \quad gases}, \qquad (3.6)$$

where n_{shaft} is a number of propeller shafts. Since both steam capacities are interdependent, then, by substituting and after repeated evaluations exact values of ξ, ξ_{sat} are found.

3.9.2. BOILER STEAM PRESSURE LOSSES.

As noticed earlier, boiler steam capacity, as well as overheated steam enthalpy is affected by steam pressure drop Δp_c in a down tube between a drum and a super-heater inlet collector, and relevant hydraulic losses in a superheater Δp_{st} (see Fig.3.3). Steam pressure

drop in a down tube is evaluated as follows - $\Delta p_c = \zeta_{st} \times w_c^2 \times 10^{-4} / [v_s \times (2 \times g)]$; and if the diameter of the down tube is fixed according the project, then the steam velocity is found accordingly - $w_c = \xi_{st} \times G_g \times v_s / F_{dt}$. Hence the respective steam pressure at the super-heater inlet is found as the difference of steam pressure in boiler drum and hydraulic losses in down tube - $p_c = p_s - \Delta p_c$; and saturation temperature t_{s_c} that corresponds to this pressure p_c, including for other pressure levels, could be found either based on data table of thermodynamically properties for water/steam or according brought out equation #3.7 [132] –

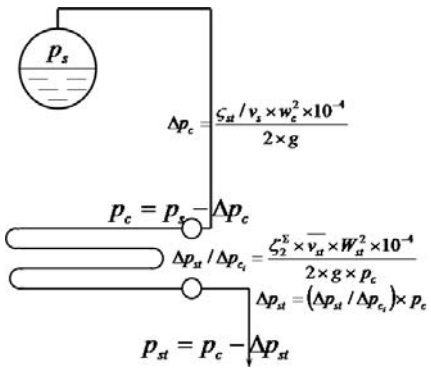

Fig.3.3. Hydraulic losses in way of superheated steam formation.

$$t_{s_c}(t_{s_i}) = \sum a_n \times \left(10^{-1} \times \ln(0.980665 \times p_c)\right)^n, {}^o C \quad (3.7)$$

where

n	0	1	2	3	
a_n	99.632	279.467	240.299	212.98	
n	4	5	6	7	8
a_n	160.22	110.97	278.81	94.6	– 849.1

.

Pressure drop in a super-heater Δp_{st} depends not only on the total steam capacity, but also on geometric parameters of the bundle and steam quality indices -

$$\Delta p_{st} / \Delta p_{c_i} = \zeta_2^{\Sigma} \times \overline{v_{st}} \times W_{st}^2 \times 10^{-4} / 2 \times g \times p_c, \quad \Delta p_{st} = \left(\Delta p_{st} / \Delta p_{c_i}\right) \times p_c, \ bar, \quad (3.8)$$

where steam velocity W_{st} in super-heater is equal to - $W_{st} = \frac{\xi_{st} \times W_g \times L}{\pi \times (d_{in}^2 / S_1)}$. Then the mean value of specific steam volume during over-heating is found according Norms or as below –

$$\overline{v_{st}} = \left(1{,}0675 + 0{,}8108 \times \left(t_{s_C} / 100\right) - 0{,}168 \times \frac{(t_{s_C} / 100)}{2 \times (p_s - \Delta p_c - \Delta p_{st}/2)}\right) \times \left(1 + \frac{0{,}961 + 0{,}25 \times (t_{s_C} / 100) - 0{,}216 \times (t_{s_C} / 100)}{1 - \Delta p_{st} / \Delta p_{c_i}}\right), \ \frac{m^3}{kg} \quad (3.9)$$

When both pressure drops Δp_c, Δp_{st} are estimated, then corresponding saturation temperature $t_{s_{ST}}$ could be made more accurate from preliminary accepted $t_{s_{ST}} = t_s$ either based on formula #3.7 or saturation temperature diminution, being evaluated as per equation #3.10, due to pressure drop in super-heater Δp_{st} –

$$\Delta t_{s_{ST}} = \left(0.0493 + 0.214 \times y_c + (0.046 + 0.08 \times y_c) \times (\Delta p_{st} / \Delta p_{c_i})\right) \times (\Delta p_{st} / \Delta p_{c_i}) \times 10^2, {}^o C, \quad (3.10)$$

where $y_c = t_{s_c} / 100$ and $t_{s_{ST}} = t_{s_c} - \Delta t_{s_{ST}}$, ${}^o C$.

Finally, overheated steam enthalpy could be made more exact according equation #3.5.

3.9.3. USEFULLY RECOVERED FLUE GAS HEAT AMOUNTS.

The useful recovered flue gas heat amount in each section is found as follows:

- in an evaporator - $\Delta h_{g_1} = \xi \times \Delta h_s / \eta_{al}$, $kJ/kg\ flue\,gases$;
- in an super heater - $\Delta h_{g_2} = \xi_{st} \times \Delta h_{st} / \eta_{al}$, $kJ/kg\ flue\,gases$;
- in an economizer - $\Delta h_{g_3} = \xi \times \Delta h_e / \eta_{al}$, $kJ/kg\ flue\,gases$.

Thereafter, in order to evaluate both flue gas temperatures at super-heater $t_{g_{sp}}$ and boiler outlet $t_{g_{exh}}$, their respective enthalpies are to be found, being equal to expressions $h_{g_{sp}} = h_{g_0} - \Delta h_{g_1}$ and $h_{g_{exh}} = h_{g_S} - \Delta h_{g_3}$. Then relevant temperatures could be determined either based on data table of thermodynamically properties for flue gases or according brought out equation #3.11 –

$$t_{g_i} = 99.52 \times \left(h_{g_i}/100\right) - 4.11 \times \left(h_{g_i}/100\right)^2 - 0.28 - a_t \times c_\alpha + b_t \times c_\alpha^2, \qquad (3.11)$$

where derivative values a_t, b_t are being expressed by formulae below -

$$a_t = 0.448 \times \left(h_{g_i}/100\right) + 6.118 \times \left(h_{g_i}/100\right)^2 - 0.393 \ ; \ b_t = 0.657 \times \left(h_{g_i}/100\right) - 0.143 .$$

Only then mean log temperature differences could be evaluated as follows:

$\Delta t_{LOG} = \left(\Delta t_{max} - \Delta t_{min}\right) / ln\left(\Delta t_{max} / \Delta t_{min}\right)$, where $\Delta t_{\max}, \Delta t_{\min}$ are respective the highest and the lowest temperature differences between heating (flue gas) and heating-up (water, steam) media. Also average gas temperature within respective surface could be found either, being used in thermal conductivity efficiency evaluations as follows –

- within evaporator - $\overline{t_{g_1}} = \left(t_{g_{sp}} - t_{g_s}\right) \times 0.5$;
- super-heater - $\overline{t_{g_2}} = \left(t_{g_0} - t_{g_{sp}}\right) \times 0.5$;
- economizer - $\overline{t_{g_3}} = \left(t_{g_s} - t_{g_{exh}}\right) \times 0.5$; and

relevant gas temperature coefficients are found accordingly $k_{t_i} = \overline{t_{g_i}} / 273.15 + 1, \ i = 1, \ 2, \ 3$.

3.9.4. THE INFLUENCE OF HYDRAULIC LOSSES IN BOILER STEAM EVAPORATOR.

The evaluation of hydraulic resistance of an evaporator is important not only from the viewpoint of the determination of circulating pump characteristics, but also because of its adverse and rather explicit influence on the heat exchange efficiency via mean-log temperature.

In the beginning part of the evaporator a considerable growth of the pressure drop Δp_1 is expected in the region of intensive steam evaporating due to the presence of the economizer section characterized by the *approach-temperature* x_3. The mode of two phase flow (steam-water) is very much dependent on its calorific properties, quantity relation of each flow constituent and tube both dimensions and disposal in tube bundle. Based on visual observations the process of boiler water evaporation could be divided in four phases followed one after another, i.e. 1) bubble, 2) when bubbles join together forming big ones - shell type, 3) circular or disperse-annular and 4) emulsive type – the end phase. In the very first boiler water is being warmed up till saturation temperature as at economizer outlet is slightly less on accepted safety factor x_3. Then bubble, size of which is around 1÷3mm with the tendency to grow in both size and concentration towards to the centre of the flow, evaporating regime occurs at high steam wetness rate. By increasing steam dryness factor x bubbles start merge into big formations, called also as shell type bubbles. During their pass through tube there is intermediate layer between moving shells; and by further heating up, when steam dryness factor is growing up considerably, these bigger formations start flow together transforming into circular or disperse-annular flow. Still until this third phase of steam evaporation some water layer is in between bubbles and tube wall inner side during the mixture pass, thus performing as some kind of lubricant. Actually, just steam bubbles, shells and other formations are those which are moving in some kind multi layer tube, consisting of base steel tube and internally covered with thin water layer at it considerably reduced speed against steam formations. By further heat adding and respective dryness factor grow up steam evaporation comes to its end phase, i.e. emulsive type one, when practically all flow is homogeneous and both steam bubbles and remaining water is evenly distributed within tube internal cross section. Despite the fact that described evaporation mechanism is more inherent to vertical tubes with natural circulation; still to some extent it could be attributed to exhaust boilers with forced circulation as well, what allows us to understand the nature of hydraulic losses in evaporator and their influence on the efficiency of surface thermal conductivity.

Although the pressure changes occur in the whole length of the evaporator, but still these hydraulic losses are so considerable in the beginning part due to the start of intensive evaporation, when dramatic changes in specific volume of media from water to steam appear (see Fig.3.4). This pressure reduction is estimated; and obtained formulae are presented based on exploration dates [27, 52, 79, 84, 96, 115, 138, 139, 144], which depend on relative steam

and water relation exchanges, pressure, media velocity, the number of heating coils. Albeit, the choice of the forced circulation coefficient k_{circ} is prescribed to observe boiler safe operation, but, if unsubstantiated high value is accepted, then it would come to both the increased circulating pump capacity and decreased efficiency of evaporator thermal conductivity. Pressure drop in evaporator coils is found in accordance equation #3.12 –

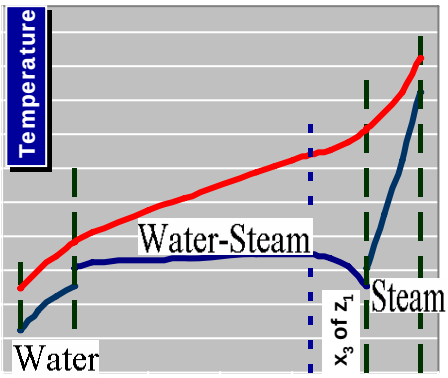

Fig.3.4. Steam-water generation temperature diagram for EB.

$$\Delta p_1 = \zeta_1^{\Sigma} \times \frac{(w \times \gamma)^2}{2 \times g \times \gamma^{|}} \times \left(1 + x \times \left(\gamma^{|} / \gamma^{||} - 1\right)\right), \quad (3.12)$$

where

- $(w \times \gamma)$ - weight speed of steam/water fluid, $kg/(s \times m^2)$;
- γ - specific weight of steam/water fluid, kg/m^3;
- $\gamma^{|}$ - specific weight of boiler water on saturation line, kg/m^3;
- $\gamma^{||}$ - specific weight of dry steam on saturation line, kg/m^3.

By solution of integral equations of functional dependence of steam dryness factor on the whole length $x = f(L_1)$ of the evaporator heating coil including its impact on specific weight of steam/water fluid changes, following expressions to find pressure losses in an evaporator are brought out -

$$\Delta p_1 = \left(a_{V_z} - b_{V_z} \times \Delta t_{sp}\right), \quad (3.13)$$

where following complexes are estimated as below -

$$a_{V_z} = 0{,}402 + (0{,}0158 + 0{,}0091 \times k_{circ}) \times (y - 2) + 0{,}136/(0{,}4 + \tau) + (0{,}0045 + 0{,}0015 \times \tau) \times k_{circ},$$

$$b_{V_z} = 0{,}073 + 0{,}0011 \times k_{circ} - (0{,}0034 + 0{,}00032 \times k_{circ}) \times \tau$$ and

$$\Delta t_{\max_1} = t_{g_{sp}} - t_s, \quad \tau = x_1 / \Delta t_{\max_1}, \quad y = t_s / 100.$$

Due to respective actual pressure changes on the whole length of evaporator also saturation temperature will be affected similarly, what will come to certain impact on heat transfer efficiency via mean log temperature at the very first Δt_{LOG_1}. Hence to the respective evaluated value Δp_1, it will correspond an appropriate saturation temperature up-growth Δt_{sp}, which is found as per below brought out equations -

$$\Delta t_{sp} = K_P \times a_{V_Z} \times \frac{(\beta_0 - K_P \times a_{V_Z} \times \beta_1)}{1 + K_P \times b_{V_Z} \times (\beta_0 - 2 \times K_P \times a_{V_Z} \times \beta_1)}, {}^{o}C, \tag{3.14}$$

Where following complexes are evaluated accordingly -

$$K_P = \zeta_1^{\Sigma} \times {k_{circ}}/{2 \times g} \times {\Delta i_s}/{r} \times v_s \times \left({W_C \times \xi}/{100 \times k_{S_1}} \right)^2 \text{ and}$$

$$\beta_0 = 37{,}378 - 29{,}576 \times y + 6{,}19 \times y^2; \quad \beta_1 = 2{,}413 - 2{,}149 \times y + 0{,}486 \times y^2$$

Based on investigations by Prof. V.A.Semeka, the following formula has been obtained, which reflects the influence on evaporator mean-log temperature difference as follows –

$$\begin{aligned} k_\delta = {} & 0{,}452 + {0{,}256}/{0{,}133 + \tau} + {0{,}26 + 0{,}18 \times \Delta t_{sp}}/{\Delta t_{\max 1}} + {0{,}4 \times \Delta t_{sp} - 0{,}7}/{x_1} + \\ & \left(\left(4{,}3 + 0{,}74/\tau - 1{,}24 \times k_{circ} \right) \times \Delta t_{sp} + \left(1{,}06 \times \Delta t_{sp} - 2{,}65 \right) \times \left(\Delta t_{sp} - 1{,}7 \right) / \left(0{,}24 + \tau \right) + \right. \\ & \left. \left(3{,}7 \times k_{circ} + 2 \times \Delta t_{sp} \right) \times \left(2 - y \right) \right) \times 10^{-3} \end{aligned} \tag{3.15}$$

$$\delta_{ev} = {\Delta t_{sp}}/{\Delta t_{\max_1}} \times k_\delta; \tag{3.16}$$

and subsequently mean-log temperature differences for evaporator will be found accordingly –

$$\Delta t_{LOG_1} = \frac{\left(\Delta t_{\max_1} - \Delta t_{\min_1} \right)}{\ln\left(\Delta t_{\max_1} / \Delta t_{\min_1} \right)} \times \left(1 + \delta_{ev} \right) \tag{3.17}$$

In addition actual delivery head of circulating pump could be considered with some safety coefficient as below –

$$p_{circ/p} = K_{safety} \times \left(p_s + \Delta p_1 \right) \tag{3.18}$$

Finally, mean log temperatures for other boiler surfaces could be estimated either as per presented equations #3.19 –

$$\Delta t_{LOG_2} = \frac{\left(\Delta t_{\max_1} - x_2 \right)}{\ln\left(\Delta t_{\max_1} / x_2 \right)}; \quad \Delta t_{LOG_3} = \frac{\left(\left(t_{g_{exh}} - t_{fw} \right) - \left(x_1 + x_3 \right) \right)}{\ln\left({t_{g_{exh}} - t_{fw}}/{x_1 + x_3} \right)} \tag{3.19}$$

3.9.5. DETERMINATION OF BOILER SURFACE SIZES.

Based on both equations of heat balance and convective heat transfer, we gain the following formula of heat amount as $Q = k \times F \times \Delta t_{LOG}$, where value k is the coefficient of convective heat exchange and value F, m^2, determines sizes of convective surface. After the formula transformation a number of tube coils in direction of flue gas outlet could be evaluated as follows -

$$z_i = \Delta h_{g_i} / \Delta t_{LOG_i} \times k_F \times W_{C_i} \times 100 / k_i \tag{3.20}$$

The basic convective heat transfer equation for **smooth** tube boiler is –

$$1/k = 1/\omega \times \alpha_1 + \varepsilon + d/d_i \times 1/\alpha_2 \tag{3.21}$$

where heat conductivity coefficient α_1 from gas to steel tube wall is determined accordingly - $\alpha_1 = c_z \times c_s \times c_\Phi \times \alpha_0$. At already evaluated geometrical complexes during boiler choice the coefficient of heat radiation impact on convective thermal conductivity is found accordingly - $c_\Phi = 4.004 - 0.163 \times \left(\overline{t_{g_i}}/1000\right) + 0.0733 \times \left(\overline{t_{g_i}}/1000\right)^2$. Subsequently, base normative value of heat conductivity α_0 could be estimated according brought out formula - $\alpha_0 = 17.85 \times c_\gamma \times c_d \times \left(W_{g_i} \times k_{t_i}\right)^{0.6}$, where W_{g_i} is gas mass-velocity in bundle narrow section between tubes, i.e. $W_{g_i} = k_w \times W_{c_i}$.

Thermal conductivity coefficient from tube to heating-up media (water, steam) α_2 is being considered in our evaluations for economizer and super-heater, while for evaporator the influence of coefficient α_2, which tends to infinity, is omitted due its insignificance. Then for both super-heater and economizer this thermal conductivity coefficient is evaluated in dependence on heating-up media both velocity and average temperature, however geometrical characteristics of tube bundle has also considerable effect. Following equation is found valid - $\alpha_2 = c_{d_{in}} \times c_{tn_i} \times \left(W_{2n_i}\right)^{0.8}$, where coefficient c_{tn_i} encounters average heating-up media temperature, i.e. for either superheated steam or feed water in economizer accordingly –

- super-heater - $c_{tn_2} = 7.08 + 1.46 \times \left(y_c - 0.48\right)^2 + \left(2.27 - 0.9 \times y_c\right) \times \left(\overline{t_{st}}/100\right)$ and
- economizer - $c_{tn_3} = 11.12 + 17.62 \times \left(\overline{t_{fw}}/100\right) - 2.27 \times \left(\overline{t_{fw}}/100\right)^2$, where
- average overheated steam temperature in super-heater - $\overline{t_{st}} = \overline{t_{g_2}} - \Delta t_{LOG_2}$
- and feed water average temperature in economizer - $\overline{t_{fw}} = \overline{t_{g_3}} - \Delta t_{LOG_3}$;
- mass velocity of heating-up media (steam/boiler) water is determined produced steam output and available tube internal cross section- $W_{2n_i} = \left(\xi_i / k_{s_i}\right) \times W_{C_i}$, $kg/\left(m^2 \times s\right)$, where ξ_i is relative consumption of warm-up media via relevant surface and following is found valid
- for super-heater - $\xi_i = \xi_2 = \xi_{st}$;

- for economizer - $\xi_i = \xi_3 = \xi \times (1 + k_{rec})$, but for WHRS with intermediate steam extraction the coefficient $k_{rec} = 0$ is equal to zero, hence $\xi_i = \xi_3 = \xi$.

With the consideration of above brought out equations the total number of heating coils for respective surface could be presented as follows -

$$z_i^{calc} = \left(\Delta h_{g_i} / \Delta t_{LOG_i}\right) \times R_i + 0{,}5573 \tag{3.22}$$

Complex R_i represents summary heat conductivity coefficient from flue gases via tube to heating-up media; and, based on analytic expressions above, formula #3.23 is brought out –

$$R_i = \frac{M_{1_i}}{c_{\Phi_i} \times k_{t_i}^{0.6}} + \left(M_{\varepsilon_i} + \frac{M_{2_i}}{c_{t_i} \times \xi_i^{0.8}}\right) \times \left(1 - \frac{0.5573}{z_i}\right), \tag{3.23}$$

- where complex representing α_{1_i} - $M_{1_i} = A_{1_i} \times W_{C_i}^{0.4}$;
- another one representing pollution from gas side ε_i - $M_{\varepsilon_i} = A_{\varepsilon_i} \times W_{C_i}$;
- and the last one of α_{1_i} - $M_{2_i} = A_{2_i} \times W_{C_i}^{0.2}$.

In a result surface amount of respective constituent could be found as per equation #3.22 for smooth tube exhaust boiler.

For **<u>finned</u>** surfaces heat transfer coefficient is expressed via the modified formula -

$$1/k = 1/\overline{\alpha_1} + H/H_{\text{int}} \times 1/\overline{\alpha_2} \tag{3.24}$$

that encounters finned surface sizes against internal one, but values $\overline{\alpha_1}$, $\overline{\alpha_2}$ are respectively average heat return coefficients from gases to tube wall and from tube wall to heating up media. In the presented formula #3.24 heat conductivity coefficient $\overline{\alpha_1}$ encounters not only heat transfer from gas to tube but also the adverse effect of pollution ε_i from gas side. In our case, when tube ribbing is ensured from gas side only, it becomes evident, that mechanism of heat conductivity from tube to steam/water will be alike as for plain tube surfaces.

The present coefficient of <u>thermal conductivity from gases to finned tube</u> is dependent on both heat conductivity efficiency to base tube and ash deposit, and rib thermal resistance. Radiant component impact on heat transfer efficiency for ribbed surface is so small, that it could be omitted, subsequently only convective constituent α_k is being considered in evaluations; and the respective equation #3.25 is applicable for surface size determination –

$$\overline{\alpha_1} = \left(\frac{H_{fin}}{H_g^{\Sigma}} \times E \times \mu + \frac{H_{sm}}{H_g^{\Sigma}}\right) \times \frac{\psi_r \times \alpha_k \times \omega}{1 + \varepsilon \times \psi_r \times \alpha_k \times \omega} \tag{3.25}$$

Ribbed surface heat conductivity efficiency coefficient E is dependent on geometrical fining characteristics, chosen material for fins, arranged gas flow and ash deposit amount being function of following - $E_i = th(\beta_i \times h_r) / \beta_i \times h_r$, where $th(x) = e^x - e^{-x} / e^x + e^{-x}$; but derivative complex of rib thermal efficiency β_i is found equal to - $\beta_i = \sqrt{\dfrac{2 \times \psi_r \times \alpha_k \times \omega}{\delta_p \times \lambda_M \times (1 + \varepsilon \times \psi_r \times \alpha_k \times \omega)}}$. With the consideration of carried out equation transformations another practical one is brought out for our calculations - $\beta_i = \sqrt{2 \times \psi_r \times A_{gk_i} \times M_{0i} / \delta_p \times \lambda_M \times (1 + A_{\varepsilon_i} \times M_{0i})}$. Coefficient due to rib widening will be equal to - $\mu_r = 1 + 0.12 \times (\beta \times h_r) \times \left(1 - \sqrt{(\delta_{r_2} / \delta_{r_1})}\right)$, being equal to one, if straight fins are in use. Effective finned tube boiler surface will be slightly less than summary geometrical one due to reduced heat transfer efficiency via ribs, therefore this factor is encountered in evaluations via relation of mentioned above surfaces, i.e. effective surface against total geometrical one - $\overline{H_{ef_i}} = (H_{fin} / H_g^{\Sigma}) \times E_i \times \mu + (H_{sm} / H_g^{\Sigma})$. Complex M_{0i} is the measure value of actual flue gas flow in particular narrow cross section between tubes, that influences thermal conductivity rate –

$$M_{0i} = k_{t_i}^{0.5014} \times (\overline{t_{g_i}} / 100)^n \times W_{C_i}^{0.65} \times \omega \;;$$
$$n = 0.0175 \;\; @\overline{t_{g_i}} \le 510^o C; \;\; n = 0.02 \;\; @510^o C < \overline{t_{g_i}} \le 600^o C \tag{3.26}$$

Finally, summary thermal conductivity coefficient $\overline{\alpha_1}$ influence in determination of boiler surface sizes could be presented via equation #3.27:

$$100 / \overline{\alpha_1} = X_{0i} = 1 + A_{\varepsilon_i} \times M_{0i} / A_{1i} \times M_{0i} \times 10^2 , \tag{3.27}$$

where average total heat return coefficients from gases to tube wall is presented by following complex - $A_{1i} = \overline{H_{ef_i}} \times \psi_r \times A_{gk_i}$. The influence of heat transfer efficiency by present coefficient of <u>thermal conductivity from finned tube to warm-up media</u> is being reflected via following expression for both super-heater and economizer -

$$100 / \overline{\alpha_2} \times H_g^{\Sigma} / H_{in} = Y_{0i} = \left(k_{s_i} / \xi_i \times W_{Ci} \right)^{0.8} \times 10^2 / c_{t_i} \times c_{d_{in}} , \tag{3.28}$$

while for evaporator surface the complex Y_{0i} is equal to zero, i.e. $Y_{0_1} = 0$.

Finally, after all transformations heating coil amount is determined as follows -

$$z_i^{calc} = \left(\Delta h_{g_i} / \Delta t_{LOG_i}\right) \times k_F \times W_C \times \left(X_{0_i} + Y_{0_i}\right) \tag{3.29}$$

As it was noted previously, initially accepted boiler surface amounts will differ from calculated ones $\Delta z_i = \left|z_i^{calc} - z_i\right| > 0$ at initially accepted temperature differences x_i. Hence, respective adjustments in $x_{i_{j+1}}$ are to be done, encountering complex influence of deviation extent of each boiler surface. So, by using different iterative methods this system of non linear equations could be solved at required accuracy $\Delta z_i = \left|z_i^{calc} - z_i\right| \le accuracy$.

3.10. DETERMINATION OF EXHAUST BOILER AERODYNAMICALLY RESISTANCE.

Boiler aerodynamically resistance is determined by surface sizes, tube bundle geometry, flue gas current speed $\Delta P_{g_i} = f\left(k_h, z_i, \overline{t_{g_i}}, W_{C_i}\right)$ [21, 86, 100, 117], adversely affecting main engine output. Usually the upper limit of boiler resistance is restricted by main engine manufacturers so, as an exceeding of it could cause both a significant efficiency drop down and come to an unreliable performance of the engine either.

Different equations are brought out in dependence on boiler surface type. So for **smooth** tube boiler aero-resistance is evaluated in accordance formulae #3.30 –

$$\Delta P_{g_i} = k_h \times \left(z_i + 1\right) \times k_{t_i}^{1.194} \times W_{C_i}^{1.73}, \quad kg/m^2 \tag{3.30}$$

At similar conditions **finned** surface boiler gas resistance will be higher due to less free space for gas passage and following expression is brought out –

$$\Delta P_{g_i} = k_{\Gamma\Gamma} \times c_{z_i}^h \times z_i \times k_{t_i}^{1.4475} \times W_{C_i}^{1.75} \times \left(\overline{t_{g_i}}/100\right)^{0.25 \times n_\Gamma}, \quad kg/m^2 \tag{3.31}$$

- Where coefficient that encounters coil amount in way of gas outflow - $c_{z_i}^h = 1 + 1.5 \times e^{-k_{z_i}^h \times z_i}$ and $k_{z_i}^h = 0.8942 - \left(z_i - 3\right) \times \left(0.107867 - \left(z_i - 3\right) \times 0.0838\right)$;
- $n_\Gamma = -0.020$ @ $\overline{t_{g_i}} \le 420^o C$ & $n_\Gamma = -0.032$ @ $\overline{t_{g_i}} > 420^o C$.

Afterwards, the total aero-gas resistance is found as the sum by each boiler constituent - $\Sigma \Delta P_{g_i} = \Delta P_{g_1} + \Delta P_{g_2} + \Delta P_{g_3}$.

3.11. DETERMINATION OF STEAM CYCLE EFFICIENCY GAIN.

Steam turbine output is dependent on both quantity $\left(\xi, \ \xi_{st} = \xi - \xi_{sat}\right)$ and quality indices of steam before nozzles $\left(t_{0_T}, \ p_{0_T}\right)$ and at condenser inlet $\left(p_x\right)$.

The pressure at the inlet of turbine nozzles depends on hydrodynamic pressure losses of supply tube Δp_T, consisting of 1) super-heater main valve, 2) a collector with one angled output, 3) collecting triple valve and 4) shut off valve. Resistance to friction of chosen fixtures could be found either in particular manufacturer handbooks or evaluated based on different Norms for hydraulic calculations. Based on accepted construction of the main for steam delivery till turbine it is found, that relative pressure drop will be within following margins - $\Delta p_T / p_{0_T} \approx 0.055 \div 0.065$ [19, 120]; then the respective saturation temperature reduction $\Delta t_{s_T} = f\left(y_{st},\ \Delta p_T / p_{0_T}\right)$ is possible to evaluate by substituting corresponding values in equation #3.10, where saturation index y_{st} is equal to $y_{st} = t_{s_{ST}} / 100$. In a result actual steam saturation temperature that corresponds to relevant pressure $p_{0_T} = p_{st} - \Delta p_T$ at turbine inlet just before nozzles will be difference of following - $t_{s_T} = t_{s_{ST}} - \Delta t_{s_T}$; $y_T = t_{s_{ST}} / 100$. Besides pressure drop in steam main there are also heat losses via insulation being dependent on its quality, temperature difference between steam and that in engine room, length of steam line, pressure and other characteristics. But in our considered cases it is found that enthalpy drop down due to heat dissipation is around following - $\Delta h_T \approx 0.1\% \times h_{st}$; then relevant overheated steam temperature decrease Δt_{st_T} at turbine 1st stage nozzle inlet will be adjusted accordingly (see relevant indices from equation #3.5) -

$$\Delta t_{st_T} = \frac{\left(\Delta h_T + \left(2 \times a_2 \times y_T - a_1\right) \times \Delta y_T\right) \times 100}{302.08 - 16.74 \times U_{st} - \left(172.3 - 32.82 \times U_{st}\right) \times y_T + \left(70.33 - 13.4 \times U_{st}\right) \times y_T^2} \tag{3.32}$$

where $U_{st} = \Delta t_{st} / 100$ and $\Delta y_T = \Delta t_{s_T} / 100$. In a result steam temperature at turbine inlet is defined more exactly - $t_{st_T} = t_{st} - \Delta t_{st_T}$, as well as its entropy –

$$\begin{aligned} S_0 = {} & 8.39228 - 1.79479 \times y_T + 0.22622 \times y_T^2 - 0.06283 \times y_T^3 + \\ & \left(0.58904 - 0.07497 \times y_T + 0.08582 \times y_T^2\right) \times U_{st} - \\ & \left(0.03317 + 0.02853 \times y_T\right) \times U_{st}^2 + 0.005547 \times U_{st}^3 \quad ; \quad kJ/\left(kg \times K\right) \end{aligned} \tag{3.33}$$

Now, steam cycle iso-entropic enthalpy difference that works out in the turbine is found -

$$Ha = h_{st_T} - h_x^{\parallel} + T_x \times \left(S_x^{\parallel} - S_0\right) \tag{3.34}$$

Thermal indicator efficiency coefficient of steam turbine η_{0i} could be evaluated either based on thorough both specification choice and calculus of turbine stages or by using some simplified equations elaborated and presented as below [6, 8, 9, 12, 42, 106]. By detailed

information processing regarding available in market advanced steam turbo-generators some common regularities were found in dependence on steam dates and turbine output range. With the considerations of similar explorations conducted by Professor Mr. V.A.Semeka following equations found valid for steam turbo-generators within range of output from 500kW till 7500/8500kW as below –

$$\eta_{0i} = \left(A_\eta - 16.342 \times y_T + \left(3.13 + 1.428 \times y_T\right) \times U_{st} - 0.36 \times U_{st}^2\right) \times k_\eta \times 10^{-2} \qquad (3.35)$$

Where following values found equal to -

- constant $A_\eta = 97.673$ for COGAS plants and $A_\eta = 90.58$ for turbo-generators in power plants with diesel engine as ships main engine;
- efficiency coefficient - $k_\eta = 0.9229 - 0.0344 \times y_T + \left(0.161 + 0.0434 \times y_T\right) \times k_N - \left(0.1072 + 0.009 \times y_T\right) \times k_N^2 + 0.0233 \times k_N^3$;
- Efficiency factor - $k_N = Ne_{ST_i} / 5000$.

By repeated substituting of evaluated values of steam turbine output Ne_{ST_i} in formulae #3.35, the exact rate is obtained finally, i.e. $Ne_{ST_i} = Ha \times \xi_{st} \times G_g \times \eta_{0i} \times \eta_{m_T}$.

3.12. EFFICIENCY ADJUSTMENTS FOR INTERMEDIATE STEAM EXTRACTION CYCLE.

For HRC with intermediate steam extraction the de-aeration and feed water pre-heating should be organized so, that within the range of normal operational load of main engine all demands in required heat will be met by this steam. With the consideration of ships' trading peculiarities the lowest durable service load level of main power plant would be around not less than 70% of MCR, that leads to similar pressure reduction both in exhaust boiler and in way of steam path. Therefore extraction point is to be *shifted up*, i.e. during designing the extraction point pressure p_{ext}, which is chosen at nominal service load technical conditions, is to be raised with the consideration that de-aerator is capable to serve at reduced main engine rating without any fresh steam supply. Based on maintenance experience, when ME actual load is 70% of MCR, the pressure drop in boiler would be around 79% of that one at nominal load [3, 95]. Such a necessity to increase extraction point pressure is lowering possible cycle net gain at nominal output; however power plant reliability is maintained within all range of operational loads as well as its average service efficiency. When extraction pressure is set up, its coordinate Y_1 is found -

$Y_1 = \left. h^{|}_{s_{ext}} - h^{|}_{x} + \delta h^{|}_{x} \right/ h^{|}_{s_T} - h^{|}_{x}$, where following boiling water enthalpies $h^{|}_{s_{ext}}$; $h^{|}_{x}$; $h^{|}_{s_T}$ correspond to pressure either in extraction point p_{ext} or condenser p_x or at turbine inlet p_{0_T} correspondingly (see equation #3.3 & 7). Then the reduction in the relative steam output due to the extraction is found:

$$\Delta\xi_{ext} = (1-\Psi)\times \left. h^{|}_{fw} - h^{|}_{fwp} \right/ h_{st} - \Psi \times Ha \times \eta_{0i} - h^{|}_{fwp} \times \xi \qquad (3.36),$$

where value $\Psi = f(Y_1, p_{st}, h_{st})$ is extraction quality coefficient [130]. For the system with thermostatic re-circulating valve this amount is equal to - $\Delta\xi_{ext} = 0$. Finally, the present value of steam turbine output is evaluated as per formula #3.37:

$$\Pi = (\xi_{st} - \Delta\xi_{ext}) \times Ha \times \eta_{0i} \times \eta_{m_T}, \quad kJ/1kg \quad flue \quad gasses \qquad (3.37),$$

where η_{m_T} is mechanical efficiency coefficient of steam turbine. Obtained characteristic Π is the measure value of steam turbine net output; and it has a little change in dependence of main engine rating. Hence, only by multiplying with total exhaust gas amount G_g, which is the passport data of the particular type of the ME at specified load level, the absolute value of the rating is obtained as follows - $Ne_{st} = \Pi \times G_g$, kW. At the same time EB aerodynamic resistance comes to reduction in the MR power as per below -

$$\Delta He_g = 2.403\times 10^{-5} \times \eta_{ig} \times \eta_{M_{GT}} \times \left(\sum \Delta P_{g_i} - 150\right) \times T_{g_0}, \quad kJ/1kg \quad flue \quad gasses \qquad (3.38).$$

In the case of common drive for any prime mover (generator, propeller or etc.) of both main engine (gas turbine) and steam turbine the determination of the net efficiency raise of the power unit in the whole, which makes the sum of two opposite constituents, is the final measure of net efficiency due to WHRS introduction:

$$\Pi_0 = \Pi - \Delta He_g, \quad kJ/1kg \quad flue \quad gasses \qquad (3.39).$$

Finally, this thermodynamic and EB dimension numerical analyze method is accomplished for both HRC with thermostatic recirculation valve and intermediate steam extraction, when different types of boiler surfaces, i.e. smooth and finned ones, are optionally assumed. Simplified flow chart of the method is presented in the figure 3.5.

3.1.13. CONCLUSIONS.

1. The novelty of the presented method is that the efficiency of HRC is evaluated on accepted, fixed dimensions of EB. Such approach is important for this type of power systems especially, as already fixed amount of heat is available only to be recovered.
2. There is a possibility to ensure the highest efficiency of the power unit within fixed dimensions being very important for vehicles, particularly for specialized vessels, when speed and cargo space are both contradictory and important matters.

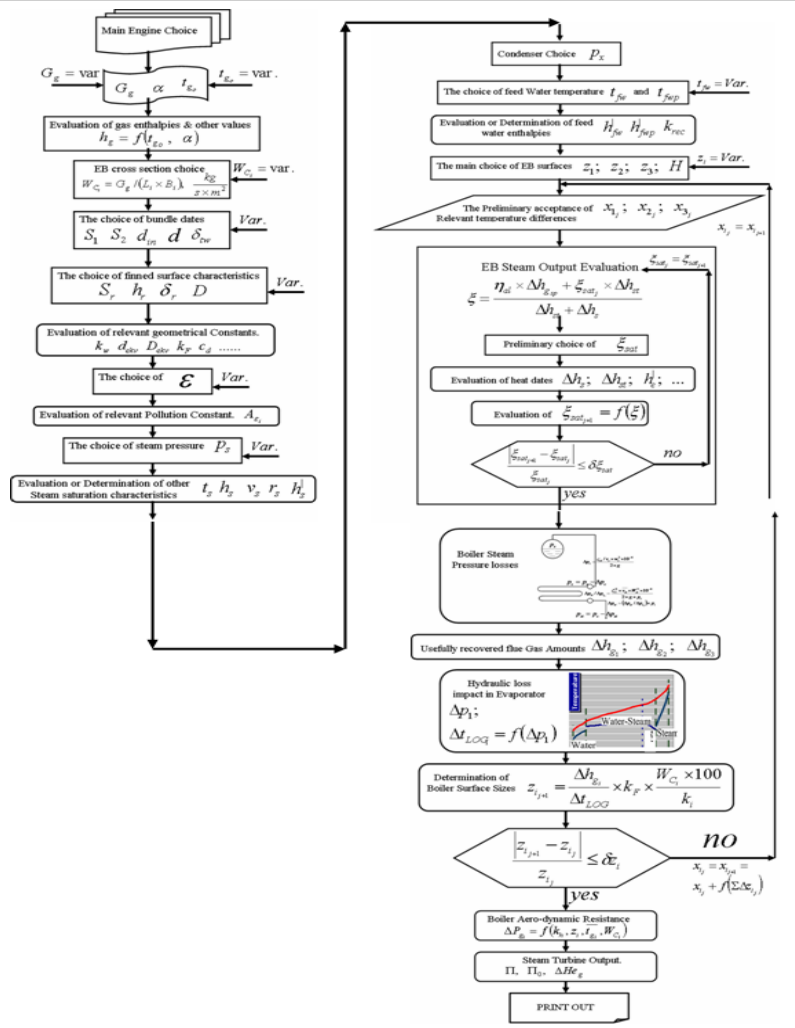

Fig.3.5. EB Mathematic Model Flowchart.

3. The use of the amount of coils as the parameter of heat exchange surface sizes is grounded from the practical view point either, as it allows us to ensure the module production of EB-s and to carry out an optimal set up of the power unit.
4. Another advantage is that obtained relative values are valid for the wide range of different type of engines at various ratings, load levels and ambient conditions.
5. The influence of other factors as geometrical and thermodynamic ones could be explored.
6. The algorithms for other different type of HRC are possible to be elaborated. More sophisticated two-stage WHRS could be attractive for highly rated both medium speed diesel engines and gas turbines, especially.

CHAPTER 4. HEAT RECOVERY CIRCUIT AND EXHAUST BOILER EQUIPMENT OPTIMIZATION FOR COMPACT HIGH RATED POWER PLANTS.

4.1. INTRODUCTION.

The object of our investigation is Waste Heat Recovery System, being incorporated in a marine power-propulsion plant with main gas (or high rated medium speed diesel engine) and steam turbine (see Fig.4.1). GT as ships' main engine is chosen due to considerably broadened tasks for our explorations, as WHRS is becoming as essential part of main propulsion plant; and that type of choice is substantiated by increased interest and application in marine industry either (see Chapter 1). At lowered gas temperatures t_{g_0} research results might be applicable for similar high rated medium speed diesel engine power plants. However all considered problems and brought out conclusions will have practical use for WHRS irrespectively of ME type but in different extent.

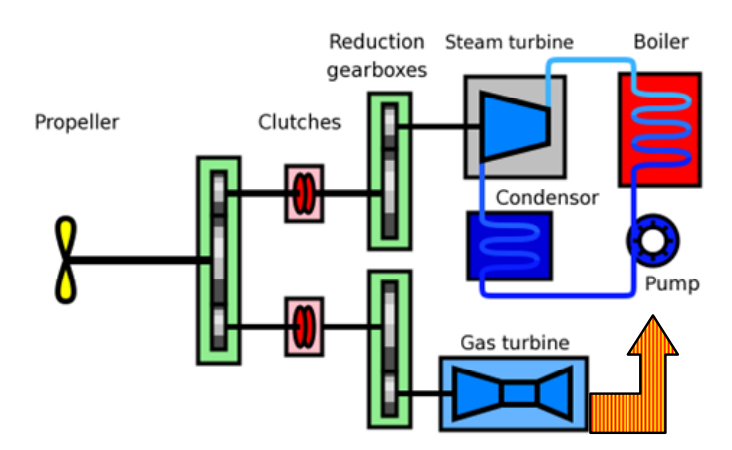

Fig.4.1 COGAS-Diagram.

The main task of these studies is to find such optimal conditions, which result in the highest thermodynamic net outcome produced by WHRS, especially, when the main constituent of the system Exhaust Boiler (EB) might be limited in sizes (especially in its height ΣH_i) due to both installation matters and cost wise. Therefore mutual and favorable convective surface re-distribution ($(\Sigma H_i)\Sigma z_i = z_{1_i} + z_{2_i} + z_{3_i}$) might be one of the ways for power plant optimization, when the highest output of power plant in total is achieved $\Pi_0 = \max.$ as difference of two constituents - $\Pi_0 = \Pi - \Delta He_G$, $kJ/1kg$ $flue$ $gasses$. By multiplying the relative increment in power output due to WHRS introduction Π by flue gas amount G_g the absolute value of steam turbine output is achieved $Ne_{ST} = \Pi \times G_g$, kW .

At the same time it would be necessary to know the influence of each separate convective surface of EB on efficiency indices of the WHRS and power plant in the whole at unlimited growth of each constituent either z_1 *or* z_2 *and* z_3, i.e. number of respective heating coils (1 - evaporator, 2 – super-heater, 3 -economizer). HRC is chosen with thermostatic recirculation valve (Fig.4.2), allowing us to achieve both the deepest cooling rate of flue gases at lowest boiler surface sizes and maintain inlet feed water temperature t_{fw}, on constant level irrespectively of power plant load level (see Chapter 1, 2). Meantime following main restrictions are to be observed based on recommendations, maintenance experience and design practice, e.g. lowest flue gas temperature at exhaust boiler outlet to be equal as follows - $t_{g_{exh}} \geq 160^o C$ and so-called *approach* temperature x_3 ($x_3 = t_s - t_e$) should be always positive value equal to $x_3 > x_3^{\min}\left(=15^o C\right)$.

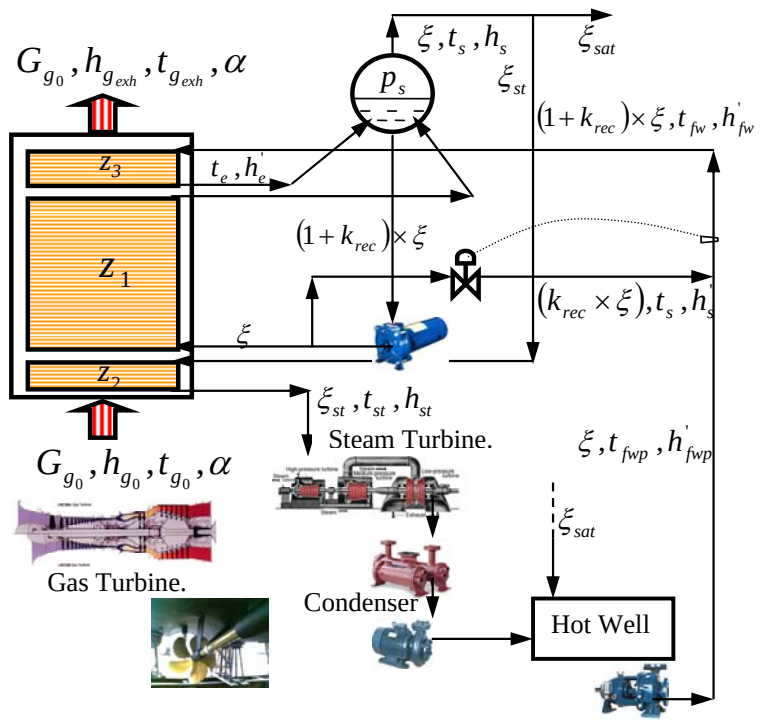

Fig.4.2 WHRS Diagram with feed water re-circulation.

At the same time when additional boiler size enlargement ΔH_i could be obtained for another similar project it comes possible adequately increase convective surface $\Delta z_i = \Sigma z_{i+1} - \Sigma z_i$ as well, so that the highest efficiency of power plant is ensured, i.e. $\partial \Pi_0 / \partial z_i = max$. But which boiler surface constituent should be enlarged and in which extent it is a task of our studies in this chapter. Meantime any changes will affect other efficiency parameters either, e.g. the choice of optimal steam pressure in EB $p_{S_{i+1}} \neq p_{S_i}$, which will be different in dependence on other WHRS technical indices. The process of investigations, how to achieve the highest output within fixed boiler dimension, is thorny problem; and therefore this chapter is proposed to be divided in separate subchapters that reflects the complexity of the optimization process.

CHAPTER 4. SUB-CHAPTER 4.I. | EB CONVECTIVE SURFACE INFLUENCE ON WHRS THERMO-DYNAMIC EFFICIENCY INDICES.

Based on said above considerations before to investigate complex and joint influence of all boiler surfaces, i.e. an economizer, a super-heater and an evaporator, the impact of each one on WHRS and power plant performance will be explore at unlimited its growth, while remaining other two boiler constituents, i.e. either economizer and evaporator or economizer and super-heater or super-heater and evaporator, remain constant.

4.I.1. SUPER-HEATER INFLUENCE AT UNLIMITED IT'S GROWTH.

The purpose of super-heater is to ensure saturated steam overheating in order both to increase thermodynamic efficiency of Rankine cycle and to ensure long-term reliable steam turbine performance. With the growth of super-heater surface $z_2 \uparrow$, when other two constituents remain invariable z_1 , $z_3 = const.$, steam overheat rate $\Delta t_{st} = t_{st} - t_s$ trends to increase till its highest theoretical limit Δt_{st}^{max} (see Fig.4.3). At unlimited super-heater sizes theoretical limit Δt_{st}^{max} will be equal to following equation: $\Delta t_{st}^{max} = t_{g_0} - t_s + \delta t$, where δt gas temperature difference between gas and steam due to heat transfer resistance impact correspondingly. The growth of value Δt_{st} & t_{st} ensures both reliable steam turbine performance and its efficiency via respective increment in iso-entropic enthalpy difference usefully worked out in turbine cycle Ha , kJ/kg (see Fig.4.4.) with following indices $\partial Ha / \partial z_2 > 0$, but $\partial^2 Ha / (\partial z_2)^2 < 0$, and $Ha \approx \overline{c_{ST}} \times (t_{st} - t_x^{'})$, where $t_x^{'}$ - temperature corresponding to enthalpy of dry exhaust steam after turbine at condenser inlet. With the overheated steam temperature raise there is slight tendency of increase in turbine internal efficiency η_{oi} with the rate equal to $\approx (2{,}8 \div 3{,}3) \times 10^{-4}\%$ on each temperature $\Delta t_{st} = 1^o C$

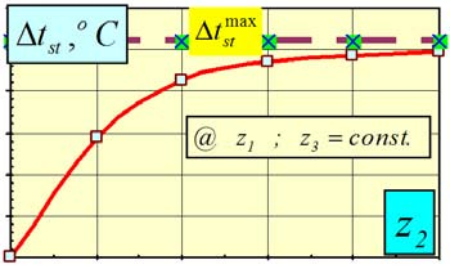

Fig.4.3. Super-heater surface influence on steam overheat rate.

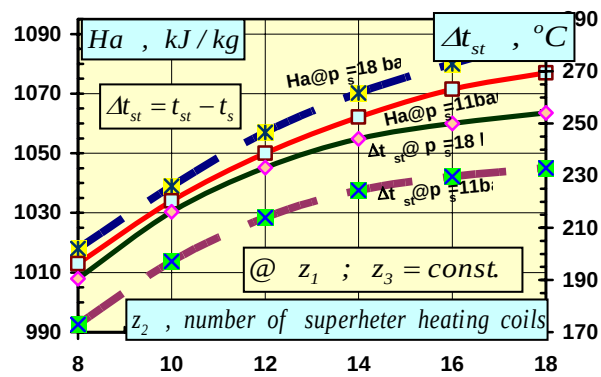

Fig.4.4. Super-heater impact on overheat rate & iso-entropic enthalpy difference at z_1; z_3=const.

increment. At the same time unlimited super-heater surface enlargement is unreasonable as any further its increment will generate less net gain in contradiction to almost direct increase in aero-dynamic resistance ΔP_{g_i} of EB as follows - $\Delta P_{g_i} \cong \Delta P_{g_0} + k_2^{\Delta P} \times \Delta z_{2_i}$, kg/m^2, where ΔP_{g_0} - boiler gas resistance at some initial its surface sizes $z_{1_0}; z_{2_0}; z_{3_0} = const.$ and Δz_{2_i} - further enlargement of super-heater surfaces, i.e. heating coil amount (see Fig.4.5). In a result power loses in main engine (gas turbine) ΔHe_g will be in direct ratio on surface growth, while value Π will tend to its ultimate theoretical maximum Π^{MAX} (see Fig.4.6). Final efficiency Π_0 of WHRS is found as a difference of two meanings, i.e. $\Pi_0 = \Pi - \Delta He_g$ with following functional dependence characteristics: $\partial^2 \Pi_0 / \partial z_2^2 \cong \partial^2 \Pi / \partial z_2^2 < 0; \partial^2 \Delta He_g / \partial z_2^2 \cong 0$. Based on these indices we can expect, that initially super-heater growth will ensure positive additional efficiency increment of the power system in the whole, i.e. $\partial \Pi_0 / \partial z_2 > 0$, while at certain critical coil number $z_{2_i} = z_2^{crit}$ value Π_0 will reach its maximum Π_0^{MAX}; and, subsequently, further super-heater enlargement $z_{2_i} > z_2^{crit}$ will result in prevailing of main engine losses $\Delta He_g = f(\Delta P_{g_i})$, i.e. $\partial \Pi_0 / \partial z_2 < 0$ (see Fig.4.7). Based on presented results it is possible to find the critical super-heater coil number z_2^{crit} in dependence on inlet gas temperature, being almost in direct ratio (see Fig.4.8), at fixed sizes of evaporator and economizer surface. Now we will try more in details to explore super-heater influence on heat transfer process. With the surface enlargement $z_2 \uparrow$ any evident flue gas additional cooling is not observed, i.e. $\partial Q_i / \partial z_2 \geq\approx 0$, due to the fact, that gas cooling rate or its equivalent outlet gas temperature $t_{g_{exh}}$ is dominating dependable on evaporator sizes z_1, to which correspond gas temperature at evaporator outlet $t_{g_{sp}}$, being equal to following expression $t_{g_{sp}} = t_s + x_1$. So called *pinch-point* temperature x_1 is being directly and dominantly dependable on evaporator surface sizes at constant other characteristics, while

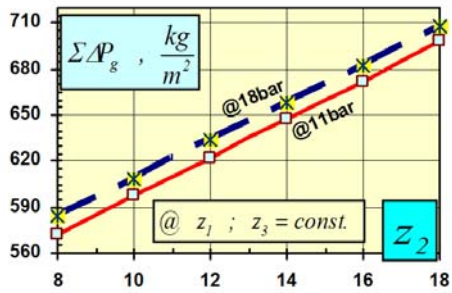

Fig.4.5 Super-heater impact on aero dynamic resistance at z_1; z_3=const.

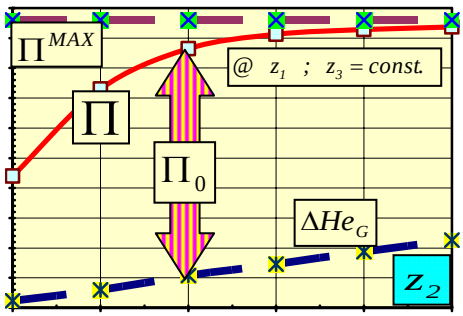

Fig.4.6 Super-heater influence on WHRS final output at z_1; z_3=const.

saturation temperature t_s is solely defined by its pressure p_s. Then considering said above on the first approximation we can expect, that transferred/recovered heat amount in both super-heater and evaporator sections will remain invariable, i.e. $(t_{g_0} - t_{g_s})_i \cong (t_{g_0} - t_{g_s})_{i+1}$, subsequently transferred heat amount $(Q_1 + Q_2)_i \cong (Q_1 + Q_2)_{i+1}$ either (see Fig.4.9a, b). On another hand super-heater surface enlargement comes to definite Q_2 value increment, thus reducing gas temperature at evaporator inlet $t_{g_{sps}}$. It results in reduction of remaining exploited heat by evaporator thus reducing steam capacity, but corresponding both inlet $t_{g_{sps}} \downarrow$ and mean temperature reduction $\overline{t_{g_1}} \downarrow$ comes to heat transfer coefficient k_1 diminution as well thus even more reducing boiler steam output ξ. In our case relative reduction in steam output constitutes around $\approx 0{,}67 \div 0{,}50\%$ *per* $\Delta z_2 = 1$ or $\approx 0{,}071 \div 0{,}053\%$ *per* $\Delta t_{st} = 1^\circ C$. Nevertheless, some further deeper cooling of flue gases in evaporator surface is observed $x_1 \downarrow$; $t_{gs} = (t_s + x_1) \downarrow$. Decrease in boiler steam capacity allows to obtain higher overheat rate $\Delta t_{st} \uparrow$; however, it also diminishes recovered heat Q_2

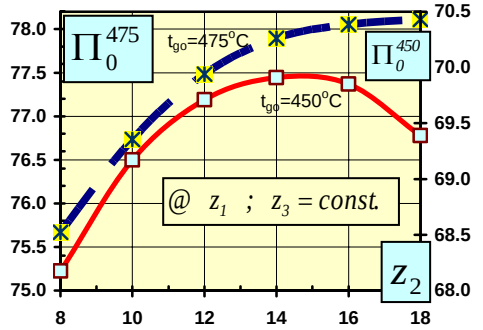

Fig.4.7 Super-heater influence on WHRS net output at z_1; z_3=const. & different inlet gas temperatures.

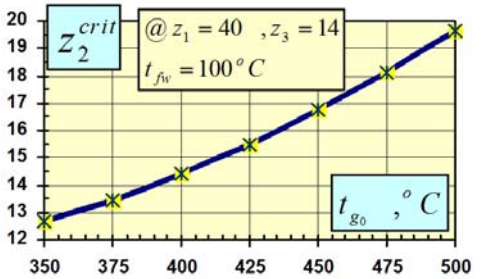

Fig.4.8. The highest amount of super-heater coils, at which the max. WHRS efficiency is obtained, on inlet gas temperature at z_1; z_3=const.

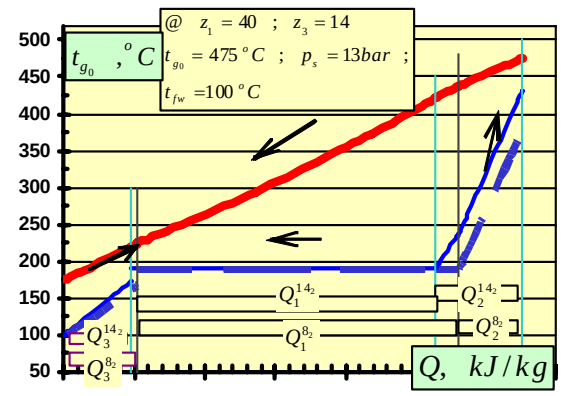

Fig.4.9b Temperature – transferred heat diagram at variable super-heater surface.

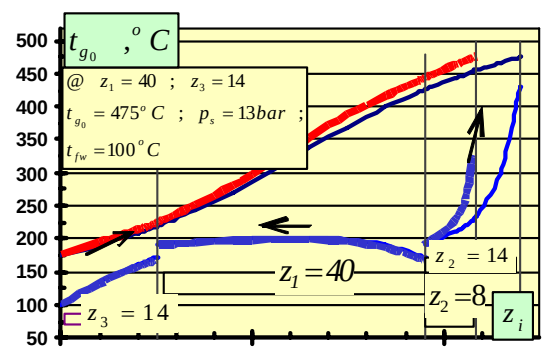

Fig.4.9a Temperature diagram - heat exchange surfaces diagram at variable super-heater surface.

to some extent. Consequently we can state that with the super-heater surface growth steam overheating and followed Rankine cycle efficiency increases due to following effects:

1. The growth of transferred heat $\partial Q_2 / \partial z_2 > 0$;
2. Reduction in steam capacity $\partial \xi / \partial z_2 < 0$ comes to even higher rate of adjoined heat to one kg of saturated steam, i.e. $\partial (Q_2 / \xi) / \partial z_2 >> 0$;
3. However, some minor ST efficiency drop is noticed due to - $\xi \downarrow; \partial \zeta / \partial z_2 |_{all=const.} < 0$.

These changes has minor influence on economizer performance, but still some decrease in so called the *approach temperature* x_3 is ensured and $\partial x_3 / \partial z_2 < 0$ due to relevant EB steam output changes. Further it comes to adequate changes in heat amount Δh_s, i.e. $\partial \Delta h_s / \partial z_2 < 0$, required for generating one kg saturated steam in an evaporator, as it is found as per equation below $\Delta h_s = r_s - (1 + k_{rec}) \times \overline{c_w} \times x_3$, where value $\overline{c_w}$ is mean specific heat of water in economizer section (others see chapter 3). This so called economizer impact, i.e. $\partial x_3 / \partial z_2 < 0$ & $\partial \Delta h_s / \partial x_3 < 0 \Rightarrow \partial \Delta h_s / \partial z_2 > 0$, contributes EB steam output rise to some extent. Anyway recovered heat amount in economizer has tendency to grow down $\partial Q_3 / \partial z_2 < 0$ (see Fig.4.9) due to both dominated steam output reduction and efficiency decrease in heat exchange, what is a result of economizer performance shift into the region of lowered gas temperatures, i.e. $\overline{t_{g_3}} \downarrow; \partial \overline{t_{g_3}} / \partial z_2 |_{all=const.} < 0$. In many cases during turbine designing steam overheat rate Δt_{st} is that initially chosen value, that influences technical parameters of turbine itself, condenser and other characteristics. Therefore it would be useful to explore efficiency parameters of WHRS in dependence on value Δt_{st} either. The iso-entropic enthalpy difference Ha is in direct dependence on steam overheat rate, as well as steam efficiency output Π with some minor ξ adjustments (see Fig.4.10). Due to the fact that any further increment in overheat rate is subject of required surface enlargement as follows (see Fig.4.4) $\partial z_2 / \partial \Delta t_{st} > 0$; $\partial^2 z_2 / \partial (\Delta t_{st})^2 > 0$, subsequently increasingly net power loses in main engine ΔHe_g due to EB aero-dynamic resistance (see Fig.4.10) will constantly decrease the positive effect of almost linear growth of steam turbine net output. Therefore, efficiency

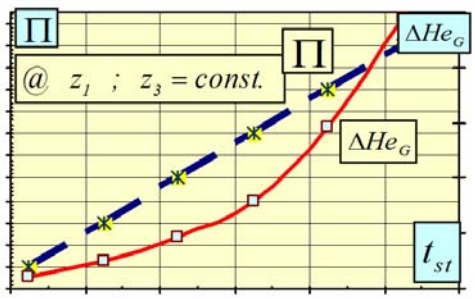

Fig.4.10. EB Super-heater influence on WHRS efficiency parameters at z_1; z_3=const. on steam overheat rate.

net outcome due to WHRS effect $\Pi_0 = \Pi - \Delta He_g$ will tend to have some maximum value Π_0^{max} at some certain level of steam overheat rate, exceeding of which will result in accelerate growth of efficiency losses (see Fig.4.11). The steam overheat value, at which the highest efficiency is obtained, will be an optimal one Δt_{st}^{opt}, and as we can see (see Fig.4.11) it is pretty much dependable on inlet gas temperature (see Fig.4.12). Steam pressure p_s has a negative influence on value Δt_{st}^{opt}, as it is found as difference of overheated t_{st} and saturated steam t_s temperatures. Actually, with the pressure raise overheated steam temperature has explicit tendency to increase, mainly due to steam output reduction. On another hand super-heater surface measure value the temperature difference x_2, being dependent on flue gases temperatures at boiler inlet t_{g_0} and superheated steam one t_{st} as follows - $x_2 = t_{g_0} - t_{st}$, is adversely influenced by the same steam pressure changes (see Fig.4.13). However at higher meanings of steam pressure the decrease rate of x_2 is being slow down due to relevant temperature gradient decrease $\Delta t_{max_2} \downarrow = t_{g_{sp}} - t_s \uparrow$, which influences mean log temperature value in relevant section. In a result saturation temperature t_s changes are more distinct against temperature difference x_2 ones, i.e. $\partial t_s / \partial p_s > |\partial x_2 / \partial p_s|$. Subsequently, due to the fact, that steam overheat rate is temperature differences of following magnitudes $\Delta t_{st} = (t_{g_0} - x_2) - t_s$, then following expression will be valid $\partial \Delta t_{st}^{opt} / \partial p_s < 0$ either (see Fig.4.13). Presented values of steam overheat rate Δt_{st}^{opt} are ultimate ones, which in reality will be lower $\Delta t_{st} < \Delta t_{st}^{opt}$, being chosen based on design parameters of WHRS and system characteristics. Apparently at higher steam pressure also the overheat should be increased to

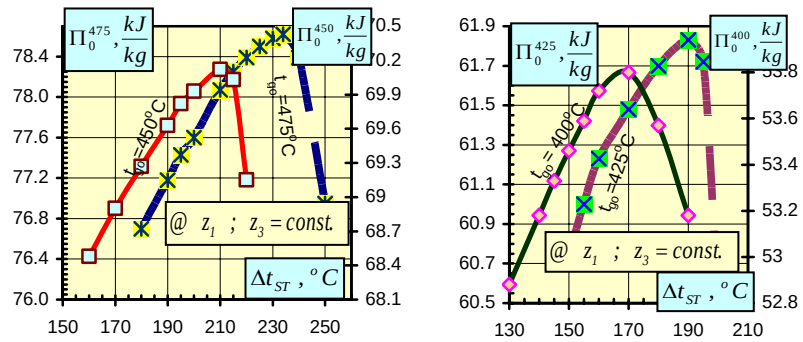

Fig.4.11 WHRS efficiency net outcome in dependence on steam overheat rate at different inlet gas temperatures and fixed heat exchange surface sizes of both evaporator and economizer.

avoid excessive humidity of exhaust steam at nozzle inlet in last stages.

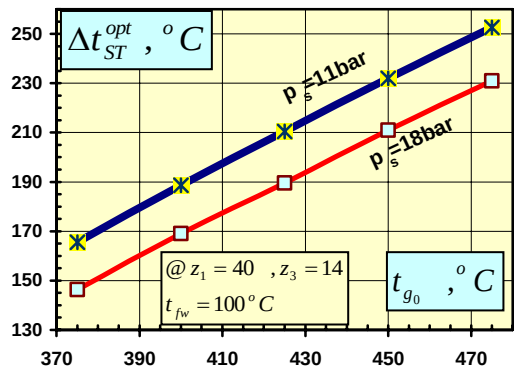

Fig.4.12.Optimal steam overheat rate, at which highest efficiency of WHRS is ensured, on t_{g_0} at z_1; z_3=const.

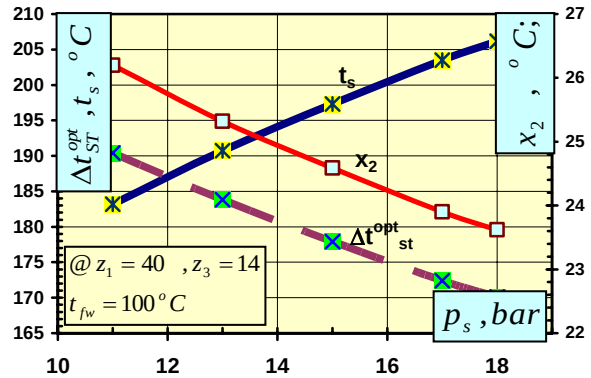

Fig.4.13 Optimal steam overheat rate, at which the highest efficiency of WHRS is ensured, on steam pressure at z_1; z_3=const.

4.I.2. ECONOMIZER INFLUENCE AT UNLIMITED IT'S GROWTH.

At fixed of both super-heater and evaporator z_1, $z_2 = const.$ sizes and other thermodynamic parameters p_s, $t_{f/w} = const.$, the growth of economizer $z_3 \uparrow$ results in considerable reduction of approach temperature x_3 (see Fig.4.14). It comes to further deeper flue gas cooling rate, i.e. $\Delta t_g^{\Sigma} = t_{g_0} - t_{g_{exh}}$, $\partial \Delta t_g^{\Sigma} / \partial z_3 > 0$, due to consequent steam output growth - $\partial \xi / \partial z_3 > 0$ (see Fig.4.15), being contributed by reduction in specific heat required for generating one kg saturated steam in an evaporator $\Delta h_s = r_s - (1 + k_{rec}) \times \overline{c_w} \times x_3$, $\partial \Delta h_s / \partial z_3 < 0$. Due to steam output growth overheat rate Δt_{st} has a tendency to grow down; however it is ensured a slight higher amount of recovered heat in super-heater, i.e. $\Delta Q_{2_i} / Q_{2_i} \times 100\% \approx 3\%$. Despite of economizer part reduction in evaporator still hydrodynamic resistance of it $\Delta p_{hydr}^{z_1}$ has an explicit tendency of the growth up (see Fig.4.15), what requires to install circulating pump with higher both delivery head and electrical consumption in a result. Exhaust boiler aerodynamic resistance is dependent almost in direct ratio, i.e. $\Delta P_{g_i} \cong \Delta P_{g_i} + k_3^{\Delta P} \times \Delta z_{3_i}$ (see Fig.4.14), where value $k_3^{\Delta P}$ is economizer surface constant of proportionality. However, any equal economizer surface increase is accompanied with less increment in value ΔP_{g_i} than the same super-heater surface growth, i.e. $\partial \Delta P_{g_i} / \partial z_2 > \partial \Delta P_{g_i} / \partial z_3$, due to higher both mean gas temperatures in section $\overline{t_{g_1}} > \overline{t_{g_3}}$ and relevant linear gas velocity in a result. Finally, efficiency net outcome due to economizer

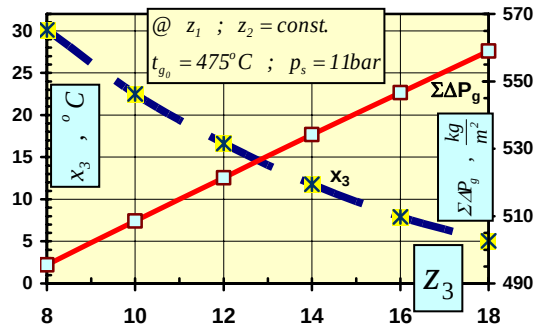

Fig.4.14 Economizer influence on EB x_3 temperature & aerodynamic resistance.

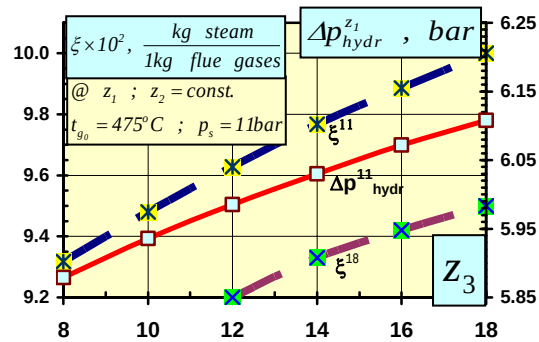

Fig.4.15 Economizer impact on EB steam output & evaporator hydraulic resistance.

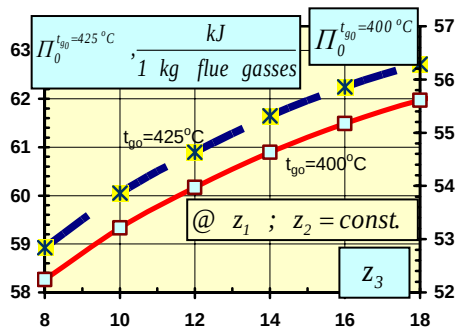

Fig.4.16 Economizer influence on WHRS efficiency - net output.

effect is ensured with following indices: $\partial \Pi_0 / \partial z_3 > 0 \,\&\, \partial^2 \Pi_0 / \partial (z_3)^2 < 0$, but within investigated limits the value Π_0 never reaches its maximum (see Fig.4.16). At the same time due to the safety matters we cannot indefinitely increase economizer surface in order to avoid feed water boiling in it, i.e. following restrictions are to be observed $t_e^{\max} < t_s$ or $x_3^{\min} = t_s - t_e^{\max} > 0$ at all long-term service conditions.

4.I.3. EVAPORATOR INFLUENCE AT UNLIMITED IT'S GROWTH.

Interrelation between evaporator z_1 heat exchange surface sizes and so called *pinch-point* $x_1 = t_{gs} - t_s$ is unequivocal (see Fig.4.17). At unlimited evaporator surface growth this temperature gap x_1 will tend to zero (see Fig.4.18), i.e. $\lim_{z_1 \to \infty} x_1 = 0$ or $\partial x_1 / \partial z_1 < 0$ and $\partial^2 x_1 / \partial (z_1)^2 > 0$, thus ensuring deeper gas cooling either. Based on equation as below $\xi = \dfrac{c_g \times (t_{g_0} - (t_s - x_1)) \times \eta_{al} + \xi_{sat} \times \Delta h_{st}}{\Delta h_{st} + \Delta h_S}$ it is evident, that EB steam output is inversely proportional to *pinch-point temperature*. So with the surface enlargement adequate recovered heat amount growth in evaporator is ensured - $\partial Q_1 / \partial z_1 > 0$, what leads to respective increase in ξ with following indices: $\partial \xi / \partial z_1 > 0$ and $\partial^2 \xi / \partial (z_1)^2 < 0$ (see Fig.4.17). Meantime it results in the more deep gas cooling rate in super-heater as well $\partial Q_2 / \partial z_1 > 0$ due to the $\xi \uparrow$ growth, thereby coming to heat transfer efficiency drop down in evaporator. On another hand

at lowered gas temperature after evaporator $\partial t_{g_s}(t_s + x_1)/\partial z_1 < 0$ heat transfer efficiency reduces in economizer either; and in combination with increased feed water flow amount $\partial \xi \times (1 + k_{rec})/\partial z_1 > 0$ the *approach* temperature x_3 will grow considerably $\partial x_3/\partial z_1 > 0$, thus enlarging economizer part in evaporator $h_s \cong r_s + \overline{c_{fw}} \times (1 + k_{rec}) \times x_3$ or $\partial h_s/\partial z_1 > 0$. These secondary post effects in both economizer and super-heater $\partial \Delta t_{st}/\partial z_1 < 0$ part of boiler decrease primary effect of evaporator surface enlargement on boiler efficiency parameters to some extent. The increment in surface sizes comes to adequate boiler aero-resistance increase as well. However some reduction in mean gas temperature in section $t_{g_1} = (t_{g_{sp}} \downarrow + t_{g_s} \downarrow\downarrow)/2$ ensures adequate diminution in the growth of this adverse effect either, but all the same almost direct dependence of value $\Delta P_g = f(z_1) = k_1^{\Delta} \times z_{1_i} + \Delta P_{g_0}$ is observed (see Fig.4.19). Hydraulic losses in evaporator Δp_1, being directly determined by surface sizes, are also dependent on the growth of relevant steam-water media velocity $(k_{circ} \times \xi)\uparrow$ due to boiler output increase. The raise of *approach* temperature x_3 also contributes the growth in hydraulic losses (see Chapter 3). Considering the total summarizing effect of these three main factors, evaporator hydro-resistance Δp_1 is found increasingly dependant on evaporator sizes as follows $-\partial(\Delta p_1)/\partial z_1 > 0$, $\partial^2(\Delta p_1)/\partial(z_1)^2 > 0$ (see Fig.4.19). Finally, net efficiency functional dependence $\Pi_0 = f(z_1)$ is found (see Fig.4.20), being directly contributed by steam output increase, while direct dependence of boiler aero-resistance comes to diminishing in the net gain. Some secondary reduction in efficiency growth is determined by steam overheat rate diminution

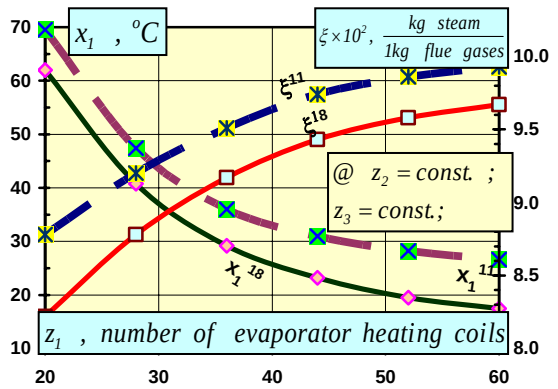

Fig.4.17 Evaporator inpact on *pinch point* x_1 & EB steam output at z_2, z_3 =const.

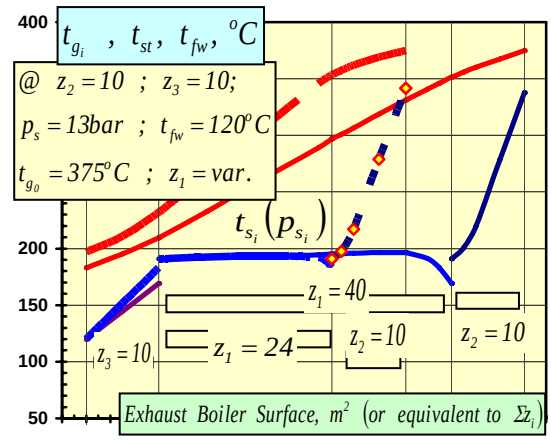

Fig.4.18. EB Temperature-surface diagram at variable evaporator sizes.

either due to $\xi\uparrow$, which is slightly compensated by some turbine efficiency increase due to higher mass flow through first stage. Still, in a result at some critical surface $z_1 = z_1^{crit}$ losses in ME will prevail over ST net output. With further rise of inlet gas temperature this critical surface has explicit tendency to grow up - $\partial z_1^{crit} / \partial t_{g_0} > 0$.

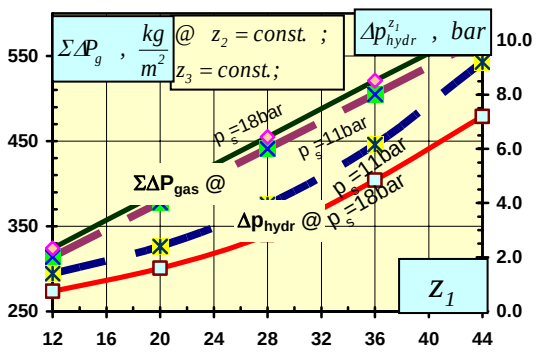

Fig.4.19. Aerodynamic & hydraulic loses dependence on evaporator sizes at fixed economizer & super-heater sizes.

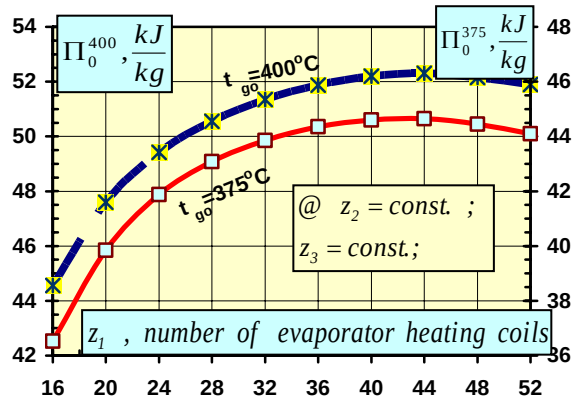

Fig.4.20. Exhaust Boiler Evaporator part influence on WHRS efficiency - net output.

4.I.4. POST FACTOR INFLUENCE ON POSSIBLE ECONOMIZER SURFACE CHANGES.

As concluded above with the growth of evaporator the increase in approach temperature is ensured $\partial x_3 / \partial z_1 > 0$ due to:

- steam output and respective feed water flow $((1+k_{rec})\times\xi)\uparrow$ rise via economizer and;
- economizer "offset" in the region of lowered temperatures $t_{g_{sp}} = (t_s + x_1\downarrow)\downarrow$ comes to temperature gradient reduction, i.e. mean log-temperature drop down $\Delta t_{LOG_1}\downarrow$;
- resulting in efficiency decrease of heat exchange process, i.e. reduction in $k_3\downarrow$.

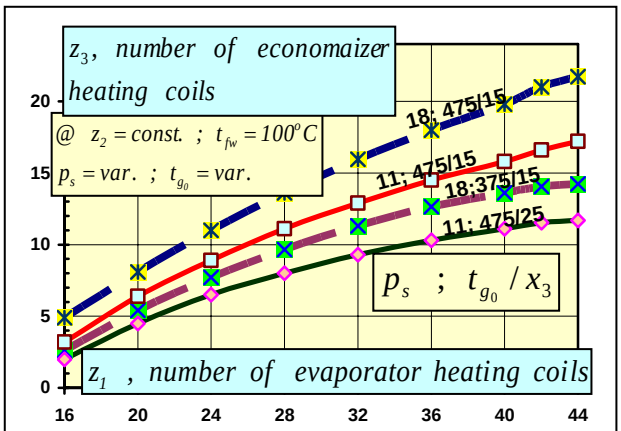

Fig.4.21. Evaporator impact on economizer sizes at fixed *approach* temperature.

At the same time the highest WHRS net efficiency rise is ensured by economizer, sizes of which are limited from the viewpoint of maintenance safety. i.e. $x_3 \geq 15^o C$. Thereby it becomes possible to enlarge economizer with the growth of evaporator $(\partial z_3 / \partial z_1)_{x_3=const.} > 0$ at fixed constant approach temperature level $x_3 = const.(=15^o C)$ (see Fig.4.21). Similar

effect is provided with steam pressure increase as recovered heat amount $Q_3 = (t_e - t_{fw}) \times (1 + k_{rec}) \times \overline{c_w^e}$ by economizer is dominantly dependent on its sizes z_3, what means that feed water temperature at economizer outlet will be almost constant value at the first approximation $t_e \cong const.$, while *approach* temperature will directly depend on pressure changes $x_3 \uparrow = t_s - t_e$ & $t_s \uparrow = f(p_s \uparrow) \Rightarrow t_s \uparrow - t_e = x_3 \uparrow$ at the same time. On another hand, the growth of pressure p_s will result in direct diminution of E steam output $\xi \cong \left(\left(t_{g_{sp}} - t_{g_{exh}} \right) \times \overline{c_g} / \left(h_s \uparrow - h^{|}_{fwp} \right) \right) \downarrow$. As a secondary effect of this ξ reduction is accelerated decrease of recovered gas heat due to exhaust temperature growth after boiler $t_{g_{exh}} \uparrow$. In a result *approach* temperature rise is slow down by boiler steam output respective changes. Anyway economizer enlargement is possible with the growth of steam pressure at fixed constant level of the approach temperature (see Fig.4.22). The growth of inlet gas temperature has similar effect on possible enlargement of economizer sizes at fixed level of $x_3 = const.(= 15^o C)$ either. In order to simplify our judgments we can consider that boiler consists of economizer and evaporator only, then produced steam output is found as per equation - $\xi \cong \left(t_{g_0} - t_{g_{exh}} \right) \times \overline{c_g} / \left(h_s - h^{|}_{fwp} \right)$, being in direct dependence on inlet gas temperature. On the first approximation, if *pinch-point* temperature x_1 is dominantly dependable on surface sizes z_1, then steam output could be determined accordingly - $\xi \cong \left(t_{g_0} - (t_s + x_1) \right) \times \overline{c_g} / r_s$ and its growth could be expressed as - $\Delta\xi \cong \Delta t_{g_0} \times \overline{c_g} / r_s$. In reality this *pinch-point* temperature x_1 is also directly dependable on heated media amount ξ; however, this tendency is being slow-down by higher heat exchange efficiency at the same time due to process offset in the region of higher temperatures, i.e. $t_{g_0} \uparrow$ and $\partial \overline{t_{g_i}} / \partial t_{g_0} > 0$, where $\overline{t_{g_i}}$ - mean gas temperature in respective surface. Then the boiler steam output changes could be expressed via equation - $\Delta\xi \cong \left(\Delta t_{g_0} - \Delta x_1 \right) \times \overline{c_g} / r_s$, or $\partial\xi / \partial t_{g_0} > 0$, despite of some temperature x_1 unequivocal, but still contradictory growth – $\partial x_1 / \partial t_{g_0} > 0$; $\partial^2 x_1 / \partial \left(t_{g_0} \right)^2 < 0$. The growth of ξ has direct influence on approach temperature x_3 as described above. Meantime with economizer performance in the region of higher temperatures $t_{g_{sp}} = \left(t_s + x_1 \uparrow \right) \uparrow$ the value x_3 increase extent is reduced due to higher heat exchange efficiency $k_3 \uparrow$. In a result it leads to

a possible growth in economizer surface providing the same safety margin (see Fig.4.23), i.e. $x_3 = const.(= 15^o C)$, i.e. $\partial z_3 / \partial t_{g_0} \big|_{x_3; z_1; z_2 = const.} > 0$.

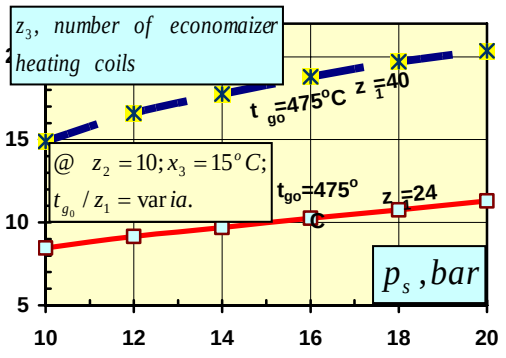

Fig.4.22 Evaporator impact on economizer sizes with changes at p_s constant *approach* temperature.

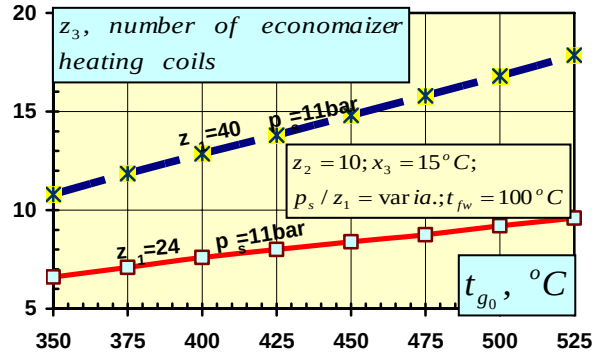

Fig.4.23 Evaporator influence on economizer surface in dependence on inlet gas temperature at fixed value of *approach temperature*.

4.I.5. CONCLUSIONS.

1. Efficiency value Π_0 is dependent on two contrary indices as - $\Pi_0 = \Pi - \Delta He_g$; and within investigated limits the growth of any convective surfaces provides efficiency increase with indices as below - $\partial \Pi_0 / \partial z_i > 0$ & $\partial^2 \Pi_0 / \partial (z_i)^2 < 0$.
2. Produced power equivalent by WHRS ST Π has tendency to reach its ultimate possible rate, i.e. $\lim_{z \to \infty} \Pi = \Pi^{max}$, while boiler aero-dynamic resistance is almost in direct ratio on heating coil amount $\Sigma \Delta P_{g_i} \cong \Sigma \Delta P_{g_0} + k_i^{\Delta P} \times z_i$.
3. The coefficient of proportionality $k_i^{\Delta P}$ for boiler gas resistance evaluation is dependent on mean gas temperature level in respective boiler section as - $k_2^{\Delta P} > k_1^{\Delta P} > k_3^{\Delta P}$.
4. Consequently, at some certain critical sizes of heat exchange surface z_i^{critic} further its enlargement is accompanied with WHRS net efficiency decrease, i.e. $(\partial \Pi_0 / \partial z_i)_{z_i = z_i^{crtic}} = 0$ or $(\partial \Pi / \partial z_i - \partial \Delta He_g / \partial z_i)_{z_i = z_i^{crtic}} = 0$.
5. Restriction in economizer surface increase is rather predetermined by boiler safe maintenance factors, i.e. $x_3 > 15^o C$, than by efficiency ones, as within investigated limits economizer contribution is always positive and the highest one - $\partial \Pi_0 / \partial z_3 > 0$ & $\partial \Pi_0 / \partial z_3 > \partial \Pi_0 / \partial z_1; \partial \Pi_0 / \partial z_2$.

6. Any dedicated boiler surface increase has an impact on another one; thereby at more developed evaporator it becomes possible to enlarge economizer part of boiler by observing the same safety margin $x_3 = const. \geq 15^o C$.
7. Similar economizer surface growth effect is ensured by relevant steam pressure changes, i.e. $\partial z_3 / \partial p_s \big|_{x_3 = const.} > 0$.
8. Finally, it is obtained such a boiler surface, after enlargement of which efficiency rise of power unit in the whole becomes negative. At this ultimate surface $\Sigma\left(z_i^{critic}\right)^{max}$ the highest efficiency of the power unit in the whole is achieved (see Fig.4.24).

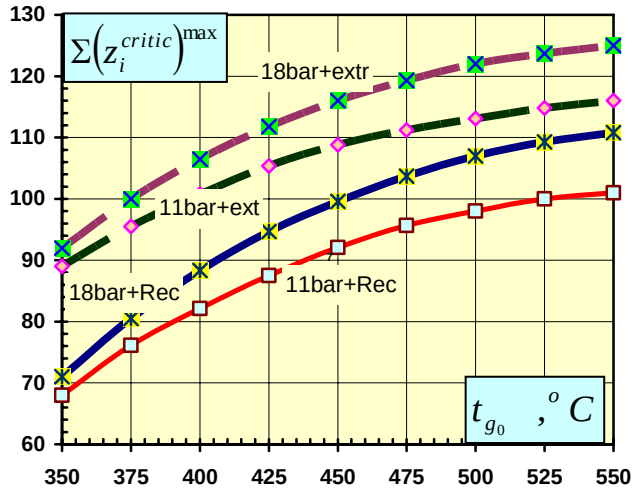

Fig.4.24. Dependence of maximum allowed EB summary surface, at which the ultimate highest thermodynamic efficiency of power unit in the whole is obtained, on inlet flue gas temperature for WHRS with feed water recirculation (*Rec*) & intermediate steam extraction (*extr*).

9. With the rise of inlet gas temperature more developed heat exchange surfaces of EB are required to recover effluent heat.
10. Despite the fact that WHRS with feed water recirculation was explored in our case, another alternative is presented also, i.e. WHRS with intermediate steam extraction for feed water heat up, being more thoroughly investigate later.

CHAPTER 4. SUB-CHAPTER 4.II. | OPTIMAL STEAM PRESSURE CHOICE FOR EXHAUST BOILER.

Steam pressure p_S is considered as one of the important particular, choice of which is justified either from viewpoint of some specific technical requirements or economical and efficiency aspects. Actually, boiler steam pressure optimisation is only one particular part of the whole task in achieving the highest output, thereby, it could be considered as completed one only, when all geometrical characteristics of tube and the bundle including thermal ones are optimised in determined and fixed boiler dimensions, its height $\Sigma H_i = const$.

4.II.1. PREAMBLE OF INVESTIGATIONS.

The proposed optimization of steam pressure is based on initially accepted exhaust boiler sizes, i.e. actually its total height $\Sigma H_i = \sum_{i=1}^{n(=3)} \Delta H_i + \Delta Hx$, or what is more true the real height of all boiler constituents (evaporator, economizer and super-heater) $H_i^{\Sigma z} = \sum_{i=1}^{n(=3)} \Delta H_i$, is that measure value of heat exchange surfaces on which is finally based our analyze. When the most favourable distribution of coils $\sum_{i=1}^{n(=3)} z_i$ amongst respective surfaces is chosen $z_2 : z_1 : z_3$ at $z_2 + z_1 + z_3 = const$, then steam pressure alteration is another possibility of power plant optimization till the highest efficiency of WHRS is achieved, to which certain optimal pressure will correspond $p_S = p_S^{opt}$. After that the goal of these researches is achieved.

WHRS efficiency is determined by the multiplication of two main indices $\Psi \times \eta_R$, i.e. flue gas cooling rate Ψ and the factor of steam (Rankine) cycle η_R, as below:

$$\Psi = \left(t_{g_0} - t_{g_{exh}}\right) / \left(t_{g_0} - t_a\right); \quad \eta_R = \left(h_{st} - h_x^{''}\right) / \left(h_{st} - h_x^{'}\right) \cong Ha / \left(h_{st} - h_x^{'}\right). \tag{4.1a}$$

The use of relative steam capacity ξ and the adiabatic enthalpy difference Ha is more practical and evident, as their multiplication characterizes ST net output $Ne_{ST} \sim \xi \times Ha$. In accordance with heat balance equations steam capacity is found equal to:

$$\xi \cong \frac{\left(t_{g_0} - t_{g_{exh}}\right) \times \overline{c_g} \times \eta_{al}}{h_{st} - h_x^{'}} = \frac{\left(t_{g_0} - t_{g_{exh}}\right) \times \overline{c_g} \times \eta_{al}}{\Delta h_{st} + \Delta h_s + \Delta h_e^{|}} \quad at \quad \overline{c_g} = const., \tag{4.2}$$

where $\overline{c_g}$ is the average meaning of the specific heat of exhaust gases, kJ/(kg×°C).

After product $\Psi \times \eta_R$ transformation the following equation is brought out:

$$\Psi \times \eta_R = \xi \times Ha / \left(\overline{c_g} \times \eta_{al} \times \left(t_{g_0} - t_a\right)\right) \quad or \quad \Psi \times \eta_R \sim \xi \times Ha . \tag{4.3}$$

In ideal occasion, when flue gases are cooled down till ambient air temperature, i.e. $t_{g_{exh}} = t_a$, the highest theoretically possible EB steam capacity ξ^0 is achieved. Then the utilization rate is reached as high as equal to $\Psi = 1$, which could be found as the division of two boiler capacities the real (#4.2) and theoretical ones either - $\Psi = \xi / \xi^0$. The achieved expression presents another explanation of flue gas cooling rate as the measure of value of steam capacity rate provided by particular WHRS (EB) against theoretically ultimate possible one.

When efficiency constituents of heat recovery circuit are determined, it becomes possible to explore their dependence on steam pressure fluctuations. But the aim of theses investigations is to find out such steam pressure meaning, to which the highest net gain by WHRS would be ensured, i.e. the highest steam turbine output. So this condition is met, when following expression becomes valid:

$$\partial\left(\Psi \times \eta_R\right) / \partial p_s\left(t_s\right) = 0 \quad or \quad \partial\left(\xi \times Ha\right) / \partial p_s\left(t_s\right) = 0 \tag{4.4}$$

4.II.2. PRESSURE INFLUENCE ON CYCLE QUANTITY INDICES.

Firstly, the pressure influence on cycle quantity characteristics Ψ, ξ should be studied out. So, boiler steam capacity could be evaluated either in accordance with the equation (4.2) or as below:

$$\xi \cong \left(t_{g_0} - \left(t_s + x_1\right)\right) \times \overline{c_g} \times \eta_{al} / \left(h_{st} - h_e^{|}\right) = \left(t_{g_0} - \left(t_s + x_1\right)\right) \times \overline{c_g} \times \eta_{al} / \left(\Delta h_{st} + \Delta h_s\right) \tag{4.5}$$

So called *pinch point* x_1, is the measure value of evaporator surface; and at it quite high developed sizes this temperature difference tends to zero, i.e. $\lim_{z_1 \to \infty} x_1 = 0$. Then on the first approximation steam output is directly conversely dependent on saturation temperature (or pressure p_s) changes $\partial\xi / \partial p_s\left(t_s\right) < 0$ (see Fig.4.25). At the same time, in real conditions value is always positive $x_1 > 0$; and the raise of steam pressure, followed by reduction in boiler steam output, ensures *pinch point* drop down as follows - $\partial x_1 / \partial \xi > 0$; and, subsequently, following

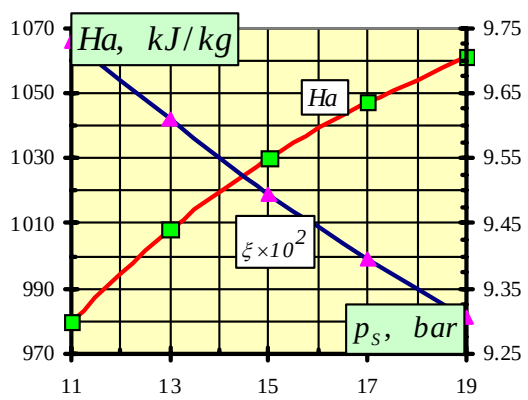

Fig.4.25 Steam pressure impact on EB output & iso-entropic enthalpy difference.

is valid - $\partial x_1/\partial p_s(t_s)<0,\ \partial^2 x_1/\partial p_s^2(t_s^2)>0$ (see Fig.4.26a, b). Such a secondary influence diminishes the impact of pressure p_s, t_s on steam capacity rate, i.e. ξ reduction is slow down by heat transfer efficiency increase. Furthermore, due to a little reduction in recovered gas heat amount by a super-heater (see Fig.4.27) $Q_2=\xi\times\Delta h_{st}/(\overline{c_g}\times\eta_{al}) \Rightarrow Q_2\sim\xi$ it results in some offset of the evaporator *working area* into a region of higher gas temperatures, which via a light increase in heat transfer efficiency ensures additional adequate diminution in x_1 meaning, thus coming to one more cut down of the pressure influence on EB steam output as following expression is valid $\partial\xi/\partial x_1<0$. Moreover, with the pressure raise specific heat, required to evaporate $\Delta h_s^{|}$ and overheat Δh_{st} 1 kg steam, has a tendency to drop off as well, thus even more amplifying the opposite, but still secondary effect on the dependence of $\xi=f(p_s)$ (see Fig.4.25). Irrespective of the fact that steam capacity ξ is the derivative value of flue gas cooling rate Ψ, nevertheless, we will separately try to study out the mechanism and substantiate its functional dependence on p_s pressure fluctuations. Based on the formula (#4.1a) it is quite evident, that only gas temperature changes at boiler outlet $t_{g_{exh}}$ are those, which have the impact on value Ψ at determined conditions. Temperature $t_{g_{exh}}$ is mainly defined by both the temperature at an evaporator outlet $t_{g_s}=t_s+x_1$ and recovered gas heat amount in an economizer. If the functional dependence of the first one value t_{g_s} is already well grounded, i.e. $\partial t_{g_s}/\partial p_s(t_s)>0$, then utilized heat extent in EB tail surface is found according formula:

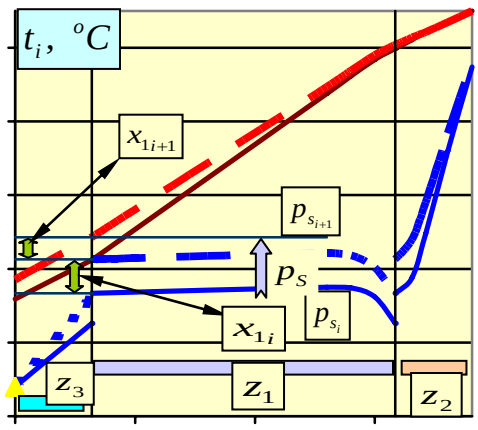

Fig.4.26a Temperature-boiler surface diagram at different steam pressure.

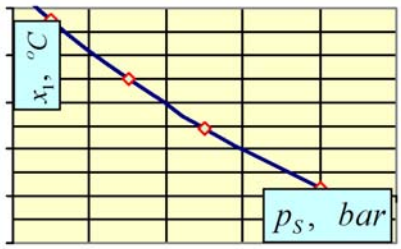

Fig.4.26b. *Pinch-point* dependence on steam pressure.

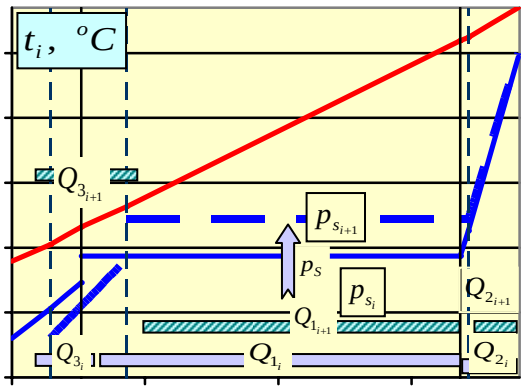

Fig.4.27 Temperature-Heat diagram at different steam pressure.

$$Q_3 = \left(\xi \times \Delta h_e^{|}\right) / \left(\overline{c_g} \times \eta_{al}\right) \tag{4.6}$$

According maintenance recommendations the *approach* temperature x_3 shall be kept at constant level not less than 15°C; in a result specific heat amount $\Delta h_e^{|}$ to warm up feed water in economizer until required temperature $t_e = t_s - x_3$ could be found as per equitation #4.7:

$$\Delta h_e^{|} = \left(1 + k_{rec}\right) \times \left(h_e^{|} - h_{fw}^{|}\right) \cong \left(1 + k_{rec}\right) \times \overline{c_w} \times \left(t_e - t_{fw}\right) = \left(1 + k_{rec}\right) \times \overline{c_w} \times \left(\left(t_s - x_3\right) - t_{fw}\right) \tag{4.7}$$

Further, specific heat amount $\Delta h_e^{|}$ could be divided in two contradictory variables, first one of which $\left(1 + k_{rec}\right)$ is fully dependable re-circulating coefficient, being found as follows - $k_{rec} = \left(h_s^{|} - h_{fwp}^{|}\right) / \left(h_s^{|} - h_{fw}^{|}\right)$; and in theoretical case, when saturated steam consumers are switch off, enthalpy before thermostatic mixing valve will be equally to that one in condenser, i.e. $h_{fwp}^{|} = h_x^{|}$ and $k_{rec} = \left(h_s^{|} - h_x^{|}\right) / \left(h_s^{|} - h_{fw}^{|}\right)$. Due to saturated steam characteristic *improvement* $\partial h_s^{|} / \partial p_s > 0$ required specific feed water amount to reach the same feed water temperature will drop down $\partial k_{rec} / \partial p_s < 0$. At constant feed water temperature $t_{fw} = const.$ another variable $\left(t_e - t_{fw}\right)$ is pre-determined by feed water temperature at economiser outlet t_e, which in its turn is the temperature difference between two contradictory constituents - $t_e = t_s - x_3$. Both values have a tendency to grow, but in different extent as follows - $\partial t_s / \partial p_s > \partial x_3 / \partial p_s > 0$, hence it results in pre-determined rise of values t_e and $\left(t_e - t_{fw}\right)$. Meantime, by both steam output reduction and the fact that due to some offset of the economizer working area into a region of higher gas temperatures (see Fig.4.27), what comes to a slight rise in heat transfer efficiency, it is ensured the diminution effect in the growth of the approach temperature x_3. Based on those substantiations, following changes are found valid - $\partial\left(1 + k_{rec}\right) / \partial p_s < 0,\ \partial\left(t_e + t_{fw}\right) / \partial p_s < 0$; and hence specific heat amount required for feed water warming up will be dependable as follows - $\partial h_e^{|} / \partial p_s > 0,\ \partial^2 h_e^{|} / \partial\left(p_s\right)^2 < 0$. Despite of some reduction in boiler steam output, still recovered gas heat amount by economizer Q_3 is dominantly defined by specific heat $h_e^{|}$ resulting in follows - $\partial Q_3 / \partial p_s > 0$ (see Fig.4.27). It becomes evident, that p_s rise comes to drop down in recovered gas heat by both evaporator Q_1 and super-heater Q_2, while in an economizer it Q_3 has a tendency for slight increase. After all that, total recovered gas heat by

EB $Q_i^{\Sigma} = Q_1 + Q_2 + Q_3$ has a tendency to go down, i.e. $\partial Q_i^{\Sigma} / \partial p_s < 0$. By joint solution of equitation (##4.2, 4.5) functional formula of gas outlet temperature is brought out as below:

$$t_{g_{exh}} = t_{g_0} - \left(t_{g_0} - \left(t_s + x_1\right)\right) \times \left(1 + k_e\right) = \left(1 - k_e\right) \times \left(t_s + x_1\right) - k_e \times t_{g_0}, where \quad k_e = \Delta h_e^{|} \Big/ \Delta h_{st} + \Delta h_s \quad (4.8)$$

and the coefficient k_e is the measure value of transferred heat in economizer against that summary one in both an evaporator and a super-heater. Based on acquired functional dependence the direct and dominant influence of pressure on gas cooling rate is evident, i.e. on exhaust gas temperature $t_{g_{exh}}$ (see Fig.4.28) and $\partial t_{g_{exh}} / \partial p_s(t_s) > 0$. Meantime some secondary and contrary impact slows down this alteration rate, firstly, due to *pinch-point* temperature reduction (see Fig.4.26b). Another factor- the coefficient k_e has a tendency to grow up with the pressure raise $\partial k_e / \partial p_s > 0$, thus even more cutting-off pressure influence. In a result second derivative of functional dependence $t_{g_{exh}} = f(p_s)$ will be slightly negative $\partial^2 t_{g_{exh}} / \partial p_s^2 (t_s^2) < 0$ (see Fig.4.28), thus pre-determining cooling rate indices as - $\partial \Psi(\xi) / \partial p_s(t_s) < 0$ and $\partial^2 \Psi(\xi) / \partial p_s^2 (t_s^2) > 0$.

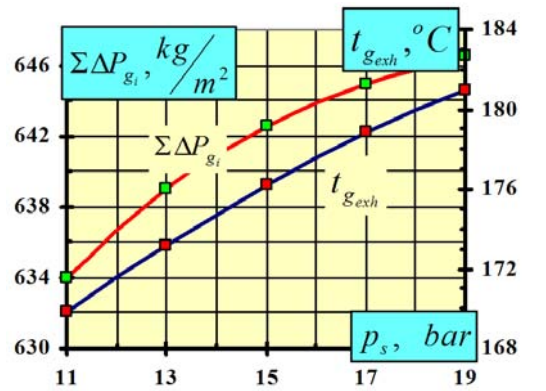

Fig.4.28 Steam pressure influence on gas cooling rate and boiler gas resistance.

4.II.3. PRESSURE INFLUENCE ON STEAM TURBINE CYCLE EFFICIENCY.

Meantime, another index of HRC efficiency, i.e. overall turbine cycle efficiency η_R, certainly grows up [9, 106, 111] - $\partial \eta_R / \partial p_s(t_s) > 0$ due to the respective increase in an adiabatic enthalpy difference Ha, which considerably depends on the pressure changes as follows: $\partial Ha / \partial p_s(t_s) > 0$, $\partial^2 Ha / \partial p_s^2 (t_s^2) < 0$ (see Fig.4.25). Moreover, due to reduced boiler capacity the slight increase in overheated steam temperature (see Fig.4.29) also contributes to the additional increment of the value Ha. Both effects have positive impact on the slight growth of turbine internal efficiency rate

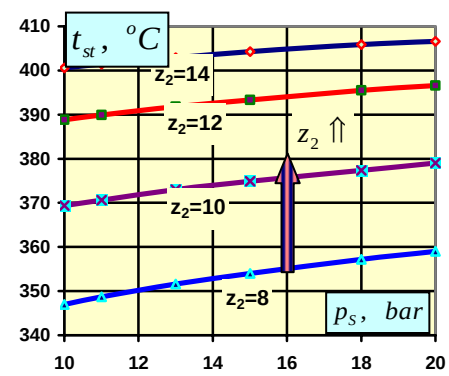

Fig.4.29 EB pressure influence on super-heated steam temperature.

η_{i_T}, $\partial\eta_{i_T}/\partial p_s > 0$, which favorably affects final cycle effectiveness as well. However, at higher pressure meanings and reduced steam capacity it leads to the rise in terminal losses on the first turbine stages, thus diminishing efficiency rate. Also with the pressure growth last turbine stages will be more affected by higher moisture content in exhaust steam, thus leading to both efficiency cut-down and wear-and-tear increase, which in its turn will adversely influence further reliable, e.g. possible stage unbalance, and effective turbine performance in a long run.

When the nature of each efficiency constituents $\Psi(\xi)$ and $\eta_R(Ha)$ have been thoroughly investigated, their common $\eta_R \times \Psi$ $(Ha \times \xi)$, but still contradictory impact (see Fig.4.25) in dependence on p_s changes should be estimated. Therefore, just concluding value Π is proposed for further explorations, which in fact represents steam turbine output; and it Π is the multiplication of above explored indices $\Pi = \eta_e \times Ha \times \xi$ *or* $\sim \Psi \times \eta_R$. Summing up final effects of all mutual interactions, the functional dependence $\Pi = f(p_s)$ is obtained, which in initial stage has a tendency to grow up with the pressure raise as follows - $\partial\Pi/\partial p_s(t_s) > 0$, $\partial^2\Pi/\partial p_s^2(t_s^2) < 0$ (see Fig.4.30). At some steam pressure level $p_{s_0}^{opt}$ positive effect due to iso-entropic efficiency increase is fully compensated by adverse steam output decrease extent, i.e. $\partial\xi/\partial p_s(t_s) + \partial Ha/\partial p_s(t_s) = 0$; and then the highest steam turbine output is achieved, i.e. $\Pi = \Pi^{max}$ and $\partial\Pi/\partial p_s(t_s) = 0$. Further steam pressure p_s growth will lead to evident efficiency cut down $\partial\Pi/\partial p_s(t_s) < 0$, $\partial^2\Pi/\partial p_s^2(t_s^2) < 0$. Thereby this particular task of WHRS optimization could be considered as accomplished for one chosen option, when at certain steam pressure level $p_{s_0}^{opt}$, considered as an optimal one, the highest ST output is achieved (see Fig.4.30) at definite boiler height (surface amount), thermic and other input dates as follows - $\sum_{i=1}^{n} z_i$, z_i, t_{g_0}, $t_{fw} = const.$

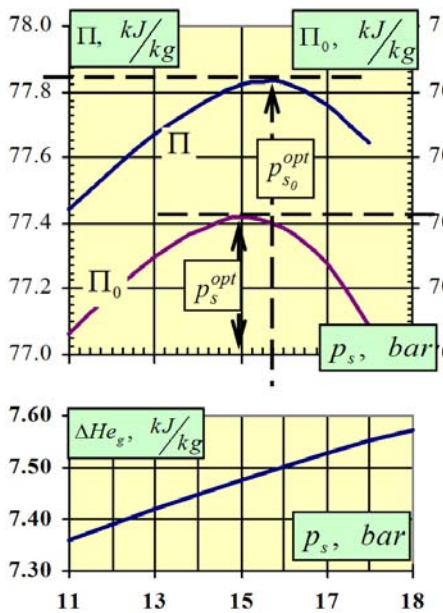

Fig.4.30 Steam temperature influence on WHRS efficiency.

Meantime, the presence of the boiler originates some backpressure $\Sigma\Delta P_{g_i}$ from gas side that adversely influences ME (gas turbine)

performance rate. This aerodynamic resistance is directly dependable on linear gas velocity, which in its turn is affected by mean temperatures in each section of respective surfaces. At the same time relevant pressure p_s (t_s) growth directly influences both outlet and average gas temperatures and EB gas resistance as well (see Fig.4.28). In a result the functional dependence of the commensurable value of power loses in the ME $\Delta He_g = f\left(\Sigma\Delta P_{g_i}\right)$ (see Fig.4.30) is found out with following alteration rate - $\partial\Delta He_g / \partial p_s(t_s) < 0,\ \partial^2\Delta He_g / \partial p_s^2\left(t_s^2\right) \approx 0$. Finally, the sum of these two efficiency Π, He_g values results in another one Π_0, representing the net increase in output generated by the power system in the whole, i.e. $\Pi_0 = \Pi - He_g$. As an outcome another magnitude of the optimal steam pressure p_s^{opt} is found, to which corresponds the highest Π_0 value. Considering the different alteration rate of efficiency parameters Π, He_g, i.e. $\partial^2 \Delta He_g / \partial p_s^2\left(t_s^2\right) \approx 0$ *and* $\partial^2 \Pi / \partial p_s^2\left(t_s^2\right) < 0$, it is found out, that the efficiency net value Π_0 will reach its maximum at another favorable pressure p_s^{opt}, which is lower (Fig.4.30) than the first one $p_{s_0}^{opt}$.

4.II.4. THE IMPACT OF HEAT EXCHANGE SURFACE GROWTH.

Further we will try to explore, how boiler surface increase influences the optimal steam pressure choice. To simplify carried out substantiations it could be considered that boiler consists of an evaporator only; and then the utilization rate will be found based on modified formulae #4.1a –

$$\Psi = \left(t_{g_0} - t_{g_{exh}}\right) / \left(t_{g_0} - t_a\right) = \left(t_{g_0} - \left(t_s + x_1\right)\right) / \left(t_{g_0} - t_a\right) \qquad (4.1b)$$

At fixed steam pressure level only the *pinch point* varies in dependence on boiler surface changes with following indices $\partial x_1 / \partial z_1 < 0$ *and* $\partial^2 x_1 / \partial z_1^2 > 0$ and, subsequently, utilization rate as $\partial\Psi / \partial z_1(\Sigma z_i) > 0$ *and* $\partial^2\Psi / \partial z_1^2\left((\Sigma z_1)^2\right) < 0$, while the steam cycle efficiency remains without any considerable changes at the constant pressure level. So, with the enlargement of EB surfaces $\sum_{i=1}^{n} z_i^k\left(z_1^k\right) + \Delta z_i^k = \sum_{i=1}^{n} z_i^{k+1}\left(z_1^{k+1}\right)$ even deeper flue gas cooling is ensured (see Fig.4.31) until temperature $t_{g_{exh}}^{k+1}$, resulting in the additional useful heat of steam cycle enclosed in the area $4 \to 4^{|} \to 3^{|} \to 3 \to 4$ ($\Delta\xi_k \sim \Delta T_k \times \Delta S_k$) and leading to adequate

growth in boiler steam output ($\partial\xi/\partial z_1(\Sigma z_i) > 0$). However, there is a possibility to provide steam pressure rise p_s^k in such degree (till p_s^{k+1}), that gained economy in $a \to 4^{II} \to 1^{II} \to 1 \to 4 \to a$ exceeds appearing losses enclosed in the area $a \to 4^{I} \to 3^{I} \to 3^{II} \to a$, what is justified until the fulfilment of the following equity - $(\partial\eta_R/\partial p_s)_{\sum z_i^{k+1}} + (\partial\Psi/\partial p_s)_{\sum z_i^{k+1}} \geq 0$ or $(\partial(\xi \times Ha)/\partial p_s)_{\sum z_i^{k+1}} \geq 0$. In addition, increased boiler steam output favorably affects the performance effectiveness of ST stages, especially the first ones. On the other hand both the pressure and the surface growth leads to appropriate changes in boiler gas resistance, thus making some corrections on the choice of the optimal pressure value. However, due to the deeper flue gas cooling $t_{g_{exh}}^{(k+1)^{opt}} < t_{g_{exh}}^{k}$ its average linear velocity drops down thus minimizing this adverse impact of EB aero resistance. Finally, it is found out that, with the growth of heat exchange surface the increase in the optimal steam pressure p_s^{opt} is ensured - $\partial p_s^{opt}/\partial z_1(\Sigma z_i) > 0$ (see Fig.4.32). Meantime, this tendency is restricted by deeper gas cooling rate, as temperature after an evaporator $t_{g_s} = t_s + x_1$ is that value, which greatly determines the level of the maximum attainable steam pressure. With a consideration of the equation #4.8 another one is found -

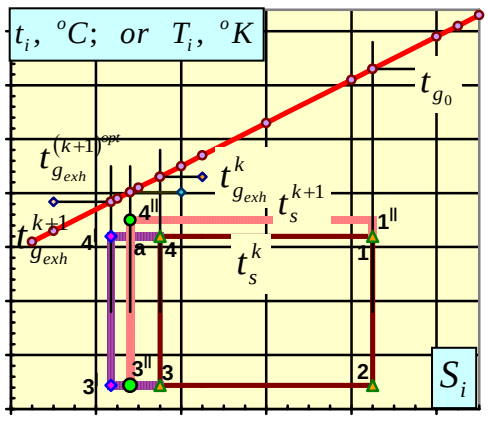

Fig.4.31 EB surface growth influence on optimal steam pressure choice.

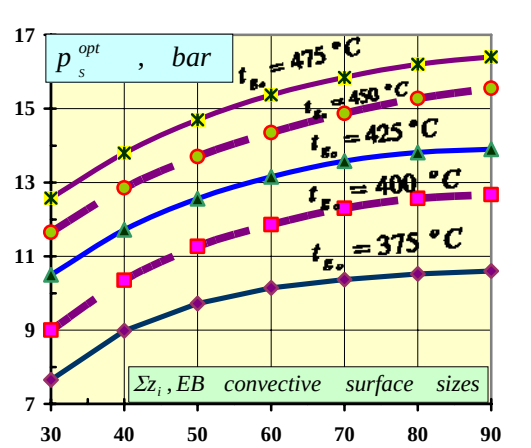

Fig.4.32 EB surface/temperature impact on optimal steam pressure choice.

$$t_s = t_{g_0} \times \left(k_e^{-1} - 1\right)^{-1} + t_{g_{exh}} \times (1 - k_e)^{-1} - x_1, \tag{4.9}$$

which demonstrative shows the dependence of steam pressure on inlet and outlet gas temperatures. If at unlimited surface the *pinch point* is equally to zero, i.e. $\lim_{z_1 \to \infty} x_1 = 0$, then the equation (4.9) reflects changes of the ultimate theoretically possible pressure $p_s^{\max}$ as follows - $\partial p_s^{\max}(t_s^{\max})/\partial t_{g_{exh}} < 0$, $\partial^2 p_s^{\max}(t_s^{\max})/\partial(t_{g_{exh}})^2 < 0$; and as to some extent the equity

sign could be inserted between outlet gas temperature and the surface amount, then in real conditions for definite boiler sizes value p_s^{opt} has a tendency to attain respective limit of $p_s^{\max}\left(t_s^{\max}\right) = f\left(t_{g_{exh}}\right)$ (see Fig.4.33). The fact, that the highest gas cooling rate $t_{g_{exh}}$ is naturally restricted by ambient conditions and feed water temperature at boiler outlet, predetermines the tendency of ultimate steam pressure that tends to some lowest theoretical level as per equation #4.9. On another hand this preconditions pre-determines the upper limit of optimal pressure changes, which with the growth of heating coil amount aspire to its possible maximum $\lim\limits_{\sum z_i \to \infty} p_s^{opt} = p_s^{opt^{MAX}} = const.$; and, subsequently, second fluxion of functional dependence $p_s^{opt} = f\left(\sum z_i\right)$ will be equal to - $\partial^2 p_s^{opt} / \partial\left(\Sigma z_i\right)^2 \left(z_1\right) < 0$.

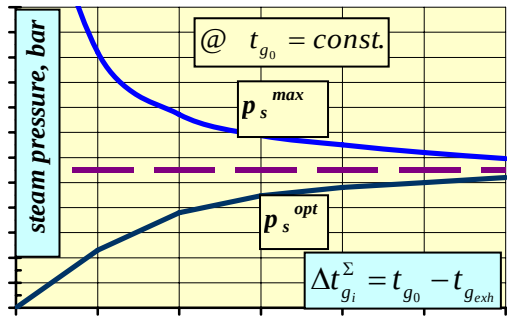

Fig.4.33 EB surface influence on optimal & ultimate steam pressure level.

4.II.5. INLET GAS TEMPERATURE FACTOR.

By increasing of inlet gas temperature t_{g_0}, which is dependable on either ME type or its load level, the additional appearing usefully recovered heat in comparison with the base option exceeds negligible losses caused by some *pinch point* rise (see Fig.4.34), which is dominantly determined by an evaporator sizes. Both cases, whether the surface enlargement or the temperature growth is ensured, are very similar due to the availability of additional heat extracted from flue gasses, what makes in general same conclusions and regularities applicable. The only difference lies in the potential of this heat located at the beginning ($t_{g_0} \uparrow$) or at the end ($\sum z_i \uparrow \left(z_1 \uparrow\right)$) of the temperature chart; hence the higher outlet temperature $t_{g_0} > t_{g_0}^{j}$ (see Fig.4.34) is that condition, when possible raise in steam pressure is ensured to a rather great extent. Moreover as per the equitation #4.9 the growth in the *upper limit* $p_s^{\max}\left(t_s^{\max}\right)$ is more considerable, thus determining respective level of favorable steam pressure either. By concluding above another similar functional dependence is brought out - $p_s^{opt} = f\left(t_{g_0}\right)$ with next indices $\partial p_s^{opt} / \partial t_{g_0} < 0$; $\partial^2 p_s^{opt} / \partial\left(t_{g_0}\right)^2 < 0$ (see Fig.4.35).

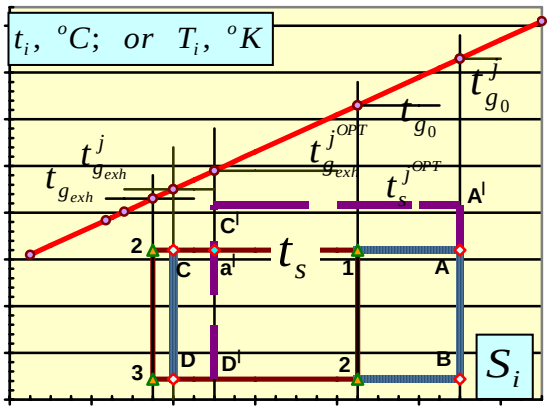

Fig.4.34 Inlet gas temperature impact on optimal steam pressure choice.

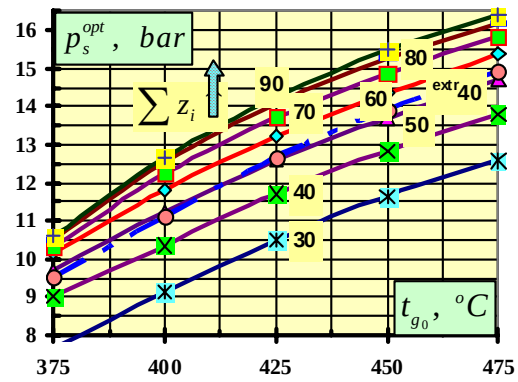

Fig.4.35 Inlet gas temperature impact on optimal steam pressure choice.

4.II.6. POST-EFFECTS.

Some aspects of joint steam pressure and evaporator influence on efficiency parameters of WHRS already partly discussed before; but we will try to develop explorations of this effect. Our conclusions will be based on dominant correlative impact between evaporator and economizer only, while super-heater impact could be omitted due to their insignificance. Steam pressure increase almost directly influences *approach* temperature x_3 alteration rate as follows $\partial x_3/\partial p_s > 0$ (see Fig.4.36 a), being affected by both economizer and evaporator sizes as well (see Fig.4.36 b). As it was stated before, at fine boiler surface tuning economizer enlargement provides the biggest beneficial impact on efficiency growth

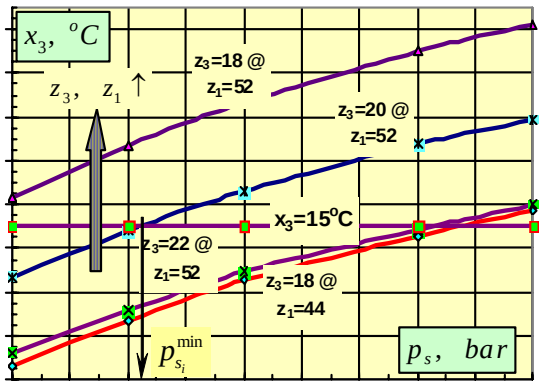

Fig.4.36a. Pressure & economizer surface impact on *approach* temperature.

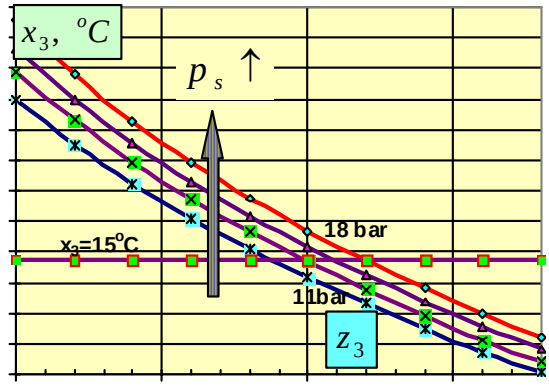

Fig.4.36b. Pressure & economizer surface impact on *approach* temperature.

$\partial \Pi_0/\partial z_3 > \partial \Pi_0/\partial z_1(z_2)$, being limited only by safety aspects $x_3 \geq 15^o C$, to which corresponds some lowest steam pressure meaning $p_{s_i}^{min}$. Then with a pressure rise by Δp_s consequently economizer surface could be more extended at accepted invariable *approach* temperature (see Fig.4.37 a), i.e. $\partial z_3/\partial p_s > 0|_{x_3=const.}$; and at new increased pressure p_s^j

possible surface enlargement will be equal to value Δz_3 or $\overline{\Delta z_3}$ (see Fig.4.37b). Meantime,

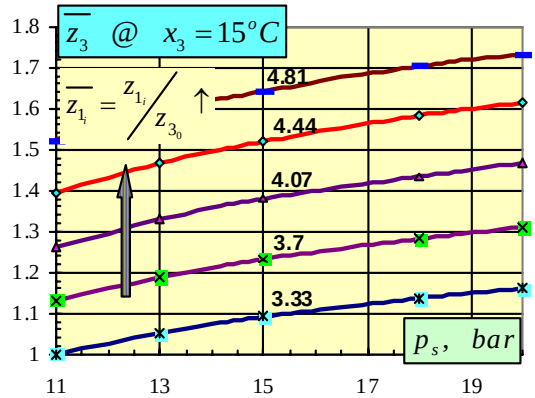

Fig.4.37a. Pressure impact on economizer surface at constant *approach* temperature.

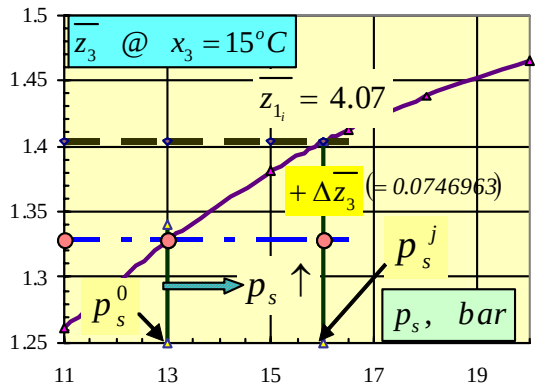

Fig.4.37b. Pressure impact on economizer surface at constant *approach* temperature.

evaporator and economizer sizes are in direct correlation (see Fig.4.38a), when the increase of the first one leads to respective changes in another one. However, at initially accepted condition, when total EB surface dimensions are to be invariable, i.e. $z_1 + z_3 = const.$; then this possible economizer enlargement $\overline{\Delta z_3}$ $(= 0.0746963)$ is to be compensated by adequate reduction in evaporator surface - $\overline{z_1} - \overline{\Delta z_3} = \overline{z_1^{j-1}}$, to which will correspond economizer with slightly reduced sizes of that one initially increased, i.e. $\overline{z_3} + \overline{\Delta z_3} = \overline{z_3^{j-1}} \Rightarrow -\overline{\delta\Delta z_3} \Rightarrow \overline{z_{3_i}^{j-1}}$ at constant *approach temperature*. In a result of these interactions, required economizer sizes, that correspond to new conditions, i.e. $\overline{z_1^{j-1}} = \overline{z_1} - \overline{\Delta z_3}$, $x_3 = const.$ and $p_s^j = p_s + \Delta p_s$, should be slightly reduced by value equally to $\overline{\delta\Delta z_3} = (0.0313472)(< \overline{\Delta z_3})$ (see Fig.4.38b). Consequently, total EB dimensions will be accordingly less than initially accepted as follows- $\left(\left(\overline{z_3} + \overline{\Delta z_3}\right) - \delta\overline{\Delta z_3}\right) + \left(\overline{z_1} - \overline{\Delta z_3}\right) < \overline{z_1} + \overline{z_3}$ at $x_3 \geq 15^oC$ (see Fig.4.38b). So, at this stage there is left free surface $\overline{\delta\Delta z_3}$, which is to be somehow utilized. Based on conclusions above, another functional dependence of $p_s = f\left(\overline{z_1} + \overline{z_3}\right)$ at $\overline{z_{1_i}} = const.$, $x_3 = const.(= 15^oC)$ so called *iso-evaporator surface line* is brought out that would foreseeable display the mechanism of theses interdependencies (see Fig.4.39.b) from another point of view. The line a_0 corresponds to initially chosen evaporator surface $\overline{z_{1_0}} = 4.074$ and in the point $(.)1$ to fixed total surface $\left(\overline{z_1} + \overline{z_3}\right)_0 = 5.40278$ at $p_s = p_{s_0}(= 13bar)$ and $x_3 = const.(= 15^oC)$. In order to increase pressure by Δp_s at $\overline{z_{1_i}} = const.$, $x_3 = const.(= 15^oC)$ from point $(.)1$ till $(.)2$ economizer is to be enlarged by value $\overline{\Delta z_3}$ as above, but in order to meet conditions of explorations that

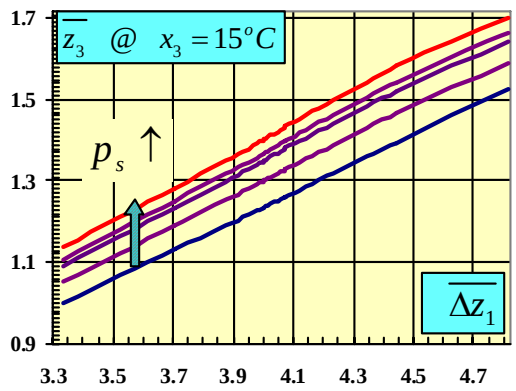

Fig.4.38a Evaporator impact on economizer at $x_3 = const.@\ p_s = \text{var}$.

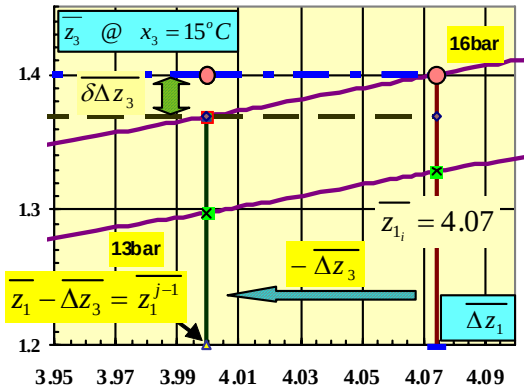

Fig.4.38b Mutual evaporator & economizer impact on their sizes at $x_3 = const.$

are carried out, i.e. $\left(\overline{z_1} + \overline{z_3}\right)_i = const.$, evaporator surface is to be reduced by the same value, i.e. from $(.)2$ till $(.)3$ on another *iso-evaporator line* a_1 at $\overline{z_{1_i}} = 3.968$ and at higher pressure $p_{s_1} = p_{s_0} + \Delta p_s$. Meantime to retain *safety factor* invariable, i.e. $x_3 = const.$, also economizer surface should be slightly diminished by $\overline{\delta\Delta z_3}$ as above. However, in order to fulfill terms of explorations, i.e. $\left(\overline{z_1} + \overline{z_3}\right)_i = const.$ and $x_3 = const.\left(= 15^oC\right)$, it becomes possible by further both economizer and pressure rise upwards *iso-evaporator* line a_1 till the $(.)4$ (see Fig.4.39.b). In reality these surface changes could be more complicated

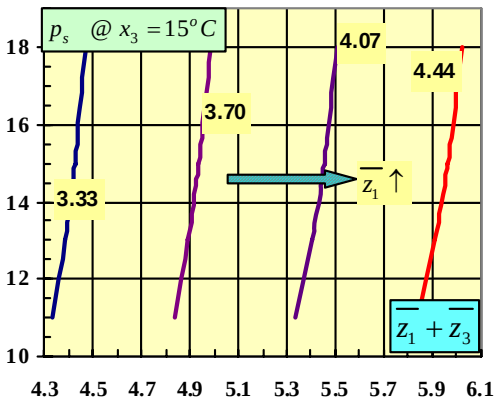

Fig.4.39a. Steam pressure dependence on boiler surface sizes at $x_3 = const.$

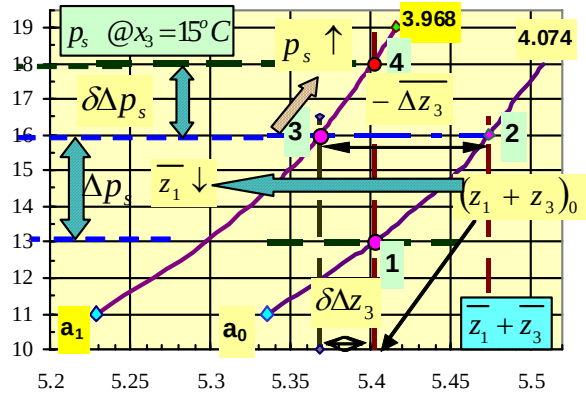

Fig.4.39b. Steam pressure alterations at $x_3 = const.$ to keep $z_1 + z_3 = const.$

accompanied with the partial shift into evaporator surface enlargement. Finally, following algorithm of correlative EB surface impact due to steam pressure raise is elaborated as below:

1. Accepted pre-conditions - $x_3 \geq 15^oC$; $\overline{z_1} + \overline{z_3} = const.$; disregard of super-heater influence due to its insignificance;

2. $p_s \uparrow + \Delta p_s \Rightarrow \Delta z_3 \uparrow \Rightarrow (z_3 + \Delta z_3) + z_1 > z_3 + z_3$, as per line a_0 till $(.)2$ (see Fig.4.39.b);
3. to observe $\overline{z_1} + \overline{z_3} = const. \quad \Rightarrow z_1 \downarrow by - \Delta z_3 \Rightarrow x_3 \downarrow \quad at \quad new \quad (z_1 - \Delta z_3) + (z_3 + \Delta z_3)$;
4. to maintain $x_3 = const. \quad (z_3 + \Delta z_3) \downarrow \quad by \quad \delta \Delta z_3$, but then $\left(\left(\overline{z_3} + \overline{\Delta z_3}\right) - \delta \overline{\Delta z_3}\right) + \left(\overline{z_1} - \overline{\Delta z_3}\right) = \overline{z_3^{j-1}} + \overline{z_1^j} < \overline{z_1} + \overline{z_3}$;
5. therefore at new $\overline{z_1^j} = \left(\overline{z_1} - \overline{\Delta z_3}\right)$ economizer shall be enlarged $\overline{z_3^{j-1}} + \delta \overline{\Delta z_3} = \overline{z_3^j} \Rightarrow$
   $\Rightarrow \overline{z_3^j} + \overline{z_1^j} = const.$ but to observe $x_3 = const. \Rightarrow (p_s + \Delta p_s) \uparrow \quad by \quad \delta \Delta p_s$.

What is the nature of such a complex interaction? As described above pressure raise directly influences steam cycle quality index Ha growth, while recovery rate and its present value steam output ξ decreases, however, being slow-down by reduction of specific evaporation heat r_s. By such EB surface re-distribution total heat for evaporation $h_s = r_s + k_{rec} \times \overline{c_w} \times x_3$ is being reduced yet more due to minimizing of economizer part in evaporator $\left(k_{rec} \times \overline{c_w} \times x_3\right) \downarrow$, as required amount of re-circulated water for feed water temperature warm up is diminishing as well, i.e. $k_{rec} = \left(\left(h'_{fw} - h'_{fwp}\right) / \left(h'_s(\uparrow) - h'_{fw}\right)\right) \downarrow$.

4.II.7. CONCLUSIONS.

1. In order to achieve the highest efficiency of the WHRS the optimization of the steam pressure value is one of the possibilities, which contradictory influences on the cooling rate Ψ and the effectiveness of the Rankine cycle η_R.
2. In the result two values of the favourable steam pressure are found. The first one value $p_{s_0}^{opt}$ ensures the highest output of ST.
3. The choice of second value p_s^{opt} is important in order to provide the highest effectiveness of the power plant in the whole.
4. Both values $p_{s_0}^{opt}$, p_s^{opt} are directly dependent on the growth of both EB surfaces $\sum_{i=1}^{n} z_i$ and the inlet gas temperature t_{g_0}, but in different rate (see Fig.4.32, 4.36).
5. With the pressure raise economizer part is becoming more developed.

CHAPTER 4. SUB-CHAPTER 4.III. FINE HEAT-EXCHANGE SURFACE OPTIMISATION OF EXHAUST BOILER WITHIN FIXED DIMENSIONS.

4.III.1. PREAMBLE OF INVESTIGATIONS.

When optimal steam pressures $p_{s_0}^{opt}$, p_s^{opt} are found at fixed EB surfaces, i.e. its height $\Sigma H_i = \sum_{i=1}^{n(=3)} \Delta H_i + \Delta Hx$, fine optimization of WHRS efficiency indices are to be carried out by mutual correlation of all boiler constituents (evaporator, economizer and super-heater). For true heat exchange, i.e. tube bundle, surface height $H_i^{\Sigma z} = \sum_{i=1}^{n(=3)} \Delta H_i$ or its representative and practical value, i.e. the total number of heating coils $\sum_{i=1}^{n(=3)} z_i$, some unique surface distribution $(z_2 + z_1 + z_3)^{opt} = const.$ shall be find out, at which the highest output Π, Π_O generated by WHRS is obtained, by observing maintenance safety conditions, i.e. $x_3 \geq 15^o C$. In order to find this optimal surface relation it is necessary to explore the impact on efficiency indices of one of them on account of another surface, i.e. if, e.g., super-heater is enlarged on account on either evaporator or economizer.

4.III.2. MUTUAL ECONOMIZER AND EVAPORATOR IMPACT.

At fixed sizes of super-heater surface $z_2 = const.$ correlative dimensional changes of both evaporator and economiser are possible as follows- $(z_1 \mp \Delta z_i) + (z_3 \pm \Delta z_i) = const$. By $\Delta z_3^{1\to3}$ enlarging economiser $z_3^{1\to3} = z_{3_0} + \Delta z_3^{1\to3}$ at the expense of evaporator $z_1^{1\to3} = z_{1_0} - \Delta z_3^{1\to3}$ (see Fig.4.40) at the condition of $p_s = const.$, the *pinch-point* temperature x_1 has a tendency to grow up thus adversely affecting steam output (see Formula #4.5). At the same time accelerated decrease in *approach* temperature is dominant in EB capacity growth $\partial\xi / \partial\Delta z_3^{1\to3} > 0$ due to *economizer part* diminution in specific heat for evaporation $\Delta h_s \downarrow$. In a result deeper gas cooling rate $t_{g_{exh}} \downarrow$ is obtained, however some slight reduction in steam over-heat rate $t_{st} \downarrow$ as well as. Meantime to provide that condition $x_3 \geq 15^o C$ is observed it becomes necessary to raise steam pressure $p_s \uparrow (t_s \uparrow)$ till to which saturation temperature growth Δt_s would be equal to the *approach one* $-\Delta x_3^{1\to3}$,

i.e. $\left|\pm \Delta x_3^{1\to 3}\right| \approx \left|\mp \Delta t_s\right|$ on the first approximation. But then as per equation #4.5, EB output has a tendency to grow down, thus coming to even more pressure increase to maintain boiler safety, i.e. $x_3 \geq 15^o C$ (see Fig.4.39, 4.40 and sub-chapter 4.II). Some slight reduction in both *pinch-point* temperature $\partial x_1 / \partial p_s < 0$ and specific heat for saturated steam generation compensates further required steam pressure growth due to positive impact on value x_3 via steam output rate. Finally, based on summarization of all contradictory effects within investigated limits relevant boiler output changes are found around equally to – $\delta\xi \approx -(1.3 \div 1.6\%)$ *at* $\Delta z_3^{1\to 3} = 1$, & $x_3 = const$. Due to these alterations, exhaust gas temperature at EB outlet has a tendency to grow, thus reducing recovery rate $\Psi \downarrow$. In a result reduced steam capacity, i.e. $\partial\xi / \partial \Delta z_3^{1\to 3} < 0\big|_{x_3 = const.}$, contributes to slight increase of steam overheat rate, i.e. $t_{st} \uparrow$ (see Fig.4.40), and with the pressure raise it results in noticeable growth of cycle quality indices, such as iso-entropic enthalpy difference $Ha \uparrow$, which within investigated limits constitutes around - $\delta Ha \approx -(2.3 \div 2.9\%)$ @ $\Delta z_3^{1\to 3} = 1$ & $x_3 = const$. Alterations in internal efficiency index η_{ST} of ST are contradictory, as reduced steam output at higher pressure originates more terminal loses in the first stage; however just those positive changes in steam quality indices dominantly determines internal efficiency η_{ST} slight increase. Meantime, last turbine stages will be more affected by steam with higher humidity content, deteriorating unit safety in long run, as pressure changes are not adequate with steam overheat rate ones. Due to higher mean gas temperature boiler aero-resistance has tendency to grow up, thus diminishing main engine output. Consequently, such a surface adjustment ensures higher efficiency of the steam cycle, ultimately removing the reasons for lowering its quantity parameters.

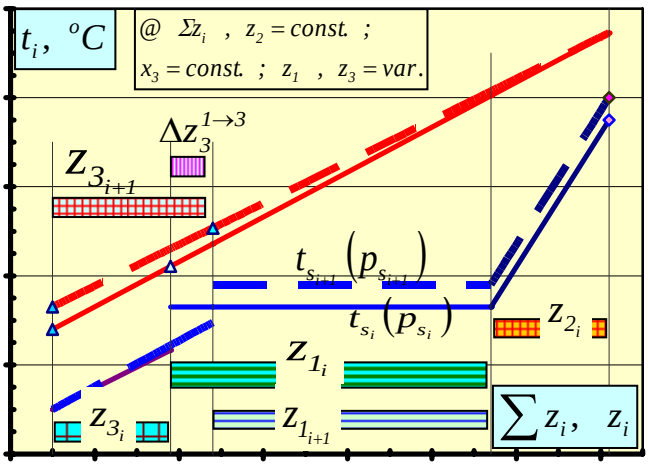

Fig.4.40. Economizer & evaporator mutual impact.

4.III.3. MUTUAL SUPER-HEATER AND EVAPORATOR IMPACT.

The reciprocal distribution of surfaces under the condition, when $z_3 = const.$ (see Fig.4.41.), is possible by altering them as follows - $(z_1 \pm \Delta z_i) + (z_2 \mp \Delta z_i) = const$. At condition of $p_s = const.$ any enlargement of the evaporator at the expense of the super-heater by some value $\Delta z_1^{2\to1}$ (see Fig.4.41.) leads to increased boiler steam output $\xi\uparrow$ and gas cooling rate in a result $\Psi\uparrow$, $t_{g_{exh}}\downarrow$, thus pre-determining some minor reduction in boiler aero-resistance $\sum \Delta P_{g_i}\downarrow$ either. Due to *approach* temperature growth $x_3\uparrow$, caused not only by feed water amount increase, but also due economizer offset in the region of lowered gas temperatures $\partial\overline{t_{g_3}}/\partial\Delta z_1^{2\to1} < 0$, steam capacity raise is being slow down. The influence of both factors as smaller super-heater surface sizes and increased steam quantity indices leads to quite considerable reduction in cycle quality factors, i.e. t_{st}, $Ha\downarrow$. In order to meet the condition $x_3 = const.$ it is necessary to reduce selected steam pressure (see Fig.4.41), thus further contributing the value $\xi\uparrow$ increase (see equation #4.5) despite of some increment in specific heat for evaporation. At the same time due to heat exchange efficiency drop down the *pinch-point* has a tendency to grow slightly less thus resulting in slow-down of steam output raise, the impact of which however is still insignificant in comparison with primary causes, i.e. $z_1\uparrow$ & $p_s\downarrow$. These changes ensure even more deep gas cooling rate; and mean temperature reduction in section $\overline{t_{g_i}}\downarrow$ results in adequate diminution of boiler gas resistance $\sum \Delta P_{g_i}\downarrow$ either. On another hand, cycle quality factors grow down even more due to both lowered superheated steam temperature $t_{st}\downarrow$ (caused by $\xi\uparrow\uparrow$) and in a result considerable drop down of specific iso-entropic expansion work $Ha\downarrow\downarrow$. Despite of pressure

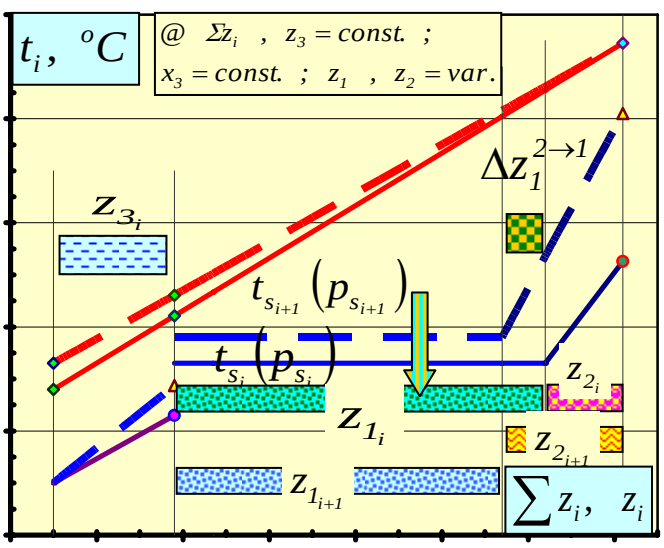

Fig.4.41. Super-heater & evaporator mutual impact.

reduction still exhaust steam dryness is coming down, as well as turbine internal efficiency rate $\eta_{ST}\downarrow$.

4.III.4. MUTUAL SUPER-HEATER AND ECONOMIZER IMPACT.

When evaporator is accepted invariable $z_1 = const.$, it becomes possible to alter other two constituents as follows - $(z_3 \pm \Delta z_i) + (z_2 \mp \Delta z_i) = const$. At initially accepted $p_s = const.$ the enlargement of the economiser $\Delta z_3^{2\to3}$ at the cost of the super-heater (Fig.4.42) leads to a rapid drop of the value x_3, thus ensuring steam output increase via *economizer part* reduction in required specific heat for evaporation as follows - $\Delta h_s = r_s + (1 + k_{rec}) \times \overline{c_w} \times x_3 \downarrow$ or $\Delta h_s = f(x_3)$ at accepted conditions and finally $\partial(\Delta h_s)/\partial \Delta z_3^{2\to3} < 0$. It has a positive impact on the growth of steam cycle quality indices t_{st}, $Ha\downarrow$. At the same time the condition of $x_3 = const.$ shall be observed therefore it becomes necessary to increase initially chosen steam pressure $p_s + \Delta p_s = p_{s_{i+1}}$ (see Fig.4.42.), that keeps the initial steam output changes on a minimum level also due to decrease of required heat for evaporation.

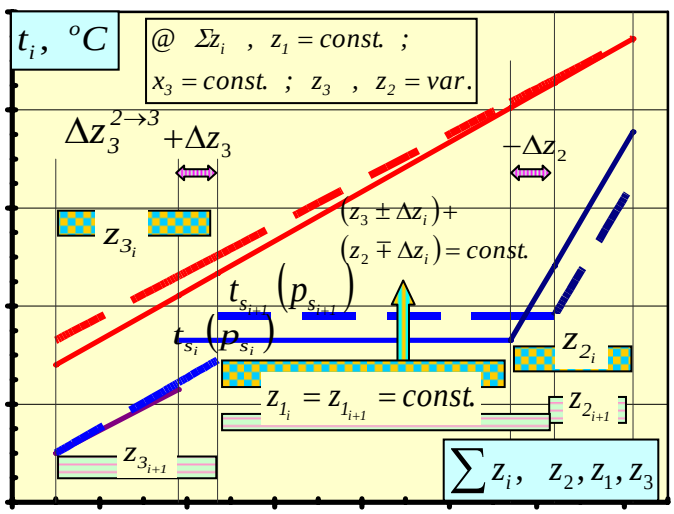

Fig.4.42 Super-heater & economizer mutual impact.

However, despite of steam overheat temperature reduction still adiabatic heat difference grows up $\partial Ha/\partial \Delta z_3^{2\to3} > 0\big|_{x_3=const.}$ due to dominant impact by relevant pressure changes, what finally results in increased relative humidity of the exhaust steam. Although economiser surface is enlarged, flue gas cooling rate is still slightly diminishing, because of the prevailing alterations in steam pressure –

$$t_{g_{exh}} = t_{g_0} - \left(t_{g_0} - \left(t_s(\uparrow) + x_1\right)\right) \times (1 + k_e), \tag{4.10}$$

where the coefficient $k_e = \Delta h_e^{|} / (\Delta h_{st} + \Delta h_s)$ represents economizer heat capacity in EB.

In a result it is noticed slight increase in boiler gas resistance.

4.III.5. OPTIMAL SURFACE RE-DISTRIBUTION AT ITS ADDITIONAL ENLARGEMENT.

When additional space, i.e. height, for boiler installation with increased dimensions is found available for new one project found, the total number of heating coils could be increased as follows - $\left(\sum_{i=1}^{n(=3)} z_i = const.\right) + \Delta z_j = \left(\sum_{i=1}^{n(=3)} z_i\right)_{j+1} = const_{j+1}$. As already concluded before economizer sizes will be those, which should be enlarged first of all; however dimensions of it z_3 are limited for safety reasons. Thereby initial evaporator enlargement $z_1 \uparrow$ is obvious followed by subsequent z_3 increase as follows - $(\partial z_3/\partial z_1)_{x_3=const.} > 0$, provided that condition $x_3 = const. \geq 15^o C$ is met (see Fig.4.43). Any additionally available heating coil amount Δz_j would be distributed as per equation -

$$\Delta z_3^j = \Delta z_j \times \left((\partial z_3/\partial z_1)^{-1}_{x_3=const.} + 1\right)^{-1}.$$

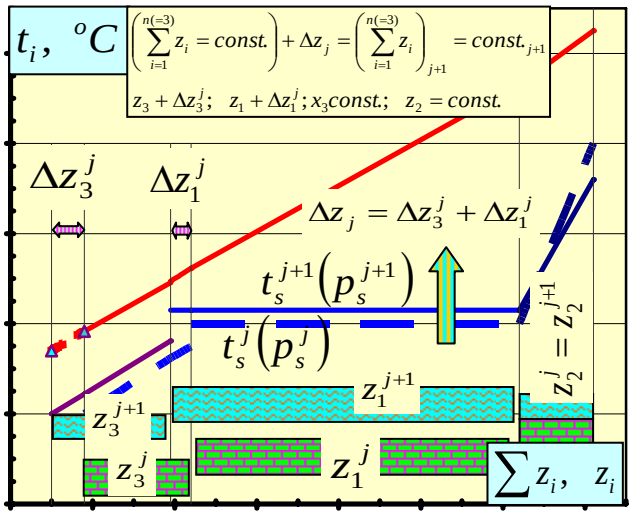

Fig.4.43 Surface enlargement impact.

Meantime as explored above for more developed surfaces optimal steam pressure level is higher; and then influence of both values $t_s \uparrow$, $\xi \uparrow$ pre-determines dominant possible economizer enlargement at the expense of other boiler constituents. Despite that specific iso- entropic expansion work $Ha \uparrow$ is increasing steam overheat rate is growing down as well as dryness of exhaust steam in the last turbine stages. Consequently, at some definite correlation between surfaces $z_1^k : z_2^k : z_3^k$ the necessity to enlarge the super-heater is self evident, when the conditions $\partial \Pi_0/\partial z_2 > \max$ and $\partial \Pi_0/\partial z_2 > \partial \Pi_0/\partial z_1(z_3)$ are fulfilled. Theoretically, in order to reach the optimum distribution all surfaces are to be altered simultaneously (see Fig.4.44a, b). However, in practice their enlargement is step-wise (see.Tab.4.1) – four (4) coils for the evaporator and two (2) for the other surfaces.

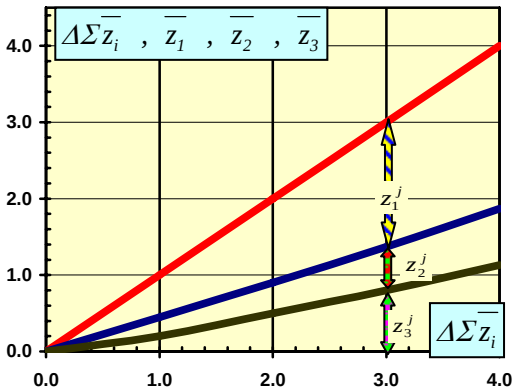

Fig.4.44a. Optimal boiler surface mutual distribution.

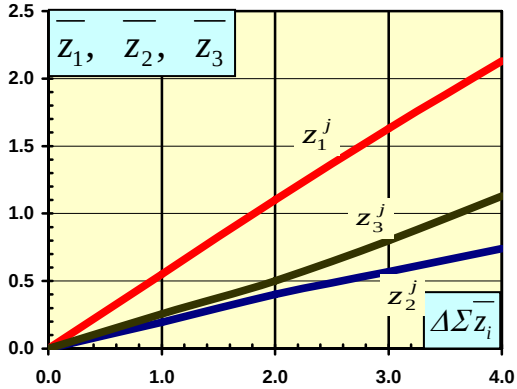

Fig.4.44b. Optimal boiler surface mutual distribution.

t_{g_o}	475°C			450°C			425°C			400°C			375°C		
Σz	z_1	z_2	z_3	z_1	z_2	z_3	z_1	z_2	z_3	z_1	z_2	z_3	z_1	z_2	z_3
70	40	14	16	40	14	16	40	14	16	44	10	16	44	10	16
68		12	16		2	16		2	16	40	12	16	40	14	14
66	36	14	16	36	14	16	36	14	16		10	16		12	14
64		12	16		12	16		12	16	36	14	14	36	14	14
62		10	16		10	16		10	16		12	14		12	14
60	32	12	16		10	14		10	14		10	14		10	14
58		10	16	32	12	16		8	14		8	14		8	14
56	28	14	14		10	14	32	10	14		8	12		8	12
54		12	14	28	12	14		10	12	32	10	12	32	10	12
52		10	14		10	14		8	12		8	12		8	12
50		10	12		10	12		8	10		8	10		8	10
48	24	12	12	24	12	12	28	10	10	28	10	10	28	10	10
46		10	12		10	12		8	10		8	10		8	10
44		10	10		10	10	24	10	10		6	10		6	10
42		8	10		8	10		8	10	24	8	10		6	8
40	20	10	10	20	10	10		8	8		8	8	24	8	8
38		8	10		8	10	20	8	10		6	8		6	8
36		8	8		8	8		8	8	20	8	8		6	6
32		6	6		6	6		6	6		6	6	20	6	6

Table.4.1 Number of heating coils for the finned tube boiler, type КУП-3100.

4.III.6. INLET GAS TEMPERATURE INFLUENCE.

The reduction of inlet gas temperature $t_{g_o} \downarrow$ makes direct impact on both boiler steam output and *approach* temperature. In order to meet condition $x_3 = const. \geq 15^o C$, enlargement of evaporator surface at the expense of others is self evident (see Fig.4.45), especially in combination with respective steam pressure drop. Based on carried out investigations it is found out that required optimal surface dimensions of just super-heater are most affected by such changes (see Fig.4.46a, b; Tab.4.1). In general, same conclusions and regularities are valid as in the case of overall enlargement/reduction of heat exchange

surfaces; only due to the fact that *high temperature part* $t_{g_O} > t_{g_{exh}} \left(= f\left(z_i\right)\right)$ in diagram $T-S$; $\sum z_i$ is affected, what makes the influence on all boiler and WHRS parameters more discernible. On another hand since *pinch-point* temperature x_1 is almost as a measure value of evaporator surface sizes, then the increase of inlet gas temperature will directly influence the growth in boiler steam output ξ (see Formula #4.5), however being slow down by some higher meaning of value x_1, i.e. $\partial x_1 / \partial t_{g_0} > 0$. Despite of followed steam pressure raise specific part of steam quality indices in Π_0 formation is diminished, mainly due to non-adequate relation between produced steam amount and required its overheat rate t_{st}. Therefore further surface re- distribution is followed by increased super-heater surface enlargement at the expense of an evaporator, while economizer growth is minor one (see Fig.4.46b). At more developed boiler surface sizes, when gas recovery possibilities are reaching its ultimate possible limit, so-called super-heater factor is becoming less important, however, within investigated limits still the growth of boiler constituent z_2 is evident.

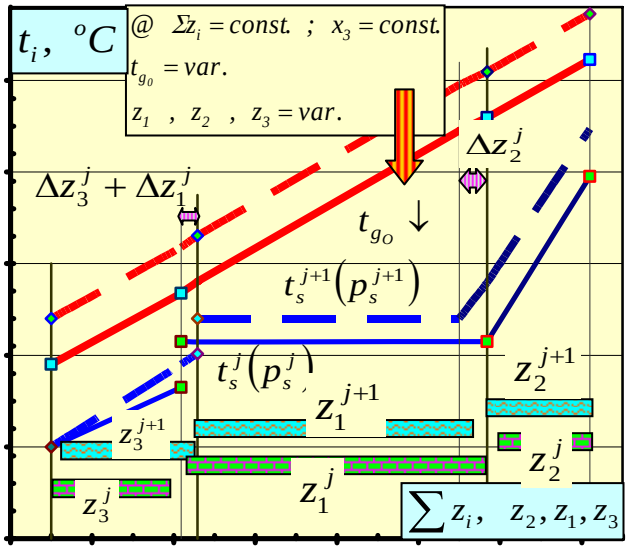

Fig.4.45 Inlet gas temperature influence.

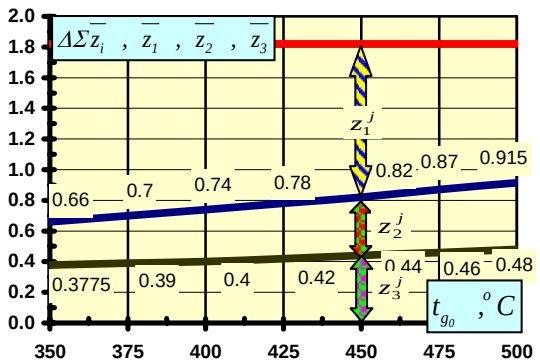

Fig.4.46a. Inlet gas temperature impact on optimal boiler surface mutual distribution.

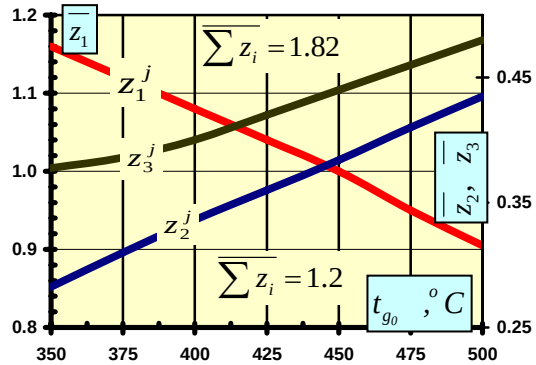

Fig.4.46b. Inlet gas temperature impact on optimal boiler surface mutual distribution.

4.III.7. CONCLUSIONS.

1. Any enlargement of the evaporator at the expense of other surface entails an immediate and directs increase in the heat recovery quantity parameters, also due to the necessity to diminish steam pressure in order to keep *approach* temperature invariable Meantime cycle quality indices have a tendency to grow down.
2. Any economiser expansion is followed by required pressure rise p_s, thus diminishing the increase rate of EB output. Consequently, specific ST iso-entropic expansion work is growing despite of diminished overheat temperature, what adversely influences ST operational safety due to higher moisture content in exhaust steam.
3. Interconnected increment/reduction in heat exchange surfaces sizes of both economiser and evaporator results in the biggest steam pressure changes, i.e. 2.2÷2.8 bar per row for finned tube boiler at $x_3 = const. \geq 15^o C$. By reciprocal expansion of both economiser and super-heater, these alterations in pressure may reach up to 1.5÷1.8 bar, but in the case of evaporator and super-heater - 0.5÷0.9 bar.
4. With the additional growth of EB height, all surfaces are being adequately altered; however at the dominance of economizer due to subsequent p_s rise either (see Fig.4.44).
5. With the inlet temperature raise, boiler steam output is dominantly increasing despite of followed pressure growth. Therefore to achieve the highest WHRS efficiency outcome, steam quality indices should be increased either, being provided by surface redistribution in favor of super-heater. For more developed boiler surfaces this *super-heater factor* is becoming less dominant (see Fig.4.46).
6. In practice for real boilers surface alterations will be carried out unevenly, e.g. by four coils for evaporator and two ones for either economizer or super-heater (see Tab.4.1).

CHAPTER 4. SUB-CHAPTER 4.IV. INTERMEDIATE STEAM EXTRACTION POSSIBILITIES.

4.IV.1. PREAMBLE OF INVESTIGATIONS.

Waste Heat Recovery System with intermediate steam extraction (see Fig.4.47) is chosen as an alternative against HRC with feed water *re-circulation*, as besides efficiency gain boiler water de-aeration in extraction (de-aerator) stage is considered as another important beneficial outcome to reduce tube oxygen corrosion occurrence internally. For stationary steam power units steam extraction is self-evident practice, what allows us to increase thermodynamic efficiency up to 13% at around 8÷10 (maximum) steam extraction points; but meantime for main power plant whether boiler sizes or available gas amount (boiler capacity) is not any restrictive factor as, if EB is installed on ME exhaust duct with already pre-determined gas dates and dimensions. In our case, one (1) extraction point is considered enough as it would provide the highest possible efficiency gain at rather low additional upgrading necessity. Extraction point coordinate Y_1 is chosen based on not only required feed water temperature at boiler inlet $t_{fw} + (10^o C)^{\min}$, but also with the consideration of both eventual changes in ME service load level and the possibility to direct this extracted steam for some low potential heat consumers also. In a result extraction point pressure p_{st}^{extr} should be around not less, than $\geq 3.2 \div 3.5 bar$, what will determine directed off steam amount to run de-aerator and pre-heater (see Fig.4.47) as per equation #3.36 (see Chapter 3).

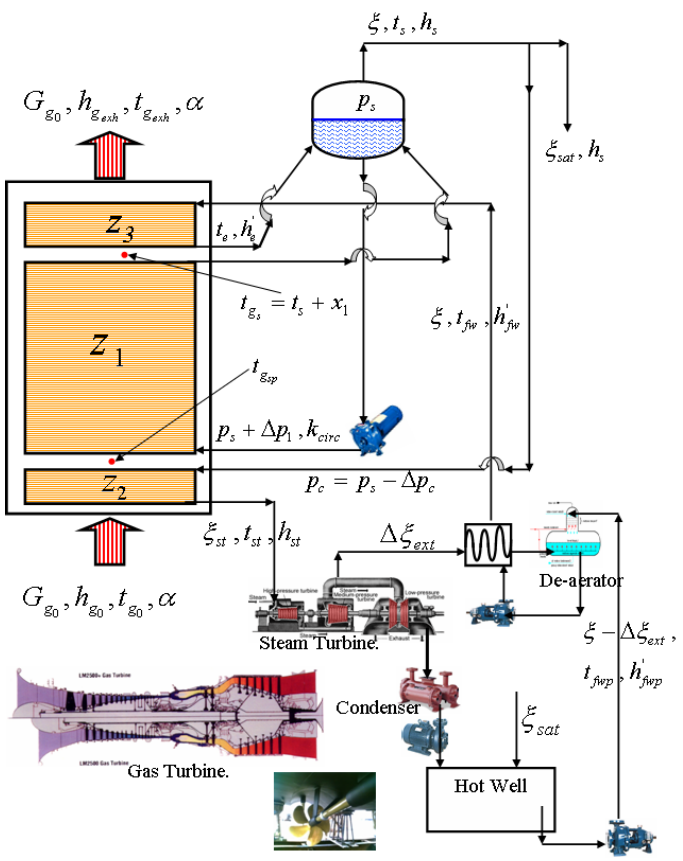

Fig.4.47. WHRS with intermediate steam extraction.

4.IV.2. AT CONDITIONS OF FIXED BOILER DIMENSIONS - $\sum z_i^{extr} = \sum z_i^{rec}$.

The regenerative Rankine cycle is so named because after emerging from the condenser (possibly as a sub-cooled liquid) the working fluid is heated by steam tapped from the hot portion of the cycle, what increases the average temperature of heat addition, resulting in the growth of thermodynamic efficiency. In another words such an arrangement of power system allows us to save losses in a condenser by partly recovery of them via latent steam evaporation/condensing heat Q_ε in a de-aeration stage (see Fig.4.48a). Then relative efficiency gain due to extraction will be equal to - $E_\varepsilon = \left(Q_T^{act} - Q_T^0\right)/Q_T^0$; but its absolute value, being not wasted (cooled) in condenser, is found as per equation - $Q_\varepsilon = \left(D_T^0 - D_x^{act}\right) \times \lambda_x$, where λ_x - specific heat for condensation or evaporation at determined pressure. Based on these main input dates comparative analyze of steam regeneration with *re-circulation* is to be carried out at equal boiler surface sizes, i.e. $\sum z_i^{extr} = \sum z_i^{rec}$, and $x_3 = const. \geq 15^o C$. In order to simplify our analytic exploration model following conjectures are accepted due to their minor impact on final results as follows:

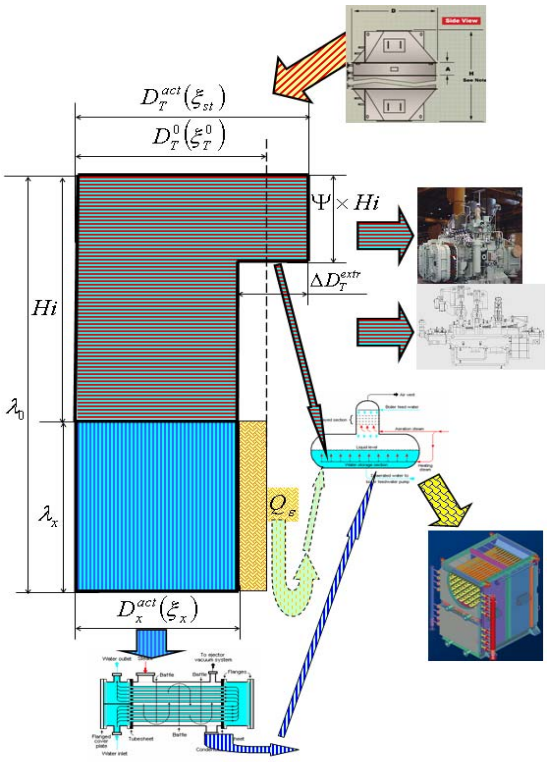

Fig.4.48a. Steam-Heat distribution Chart for *regenerative* cycle.

- Saturated steam consumption is accepted equal to zero - $\xi_{sat} = 0$;
- Both internal and mechanical efficiency factors are invariable and equal for both regenerative and feed water *re-circulation* steam cycles.

Then steam turbine output is found equal for:

- Regenerative steam cycle - $Ne_{ST}^{extr} = D_T^0 \times Hi \times \eta_{ST} = \left(D_T^{act} - \Delta D_T^{extr} \times (1 - \Psi)\right) \times Hi \times \eta_{ST}$;
- Feed water *re-circulation* - $Ne_{ST}^{rec} = D_T^{rec} \times Hi \times \eta_{ST}$.

In a result the relation $\overline{N}$ between steam turbine powers is obtained as –

$$\overline{N} = Ne_{ST}^{extr} / Ne_{ST}^{rec} = \left(\xi^{ext} / \xi^{rec}\right) \times A^{extr}, \tag{4.11}$$

where value $A^{extr} = 1 - \left(h_{fw}^{|} - h_x^{|}\right) / \left(h_{st}^{extr} - h_x^{|}\right) \times (1 - \Psi)$ is *extraction factor*, representing eventual steam turbine power loses due to consumption reduction (see Fig.4.48b) as if all steam amounts would be usefully worked out in ST. By numerical meaning substituting in equations this reduction is found out within limits from 5.5 until 9.7%, i.e. $A^{extr} \approx 0.90 \div 0.95$. But what do about boiler steam capacities? Firstly, the relation of steam capacities would be equal to $\overline{\xi} = \xi^{ext} / \xi^{rec} = 1$, as equal *approach* temperatures, pressures and evaporator sizes (*pinch-point* x_1) are those dominant factors, which determine EB output. However, boiler water warm up by means of *re-circulation* results in the growth of feed water flow rate k_{rec} through economizer up to 60÷130% in dependence on required feed water temperature and pressure. In order to maintain condition $x_3 = const.$ surface mutual distribution should be re-arranged towards economizer $z_3 \uparrow$ enlargement at the expense of evaporator $z_1 \downarrow$ (see Fig.4.49). After equation #4.5 modification another one is brought out to determine boiler capacity –

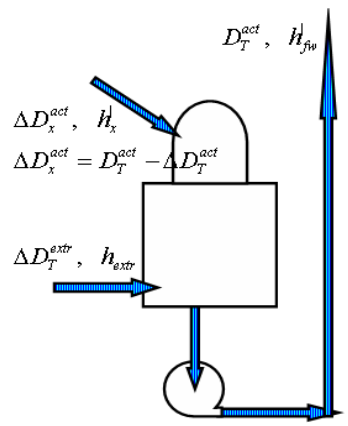

Fig.4.48b. Heat Distribution Chart for De-aeration Stage.

$$\xi = \left(t_{g_0} - \left(t_s + x_1\right)\right) \times \overline{c_g} \times \eta_{al} / \Delta h_s \tag{4.12}$$

First of all, it is quite evident that required specific heat for evaporation Δh_s will be lower for steam cycle with intermediate extraction $\Delta h_s^{extr} = h_s - h_e^{|}$ than for *re-circulation* - $\Delta h_s^{rec} = h_s - h_e^{|} + k_{rec} \times \overline{c_w} \times x_3 = \Delta h_s^{extr} + k_{rec} \times \overline{c_w} \times x_3$; and their relation will reflect the impact on steam capacity reduction as follows –

$$\overline{\xi}_{\Delta h_s} = 1 + \frac{k_{rec} \times \overline{c_w} \times x_3}{\Delta h_s^{extr}} = 1 + \frac{k_{rec} \times \overline{c_w} \times x_3}{r_s + \overline{c_w} \times x_3} = 1 + \frac{k_{rec}}{r_s / \left(\overline{c_w} \times x_3\right) + 1} = 1 + \frac{k_{rec}}{r_s / \delta h_e^{|} + 1} \tag{4.13}$$

As per equation #4.12 this value will be always equal to $\overline{\xi}_{\Delta h_s} > 1$, what corresponds to reduced boiler steam output for *re-circulation*. Meantime due to required boiler surface re-distribution *pinch -point* will be lower for regenerative cycle, i.e. $x_1^{extr} < x_1^{rec}$; then with the consideration of equation #4.12 steam changes due evaporator diminishing will be equal to –

$$\overline{\xi}_{\delta x_1} = \left(1 - x_1^{extr} / \left(t_{g_0} - t_s\right)\right) \times \left(1 - x_1^{rec} / \left(t_{g_0} - t_s\right)\right)^{-1} \tag{4.14}$$

Both steam capacity alteration factors are found equal to $\bar{\xi}_{\delta x_1} > 1.0$ and $\bar{\xi}_{\Delta h_s} > 1.0$, subsequently boiler output will be higher for regenerative cycle - $\bar{\xi} = \bar{\xi}_{\delta x_1} \times \bar{\xi}_{\Delta h_s} > 1.0$; and after real figure substitution the relative steam output difference will constitute around $6 \div 10\%$, i.e. $\bar{\xi} = \bar{\xi}_{\delta x_1} \times \bar{\xi}_{\Delta h_s} = 1.06 \div 1.10$. In a result there will be no any efficiency, power gain due to intermediate steam extraction, i.e. $\bar{N} = \bar{\xi} \times A^{extr} \cong 1.0$ at $\sum z_i^{extr} = \sum z_i^{rec}$ and equality of other main parameters.

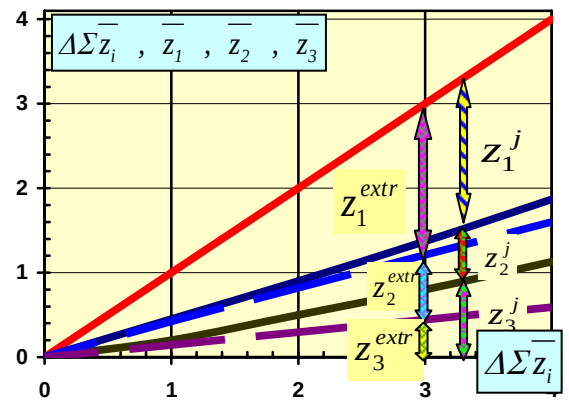

Fig.4.49 Optimal EB surface distribution for HRC with Regeneration & *Re-Circulation*.

On another hand recovered heat from exhaust gases is equal to that one adjoined to water-steam media in exhaust boiler, i.e. –

- For *re-circulation* - $Q_{ST}^{rec} = D_T^{rec} \times \lambda_0 = D_T^{rec} \times (Hi + \lambda_x)$;
- For regenerative cycle - $Q_{ST}^{extr} = D_T^{act} \times (1 - \Theta \times (1 - \Psi)) \times (Hi + \lambda_x)$, where Θ extraction quantity coefficient is equal to $\Theta_{extr} = \Delta D_T^{extr} / D_T^{act} = h_{fw}^{|} - h_x^{|} / h_{st}^{extr} - h_x^{|}$ (see Fig.4.48) and - $h_{st}^{extr} = h_{st} - \Psi \times Hi$.

On above accepted terms, when steam turbine output remains invariable (see as above), efficiency effect due to *regeneration* is found as per equation –

$$E_\varepsilon = \left(Q_T^{rec} - Q_T^{extr}\right) / Q_T^{rec} = Q_\varepsilon / Q_T^{rec}; \tag{4.15}$$

and after formula transformation following expression is brought out –

$$E_\varepsilon = \chi_{extr} \times \left(1 - \eta_{ST_i}\right) \times \Theta \times \Psi, \tag{4.16}$$

where following coefficients are found as follows - $\chi_{extr} = \left(1 - \Theta \times (1 - \Psi)\right)^{-1}$ and $\eta_{ST_i} = Hi / \lambda_0$. Then by substituting numerical values heat efficiency gain E_ε is found equal within range from $E_\varepsilon \approx 2.5\%$ (at lower p_s meanings and higher feed water temperature t_{fw}) till $E_\varepsilon \approx 3.5\%$. But in accordance as above brought out conclusions there is no any additional turbine power growth; then where and how can we sense this gain? As discussed above (see equations #4.16) less gas heat on value equal to $\delta\Delta h_g^{rec/extr} = E_\varepsilon \times \xi_T^0 \times \lambda_0$ is required to obtain the same result; and it means the relevant increase in outlet gas temperature

at boiler outlet. But in which part of the boiler does this gain appear? The main difference is due to different feed water warm up arrangement, as for *re-circulation* gas heat is used and subsequently recovered heat in economizer will be found as per equation - $\Delta h_{g_3}^{rec} = (1 + k_{rec}) \times \Delta h_e^{|} \times \xi^{rec} / \eta_{al}$, while for *regenerative* cycle obtained heat is used more efficient, therefore gas enthalpy drop in economizer will be less - $\Delta h_{g_3}^{extr} = \Delta h_e^{|} \times \xi^{extr} / \eta_{al}$. In a result cooling rate increase due to recirculation is obtained as follows –

$$\delta \Delta h_g^{rec/extr} = \Delta h_{g_3}^{rec} - \Delta h_{g_3}^{extr} = \left((1 + k_{rec} - (1.06 \div 1.10)\right) \times \Delta h_e^{|} \times \xi^{rec} / \eta_{al} = \\ = \left((k_{rec} - (0.06 \div 0.10)\right) \times \Delta h_e^{|} \times \xi^{rec} / \eta_{al} \qquad (4.17)$$

At the same time increased both evaporator surface and steam output results in reduction of relevant gas temperature $t_{g_s} \downarrow = t_s + x_1 \downarrow$, but nevertheless within investigated limits this additional heat difference constitutes around $\delta \Delta h_g^{rec/extr} \approx 6 \div 14\, kJ/kg$, to which corresponds increased outlet gas temperature for *regenerative* cycle EB till $\delta \Delta t_{g_{exh}}^{rec/extr} \approx 7 \div 12^o C$ at equality of all other HRC parameters. Consequently higher mean gas temperatures are observed for *intermediate steam extraction* option, coming to increased boiler aero-resistance $\sum \Delta P_g^{extr} > \sum \Delta P_g^{rec}$ and corresponding losses in main engine ΔHe_g. In average summary additional efficiency growth of power plant due to WHRS is higher for system *with re-circulation* on $\overline{\Delta \Pi_0} \approx 1 \div 2\%$ in the maximum. On another hand higher exhaust temperatures at boiler outlet minimizes the risk of acid corrosion occurrence in tail surfaces, but increased linear gas velocity comes to lowered surface pollution from gas side $\varepsilon^{extr} < \varepsilon^{rec}$. Some minor but still favorable impact on ST internal efficiency growth is ensured, as due to higher steam output for *regenerative* cycle there will be reduction in terminal losses on blades of the first stage, while followed cut down in steam consumption reduction ensures reduction in blade height of the last stages, thus minimizing their profile losses.

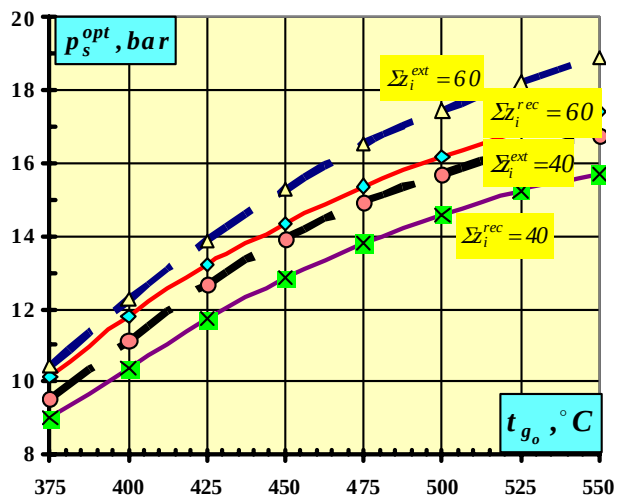

Fig.4.50 Optimal steam pressure dependence on inlet gas temperature for cycles with intermediate steam extraction and *Re-Circulation*.

The nature of optimal steam pressure choice is similar as described previously, but as per carried out studies, it has a slight tendency to be higher then for *re-circulation* option (see Fig.4.50). After equation #4.9 modification another one #4.18 is brought out, that reflects ultimate steam pressure dependence at unlimited surface -

$$t_s^{\max} = t_{g_0} \times \left(k_e^{-1} - 1\right)^{-1} + t_{g_{exh}} \times \left(1 - k_e\right)^{-1} \tag{4.18}$$

Despite of some opposite, but minor coefficient k_e (see formulae #4.8) impact ultimate possible steam pressure will be higher due to relevant exhaust gas temperature differences, i.e. $t_{g_{exh}}^{extr} - t_{g_{exh}}^{rec} \approx 12 \div 14^o C$, thus directly influencing the optimal pressure level as well. In reality for specific and fixed boiler sizes *pinch point* has also certain influence on the pressure choice, i.e. $t_s = t_s^{\max} - x_1$; and due to required surface distribution as above this temperature difference is lower for regenerative cycle, i.e. $x_1^{rec} > x_1^{extr}$, thus increasing t_s^{extr} level.

4.IV.3. AT FIXED COOLING RATE.

When further deeper gas cooling is limited exclusively by safety matters only, then it becomes possible to enlarge boiler dimensions for *regenerative* ST cycle at equal recovery rate, i.e. $\sum \Delta t_g^{EB} = t_{g_0} - \left(t_{g_{exh}}^{extr} = t_{g_{exh}}^{rec}\right) = const$. At rather low outlet gas temperatures required surface increase $\overline{\Delta z_i}$ might constitute rather considerable figure (see Fig.4.51). In a result tangible benefit of net efficiency growth would be obtained, which absolute value has its explicit maximum level $\Delta\Pi_0^{\max} = \Pi_0^{extr} - \Pi_0^{rec} = \max$. at certain cooling rate (see Fig.4.52).

Further gas cooling requires more extensive surface development (see Fig.4.51) with consequent accelerated power losses due to boiler gas resistance (see Fig.4.53) with a tendency to grow up till unlimited level. Theoretically ST output or its representative value Π is directly proportional to gas cooling rate, which however has its ceiling $\sum \Delta t_{g_{MAX}}^{EB}$ at unlimited boiler surfaces (see Chapter 4.I); consequently the maximum value Π_{MAX} will be obtained (see Fig.4.53), that is higher for *extraction* on around up to $\overline{\Delta\Pi^{\Delta t_g}} \approx 4\%$ than for *re-circulation* due to cycle efficiency (see Fig.4.54). Meantime at unlimited surface dimensions different recovery rates would be obtained, which would be higher for *re-circulation*, corresponding to lines $1-2$ and $3-4$ respectively, i.e.

$\sum \Delta t_{g_{MAX}}^{EB-rec} > \sum \Delta t_{g_{MAX}}^{EB-extr}$ @ $\sum \Delta z_i \to \infty$. At these marginal conditions the impact of boiler aero-resistance will be unlimited thus coming to zero outcomes for power plant in the total,

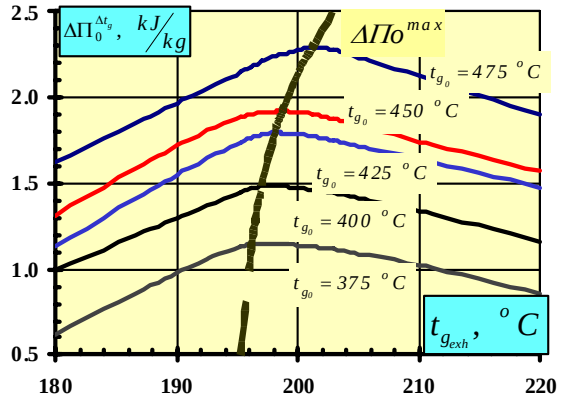

Fig.4.52 Max. efficiency increase due to *regeneration* at $t_{g_0} - \left(t_{g_{exh}}^{extr} = t_{g_{exh}}^{rec}\right) = const.$ for different outlet gas temperatures.

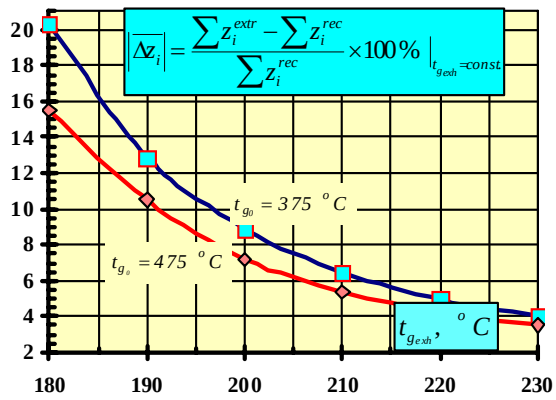

Fig.4.51. Relative EB surface increase for *regeneration* at $t_{g_0} - \left(t_{g_{exh}}^{extr} = t_{g_{exh}}^{rec}\right) = const.$ in dependence on outlet gas temperature.

i.e. $\lim\limits_{\sum \Delta z_i \to \infty} \Pi_0 = 0$; however in different extent as by reaching line $1-2$ there will be still left enough efficiency gain for HRC with *re-circulation*, while nothing for *regeneration*. It means that at certain gas cooling rate or $t_{g_{exh}}$ there will be ME power loss prevalence by *extraction* over *re-circulation*, which results in explicit peak of additional efficiency gain due to de-aeration stage introduction in the cycle (see Fig.4.54). At the best the relative gain

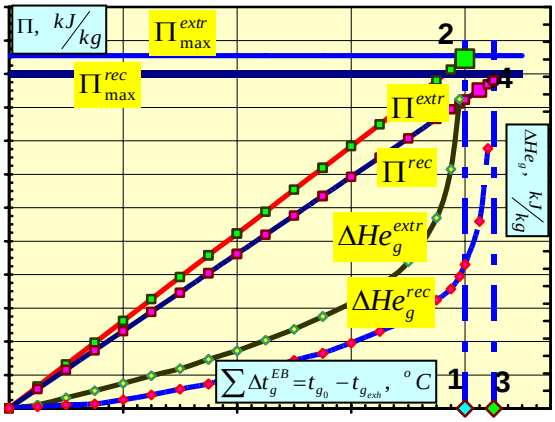

Fig.4.53 Dependence of WHRS Efficiency parameters for both *regeneration* & *Re-Circulation* at different gas cooling rate.

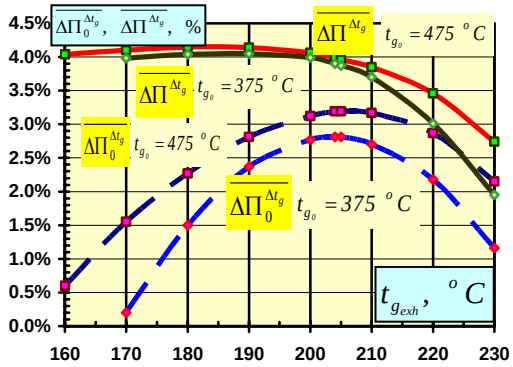

Fig.4.54 Relative WHRS & Power Plant efficiency increase due to intermediate steam extraction at constant gas cooling rate for different outlet gas temperatures.

constitutes around - $\left(\Pi_0^{ext} / \Pi_0^{rec} - 1\right) \times 100\% \Big|_{t_{g_{exh}}=const.} = \overline{\Delta\Pi_0^{\Delta t_g}} \approx 3 \div 3.3\%$.

4.IV.4. CONCLUSIONS.

1. Heat recovery circuit with *intermediate steam extraction* is justified alternative, the main purpose of which is to ensure power plant safety via feed water de-aeration.
2. At fixed equal boiler dimension following is obtained due to steam regeneration:

a. Despite that steam turbine cycle efficiency is higher due to latent heat losses reduction in a condenser by recovering it in a heating stage, any additional rise in turbine output is doubtful;
b. Meantime less gas heat is required, i.e. $t_{g_{exh}}^{extr} < t_{g_{exh}}^{rec}$, due to reduced feed water amount flow through economizer, thus reducing sulfuric acid corrosion of tail surfaces;
c. But due to higher outlet temperatures and respective EB gas resistance growth final efficiency gain for the power plant in total is found slightly less, i.e. $\Pi_0^{extr} \leq \Pi_0^{rec}$.

3. Due to feed water quantity reduction the favorable mutual surface distribution is shifted towards evaporator part enlargement at the expense of economizer.
4. By observing the condition of fixed, equal flue gas cooling rate there is a possibility to increase efficiency by adequate surface enlargement, which provides us relative steam turbine output increase up to $\approx 4\%$,
5. But required boiler surface enlargement is accompanied with relevant loses in ME, which finally results into zero efficiency gain at high enough flue gas cooling rate.
6. Nevertheless total efficiency gain could reach till the value of $\approx 3\%$ to the utmost at equal recovery rates with relative surface growth up to $\approx 10 \div 18\%$.

CHAPTER 4. SUB-CHAPTER 4.V. EXHAUST BOILER TUBE FINNING IMPACT ON WHRS EFFICIENCY AND DIMENSIONAL INDICES.

In order to increase WHRS efficiency exhaust boiler tube ribbing is considered as an alternative versus smooth surface in our investigations. Meantime this eventual efficiency gain shall be somehow estimated, being thoroughly investigated as below.

4.V.1. FINNING EFFICIENCY AT EQUAL BOILER DIMENSIONS, HEIGHT.

Since boiler cross section is accepted constant $L \times B = const.$ for any boiler type, then just its dimensional height ΣH_i $\left(or \;\; \Sigma z_i = z_{1_i} + z_{2_i} + z_{3_i}\right)$ will represent heat exchange surface sizes. At condition, when both EB heights smooth ΣH_i^{sm} tube and finned ΣH_i^{fin} one are equal and constant, i.e. $\Sigma H_i^{fin} = \Sigma H_i^{sm} = const.$, real surface (in m^2) sizes $\Sigma F_i^{\,j}$ will be evidently bigger for ribbed tubes, i.e. $\Sigma F_i^{\,fin} > \Sigma F_i^{sm} \;\; @\Sigma H_i^{\,j} = const.$, at accepted conditions (see Chapter II) , what results in deeper gas cooling rate $t_{g_0} - t_{g_{exh}}^{fin} > t_{g_0} - t_{g_{exh}}^{sm} \;\; @\Sigma H_i^{\,j} = const.$ and subsequent WHRS total efficiency increase $\Pi_0^{fin} > \Pi_0^{sm}$. In a result self-evident measure value for fining efficiency is brought out that represents additional net gain of the power plant in the whole, i.e.

$$K_{\Pi o}^{\Sigma H} = \left(\Pi_0^{fin} - \Pi_0^{sm}\right) / \Pi_0^{fin} \times 100\% \;\Big|_{H_i = const.} \tag{4.19}$$

This coefficient might be convenient, when specific ship project is investigated and different alternatives economically compared. Total boiler surface is evaluated according equations

– for plain tube boiler $\Sigma F_i^{sm} = \pi \times d \times L \times \Sigma z_i^{sm} \times n_t$, where $\Sigma z_i^{sm} = \Sigma H_i^{sm} / S_2^{sm} + 3$ and $n_t = B / S_1^{sm} + 1$, subsequently $\Sigma F_i^{sm} = \pi \times d \times L \times \left(\Sigma H_i^{sm} / S_2^{sm} + 3\right) \times \left(B / S_1^{sm} + 1\right), \;\; m^2$;

– for fined tube boiler $\Sigma F_i^{fin} = \pi \times d \times L \times \left(1 - F_{ribs} / F\right) \times \left(\Sigma H_i^{fin} / S_1^{fin} + 1\right) \times \left(B / S_1^{fin} + 1\right), \;\; m^2$, where F_{ribs} / F relation between surfaces of ribs and total one, being found in dependence on finned tube characteristics [21, 52, 87, 89, 109, 138]. The specific costs, price of one square meter of respective boiler surface will depend on material grade and quantity, involved labor, production costs and could be specified as - C_i^{sm}, C_i^{fin}, $\$(EUR)/m^2$. Then total expenses $E_i^{\Sigma j}$ for specific boiler manufacturing could be evaluated as $E_i^{\Sigma j} = C_i^{\,j} \times \sum F_i^{\,j}$, $\$(EUR)$. Based on theses assumptions another coefficient of comparative expense growth for fined tube boiler manufacturing could be introduced, which reflects additionally involved costs -

$$K_E^{\Sigma H} = \frac{C_i^{fin} \times \Sigma F_i^{fin} + C_i^{sm} \times \Sigma F_i^{sm}}{C_i^{sm} \times \Sigma F_i^{sm}} \times 100\% = \left(\frac{C_i^{fin}}{C_i^{sm}} \times \frac{\Sigma F_i^{fin}}{\Sigma F_i^{sm}} - 1 \right) \times 100\% \qquad \text{or}$$

$$K_E^{\Sigma H} = \left(\overline{C_i} \times \left(1 - \frac{F_{ribs}}{F} \right) \times \frac{\Sigma H_i - S_2^{fin}}{\Sigma H_i - S_2^{sm}} \times \frac{S_2^{sm}}{S_2^{fin}} \times \frac{B - S_1^{fin}}{B - S_1^{sm}} \times \frac{S_1^{sm}}{S_1^{fin}} - 1 \right) \times 100\%, \qquad (4.20a)$$

where value $\overline{C_i} = C_i^{fin} / C_i^{sm}$ is specific either self-cost or price relation between ribbed and plain tube surface boiler. At quite high meanings of boiler dimensions ΣH_i & B it becomes possible the equation above to convert as below:

$$K_E^{\Sigma H} = \left(\overline{C_i} \times (1 - F_{ribs}/F) \times \left(S_2^{sm} / S_2^{fin} \right) \times \left(S_1^{sm} / S_1^{fin} \right) - 1 \right) \times 100\% \qquad (4.20b)$$

For accepted type and geometry of tube bundles the coefficient of comparative expense growth will be equal to follow - $K_E^{\Sigma H} \cong \left(\overline{C_i} \times 2{,}938 - 1 \right) \times 100\%$ at $\Sigma H_i^{fin} = \Sigma H_i^{sm} = const$. Relation of two indices efficiency and price ones $K_{\Pi o}^{\Sigma H} / K_E^{\Sigma H}$ *or* $\partial K_{\Pi o}^{\Sigma H} / \partial K_E^{\Sigma H}$ is reflecting the efficiency of eventual fuel savings $K_{\Pi o}^{H}$ versus added investments $K_E^{\Sigma H}$. At the same time this fuel gain will tend to some theoretical limit with surface size growth (see Fig.4.55), while manufacturing costs would be close in direct ratio, what means that at some critical EB sizes equally to ΣH_0^{crit} the tube ribbing is capable to produce the highest net savings. With the growth of boiler height another critical level ΣH_1^{crit} is reach, when, e.g., in order to avoid dangerous vibrations evaporator coils are to be divided in two sections due to its high length. Such a modification unevenly will come to boiler production cost increase. By reaching the third critical level ΣH_2^{crit} flue gas temperature at EB outlet might be quite low coming to highly probable acid corrosion in tail surfaces, especially, when residue fuel oils with high sulfur content are being consumed by ME. Consequently, economizer manufacturing of alloy steels might be considered economically beneficiary during long term operation, what results in additional cost increase for boiler manufacturing (see Fig.4.55). Based on this cost-expense analyze chart net gain,

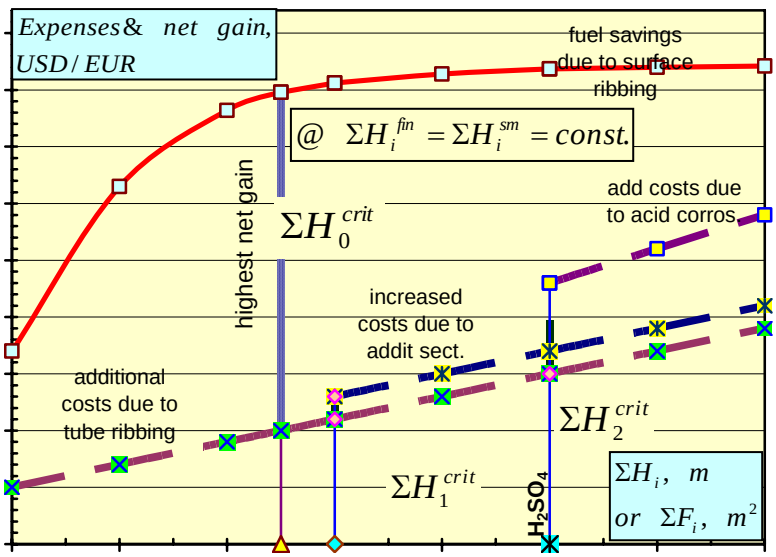

Fig.4.55 Surface fining effect– fuel savings & cost diagram.

that is the difference between additional fuel savings and initial EB expenses, could be presented in way of functional dependence (see Fig.4.56), which has an explicit maximum and in general would be valid for both manufacturers and ship owners, only at different meanings. Meantime, we are not going to explore economical aspects in our researches, it is just an example, how results could be utilized and the usefulness of introduced coefficients of surface ribbing efficiency.

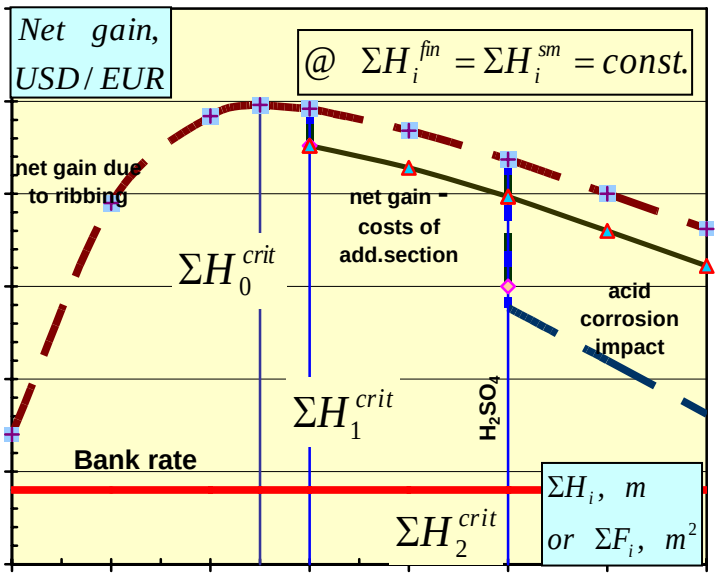

Fig.4.56 EB surface fining effect – net saving diagrams.

In order to simplify our justifications the impact of EB gas resistance $\Sigma\Delta P_{G_i}$ could be preliminary omitted, then WHRS gain would be equal to ST output, i.e. $\Pi_0 \cong \Pi$. Consequently the coefficient of power plant net gain $K_{\Pi o}^{\Sigma H}$ is found accordingly - $K_{\Pi o}^{\Sigma H} = \left(\Pi_H^{fin} / \Pi_H^{sm} - 1\right) \times 100\%$, where Π_H^{fin}, Π_H^{sm} relative WHRS steam turbine output at equal heights for both finned and plain tube boiler. Further, to make our conclusions more comprehensible, super-heater sizes are chosen so, that equal steam overheat rates Δt_{st} is obtained, i.e. $\Delta t_{st}^{fin} = \Delta t_{st}^{sm}$, then surface ribbing efficiency will be dependable on relevant capacity relation - $K_{\Pi o}^{\Sigma H} \cong \left(\left(\xi^{fin} / \xi^{sm}\right) - 1\right) \times 100\% \big|_{H=const}$. However at equal both pressures and *approach* temperatures with the equation #3.4 consideration this surface intensification efficiency could be reflected via *pinch-point* temperatures as follows –

$$K_{\Pi o}^{\Sigma H} \cong \overline{c_{p_g}} \times \left(x_1^{sm} - x_1^{fin}\right) \Big/ h_{g_0} - h_{g_S}^{sm} \times 100\% \quad \text{or} \quad K_{\Pi o}^{\Sigma H} \cong x_1^{sm} - x_1^{fin} \Big/ t_{g_0} - \left(t_s + x_1^{sm}\right) \times 100\% \qquad (4.21a)$$

With the surface growth, i.e. $\sum H_i \uparrow$ & $\sum z_i \uparrow$, the *pinch-point* will go down, but in different extent (see Fig.4.57) for plain and finned tubes respectively. At unlimited EB surface increase both differences x_1^{sm}, x_1^{fin} will tend to zero, i.e. $\lim_{H_i \to \infty}\left(x_1^{sm};\ x_1^{fin}\right) = 0$, thus reaching ultimate the highest recovery rate $\Delta t_{g_{MAX}}^{\Sigma}$ (see Fig.4.58), consequently determining

coefficient $K_{\Pi o}^{\Sigma H}$ functional dependence rate as well. On the other hand WHRS efficiency

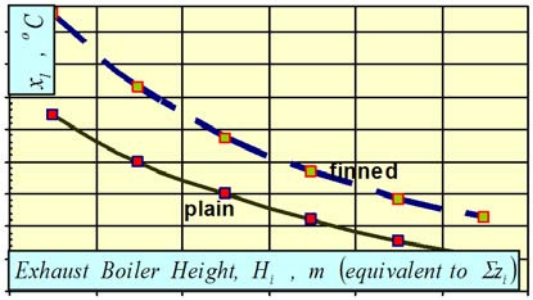

Fig.4.57 Pinch point dependence on EB height for smooth & fined surface.

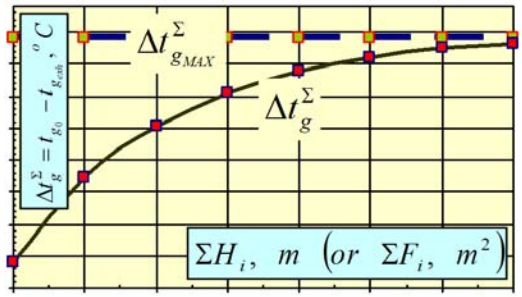

Fig.4.58 Recovery rate dependence on EB surface (height).

index Π_0 is equivalent to transferred heat from gases Q utilized by heat exchange surfaces, and then the coefficient is found as - $K_{\Pi o}^{\Sigma H} \cong \left(Q^{fin}/Q^{sm} - 1\right) \times 100\%$. Taking into consideration equations of heat balance and convective heat transfer, i.e. $Q = k \times F \times \Delta t_{LOG} = G_g \times \Delta h_g \times \eta_{al}$ (see Chapter #3), *ribbing* efficiency gain is modified accordingly –

$$K_{\Pi o}^{\Sigma H} \cong \left(\Delta h_g^{fin} / \Delta h_g^{sm} - 1\right) \times 100\% \cong \left(t_{g_{exh}}^{sm} - t_{g_{exh}}^{sm}\right) / \left(t_{g_0} - t_{g_{exh}}^{sm}\right) \times 100\% \qquad (4.21b)$$

With consideration of convective heat transfer equation following expression of fining efficiency coefficient is obtained - $K_{\Pi o}^{\Sigma H} \cong \left(\frac{\Sigma k_i^{fin} \times F_i^{fin} \times \Delta t_{LOG_i}^{fin}}{\Sigma k_i^{sm} \times F_i^{sm} \times \Delta t_{LOG_i}^{sm}} - 1 \right) \times 100\%$; and if consider only evaporator dominance over other constituents then simplified expression is brought out –

$$K_{\Pi o}^{\Sigma H} \cong \left(\left(k_1^{fin}/k_1^{sm}\right) \times \left(F_1^{fin}/F_1^{sm}\right) \times \left(\Delta t_{LOG_1}^{fin}/\Delta t_{LOG_1}^{sm}\right) - 1\right) \times 100\% \qquad (4.21c)$$

By presenting value $K_{\Pi o}^{\Sigma H}$ in so many different ways, the nature of it is being reflected extensively $K_{\Pi o}^{\Sigma H} = f\left(H_i\right)$ (see Fig.4.59). The highest benefit due to tube fining is obtained for EB with less developed surfaces; and with the growth of it we have less and less available heat will remain to recover as well as eventual additional savings, thus determining functional dependence $K_{\Pi o}^{\Sigma H} = f\left(H_i\right)$ with following indices $\partial K_{\Pi o}^{\Sigma H} / \partial H_i < 0$; $\partial^2 K_{\Pi o}^{\Sigma H} / \partial \left(H_i\right)^2 > 0$; and at marginal conditions following is valid - $\lim_{H_i \to \infty} K_{\Pi o}^{\Sigma H} = 0$. In one way EB is performing as some kind of heat compensator by smoothening outlet gas temperature fluctuations, being dependent on inlet and/or ambient ones t_a, i.e. $\partial t_{g_0} / \partial t_{g_0}\left(t_a\right) > \partial t_{g_{exh}} / \partial t_{g_0}\left(t_a\right) > 0 \big|_{H=const.}$, especially at bigger EB sizes. Therefore just minor coefficient $K_{\Pi o}^{\Sigma H}$ growth is observed due to inlet temperature rise $t_{g_0} \uparrow$ (see Fig.4.59 & 4.60). At enough high meaning of EB height outlet gas temperatures will be almost equal $t_{g_{ex}}^{fin} \approx t_{g_{ex}}^{sm}$, thus ensuring equal mean log gas

temperatures in relevant sections either, i.e. $\Delta t_{LOG_i} = const.$; and in a result another simplified dependence of the coefficient $K_{\Pi o}^{\Sigma H}$ is found - $K_{\Pi o}^{\Sigma H} \cong \left(\left(\Sigma k_i^{fin} / \Sigma k_i^{sm}\right) \times \left(F_i^{fin} / F_i^{sm}\right) - 1\right) \times 100\%$.

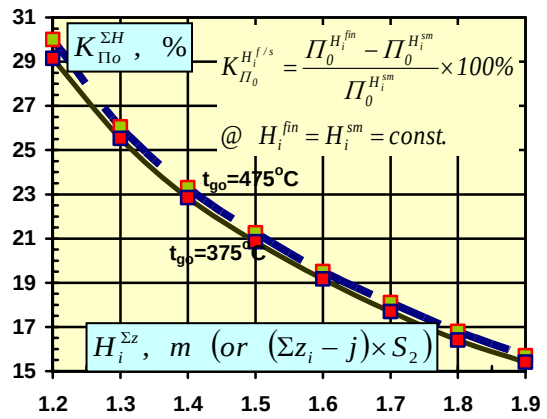

Fig.4.59 Tube fining efficiency coefficient dependence on EB surface height.

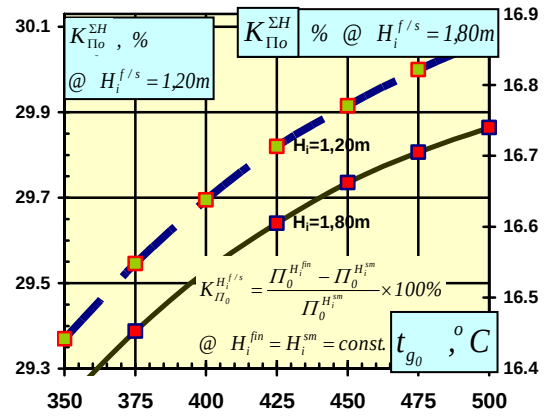

Fig.4.60. EB surface fining efficiency coefficient on inlet gas temperature.

Meantime surface relation will be constant at fixed EB height, i.e. $F_i^{fin} / F_i^{sm}\big|_{H=const.} = const.$, and then surface fining efficiency will solely depend on heat transfer efficiency relation - $k^{fin} / k^{sm} = \bar{k}$. Considering only evaporator section and the fact that high grade fuel is burnt in ME, when the influence of pollution coefficient ε on heat transfer coefficient could be neglected, i.e. $\varepsilon = 0$, following expression is obtained -

$$K_{\Pi o}^{\Sigma H} \sim k^{fin} / k^{sm}\big|_{H=const.} = \bar{k} = \overline{C_k^g} \times W_C^{0.05} \times k_{t_g}^{-0.0986} \times \left(\bar{t}_g / 100\right)^{0.0175} \times \left(1 / c_\Phi\right), \qquad (4.22)$$

where value $\overline{C_k^g}$ is so called comparative fining density volumetric geometry index that represents relation of tube bundle geometrical characteristics between fined and smooth surface boilers. The influence of gas temperature on values $\bar{t}_g$, c_Φ, k_{t_g} is unequivocal, what finally pre-determines the nature functional dependence $K_{\Pi o}^{\Sigma H} = f\left(t_{g_0}\right)$ of surface fining efficiency with following indices $\partial K_{\Pi o}^{H} / \partial t_{g_0} > 0$; $\partial^2 K_{\Pi o}^{H} / \partial \left(t_{g_0}\right)^2 < 0$ (see Fig.4.60). On other hand it could be conditionally accepted, that WHRS efficiency Π_0 is directly dependent on flue gas cooling rate - $\Delta t_g^{\Sigma} = t_{g_0} - t_{g_{exh}}$; then at equal boiler dimensions effective (with the consideration of heat transfer coefficient impact) surface will be bigger for finned tubes, i.e. $F_{ef}^{fin} > F_{ef}^{sm}$, to which correspond different meanings of temperature difference Δt_g^{Σ} and efficiency outcome (*line O-A* see Fig.4.61). Due to limitation in recovery rate gain that tends to zero, i.e. $\partial \Delta t_g^{\Sigma} / \partial H_i < 0$, surface ribbing is becoming less efficient with further EB height

rise, i.e. $\partial K_{\Pi o}^{\Sigma H} / \partial H_i < 0$ (see above). As described before inlet gas temperature rise has similar, however rather diminished, impact on exhaust temperature growth either; and in a result expected increase in recovery rate will be slightly less on value $\delta \Delta t_{g_i}^{0-exh}$ (*line O-B* see Fig.4.61), that is a difference of respective temperature deviations, i.e. $\delta \Delta t_{g_i}^{0-exh} = \left(t_{g_{0_{i+1}}} - t_{g_{0_i}}\right) - \left(t_{g_{exh_{i+1}}} - t_{g_{exh_i}}\right)$ or $\delta \Delta t_{g_i}^{0-exh} \sim \left(1 - \partial t_{g_{exh}} / \partial t_{g_0}\right)$. Meantime this temperature deviation is directly affected by EB surface sizes, i.e. $\partial\left(\delta \Delta t_{g_i}^{0-exh}\right) / \partial F_i < 0$; and since at equal heights ribbed tube surface is bigger, then respective cooling rate deviation will be less influenced by exhaust gas temperature $t_{g_{exh}}$, what finally determines *surface intensification* efficiency growth (see Fig.4.60).

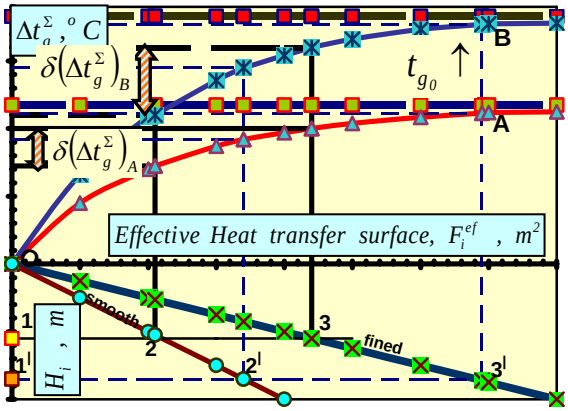

Fig.4.61. Flue gas cooling rate on EB sizes.

Also steam pressure p_s has some impact on *fining* efficiency; and as per equation #4.22 the coefficient $K_{\Pi o}^{\Sigma H}$ is found directly influenced by mean gas temperature $\overline{t_{g_i}}$, which in its turn is determined by pressure via saturation temperature, i.e. $\overline{t_g} = \left(t_{g_0} + \left(t_s + x_1\right)\right) \times 0.5$. Despite of some contrary, but still secondary impact of *pinch point*, functional changes of *surface intensification* efficiency is found with following indices $\partial K_{\Pi o}^{\Sigma H} / \partial p_s\left(t_s\right) > 0$. On the other hand power plant efficiency increase Π_0 is being adversely affected by aerodynamic resistance; and despite of increased losses ΔHe_g for fined tube boiler its effective surface is considerably bigger than for plain tube ones, what finally predetermines higher net output (see Fig.4.62).

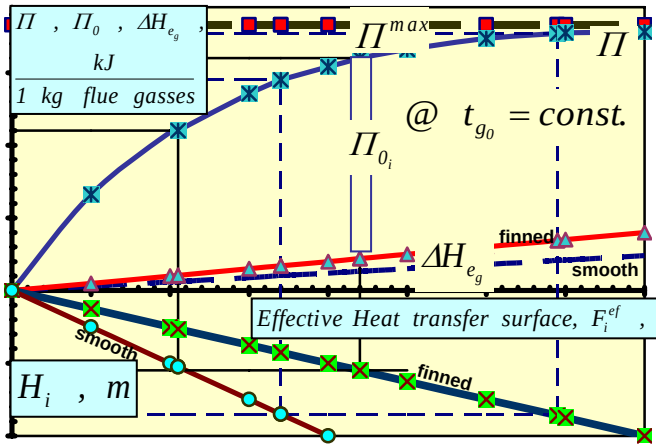

Fig.4.62 WHRS efficiency indices on boiler sizes.

Meantime value Π_0 has its maximum, however, different in dependence on surfaces type (see Fig.4.63). Based on carried out investigation (see Chapter 4.II) following functional alteration rates of WHRS efficiency are found valid - $\partial \Pi_0 / \partial p_s \big|_{H=const}^{fin} > \partial \Pi_0 / \partial p_s \big|_{H=const}^{sm}$ or

$(\partial \Pi_0 / \partial p_s)^{fin} - (\partial \Pi_0 / \partial p_s)^{sm} > 0$, what again pre-determines relevant efficiency index changes with following rates $\partial K_{\Pi o}^{\Sigma H} / \partial p_s(t_s) > 0$; $\partial^2 K_{\Pi o}^{\Sigma H} / \partial (p_s(t_s))^2 > 0$ (see Fig.4.64).

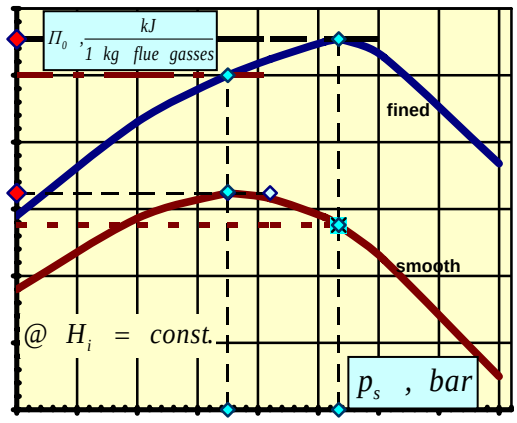

Fig.4.63 WHRS Efficiency net gain dependence on steam pressure.

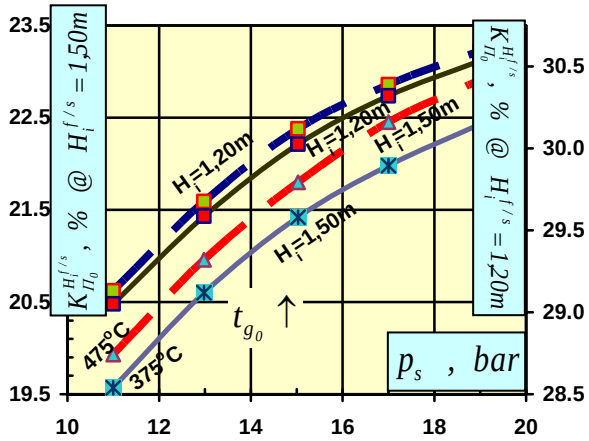

Fig.4.64 Fining efficiency on steam pressure.

Based on presented investigations due to tube fining relative efficiency increase is found around 20÷28% at constant boiler dimensions.

4.V.2. FINNING EFFICIENCY AT EQUAL WHRS NET GAIN.

When fining efficiency is carried out based on constant WHRS net gain, i.e. $\Pi_0 = const.$, the reduction in boiler height is becoming possible, being presented via the coefficient $K_{\Sigma H}^{\Pi o}$ as per equation –

$$K_{\Sigma H}^{\Pi o} = \left(1 - \left(\Sigma H_{i_{fin}}^{\Pi o} / \Sigma H_{i_{sm}}^{\Pi o}\right)\right) \times 100\%, \qquad (4.23\ a)$$

where values $\Sigma H_{i_{fin}}^{\Pi o}$, $\Sigma H_{i_{sm}}^{\Pi o}$ are summary heights of EB at $\Pi_0 = const$. Actually this economy is ensured in convective surfaces, i.e. $H_i^{\Sigma z}$, $(or\ \ (\Sigma z_i - j) \times S_2)$ (see Chapter 3), not in clearances ΔHx, therefore it is found other coefficient of direct surface reduction -

$$K_H^{\Pi o} = \left(1 - \left(\sum_{i=1}^{n(=3)} H_{i_{fin}}^{\Pi o} / \sum_{i=1}^{n(=3)} H_{i_{sm}}^{\Pi o}\right)\right) \times 100\% \qquad (4.23\ b)$$

The interrelation between these two coefficients is dependent on specific weight of clearances, which could be different for other project, being reflected as follows –

$$K_{\Sigma H}^{\Pi o} = K_H^{\Pi o} \times K_{\Delta Hx}^{\Pi o}, \quad K_{\Delta Hx}^{\Pi o} = \left(1 - \left(\Delta Hx / \sum_{i=1}^{n(=3)} H_{i_{sm}}^{\Pi o}\right)\right)^{-1} \qquad (4.23\ c)$$

At both borderlines, when either clearances are tend to zero $\Delta Hx \to 0$ or boiler surface to infinity (or big enough), tube ribbing effect might be presented via coefficient $K_H^{\Pi o}$, as

following is valid - $\lim\limits_{\Delta Hx \to 0 (or\ \Sigma z \to \infty)} \left(K_{\Sigma H}^{\Pi o}\right) = K_H^{\Pi o}$. In order to simplify our conclusions pre-conditions as above might be accepted, i.e. evaporator dominance over other boiler constituents and the use of high quality grade fuel oil with zero ash content, then

$$K_H^{\Pi o} = \left(1 - 1.2717 \times \overline{C_k^g} \times W_C^{-0.05} \times k_{t_g}^{0.0986} \times \left(\overline{t_g}/100\right)^{-0.0175} \times c_\Phi\right) \times 100\% \qquad (4.24)$$

By inserting real figures, EB height reduction is obtained around $K_{\Sigma H}^{\Pi o} \cong 24 \div 25\%$, what actually corresponds to results of our investigations. By disregarding adverse impact of boiler aero-resistance on the first approximation due to its minor impact, required height to ensure equal steam turbine output $\Pi(\Pi_0) = const.$ will differ either for smooth or fined tubes, i.e. $\partial \Sigma H_i^{\Pi o} = \Sigma H_{i_{sm}}^{\Pi o} - \Sigma H_{i_{fin}}^{\Pi o}$. Further efficiency growth, i.e. $\Pi_{i+1} = \Pi_i + \Delta \Pi_i = const_{i+1}.$, is possible by extensive development of convective surfaces and its height in a result, which is more explicit for plain tube boiler than for ribbed one, i.e. $\partial \Sigma H_{i+1}^{\Pi o} > \partial \Sigma H_i^{\Pi o}$ (see Fig.4.65); and it predetermines the coefficient $K_{\Sigma H}^{\Pi o}$ functional dependence rate - $\partial K_{\Sigma H}^{\Pi o} / \partial \Pi_0 > 0$ (see Fig.4.66). In reality boiler gas resistance ΔP_{g_i} shall be also taken into account, as at condition $\Pi = const.$, to which correspond equal flue gas cooling rate $t_{g_{exh}} = const.$, the relation of relevant fined $\Delta P_{g_i}^{fin}$ and plain $\Delta P_{g_i}^{sm}$ tube bundle resistances is evaluated as below –

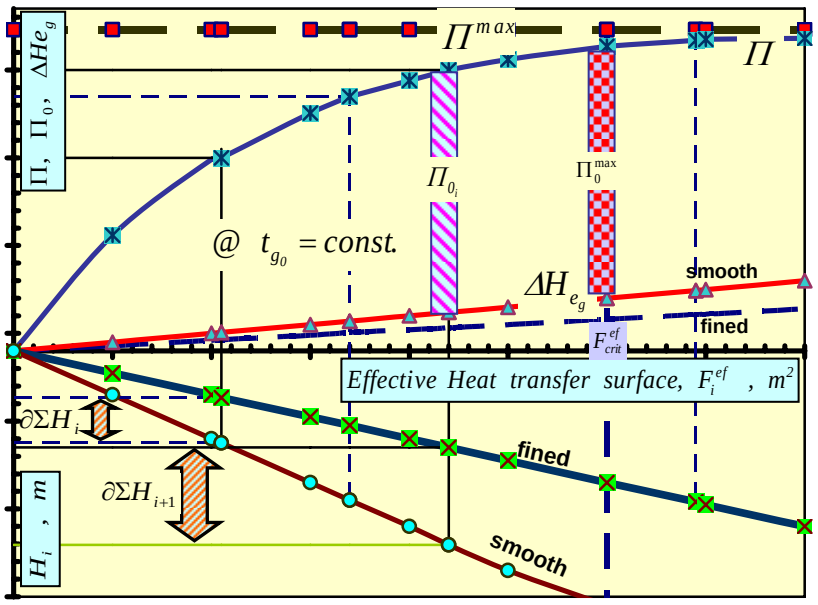

Fig.4.65. Boiler dimension reduction due to tube fining effect.

$$\Delta P_{g_i}^{fin} / \Delta P_{g_i}^{sm} = \Gamma_{\Delta P} \times \left(S_1^{fin} / S_1^{sm}\right) \times d / D_{ekv} \times W_{C_i}^{0.02} \times k_{tg_i}^{0.2535} \times \left(\overline{t_g}/100\right)^{-0.005}, \qquad (4.25)$$

where $\Gamma_{\Delta P}$ - constant comparative complex of geometrical characteristics between smooth and fined tube bundle. In average it ΔP_{g_i} is higher for smooth tube boiler on ≈10÷15%, i.e. $\Delta P_{g_i}^{fin} / \Delta P_{g_i}^{sm} \cong 0.90 \div 0.80$ for our chosen case, thus ensuring minor, but positive post

effect on the accelerated growth of efficiency index $K_{\Sigma H}^{\Pi o}$ accordingly - $\partial^2 K_{\Sigma H}^{\Pi o} / \partial(\Pi_0)^2 > 0$ (see Fig.4.66). Meantime according previous investigations Π_0 is limited due to accelerated ΔP_{g_i} impact; and, when maximum efficiency is reached $\Pi_0 = \Pi_0^{max} \big|_{F_i^{ef} = F_{crit}^{ef}}$ at some critical surface F_{crit}^{ef} for fined surfaces; investigations become needless (see Fig.4.65) above this level. Inlet gas temperature has definite impact on fining effectiveness either, but comparison is inadequate due to its t_{g_0} dominant impact on efficiency output indices Π, Π_0, ΔHe_g, which are measure values in our case.

Based on the equation #4.24 dependence characteristics of fining efficiency on steam pressure p_s are found equal to - $\partial K_{\Sigma H}^{\Pi o} / \partial p_s > 0$, $\partial^2 K_{\Sigma H}^{\Pi o} / \partial(p_s)^2 < 0$, as due to saturation temperature t_s direct influence on mean gas one $\overline{t_{g_i}}$. So at certain pressure $p_{s_i} = const.$, when effective surfaces are equal $F_{i_{sm}}^{ef} = F_{i_{fin}}^{ef}$ that corresponds to the same cooling rate, there will be still higher meaning of power losses in ME $\Delta He_{g_i}^{fin} < \Delta He_{g_i}^{sm} \big|_{F_{i_{sm}}^{ef} = F_{i_{fin}}^{ef}}$ for smooth tube EB as per equation #4.25, while ST outputs remain equally constant, i.e. $\Pi^{sm} = \Pi^{fin} \big|_{F_{i_{sm}}^{ef} = F_{i_{fin}}^{ef}}$. Therefore to meet the condition of our explorations, i.e. $\Pi_0 = \Pi - \Delta He_g = const.$, effective surface of plain tube, or respective cooling rate, shall be increased by the value $\Delta F_i^{ef} > 0$, i.e. $F_{i+1_{sm}}^{ef} = F_{i_{sm}}^{ef} \left(= F_{i_{fin}}^{ef}\right) + \Delta F_i^{ef} \big|_{\Pi_0 = const.}$, resulting in additional height rise $\delta H_i^z \big|_{\Pi_0 = const.}$ over already increased one. Finally smooth tube EB height constituents could be presented as follows –

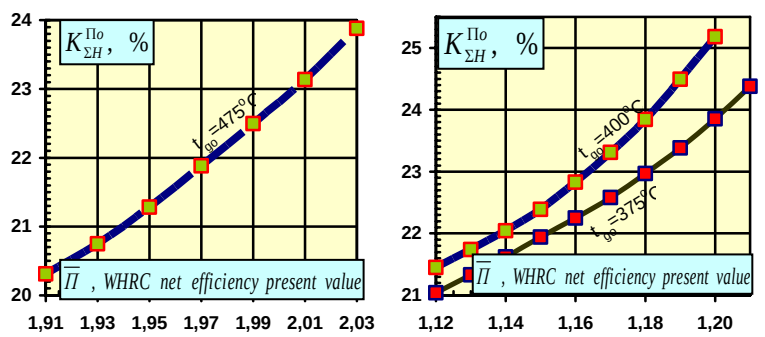

Fig.4.66 EB height reduction due to tube fining at $t_{g_0} = \text{var}$.

$$\Sigma H_{i_{sm}}^{\Pi_o} = \Sigma H_{i_{fin}}^{\Pi_o} + \Delta H_i^z \big|_{F_i^{ef} = const.} + \delta H_i^z \big|_{\Pi_0 = const.}, \tag{4.26}$$

where value $\Delta H_i^z \big|_{F_i^{ef} = const.}$ represents additional smooth tube boiler height increase over fined one at equal effective surfaces $F_{i_{sm}}^{ef} = F_{i_{fin}}^{ef}$ or recovery rate. At fixed of all other WHRS parameters, EB gas resistance is found almost in direct ratio on pressure, i.e. $\Delta P_{g_i} \cong C_{\Delta P} \times p_s$,

as well as power losses $\partial \Delta He_g / \partial p_s > 0$, what results in immediate influence on both effective surface growth and relevant changes in boiler height - $\partial\left(\delta H_i^z\big|_{\Pi_0=const.}\right)/\partial p_s > 0$, thus finally pre-determining fining efficiency functional dependence (see Fig.4.67).

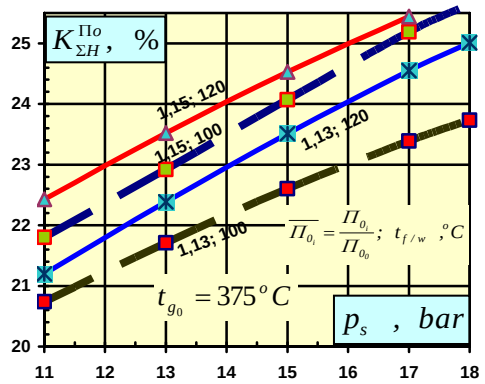

Fig.4.67. Fining efficiency on p_{s_i}.

4.V.3. CONCLUSIONS.

1. At fixed both boiler height, i.e. $\Sigma H_i^{fin} = \Sigma H_i^{sm} = const.$, due to surface intensification per one volume unit it becomes possible to ensure deeper gas cooling, resulting in higher relative net output, what constitutes around $K_{\Pi o}^{\Sigma H} = 16 \div 30\%$;
2. In order to achieve the same net output $\Pi_0 = const.$ height for fined tube boiler will be less on $K_{\Sigma H}^{\Pi o} = 21 \div 25\%$ than for plain tube one in average.
3. At higher inlet temperatures t_{g_0} both tube fining efficiency coefficients are increasing, as well as with the steam pressure growth.

CHAPTER 5. WASTE HEAT RECOVERY AT LIMITED RESOURCES.

5.1. INTRODUCTION.

As it was already mentioned advanced SSDE are dominantly used as ships' ME. During the years of engine technical development diesel efficiency has been approaching its theoretical upper limit by reducing all possible heat losses, and first of all those in exhaust gasses (see Fig.5.1). In a result any developed waste heat recovery became economically unattractive because of required high investments at doubtful outcome. However in recent years due to both significant fuel price and engine output growth (see Chapter 1, Introduction), waste both gas and coolant heat recovery is becoming considered as potential benefit, that might save not only fuel, but also initial and maintenance costs in required electrical power plant. Also different International Requirements targeted for environmental safety urge reconsider the usefulness of WHRS installation possibility. Since the main constituent of all potential heat losses is enclosed in effluent exhaust gasses (see Fig.1.12), then the main goal is to ensure as deep as possible gas cooling in a steam EB. Based on carried out explorations in chapter #4 optimal steam might be expected rather low, therefore some higher meaning i.e. $p_s > p_s^{min}$, shall be accepted due to some practical limitations.

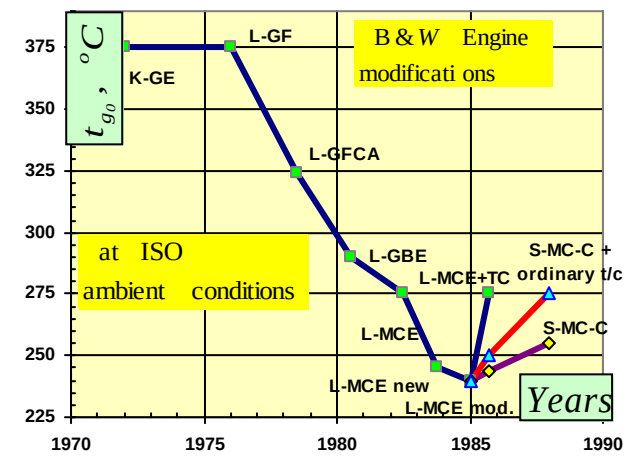

Fig.5.1 WHR potential with SSDE development.

In a result there could be presented following main differences that should be considered during our studies regarding WHRS usefulness for advanced slow speed diesels:

1. Limited resources for waste heat recovery;
2. Therefore ultimate recovery of all heat losses might be the main target;
3. Different arrangement, i.e. WHRS and its ST engagement in ship's electrical plant;
4. And in a result limited possibilities to utilize this recovered heat;
5. Steam pressure choice is determined either by technical conditions or gas cooling rate

Based on these considerations studies presented in Chapter #5 are being divided in following three subchapters, that are mostly specific for SSDE power plants, however a lot of common regularities, approaches and conclusions are universal irrespectively of WHRS application.

CHAPTER 5. SUB-CHAPTER 5.I. SOME ASPECTS OF HEAT RECOVERY POSSIBILITIES AT LOW GAS TEMPERATURE POTENTIAL.

5.I.1. MAIN INPUT DATES.

In order to ensure the highest WHRS output for advanced SSDE gas cooling rate shall be as high as possible due to ultimately reduced and pre-determined meanings of gas temperature at main engine outlet, i.e. at EB inlet t_{g_0}. At the same time limitations in lowest flue gas temperature are to be considered during designing, which shall be not less than follows - $t_{g_{exh}} \geq 160^o C$ [70, 74, 88, 118, 129, 147]. Subsequently, by accepting recovery rate of exhaust gas cooling as initial input data, being a difference of relevant gas temperatures $\Delta t_g^{\Sigma} = t_{g_0} - t_{g_{exh}}$, it becomes possible to determine and choose other thermodynamic and geometrical characteristics of WHRS and steam boiler.

As mentioned before the lowest level of steam pressure p_s should be around not less than 7 bars [27, 34, 133, 134, 147] to ensure fuel preheating at ME inlet either. Further, another important thermo characteristic, defining either boiler sizes or heat recovery rate, is found as a difference between inlet gas t_{g_0} and steam saturation temperatures t_s, i.e. the ultimate cooling capacity by evaporator $\Delta t_s^0 = t_{g_0} - t_s$. At unlimited boiler sizes there could be a possibility to cool down exhaust gases as low as till the feed water temperature t_{fw} at boiler outlet; and in a result the highest possible gas recovery is ensured equal to - $\Delta t_g^{\Sigma\Sigma} = t_{g_0} - t_{fw}$. As substantiated before, *approach temperature* $x_3 = t_s - t_e$ shall be always positive value, being accepted in our investigations equally to - $x_3 \geq 15^o C$ [23, 45, 72, 104].

5.I.2. MAIN ANALYTIC EQUATIONS.

Relative steam overheat rate χ is given as relation between the real temperature drop $\Delta t_{st} = t_{st} - t_s$ and theoretical one $\Delta t_s^0 = t_{g_0} - t_s$ as follows -

$$\chi = (t_{st} - t_s)/(t_{g_0} - t_s) = (t_{st} - t_s)/\Delta t_s^0 , \tag{5.1}$$

which is one of the objects of our explorations. Then overheated steam temperature would be evaluated accordingly - $t_{st} = \chi \times \Delta t_s^0 + t_s$, including its enthalpy h_{st} (see Chapter 3). In order to simplify acquired and presented below equations and judgments it is accepted constant meaning of specific calorific capacity of flue gases within the range of temperature drop down

at reasonably acceptable accuracy, i.e. $\overline{c_g\Big|_{t_{g_{ex}}}^{t_{g0}}} = const.$. However, more exact values of respective gas temperatures and enthalpies could be evaluated according equations given in different technical papers and norms (see chapter #3). Theoretical the highest relative steam output ξ_0 is achieved, when coefficient χ is equal to zero, i.e. lack of superheater section –

$$\xi^0 = \Delta t_g^{\Sigma} \times \overline{c_g} \times \eta_{al} \Big/ \left(\Delta h_s + \Delta h_e^{|}\right) \tag{5.2}$$

In reality, when some overheat is ensured $\chi > 0$, boiler capacity is found as follows - $\xi = k_G \times \xi^0$, where coefficient k_G represents relative part of recovered flue gas heat in order to generate one kg overheated steam. This coefficient is evaluated according formulae –

$$k_G = \left(1 + \Delta h_{st} \Big/ \left(\Delta h_s + \Delta h_e^{|}\right)\right)^{-1} = \left(1 + \overline{c_{st}} \times \chi \times \Delta t_s^0 \Big/ \left(\Delta h_s + \Delta h_e^{|}\right)\right)^{-1}, \tag{5.3}$$

where value $\overline{c_{st}}$ is mean specific calorific capacity of superheated steam. When part of saturated steam ξ_{sat} is diverted for heating purposes, e.g. fuel, accommodation, water, and then boiler total steam capacity will be equal to -

$$\xi = k_G \times \xi^0 + (1 - k_G) \times \xi_{sat} \tag{5.4}$$

Further usefully recovered flue gas heat amount in each section is found as follows:

- In an evaporator $\Delta h_{g_1} = \overline{c_g} \times \Delta t_g^{\Sigma} \times k_E \times k_G$, where coefficient k_E reflects economizer part impact on saturated steam generating capacity, being equal to –

$$k_E = (1 + \Delta h_e^{|} \big/ \Delta h_s)^{-1} \tag{5.5}$$

- In a superheater it will be found as follows - $\Delta h_{g_2} = \overline{c_g} \times \Delta t_g^{\Sigma} \times (1 - k_G)$;
- And in an economizer part - $\Delta h_{g_3} = \overline{c_g} \times \Delta t_g^{\Sigma} \times (1 - k_E) \times k_G$.

After formulae transformation mean log temperatures in respective convective surfaces could be evaluated as below:

- $$\Delta t_{LOG_1} = \frac{\Delta t_g^{\Sigma} \times k_E \times k_G}{\ln\left(\dfrac{\Delta t_s^0 - \Delta t_g^{\Sigma} \times (1 - k_G)}{\Delta t_s^0 - \Delta t_g^{\Sigma} \times (1 - k_G + k_E \times k_G)} + 1\right)}; \quad \Delta t_{LOG_2} = \frac{\Delta t_s^0 \times \chi - \Delta t_g^{\Sigma} \times (1 - k_G)}{\ln \dfrac{1 - \Delta t_s^0 / \Delta t_g^{\Sigma} \times (1 - k_G)}{(1 - \chi)}}$$

- $$\Delta t_{LOG_3} = \frac{\Delta t_g^{\Sigma\Sigma} - \Delta t_g^{\Sigma} \times (1 - k_E) \times k_G - \Delta t_s^0 - x_3}{\ln \dfrac{\Delta t_g^{\Sigma\Sigma} - \Delta t_g^{\Sigma}}{\Delta t_s^0 - \Delta t_g^{\Sigma} \times (1 - k_G + k_E \times k_G) + x_3}} \quad or = \frac{\Delta t_g^{\Sigma\Sigma} - \Delta t_g^{\Sigma} \times (1 - k_E) \times k_G - \Delta t_s^0 - x_3}{\ln \dfrac{t_{exh} - t_{fw}}{\Delta t_s^0 - \Delta t_g^{\Sigma} \times (1 - k_G + k_E \times k_G) + x_3}}$$

Based on the joint solution of equations of heat balance and convective heat transfer and after formulae transformation respective amount of convective surfaces (number of heating

coils z_i) is found according expression #3.20 (see chapter 3.9.5). Afterwards respective aerodynamic resistance of boiler $\Sigma\Delta P_g$ and steam turbine output Ne_{TG} are evaluated.

Based on the method above we try to explore and find common regularities of WHRS efficiency indices at fixed and determined gas recovery rate, i.e. at $\Delta t_g^{\Sigma} = t_{g_0} - t_{g_{exh}} = const.$

5.I.3. THE INFLUENCE OF STEM OVER-HEAT RATE.

Despite of direct influence by steam overheating rate on ST efficiency, still its χ unlimited growth is unreasonable as stated in previous chapters. Due to z_2 presence the effectiveness of heat transfer in an evaporator part slightly reduces due to gas temperature offset in region of lower temperatures, what comes to adequate minor, but definite increase in z_1 sizes. Due to the fact that steam output $\xi = k_G \times \xi^0$ has a tendency to go down with the rise of value χ, i.e. $\partial\xi / \partial\chi < 0$, it comes to slight reduction in economizer sizes at $x_3 = const.$ - $\partial z_3 / \partial\chi < 0$. At the same time total EB surface sizes Σz_i has a tendency to grow up due to predetermined influence of super-heater $\partial z_2 / \partial\chi >> 0$ (see Fig.5.2a). Due to iso-entropic enthalpy difference Ha direct dependence on steam overheat rate, it comes to adequate increase in steam turbo-generator output Ne_{TG} (see Fig.5.2c), concurrently with

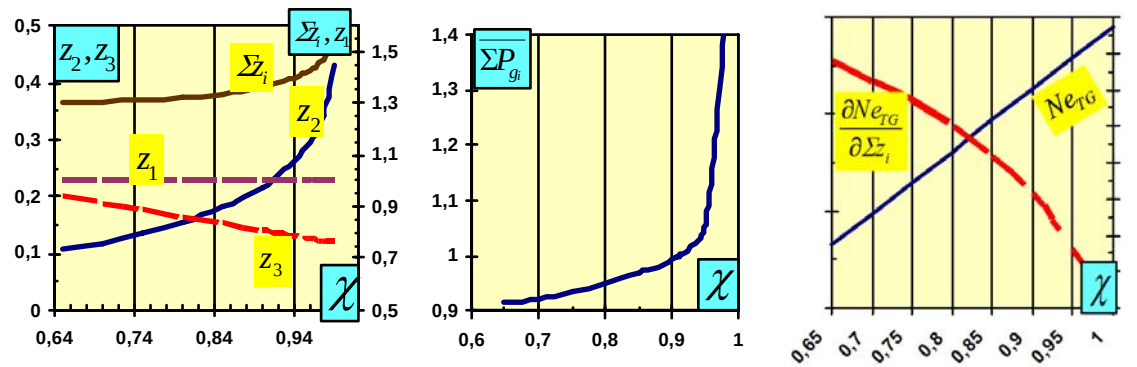

Fig.5.2a. Relative EB surface distribution

Fig.5.2b Relative EB aero-resistance

Fig.5.2c. WHRS relative efficiency

dependence on steam overheat rate $= f(\chi)$ @ Δt_g^{Σ}; x_3; $p_s = const.$

accelerated growth in boiler aero-resistance ΣP_{g_i} (see Fig.5.2b), what adversely affects ME performance and output. Based on obtained results we will try to find efficiency growth ΔNe_{TG} tendency per one surface unit $\Delta\Sigma z_i$ (one coil) in dependence on steam overheat rate, i.e. $\partial Ne_{TG} / \partial\Sigma z_i = f(\chi)$ (see Fig.5.3c), that reflects specific fuel savings against initial costs for EB. According presented analytic characteristics, the most optimal value of χ

should not exceed the level of $\chi \leq 0{,}9$, as further steam overheating would come to rapid decrease in efficiency indices of power unit in total.

5.I.4. THE IMPACT OF FLUE GAS POTENTIAL CHANGES.

Since the lowest level of outlet gas temperature is already pre-determined and fixed, i.e. $t_{g_{exh}} \geq 160^o C$, then flue gas cooling rate Δt_g^{Σ} would be affected by inlet gas temperature only $t_{g_{exh}} = var.$, being a characteristic of either diesel engine modification or ambient conditions, load level and other factors. Eventual reduction in gas temperature directly influences WHRS efficiency, first of all steam output ξ, as due to process offset in region of lowered temperatures heat transfer rate slows down. Then at reduced boiler water flow $\xi \times (1 + k_{rec}) \downarrow$ less developed economizer surface is needed, and in a result recovered flue gas heat Δh_{g_3} would be reduced either. Meantime, to ensure condition $t_{g_{exh}} = const.$, the enlargement boiler evaporator part shall be carried out (see Fig.5.3). For the sake of clarity let's consider, that overheating rate is zero $\chi = 0$, i.e. lack of superheater, then following expression is obtained –

$$t_s + x_1 = t_{g_0} \times (1 - k_E) - t_{g_{exh}} \tag{5.4a}$$

What does it explain us? The fact that gas temperature after evaporator is that the main value, which determines gas cooling deepness rate. This temperature t_{g_S} consists of two constituents; the first one is saturation temperature t_s, being equivalent to steam pressure p_s, and another value is so called *pinch point* temperature x_1, which represents evaporator surface sizes z_1. Value k_E remains without changes at constant steam pressure and *approach* temperature x_3, and then by changing meaning of gas temperature t_{g_0}, it becomes necessary to adjust *pinch point* temperature equally to value $\Delta x_1 = \Delta t_{g_0} \times (1 - k_E)$. At unlimited growth of evaporator surface sizes this temperature difference tends to zero, i.e. $\lim_{z_1 \to \infty} x_1 = 0$, but on another hand, relevant and necessary reduction in value x_1 leads to rapid increasing of evaporator sizes. Based on equation #5.4a another expression is obtained, which determines gas temperature at boiler outlet as follows –

$$t_{g_{exh}}^{\min} = t_{g_0} \times (1 - k_E) - (t_s + x_1) \tag{5.4b}$$

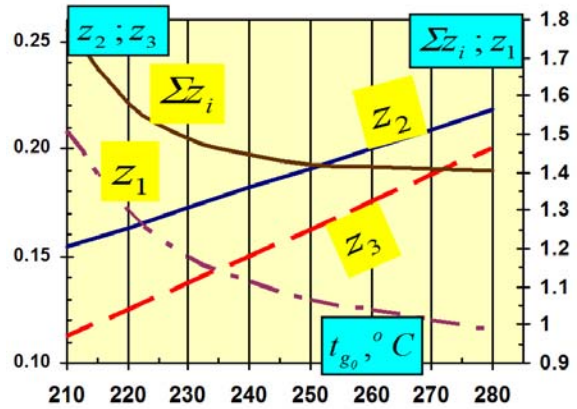

Fig.5.3 Inlet gas temperature influence on EB surface distribution at $t_{g_{ex}}$; x_3; p_s =const.

This formula reveals functional interdependence between steam pressure and achievable the highest possible flue gas cooling rate. Due to the fact that boiler steam output is dependant practically in direct ratio on gas cooling rate (see equation # 5.1), then it will have direct impact on both economizer and superheater sizes, which both will tend to grow down (see Fig.5.3) with the value Δt_g^{Σ} diminution, i.e. temperature t_{g_0} reduction.

5.I.5. APPROACH TEMPERATURE IMPACT.

Although approach temperature is accepted to be constant $x_3 = 15^oC$ due to boiler safety aspects, nevertheless it could be possible to adjust and vary it by means of thermo mixing valve for chosen WHRS, always keeping value x_3 positive. First of all, reduction in *approach temperature* is ensured by appropriate enlargement of economizer part of EB, but on another hand it diminishes economizer constituent in an evaporator, i.e. $\partial \Delta h_s / \partial x_3 > 0$, and subsequently evaporator surface is coming less developed (see Fig.5.4). At accepted pre-conditions, when other cycle characteristics remain invariable, i.e. $p_s, t_{g_0}, t_{g_{exh}}, \chi, ... = const.$, *approach temperature* has no influence on super-heater sizes, as well as on boiler steam output ξ. Due to higher heat transfer efficiency in economizer part of boiler rather than in evaporator one, it is ensured total reduction in boiler surface sizes. It also gives another benefit –drop down in EB aero-resistance ΣP_{g_i}, thus favorably affecting main engine performance.

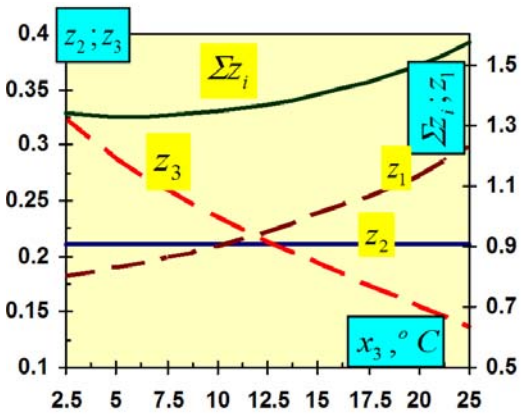

Fig.5.4 Approach temperature impact on EB heating surfaces distribution.

5.I.6. CONCLUSIONS.

1. Proposed method based on fixed gas cooling rate $\Delta t_g^{\Sigma} = const.$ is valuable, when the highest possible efficiency output of WHRS is primary required at lowered gas temperature t_{g_0}, e.g. for power units with advanced low speed diesel engines.
2. In order to obtain the highest reasonable output, recommended steam overheating rate shall be equal to $\chi \leq 0{,}9$; and then relative optimal boiler heat exchange surface mutual distribution will be within range of following figures - $z_1 = 1.000 \div 1.004$; $z_2 = 0.200 \div 0.210$; $z_3 = 0.190 \div 0.200$. Further increase in value χ should be considered based on case by case.
3. Gas temperature reduction at EB inlet adversely influences on heat transfer efficiency, what comes to further dominance of evaporator and, in a result, the growth of total boiler sizes.
4. Reduction in *approach* temperature is economical benefit, although its lowest value is limited with the consideration of boiler safety factors.

CHAPTER 5. SUB-CHAPTER 5.II. SOME MATTERS REGARDING STEAM PRESSURE CHOICE.

5.II.1. INTRODUCTION.

Despite that the choice of steam pressure was thoroughly substantiated in previous chapters, nevertheless, when low potential gas heat is being recovered, other considerations would be important to ensure both reliable power plant performance and its high effectiveness at possibly minimized boiler dimensions, i.e. height. So, when gas temperature at EB inlet is considerably reduced, then steam pressure is to be kept as low as possible to ensure recovery rate as high as possible at reasonable convective surface sizes. Meantime pressure is chosen based on available ST in the market; and also designed technical parameters of low potential heat consumers should be taken into account, which finally prescribes the lowest admissible limit of steam pressure for WHRS. Therefore it p_s shall be kept as high as possible in order to ensure effective and reliable performance of incorporated equipment (heaters, turbines) with the consideration of their dimensions as well. But as it was partly described before, then all both inlet gas temperature and cooling rate, and steam pressure, and boiler dimensions are interconnected. Hence, based on consideration above the highest attainable steam pressure shall be found out and substantiated for different service and design conditions. Effectiveness of WHRS is determined by temperature gradient recovered in EB - $t_g^{\Sigma} = t_{g_0} - t_{g_{exh}}$. If inlet t_{g_0} gas temperature is characteristic of both chosen ME type and service performance conditions, then gas cooling temperature $t_{g_{exh}}$ will be determined by both boiler surface sizes and thermo-dynamical parameters of steam-feed water. At fixed gas cooling rate relative boiler steam output is found either as per equation #4.2 or #4.5 (see Chapter 4.II).

5.II.2. MAIN ANALYTIC EQUATIONS.

At unlimited evaporator surface enlargement *pinch-point* x_1 has a tendency to grow down till zero, i.e. $\lim\limits_{z_1 \to \infty} x_1 = 0$ or $\lim\limits_{z_1 \to \infty} t_{g_S} = t_s = t_s^0$. Theoretically the highest steam output, at the absence of super-heater and zero *pinch-point*, is found as per equations #5.1 and #5.5–

$$\xi^0 = \left(t_{g_0} - t_s\right) \times \overline{c_g} \times \eta_{al} \big/ \Delta h_s = \left(t_{g_0} - t_{g_{exh}}\right) \times \overline{c_g} \times \eta_{al} \big/ \left(\Delta h_s + \Delta h_e^{|}\right) \tag{5.5}$$

After formulae #5.4 and #5.5 transformation at condition $\overline{c_g} = const.$ fulfillment following next functional dependence is brought out -

$$t_{g_{exh}} = t_{g_0} \times \left(1 - \left(k_E\right)^{-1}\right) + t_s^0 \times \left(k_E\right)^{-1}, \tag{5.6}$$

where t_s^0 the highest attainable saturation temperature corresponding to relevant ultimate the highest steam pressure p_s^0, the coefficient k_E (see Chapter 5.I), which $p_s^0\big|_{x_1=o}$ could be found as per corresponding saturation temperature (5.7) -

$$t_s^0\big|_{x_1=o} = t_{g_0} \times \left(1 - k_E\right) + t_{g_{exh}} \times k_E \tag{5.7}$$

Coefficient k_E always is positive value, but less than one $k_E < 1.0$; and for our considered conditions, when specific heat relation is around $\Delta h_e^{|} / \Delta h_s \approx 1/6 \div 1/5$, then respectively $k_E \approx 0.83 \div 0.86$. With a consideration of this mean average value $\overline{k_E}$ equation #5.6 could be simplified and presented as follows -

$$t_{g_{exh}} = t_s^0 \times 1.19 - t_{g_0} \times 0.19 \tag{5.6a}$$

It explains, that any pressure changes has direct impact on gas cooling rate, while inlet gas temperature growth influence is contrariwise and in less extent, i.e. $\partial t_{g_{exh}} / \partial t_s^0\left(t_s\right) > \left|\partial t_{g_{exh}} / \partial t_{g_0}\right|$. Subsequently, in the same way saturation temperature is found -

$$t_s^0\big|_{x_1=0} = t_{g_0} \times 0.16 + t_{g_{exh}} \times 0.84 \tag{5.7a}$$

and following functional dependence rates are valid $\partial t_s^0\left(t_s\right) / \partial t_{g_{exh}} > \partial t_s^0\left(t_s\right) / \partial t_{g_0}$. Presented equation ##5.6a, 5.7a allows us to make some conclusions:

- Further gas cooling is possible by appropriate and considerable steam pressure decrease;
- While any inlet gas temperature rise leads to p_s growth, but in less extent;
- Thus theoretically the highest gas cooling rate is determined by one specific meaning of steam pressure at unlimited evaporator sizes, being the ultimate possible level $p_s^{0^{MAX}}$;
- For real cases saturation temperature will be lower on specified *pinch-point* temperature value corresponding to accepted evaporator sizes, i.e. $x_1 = f\left(z_1\right)$; and subsequently the real steam pressure meaning will be lower than theoretical one, being dependent on EB technical characteristics either, i.e. $p_s^{0^{MAX}} > p_s^{\max} = p_s^{0^{MAX}} - f_{\Delta p}\left(x_1\right)$;

5.II.3. INLET/OUTLET GAS TEMPERATURE INFLUENCE.

At specified marginal conditions, i.e. $x_1 = 0$, it comes out that just economizer part of EB will have dominant impact on either recovery rate or p_s. So inlet gas temperature

rise $t_{g_0} \uparrow$ ensures adequate boiler steam output growth (see formulae #4.5, #5.5). However at preliminary invariable steam pressure $p_{s_i}^{0^{MAX}} = const.$ outlet gas temperature will tend to decrease, i.e. $\partial t_{g_{exh}} / \partial t_{g_0} < 0 \big|_{p_s = const.}$ due to adequate rise in recovered heat amount - $\Delta h_{g_3} = \xi^0 \times \Delta h_e^{|} / \eta_{al}$; and with the consideration of formulae #4.5 and #5.6following is brought out - $\Delta h_{g_3} = \left(t_{g_0} \uparrow - t_{s_i}^0\right) \times \overline{c_g} \times \left(\left(k_E\right)^{-1} - 1\right)$, what confirms the nature of outlet gas temperature drop down (see Fig.5.5a). In order to secure our accepted condition $t_{g_{exh}} = const.$, some pressure increment till value $p_{s_{i+1}}\left(t_{s_{i+1}}\right)$ shall be carried out (see Fig.5.5b); and, based on equation #5.7, following functional dependence is brought out - $t_{s_{i+1}} - t_{s_i} = \delta t_{s_i} = \delta \Delta t_{g_i} \times \left(1 - k_E\right)$,

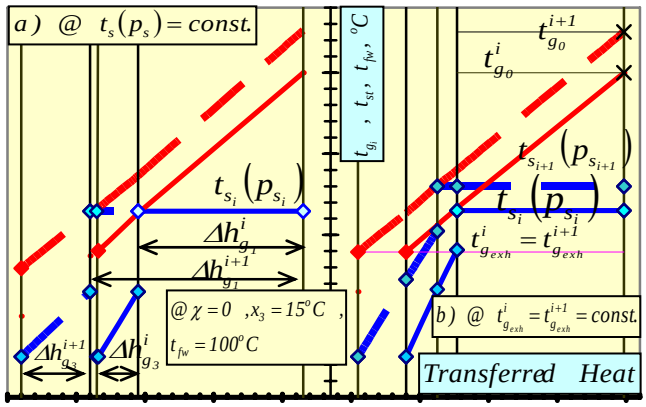

Fig.5.5 a, b. Transferred Heat-temperature diagram at inlet gas temperature rise.

where value $\delta \Delta t_{g_i} = t_{g_0}^{i+1} - t_{g_0}^{i}$ reflects variations in gas temperature at boiler inlet. In order to simplify our conclusions at small deviations of $p_s\left(t_s\right)$ the coefficient k_E influence could be omitted. Then additional acquired $\delta \Delta h_{g_i} = \delta \Delta t_{g_i} \times \overline{c_g} \times \eta_{al}$ heat due to inlet gas potential growth is being somehow distributed between evaporator and economizer surfaces at these new conditions as follows –

- Economizer - $\delta \Delta h_{g_3} = \Delta h_{g_3}^{i+1} - \Delta h_{g_3}^{i} = \delta \Delta h_{g_i} \times \left(1 - k_E\right) = \delta \Delta t_{g_i} \times \left(1 - k_E\right) \times \overline{c_g} \times \eta_{al}$;
- Evaporator - $\delta \Delta h_{g_1} = \Delta h_{g_1}^{i+1} - \Delta h_{g_1}^{i} = \delta \Delta h_{g_i} \times k_E = \delta \Delta t_{g_i} \times k_E \times \overline{c_g} \times \eta_{al}$

As we can see the biggest part of additional originating heat is utilized by evaporator, however by accompanied pressure rise coefficient k_E has a tendency to grow down due to specific evaporation heat decrease. In a result functional dependencies $p_s^{0^{MAX}} = f\left(t_{g_0}\right)$ are brought out with following alteration rates $\partial p_s^{0^{MAX}} / \partial t_{g_0} > 0$; $\partial^2 p_s^{0^{MAX}} / \partial \left(t_{g_0}\right)^2 > 0$ (see Fig.5.6). Outlet gas temperature $t_{g_{exh}}$ impact on steam pressure value is similar to inlet one (see formulae ##5.7, 5.7a), but the dependence rate is more explicit one (see Fig.5.7). Any increase in $t_{g_{exh}}$ comes to transferred heat reduction in economizer part of boiler; and then the

pressure raise is self evident action $\partial p_s^{0^{MAX}} / \partial t_{g_{exh}} > 0;\ \partial^2 p_s^{0^{MAX}} / \partial (t_{g_{exh}})^2 > 0$, at the condition $x_3 = const.$ observation either.

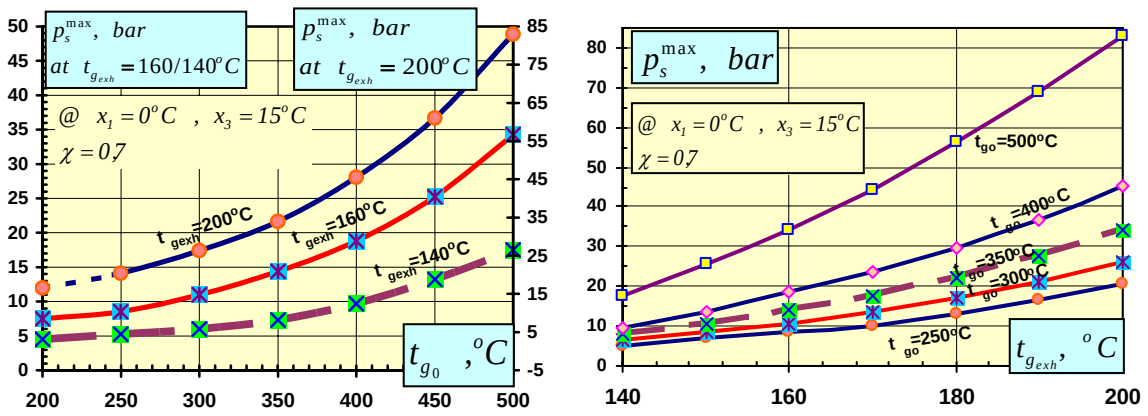

Steam pressure choice in dependence on

Fig.5.6 - t_{g_0} at $t_{g_{exh}} = const$. | Fig.5.7 - $t_{g_{exh}}$ at $t_{g_0} = const$

5.II.4. SUPER-HEATER FACTOR.

In reality super-heater is a mandatory part of exhaust boiler, therefore its influence via relative steam over-heat rate χ shall be considered as well. With the consideration of super-heater weight factor k_G (Formula #5.3) relative boiler steam output will be equal to - $\xi = \xi^0 \times k_G$. In this case ultimate the highest steam pressure $p_{s_\chi}^0$ could be found as follows-

$$t_{s_\chi}^0 \Big|_{x_1=0} = t_{g_0} + \left(t_{g_0} - t_{g_{exh}}\right) \times \left(1 - k_G \times \left(1 - k_E\right)\right) \tag{5.9}$$

At $\chi \approx 0.7 \div 0.9$ the relation $\Delta h_{st} / \Delta h_s$ is equal to $\Delta h_{st} / \Delta h_s \approx 1/6 \div 1/8$ in average, hence coefficient is close but less than $k_G < 1.0$, and respectively - $\xi < \xi^0$. Due to reduced steam output it comes to adequate and direct changes in recovered heat amount by economizer, i.e. $\partial \Delta h_{g_3} / \partial \chi < 0$, and in a result exhaust gas temperature at boiler outlet is increasing. Therefore, to ensure condition $t_{g_{exh}} = const.$ observation it becomes necessary to reduce steam pressure (see Fig.5.8), thus compensating diminution effect of steam over-heat rate χ on boiler output ξ. Anyway, super-heater presence adversely influences on achievable the highest steam pressure level $p_{s_\chi}^{0^{MAX}}$; and with its χ development the functional dependence of $p_{s_\chi}^{0^{MAX}} = f(\chi)$ has explicit tendency to grow down with following characteristics $\partial p_{s_\chi}^{0^{MAX}} / \partial \chi < 0;\ \partial^2 p_{s_\chi}^{0^{MAX}} / \partial \chi^2 > 0$ (see Fig.5.9).

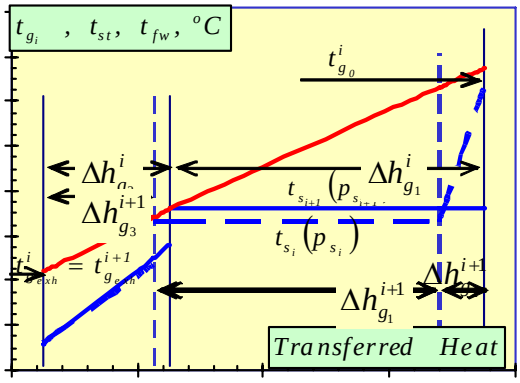

Fig.5.8 Transferred Heat-temperature diagram when super-heater added.

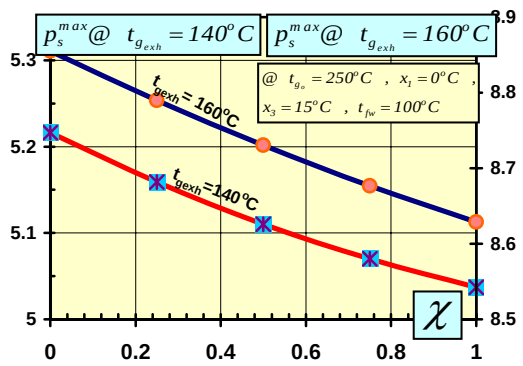

Fig.5.9 Steam pressure choice in dependence on over-heat rate.

5.II.5. APPROACH TEMPERATURE IMPACT.

Despite of considered maintenance safety issues, still there are certain possibilities to govern *approach temperature* at partial loads by feed water temperature altering, the impact of which x_3 is being explored below. Such a practice would be quite useful from the viewpoint of safety as well, so as at reduced loads possible high risk of tail surface acid corrosion could be minimize by feed water temperature increase $t_{fw}\uparrow$. Therefore by relevant economizer enlargement it might become possible to lower the accepted limit of *approach temperature*, i.e. $x_3\downarrow<15^oC$, but $x_3>0^oC$, what results in specific heat increase $\Delta h_e^{|}\uparrow$ (see Formula #4.7 chapter 4.II) with subsequent economizer part reduction in evaporator -

$$\Delta h_s = r_s + (1+k_{rec})\times\overline{c_w}\times x_3\downarrow \qquad (5.10)$$

Hence, adequate steam output growth $\partial\xi/\partial x_3<0$ (see formula ##4.5, 5.5) is ensured. Finally, *approach temperature* reduction contributes to further and accelerated deeper gas

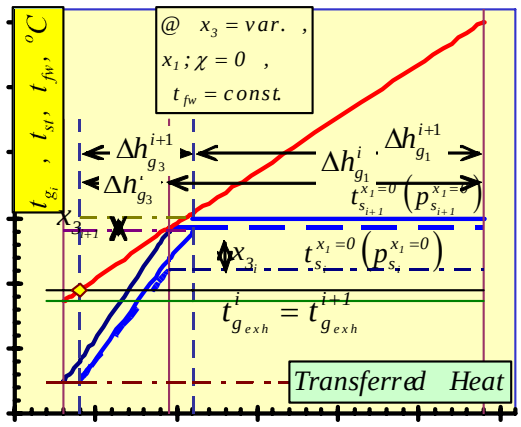

Fig.5.10 Heat-temperature diagram

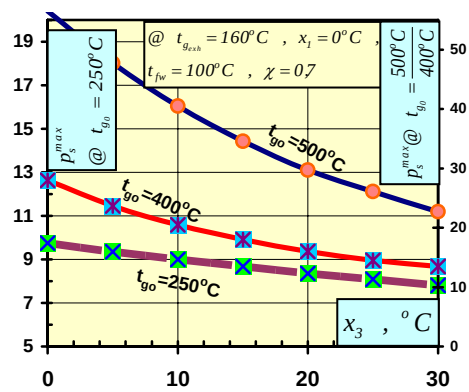

Fig.5.11 Steam pressure choice at variable *approach temperature*.

cooling as recovered heat by economizer from flue gases is directly dependent on both

considered magnitudes, i.e. $\Delta h_{g_3} = \Delta h_e^{|} \uparrow \times \xi \uparrow$ (see Fig.5.10). To keep gas cooling rate invariable additionally recovered heat amount should be reduced by means of adequate steam pressure growth, i.e. $\partial p_s^{0^{MAX}} / \partial x_3 < 0;\ \partial^2 p_s^{0^{MAX}} / \partial (x_3)^2 > 0$ (see Fig.5.11).

5.II.6. FEED WATER TEMPERATURE IMPACT.

Feed water temperature t_{fw} value is to be chosen high enough in order to avoid acid corrosion of tail surfaces; at the same time this safety margin should be reasonably low as possible with the consideration of required boiler surface sizes. In fact tube steel temperature t_{steel} is that limiting factor for acid corrosion, being determined by gas temperature either. So with ME service load level alterations also gas temperatures will vary; and at lower their t_{g_0}, $t_{g_{exh}}$ meanings, when flue gas speed is the lowest either, acid corrosion occurrence risk is the highest one. Therefore tube steel temperature should be preferably maintain on higher level by re-circulation valve opening thus increasing feed water temperature (see Fig.5.12). At the same time, when ME is heavily loaded this temperature t_{fw} could be possibly lowered, thus contributing to further and deeper gas cooling at still the same risk level of possible acid corrosion. So based on presented above suggestions decisive efficiency parameters and considerations of WHRS usefulness could be made at some durable main engine service load MCR_S, which a s rule is less than nominal one. When safe service feed water temperature t_{fw}^S is chosen at accepted MCR_S, then it might becomes possible to slightly alter this temperature t_{fw}^R (line $A_0^{fw} \div B_0^{fw}$) directly on main engine load level. In a result gas cooling could be optimized from the view point of both safety and efficiency in dependence on various MCR; and this so called Equalized acid corrosion Risk flue gas Cooling Line (ERCL) $t_{g_{exh}}^R$ (line $A_0 \div B_0$) will be less inclined than that one $t_{g_{exh}}$

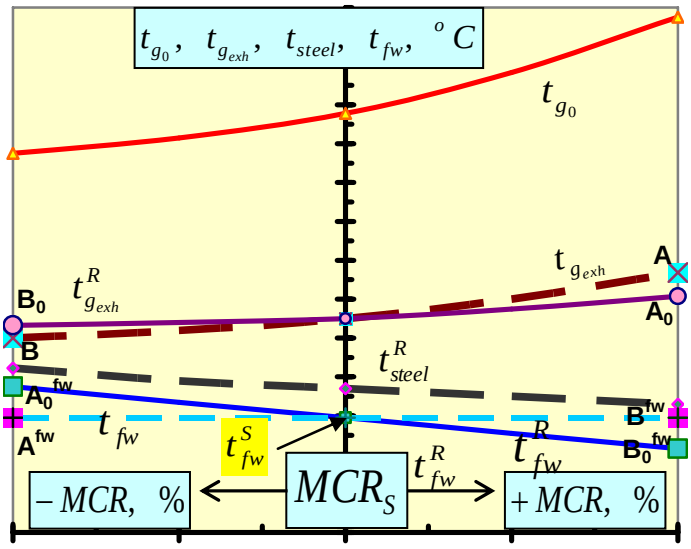

Fig.5.12 Temperature changes at different ME MCR.

(line $A \div B$) at constant feed water temperature corresponding to line $A^{fw} \div B^{fw}$ (see Fig.5.12). This type of optimization ensures additional output generation by WHRS at most frequent service loads, when even any of low figure shortage could be critical at controlled service risk. When we have substantiated one of the reason for such investigation necessity, then feed water temperature impact on pressure choice could be further thoroughly explored. The value t_{fw} growth comes to increase in required water amount for re-circulation k_{rec}, thus adequately influencing economizer part in evaporator $\Delta h_s \uparrow$ (see formula #4.7) and subsequently coming to steam output reduction (see formula #4.5, 5.5). In a result boiler efficiency is growing down as well due less recovered heat amount in economizer $\Delta h_{g_3} \downarrow$ and relevant exhaust gas temperature rise is ensured. Therefore steam pressure is to be lowered; and despite of some growth of coefficient k_{rec} steam output is being increased

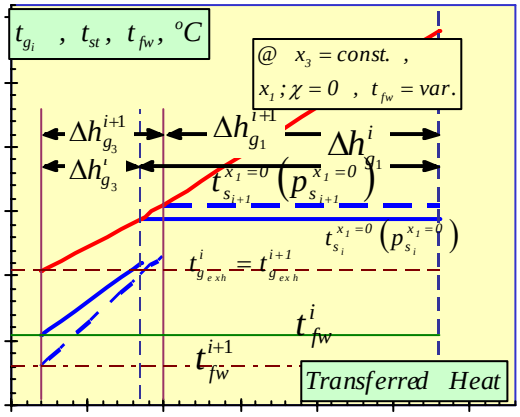

Fig.5.13 Heat-temperature diagram

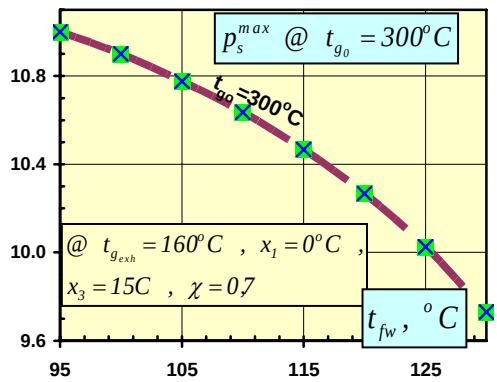

Fig.5.14 Steam pressure choice at variable feed water temperature.

till preliminary accepted constant exhaust gas temperature $t_{g_{exh}}$ (see Fig.5.13). Based presented above considerations the functional dependence of $p_s^{0^{MAX}} = f\left(t_{fw}\right)$ is elaborated with o following alteration indices $\partial p_s^{0^{MAX}} / \partial t_{fw} < 0$; $\partial^2 p_s^{0^{MAX}} / \partial \left(t_{fw}\right)^2 < 0$ (see Fig.5.14).

5.II.7. AT REAL CONDITIONS FOR SPECIFIC BOILER.

Explored steam pressure $p_s^{0^{MAX}}$ is theoretical value corresponding at unlimited boiler sizes, particularly evaporator one, i.e. when $\lim_{z_1 \to \infty} x_1 = 0$. In reality, when specific boiler is installed, *pinch-point* is always positive value $x_1 > 0$; and, respectively less heat will be recovered in both the boiler and the evaporator, i.e. $t_{g_S} = t_s + x_1 > t_s$, what comes to steam

output grow down on value equal to $\Delta\xi = x_1 \times \overline{c_g} \times \eta_{al} / (\Delta h_{st} + \Delta h_s)$. In a result economizer heat capacity $\Delta h_{g_3} \downarrow$ is coming down as well as exhaust gas temperature $t_{g_{exh}} \downarrow$ (see Fig.5.15). Thereby to maintain gas cooling rate constant steam pressure is to be lowered respectively, thus ensuring output $\xi \uparrow$ growth; only the *heat weight* of economizer is increasing at the expense of evaporator. Further surface diminishing, particularly the evaporator part at the very first, comes to respective *pinch point* increase, what considerably influences steam pressure level as follows - $\partial p_s^{MAX} / \partial x_1 < 0;\ \partial^2 p_s^{MAX} / \partial (x_1)^2 > 0$ (see Fig.5.16). For these accepted conditions t_{g_0}, $t_{g_{exh}}$, p_s, x_1, x_3, t_{st} it will correspond to some real boiler with definite convective surface sizes (see Fig.5.17). Despite the fact that acquired number of heating coils is for concrete boiler with spiral ribbed tubes type KYP-3100, nevertheless common regularities are universal. As we can see, *pinch point* $x_1 \downarrow$ reduction results in accelerated boiler surface enlargement; and evaporator at the very first, accompanied by respective pressure growth (see Fig.5.16).

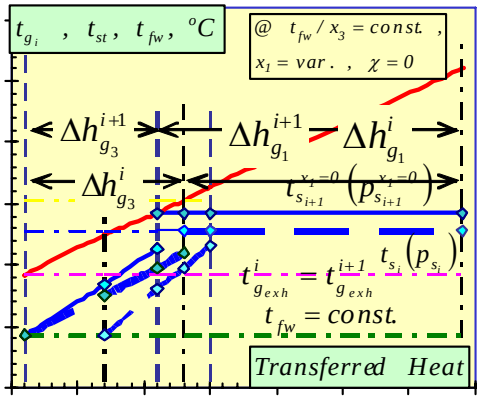

Fig.5.15. Transferred Heat-temperature diagram at $x_1 = \text{var}$.

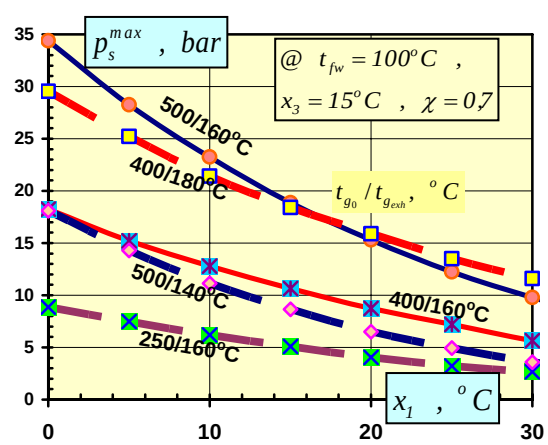

Fig.5.16. Steam pressure in dependence on *pinch-point* temperature.

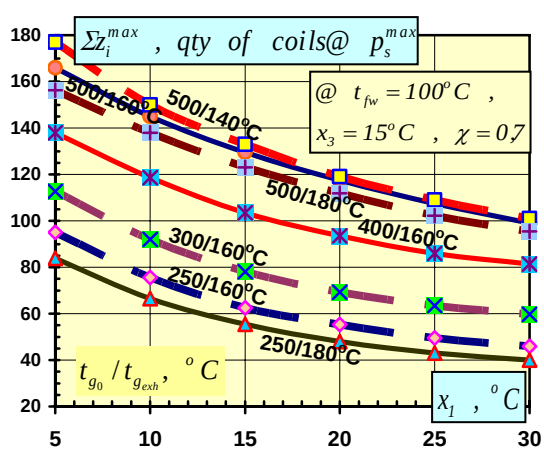

Fig.5.17. Boiler sizes in dependence on *pinch-point* temperature.

However, in order to keep both steam over-heating rate χ and *approach-temperature* x_3 invariable corresponding super-heater and economizer surface enlargement is necessary in different extent due to followed steam output rise (see formulae ##4.5, 5.5). However, boiler surface mutual optimization is thoroughly explored and described in other chapters.

5.II.8. CONCLUSIONS.

1. When service steam pressure should be around equal to recommended one $p_s \geq 7bar$, targeted the lowest gas cooling level $t_{g_{exh}} = 160^o C$ is possible, but by means of EB with developed surfaces, as recovery rate is close to ultimate one.
2. At lowered inlet gas temperatures either steam pressure shall be reduced, or outlet gas temperature increased. Since power plant operation at pressures below $p_s < 7bar$ is problematic, then whether steam consumption is to be reduced or auxiliary boiler is to be put in parallel operation with exhaust one.
3. To ensure more deeper gas cooling below $t_{g_{exh}} < 160^o C$ it might be more practical and efficient by introducing double pressure stage EB and WHRS
4. A bit more beyond the scope of this chapter investigations feed water temperature factor was substantiated and explored. In a result the necessity to govern it t_{fw} in dependence on either ME load or exhaust gas temperature levels or both might be useful from the view point of both safety and efficiency.

CHAPTER 5. SUB-CHAPTER 5.III. HEAT RECOVERY POSSIBILITIES FOR ADVANCED SLOW SPEED DIESEL ENGINE POWER PLANTS.

Due to the fact that heat recovery possibilities are limited for advanced SSDE further investigations are extended for real ships' power plant as per below stated directions:

1. to ensure ship demands in electricity and low-potential heat (by means of saturated steam consumption) via the deepest gas cooling in a steam EB;
2. the effective use of cooling water heat for boiler feed water warm-up and low-potential heat supply, substituting and reducing saturated steam consumption;
3. with a consideration of said above, it is important to evaluate the rate of ship's provision in electricity and heat in dependence on main engine (advanced slow-speed diesel) load level and sailing regions (ambient conditions),
4. Finally, based on research results it should be possible to estimate the effective ways of electricity/heat shortage compensation.

5.III.1. MAIN INPUT CONDITIONS.

Exhaust gas heat recovery is ensured by means of Waste Heat Recovery System, consisting of exhaust boiler, where superheated steam is directed to steam turbine driving alternator and producing electricity for ships demands. Saturated steam is used for low potential heat consumers, e.g. fuel oil preheat, bunker, accommodation, etc. The lowest level of steam pressure p_s in boiler is recommended to be not less than 7 bars to ensure heavy fuel oil (IFO 380) preheating at main engine inlet as well. As noted before, due to low potential of exhaust gas heat, its recovery rate should be obtained as deep as possible at the lowest possible boiler outlet gas temperature, i.e. $t_{g_{exh}} \geq 160^o C$. Boiler feed water warm-up till around $t_{fw} \geq 120^o C$ is provided by means of recirculation, allowing to achieve effective gas heat recovery at safe operation conditions. However, when feed water pre-heat is ensured by means of cooling water of either jacket ($t_{cyl} \approx 80 \div 90^o C$) or scavenging air one ($t_{cyl} \approx 105 \div 110^o C$) or both of them till temperature $t_{fwp_{II}} \approx 100^o C$, further WHRS efficiency growth is obtained by reducing required boiler water amount for recirculation $k_{rec} \downarrow \approx 3{,}6 \times$, thus increasing steam output. In order to reduce saturated steam consumption ξ_{sat} by substituting with cooling water, consumers of low-potential heat should be defined, being found divided in two groups [30, 70, 118, 148, 149]:

A. Consumers of heat that are independent on ambient conditions:

A.1. Fuel oil preheat at ME inlet, which could be ensured only by means of saturated steam as required temperature might be up to $130 \div 150^o C$;

A.2. Fuel oil preheat at separator inlet and could be covered by turbocharger scavenging air heat as required temperature is around $70 \div 90^o C$;

A.3. Required preheat temperature for lubricating oil at separator inlet is lower, i.e. $\leq 70^o C$; therefore possible heat supply could be arranged either by turbocharger scavenging air or even by jacket cooling water;

B. Consumers of heat being dependent on ambient conditions:

B.4. Bunker (and settling) tanks, etc.

B.5. Service tanks

B.6. Accommodations, laundry/washing water and etc.

Heat consumers ##B 4, 5, 6 could be covered either by jacket cooling water heat or turbocharger scavenging air heat, when it is whether available and/or required. Definitely such extensive heat recovery comes to complexity in heat exchange system (see Fig.5.18), requiring additional investments and electrical supply either. Hence, briefly summarizing said, above our plan of action targeted on ships' power plant efficiency increase via waste heat recovery (turbo-generator power output growth) consists of following steps:

1. flue gas heat recovery in EB, supplying electro-energy by STG and low potential heat;
2. feed water preheating from $50^o C$ till $\approx 100^o C$ by means of:

   2.1. jacket cooling water till $70^o C$ and ensuring additional growth in turbine output equally to value ΔNe_{TG}^{3} followed by

   2.2. turbocharger air cooling water till $100^o C$ thus reducing economizer part in boiler and coming to growth in both steam and turbine output on value $\Delta Ne_{TG_{\Delta t}}^{t/c}$;

3. Reduction in saturated steam consumption on corresponding value $\Delta\xi_{sat}^{j}$ by its substituting with cooling water (jacket $\Delta\xi_{sat}^{cyl}$ and turbocharger $\Delta\xi_{sat}^{t/c}$) heat for relevant consumers (see Fig.5.18), and in a result another additional TG output increase by value ΔNe_{TG}^{cyl} or $\Delta Ne_{TG_{\xi}}^{t/c}$ is obtained. Finally, saturated steam consumption will be reduced accordingly - $\xi_{sat}^{0} = \xi_{sat} - \Delta\xi_{sat}^{cyl} - \Delta\xi_{sat}^{t/c}$, where value ξ_{sat}^{0} is the lowest, but required steam consumption to ensure ME operation on heavy fuels.

Such an extensively developed system is to be called as Complex Waste Heat Recovery System (CWHRS) and based on considerations above following main tasks should be explored in this article:

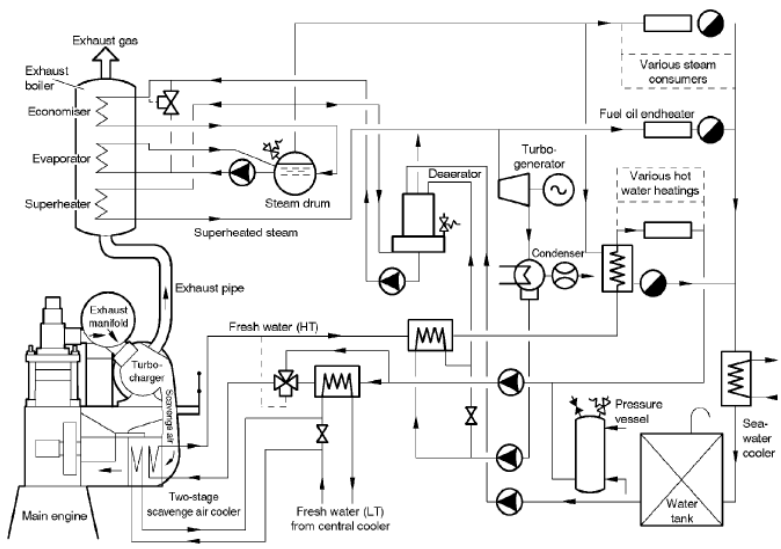

Fig.5.18. Complex Heat Recovery system layout.

1. Efficiency outcome due to exhaust gas and cooling water heat recovery extent;
2. Ambient condition ($t_{s/w}$-sea water and t_a - ambient air temperatures) impact on both main engine output dates (flue gas temperature t_{g_0} and amount G_{g_0}) and low potential heat consumers is significant;
3. ME (advanced SSDE) type ($t_{g_0} = var.$), output ($G_{g_0} = var.$) and work load impact;
4. Electrical and heat shortage determination and ways of compensation.

5.III.2. EFFECTIVE UTILIZATION OF ELECTRICAL ENERGY.

The main efficiency index of CWHRS is turbo-generator output; and especially its utilizing extent by ship consumers. What does it mean? Of course, first of all we are interested in gaining maximum output by CWHRS; and in case of heat/electrical energy surplus safety margin will be enough to run unit in off-line operation mode at different load and ambient conditions with the consideration of equipment wear and tear impact. Meantime, shortage in heat/electricity is more frequent event, which should be effectively compensated, as in case of the absence of such technical sources it might come to CWHRS disabling and total loss of recovered energy. Therefore just an effective utilization of this energy gain implies also effective any shortage compensation during the whole ship's sailing time. Although the problem above is utmost important, nevertheless it is not the main core of our topic to analyze and compare the effective ways how to either compensate or utilize heat/electricity shortage and surplus, but without mentioning the problem and defining the possible solutions our investigations would not be considered as accomplished ones. Therefore different technical solutions will be briefly described only for proposal. Meantime, the level of electrical consumption shall be determined either, being dependable on both ambient conditions and

specific ship type, which might significantly differ with the equipment saturation. As a rule electricity shortage is the issue for our investigated power plants; and the most common way how to effectively solve the problem is introduce auxiliary boiler in the system (see Fig.5.19) and use it as steam drum during WHRS operation. When steam pressure is dropping below some lowest limit, burner will start run to maintain required steam consumption for turbo-generator. Taking into consideration the fact that oxygen content in exhaust gases is around 16%, it would be possible to arrange additional fuel burning in it, being introduced on m/v "K.Ciolkovskis" with some good experience and also considered for some new-building projects under SO_X, NO_X monitoring projects [82]. With the growth of heat/electricity shortage level AB back up might be inefficient; consequently, parallel work with DG should be considered as another alternative, being proposed as two main options:

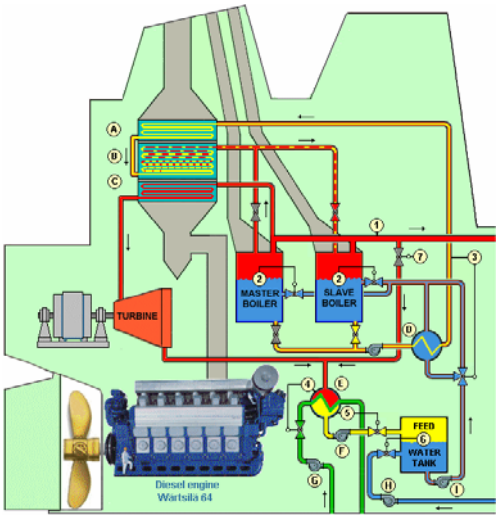

Fig.5.19. Ships' power plant with WHRS+AB in parallel engagement.

A. Parallel operation with diesel of the same output. Such an arrangement simplifies the electrical power plant set up during new-building stage and in future operation/ maintenance scheme; but on another hand even at low level of shortage power distribution amongst diesel and turbine would be so, that it comes to un-complete recovered energy use, thus artificially reducing CWHRS efficiency.

B. Parallel operation with diesel of the reduced output, i.e. so-called peak-engine. The level of possible power turbo-generator shortage should be estimated with the consideration of wide range of different factors, e.g. ME load level, ambient conditions; and the choice of peak-diesel type/modification should be so, that safe parallel operation is ensured during as long as possible voyage time. In this case diesel engine governor line will be more a-static, when running together with steam turbine; and during running alone, governor should be readjusted. Meantime, to save both initial and maintenance costs for diesel EPP peak engine output should be enough to serve at some conditions, e.g. during either ship's stay without cargo operations or specific loading conditions in parallel with base DG or something else. Anyway it would be also benefit to have engines of the same modification, as besides reduction of initial costs, there will be no increase in spare part nomenclature, thus keeping maintenance costs at the lowest possible level.

Another alternative could be also shaft generator application and possible parallel operation with turbo-generator with different arrangement of engagement [49, 75, 110, 118, 148]. Also gas by-pass around turbocharger could be considered as effective solution despite of SFOC (specific fuel oil consumption) drop down, thus increasing gas temperature at boiler inlet. During new building stage the *high efficiency turbocharger* could be substituted with a *conventional* one. Then the amount of air required for combustion purposes can, however, be adjusted to provide a higher flue gas temperature, if this is needed for EB. The matching of the engine and the turbo-charging system is then modified, thus increasing exhaust gas temperature by 20°C. This modification will lead to a 7-8% reduction in the exhaust gas amount, and involve an SFOC penalty of up to 2 g/BHPh [70, 74]. Also it could be possible to find the ways how to reduce electricity consumption level, e.g.:

A. Different mounted on ME service pumps;
B. Central cooling system arrangement by introducing central scoop type sea-water heat-exchanger

5.III.3. SYSTEM OPTIONS.

In our investigations it is explored complex waste heat recovery system (CWHRS) of exhaust gases and cooling water, i.e. jacket and turbocharged air one by means of high temperature stage (HTS) (see Fig.5.18). And such a complex combination (CWHRS +HTS) is accompanied by both highest investments and maintenance costs, but it also ensures the best efficiency of power plant in total. In some cases this type of upgrading might be economically unattractive, especially for ships already in operation; therefore following options are considered for comparison:

Option # 1 - "CWHRS + HTS (+ t/c air)", when the highest steam TG output Ne_{TG}^{1} is delivered at certain ambient conditions, ME load level and the lowest saturated steam consumption demands ξ_{sat}^{0};

Option # 2 - "CWHRS", when only heat of exhaust gases and jacket cooling water is recovered. The performance of heat consumers ##4, 5, 6 are ensured by jacket cooling water only, thus reducing saturated steam amount on value equal to $\Delta\xi_{sat}^{cyl}$ only, i.e. $\xi_{sat} - \Delta\xi_{sat}^{cyl}$, as well as feed water preheating till $70^{o}C$ after hot well. In a result steam turbo-generator output Ne_{TG}^{2} will be lower than the first one.

Option # 3 - "WHRS + 70^oC", when jacket cooling water heat is used only for feed water preheating till 70^oC. Such a modification is easy for implementation even for ships already in operation and steam turbine output will be equal to value Ne_{TG}^3.

Option # 4 - "WHRS", when only flue gas heat is recovered and turbo-generator output Ne_{TG}^0 is the lowest one as well as investments.

Based on these considered options efficiency of system complexity, i.e. recovery extent of ME cooling water heat, could be presented and compared by a value of relative increase in steam turbo-generator output - $K_{\Delta\eta} = \left(Ne_{TG}^{1,2,3} - Ne_{TG}^0\right) / Ne_{TG}^0 \times 100\%$. Such an optional division is based not only on different complexity of the system, but it is also dependent on the fact, that both cooling water heat availability and heat consumer demands are very much affected by both ambient conditions and ME load level. Therefore it might come that at certain service conditions *CWHRS + HTS (+ t/c air)* will transform into simple *WHRS* only.

5.III.4. AMBIENT CONDITIONS AND ME LOAD LEVEL INFLUENCE.

In our investigations three main ambient conditions are considered, which would cover the whole range of both sailing area and period, as follows [30, 70, 118]:

1. **ISO Ambient Conditions** at equally sea water and ambient air temperatures, i.e. $t_{s/w} = 27^oC$ & $t_a = 27^oC$. Based on investigations around $28 \div 37\%$ of sailing time lies in this weather zone, which characterizes with high gas temperatures at low demands in consumption of heat (saturated steam, cooling water heat). Meantime the electrical consumption will be the highest one due to air conditioner performance;
2. So called **B&W Ambient Conditions** with following sea water and air temperatures - $t_{s/w} = 18^oC$ & $t_a = 20^oC$, corresponding to summer conditions in temperate zone. Average total sailing time could reach up to $30 \div 38\%$. As outlet from ME gas temperature is very much dependent on ambient one, then it $t_{g_0} \downarrow$ drops down considerably till $\approx -15^oC$, while gas charge has a tendency to rise slightly $\approx +3\%$.
3. **Nordic Ambient Conditions** corresponds to autumn/spring season in temperate zone at equally, but significantly lower sea water and ambient air temperatures as follows: $t_{s/w} = 10^oC$ & $t_a = 10^oC$. Average total sailing time could reach up to 10%.

Also ME load level has a significant influence on gas dates, especially on flue gas amount, therefore 60% of Maximum Continuous Rating (MCR) is considered as the lowest reasonable level to be investigated as per service experience. ME modification impact is reflected via inlet gas temperature different levels, being also considered in our researches. In a result some common regularities are brought out. When ship is sailing in warm climate zones, demands in low potential heat are the lowest ones, while its eventual provision is the highest one. Nevertheless al low potential heat consumers type B ##4, 5, 6 could be provided by jacket cooling water heat only in the whole region of working load levels of ME, i.e. from 100% till 60% of MCR. Next-important value of effective utilization is turbocharged air cooling water heat, which is much more dependent on both ME load level and ambient temperatures. In a result it is found generated electrical power by CWHRS + HTS in dependence on ME output/ modification and load level (see Fig.5.20a, b). Despite the fact that **ISO** conditions are most

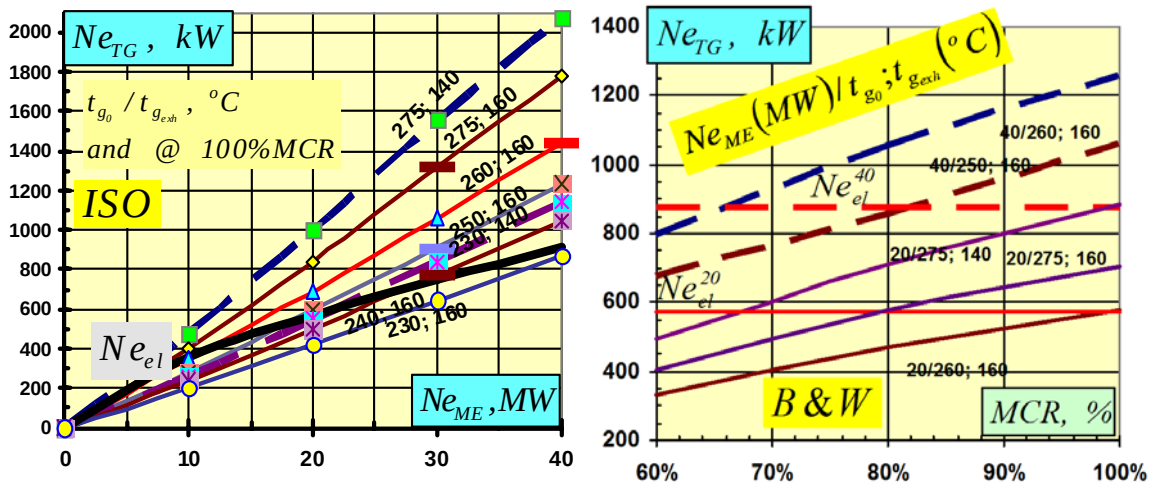

Fig.5.20 TG output by CWHRS in dependence on ME output /modification & load level
a) - @ ISO ambient conditions b) - @ B&W ambient conditions

favorable ones in order to obtain the highest TG output, still the main engine rating should be high enough up to $Ne_{ME}^{ISO} \geq 15 \div 20MW$ in order to ensure autonomous *CWHRS+HTS* performance @ $80\%MCR$ ME load level. For **B&W** conditions it constitutes not less than $Ne_{ME}^{B\&W} \geq 18 \div 25MW$. Subsequently, by choosing such a ME nominal output level at specific MCR , when following precondition $Ne_{TG} > Ne_{el}$ is met, we could expect in full supply of both electrical power and heat solely by ST, EB and cooling water heat exchangers during around $\approx 50 \div 80\%$ of total sailing time respectively. For **Nordic** sailing area lowest required ME output would be even more higher up to $Ne_{ME}^{Nord} \geq 25MW$ at $\geq 80\%MCR$, when autonomous TG performance could be ensured with some back-up by AB. Nevertheless in dependence on ME output and load level average shortage in electrical consumption

constitutes up to $50 \div 70\%$, therefore parallel operation with base DG would be the solution. Complexity of HTS performance could be described and represented via below presented functional dependencies (see Fig.5.21a, b). Considering the fact, that cooling water heat of

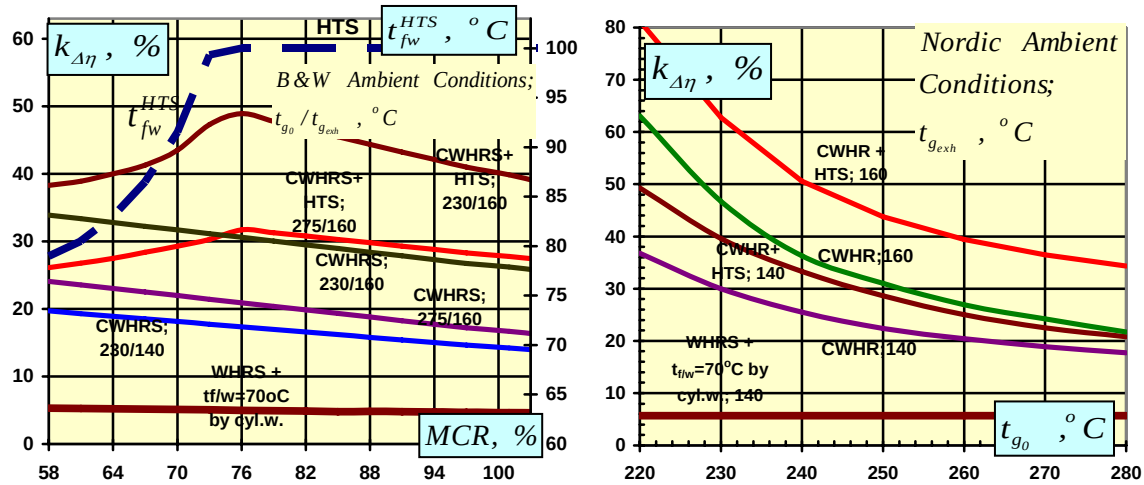

With various complexity of ME cooling water heat recovery WHRS relative thermo efficiency dependence on **Fig.5.21a** ME load level & **Fig.5.21b** inlet gas temperature @ B&W/Nordic ambient conditions for different ME modifications & gas cooling rate.

turbocharged air is very much dependable on both ME load level and sailing region, following common regularities are found:

- HTS cannot supply enough recovered cooling heat for consumers type A ##2, 3, thus slightly increasing saturated steam consumption and diminishing power gain $\Delta Ne_{TG_\xi}^{t/c} \downarrow$, when ME load level is below:
  - $\approx 72\% MCR$ at **ISO**;
  - $\approx 76\% MCR$ at **B&W** and
  - $\approx 83\% MCR$ at **B&W** ambient conditions (see Fig.5.21a).
- With further ME load level reduction there is even not enough heat to ensure feed water preheating till designed temperature; in a result relevant ST power gain drops down $\Delta Ne_{TG_{\Delta t}}^{t/c} \downarrow$. The critical MCR levels for different ambient conditions are as follows:
  - $\approx 67{,}5\% MCR$ for **ISO**, but at $\approx 60\% MCR$ feed water temperature before thermostatic mixing valve will drop down till $90^o C$;
  - $\approx 73\% MCR$ for **B&W**, but further reduction in ME load level is accompanied by relevant cooling water temperature decrease after HTS till $\approx 80^o C$ at $60\% MCR$ and feed water preheating temperature as well (see Fig.5.21a);

- $\approx 79\% MCR$ in **Nordic** conditions with further cooling water temperature after HTS drop down till $\approx 70^{o}C$ at $68\% MCR$, when this cooling stage is switched off.

Based on above conclusions functional dependence of efficiency outcome $K_{\Delta\eta}$ due to different complexity of WHRS could be interpreted as below (see Fig. 5.21a, b):

- With reduction of ME load level $K_{\Delta\eta}$ has a tendency to grow up due to the fact, that:
  - TG output of so called *gas factor* part reduces $Ne_{TG}^{0} \downarrow$ due to its direct dependence;
  - While low potential heat consumer demands remain without changes;
  - Recoverable heat amount from t/c air cooling water is almost in direct dependence.
- Below some certain ME load level the coefficient $K_{\Delta\eta}$ has a tendency to decrease due to switching off HTS, what results into power loss $\Delta Ne_{TG}^{t/c}$, or gain as appropriate, being a difference between two values as follows - $Ne_{TG}^{1} - Ne_{TG}^{2} = \Delta Ne_{TG}^{t/c}$. Meantime, this power gain is built up by two constituents, i.e. $\Delta Ne_{TG}^{t/c} = \Delta Ne_{TG_{\xi}}^{t/c} + \Delta Ne_{TG_{\Delta t}}^{t/c}$, due to substitution of saturated steam consumption and feed water warm up in HTS;
- Hence at some certain load level "CWHRS + HTS (+ t/c air)" converts into either CWHRS only or with partial HTS use (see Fig. 5.21a);
- With a reduction of inlet gas temperature the specific part of cooling water factor $K_{\Delta\eta}$ grows up (see Fig. 5.21b) due to reduction of exhaust gas constituent $Ne_{TG}^{0} \downarrow$, while it comes to opposite result by ensuring more deep gas cooling rate $t_{g_{exh}} \downarrow$;

With a ship's movement into sailing zones with lower ambient temperatures $K_{\Delta\eta}$ has a tendency to increase due to the fact, that gas constituent is very much affected by it; and so the average additional net gain $K_{\Delta\eta}$ "CWHRS + HTS (+ t/c air)" constitutes around:

- $\approx 25 \div 34\%$ for **ISO**;
- $\approx 35 \div 40\%$ for **B&W** and
- $\approx 45 \div 50\%$ for **Nordic** ambient conditions.

Meantime $K_{\Delta\eta}$ is more sensitive to load level changes in colder sailing regions due to HTS performance peculiarities. Based on presented dates, required for autonomous CWHRS performance level of ME nominal output could be determined in dependence on load level and inlet gas temperature (see Fig.5.22a, b). These dates would be important during new-building project stage; and following interpretations are described as below:

- Till around $\approx 85\% MCR$ level there is slight increase in required ME output $Ne^{nom}_{ME_{min}}$,
- What predetermines quite reliable and effective performance of "CWHRS+HTS";
- But at load levels below $\approx 75\% MCR$ $CWHRS+HTS$ efficiency drop down is increasingly dominating;
- As well as inlet gas temperature reduction below $t_{g_0} \downarrow \leq 260 \div 255^o C$;
- Combination of both factor MCR and t_{g_0} reduction is the worst scenario for efficient CWHRS introduction and performance.

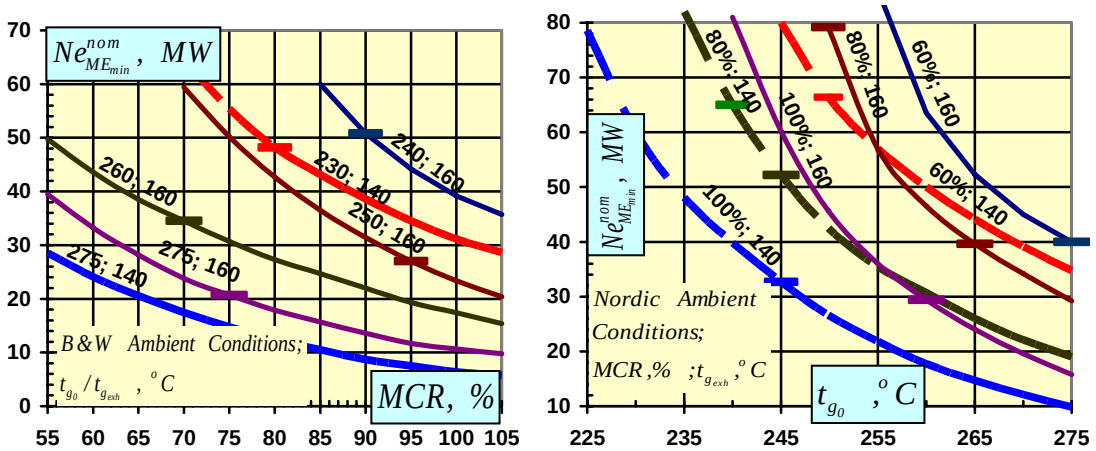

The lowest ME nominal output, at which ship demands in both electricity & heat are met by CWHRS+HTS only, in dependence on **Fig.5.22a** ME load level & **Fig.5.22b** inlet gas temperature @ B&W/Nordic ambient conditions & various gas cooling rate.

5.III.5. CWHRS EFFICIENCY FOR DIFFERENT SHIPPING TRADE LINES.

Investigated above ambient conditions for WHRS efficiency evaluation cannot be considered as comprehensive and completed for real ship, which is moving from one destination port to another one, where ambient temperature changes could be dramatic ones during just one voyage. For example, air temperature during sea voyage from Rotterdam till Montreal (Canada) could vary from $+10^o C$ till $-20^o C$ in early spring time within some 20/30 days of a sea passage. Based on long-term observations it comes out, that yearly average difference between sea water and ambient air temperatures constitute only around $1 \div 2^o C$, i.e. $t_{s/w} - t_a = \Delta t_a^{s/w} = 1 \div 2^o C$ [140]. Based on this statement functional dependence of TG output on sea water temperature is build up as follows $Ne^1_{TG} = f(t_{s/w_i})$ for different ME modifications ($t_{g_0} = var.$), load levels, nominal output (see Fig.5.23). In a result it becomes possible to investigate CWHRS application suitability for each, concrete trade line

with respect of ME particulars and ship type. By evaluation of long-term observations yearly mean-weighing sea water temperature $\overline{t_{s/w}}$ changes during one particular voyage could be established as dependence of relative time τ_{t_n} of sailing, i.e. $\overline{t_{s/w}} = f\left(\tau_{t_n}\right)$, where $\tau_{t_n} = \sum_{\Delta t_{min}} a_i / S$ - relative sailing time in zone at specified sea water temperature; Δt_{min} - sea water temperature fluctuations within marginal range; a_i - sailing time (distance), during which specified sea water temperature fluctuates within minimum range equal to $\Delta t_{\min}$; S - total sailing time (distance) of one specific voyage.

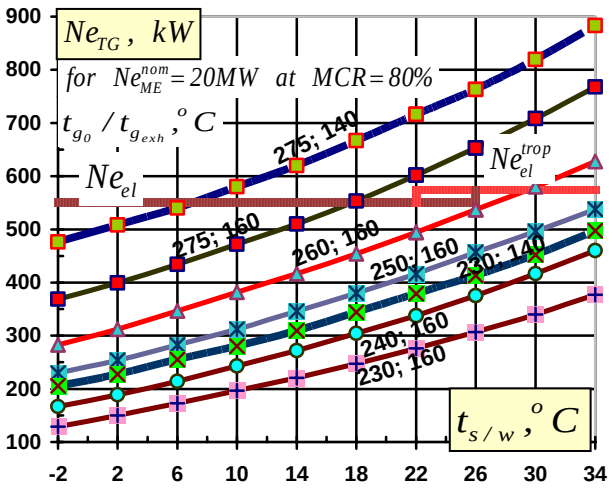

Fig.5.23. Output by CWHRS+HTS TG in dependence on yearly mean s/w temperature at various ME outputs, MCR & modifications.

Finally, it is elaborated functional dependence of TG output, i.e. $Ne_{TG}^{1,2,3} = f\left(\tau_{t_n}\right)$, on relative sailing time providing that all low potential heat consumers are maintained either by ME cooling water heat or saturated steam from EB only. That sort of analyze allows us:

- to define total sailing time, when TG (CWHRS) is working in off-line mode;
- to estimate shortage $-\Delta Ne_{TG}^{1,2,3}$ in electro-energy production by STG, its duration so that the most effective way of this energy shortage compensation could be found out;
- in a result to ensure the optimal set up of power equipment, e.g. AB, DG choice.

Following trade lines are investigated as below:

1. Baltic sea – Caribbean Sea (Central America) (see Fig.5.24);
2. Baltic sea – Gulf of Guinea (West coast of Central Africa);
3. Black sea – Caribbean Sea (Central America);
4. Black sea – Gulf of Guinea (West coast of Central Africa) (see Fig.5.25);
5. Black sea – ports of Japan around Africa(see Fig.5.26);
6. Black sea – ports of Japan via Suez Canal;
7. Baltic sea – Gulf of St. Lawrence
8. Black sea – ports of Italy (see Fig.5.27).

This choice is fortified on the ground of the fact, that it practically covers the whole sailing area with possible ambient temperature changes; and obtained results could be easily adjusted for other trade lines either. On the presented graphs above we have different estimations of

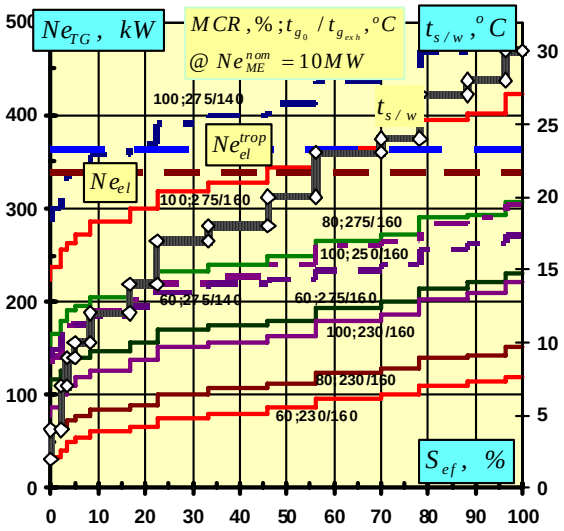

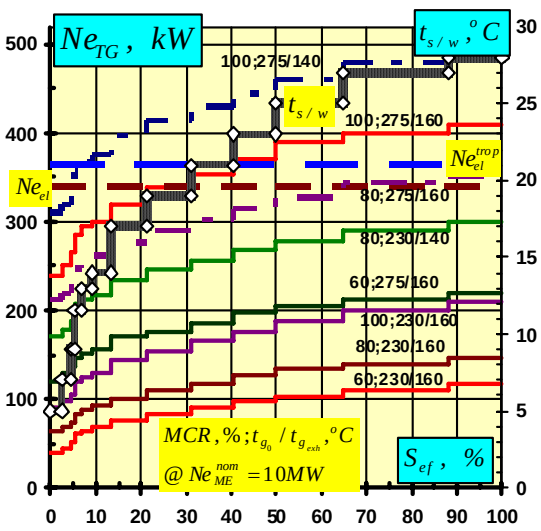

Yearly mean weighing steam turbo-generator output produced by CWHRS+HTS in dependence on relative sailing time for trade lines

Fig.5.24. Baltic sea – Caribbean Sea (Central America).

Fig.5.25. Black sea -Gulf of Guinea (West Coast of Central Africa).

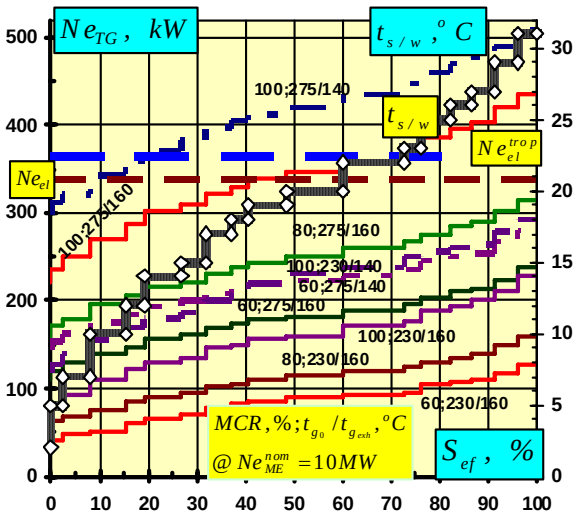

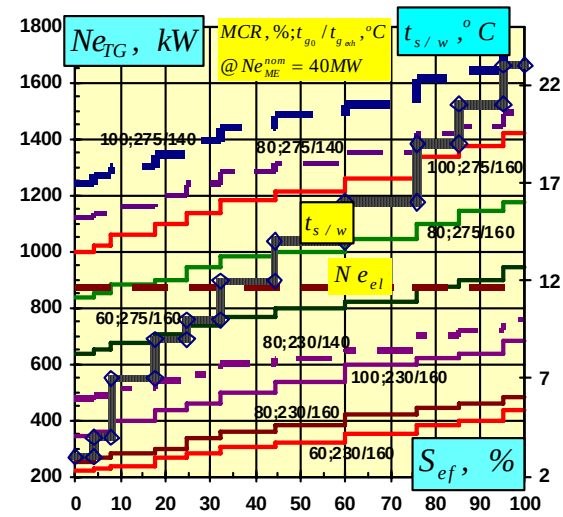

Yearly mean weighing steam turbo-generator output produced by CWHRS+HTS in dependence on relative sailing time for trade lines

Fig.5.26. Black sea - ports of Japan around Africa. Fig.5.27. Black sea - ports of Italy.

expected electro energy either shortage or surplus within sailing time. Followed comparison is based in dependence on ME nominal output and modification, as there is quite distinguished distribution in total fleet number based on these parameters. It is close to common for all trade lines that with reduction of ME nominal output below $Ne_{ME_{MIN}}^{nom} \leq 15 \div 20MW$ and load level $MCR \leq 80 \div 85\%$ autonomous performance of *CWHRS+HTS* is ensured only $10 \div 50\%$ of total sailing time S_{ef} on the best. The ways how to effectively compensate electro energy shortage could be all possible proposals above in dependence on ME modification. With the

reduction of nominal output below $Ne_{ME_{MIN}}^{nom} \leq 12MW$ and load level $MCR \leq 80 \div 75\%$ there could be offered only one way of shortage recovery, i.e. parallel operation of TG and diesel one with reduced power as the most optimal and possible choice in many cases.

For power plants with ME output above $Ne_{ME_{MIN}}^{nom} \geq 20MW$, but not more than $Ne_{ME_{MIN}}^{nom} = 25 \div 27MW$ shortage duration in electricity is reduced till $S_{ef} = 30 \div 40\%$ only at $MCR \approx 80\%$; and this deficit is small enough to choose either additional steam supply from AB or some other equivalent solution, except additional diesel generator installation.

For power plants with ME output above $Ne_{ME_{MIN}}^{nom} \geq 27 \div 30MW$ at $MCR \approx 80\%$ effective autonomous "CWHRS+HTS" is ensured during the whole sailing time for ME modifications, which inlet gas temperature is not less than $t_{g_0}^{ISO} \geq 250^o C$. Any electrical energy shortage could be compensated without DG engagement. Presented conclusions generally are applicable for all investigated lines except following two ones, which should be specially considered. Trade line Baltic Sea – Gulf of St. Lawrence is characterized not only by the lowest sea-water/air temperatures, but also due to the fact that severe ambient conditions, when wind force is around and more than 5-6 balls after Bofort scale, is quite a frequent natural phenomenon; and it means that ships will be serviced at lowered ME load level to avoid its overcharge. In addition, unstable propulsion plant performance, especially during ballast voyage, when propeller frequently comes out from water, it might come to impossibility to run WHRS. Therefore the system introduction might be of economical beneficence for big ships with high rated ME output such like container, Ro-Ro type ships.
For shipping line Black sea – ports of Italy (see Fig.5.27) total sailing time is quite short accompanied with considerable longer ME idle time due to cargo operations in ports at considerably low ambient average temperatures, however being more stable during the year. Therefore *CWHRS+HTS* could be able to ensure ships' demands in electricity and heat already at ME output equally to $\geq 15 \div 16MW$ at 80% MCR.

After summarizing presented sailing lines mean-weighing sea water temperatures during the whole voyage $\overline{t_{s/w}^{S_i}}$ could be evaluated accordingly: $\overline{t_{s/w}^{S_i}} = \sum_{i=1}^{n} t_{s/w_i} \times a_i \Big/ S^{\Sigma}$; and following mean temperature values were found for above mentioned lines:

1. Baltic sea – Caribbean Sea (Central America) (see Fig.5.24) - $\overline{t_{s/w}^{S_i}} = 19{,}85^o C$;
2. Baltic sea – Gulf of Guinea (West coast of Central Africa) - $\overline{t_{s/w}^{S_i}} = 17{,}23^o C$;

3. Black sea – Caribbean Sea (Central America) - $\overline{t_{s/w}^{S_i}} = 22{,}80^o C$;
4. Black sea – Gulf of Guinea (see Fig.5.25) - $\overline{t_{s/w}^{S_i}} = 22{,}10^o C$;
5. Black sea – ports of Japan around Africa(see Fig.5.26) - $\overline{t_{s/w}^{S_i}} = 18{,}93^o C$;
6. Black sea – ports of Japan via Suez Canal - $\overline{t_{s/w}^{S_i}} = 26{,}90^o C$;
7. Baltic sea – Gulf of St. Lawrence - $\overline{t_{s/w}^{S_i}} = 9{,}63^o C$;
8. Black sea – ports of Italy (see Fig.5.27) - $\overline{t_{s/w}^{S_i}} = 14{,}98^o C$.

Obtained average sea water temperature $\overline{t_{s/w}^{S_i}}$, and in a result ambient air $\overline{t_a^{S_i}}$ as well, during the whole sea voyage could serve as some important efficiency index, however ship type and trade features could have predominant influence via ME performance level. Nevertheless based on these temperatures some conclusive regularity are elaborated and presented in charts (see Fig.5.28-5.31). In a result effective time S_{ef}^{aut},%, when autonomous performance of

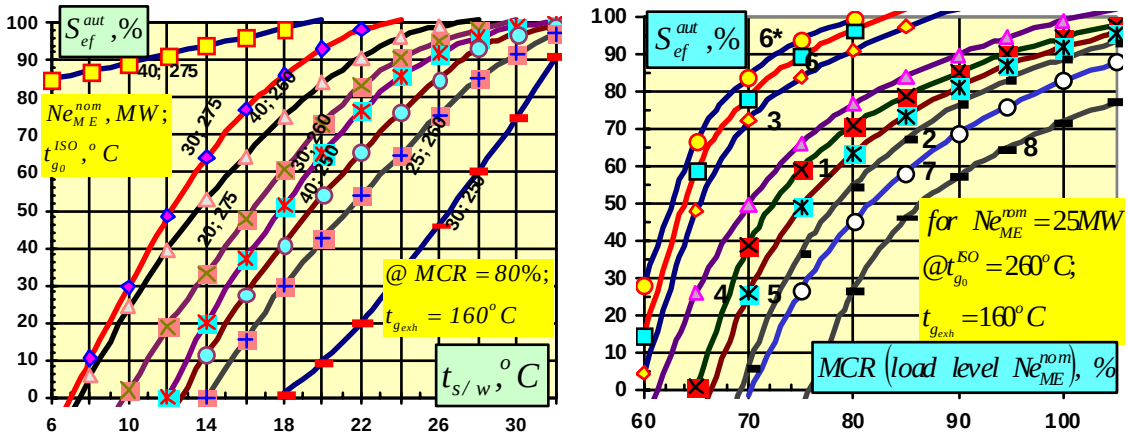

Relative sailing time, when ship demands in el-power & heat are fully met by *CWHRS+HTS* for different trade lines in dependence on
Fig.5.28 yearly mean weighing sea water temperature. Fig.5.29 ME load level.

CWHRS+HTS is ensured and presented as functional dependence $S_{ef}^{aut} = f(t_{s/w})$ for different ME modifications (t_{g_0}), nominal output (Ne_{ME}^{nom}) and load level (see Fig.5.28). As noticed before, CWHRS efficient performance is very sensitive on ME load level (see Fig.5.30), as practically for all shipping lines by reduction in MCR below 80% it comes to accelerated decrease in value S_{ef}^{aut}. Also by reducing ME nominal output below some critical minimum $Ne_{ME}^{nom/crit}$ effective time of autonomous WHRS performance starts reduce significantly; and at accepted conditions this level would be around $Ne_{ME}^{nom/crit} \le 18MW$. The choice of ME

modification should be thoughtful, when heat recovery is considered, as inlet gas temperature reduction below value $t_{g_0} \le 250^o C$ (see Fig.5.31) could result in doubtful usefulness of

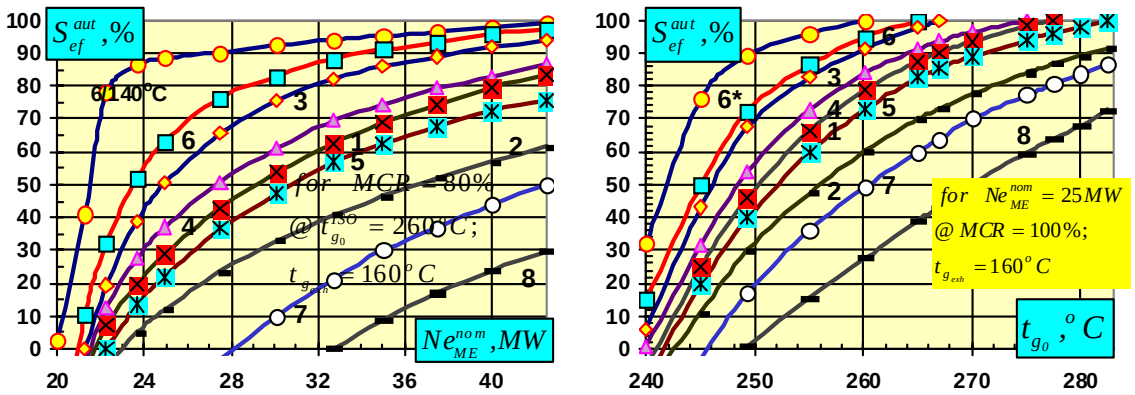

Relative sailing time, when ship demands in el-power & heat are fully met by *CWHRS+HTS* for different trade lines in dependence on

Fig.5.30. ME output. Fig.5.31. inlet gas temperature.

CWHRS. Based on presented above results, conclusions the minimum level of sea water temperature, at which autonomous performance of $CWHRS + HTS$ is ensured, could be finally extracted as functional dependence of following:

$$t_{s/w}^{\min} = f\begin{pmatrix} Ne_{ME}^{nom} & , & t_{g_0} & , \\ t_{g_{exh}} & , & MCR & \end{pmatrix}$$ (see Fig.5.32).

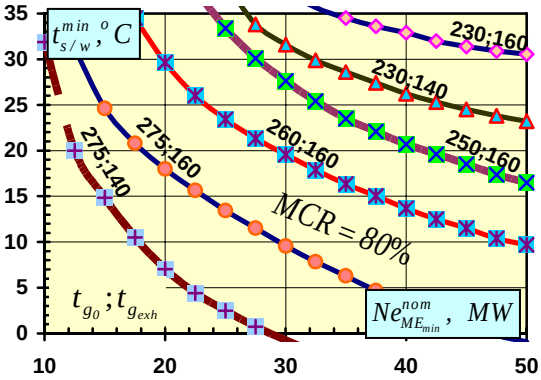

Fig.5.32. The lowest s/w temperature at which $Ne_{TG} > Ne_{el}$ and @ 80%MCR.

This diagram could be valuable during new-building stage, when ME dates are chosen for known trade. Actually this is a diagram of so-called 100% supply, but also another functional dependencies, at conditions when, for example, only 80% of total sailing time ship demands are fully covered by CWHRS, could be elaborated and considered as economically beneficent.

5.III.6. EXAMPLES OF POSSIBLE CWHRS EQUIPMENT OPTIMIZATION.

Based on presented dates, some specific example, how to manage system equipment choice to get the highest efficiency in the whole ship service range, would be examined. It might happen, that durable engine service load is in so-called variable efficiency region (zone $A \div B$) (see Fig.5.33), when for example t/c air cooling heat is not in sufficient amount to

heat-up boiler feed water till designed temperature. It is quite often, that water flow adjustment is performed manually, i.e. by opening inlet/outlet valves. With the consideration of human factor, due to the fact of reduced crew members onboard present-day ships, it would be very likelihood, that in this region efficiency would be reduced till the minimum, i.e. with the temperature changes, when alarm would appear, motormen will close feed water valves via HTS, thus unevenly both increasing required re-circulated saturated water consumption and reducing CWHRS+HTS efficiency till regular CWHRS (see Fig.5.33 – line $A_{ef} \div B_{ef}$). In order to use this recoverable heat with high efficiency in this variable zone $A \div B$ it would be necessary to install some additional self-governing valve, the costs of which would vary within range of 800÷1500$ including installation. Let's assume, that ME is permanently loaded for some time at the level $MCR = 76\%$, what means additional gain $\Delta k_{\Delta\eta} = 6{,}32\% = 35{,}60\% - 29{,}28\%$ if thermostatic self-governing valve is installed. If, for example, TG output constitutes $Ne_{TG} = 800kW$, then absolute gain is equal to - $\Delta Ne_{TG} = 800kW \times 6{,}32\% = 50{,}56kW$. For equivalent diesel-generator specific fuel oil consumption (SFOC) would be around to $SFOC \cong 0,200 \quad kg/(kW \times hr)$, what will result in specific fuel savings equally to $10{,}112 \quad kg/hr$. In reality, it might be very likelihood, that, when ship is either reaching or leaving a port, ME is serviced at reduced load level due to different factors, e.g. trade, fairway and other factors; and as a rule this time is not less than 12 hrs both sides (see Fig.5.34). In general, any average sea passage might be from 17 till 20 days, where full one day ME is serviced at reduced power. Ship's service lifetime could be divided in 2½ years, when docking for approximately 30 days is required. Then total time for shipping would constitute $2{,}5\,years \times 365\,days - 30\,days = 882{,}5\,days$, what results in average $353\,shipping\ days\ per\ year$ or $18 \div 21\ sea\ voyages\ per\ year$; and it means that in total

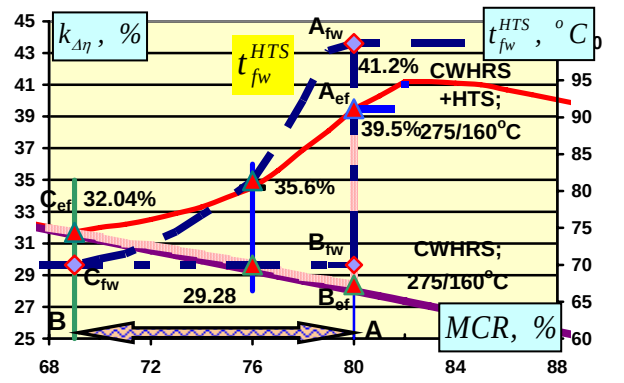

Fig.5.33 CWHRS equipment optimization possibilities to ensure highest service output.

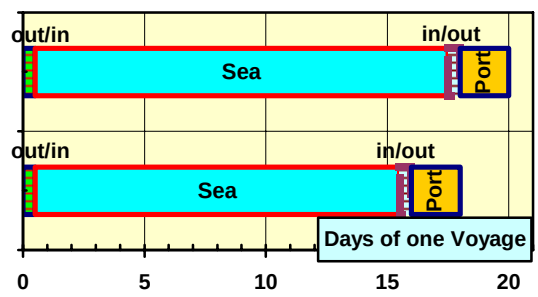

Fig.5.34 Eventual sea voyage distribution.

$18 \div 21$ *days per year* ship's power plant will be operated in region $A \div B$ of *unstable CWHRS efficiency* (see Fig.5.34). At the fuel IFO380 price equal to ≈250÷300 (LS180) $/m.t. net savings per year would be around $2530 \div 3030$\$; and relevant pay-back time is approximately just half a year. Meantime, just the provision of autonomous CWHRS performance as long as possible is rather important than these savings. Further improvements in safe performance of SEPP could be elaborated with the consideration that TG output should be in excess to that required one, i.e. $Ne_{TG} > Ne_{el}$; and it means setting up some power safety levels, at which plug-in of additional energy sources are to be considered. It proposed to introduce both Upper U_{SLel} and Lower L_{SLel} Safety Limits of required Electrical energy as follows - $U_{SLel} > L_{SLel} > Ne_{el}$. So by reaching zone "A" (from right to left, so-called Performance Zone of Reduced Reliability **PZRR**) (see Fig.5.35) it is not anymore so safe to run CWHRS in autonomous regime, some eventual preparatory precautions shall be taken into consideration. When the ship is entering zone "B" it might be necessary to activate back-up sources and run them in parallel with TG, i.e. either additional steam supply from AB or joint performance with DG or something else. In reality, based on available results of our investigations there could be different solutions and approaches to solve this problem safely both during new-building stage and in operation, besides what was considered before as following:

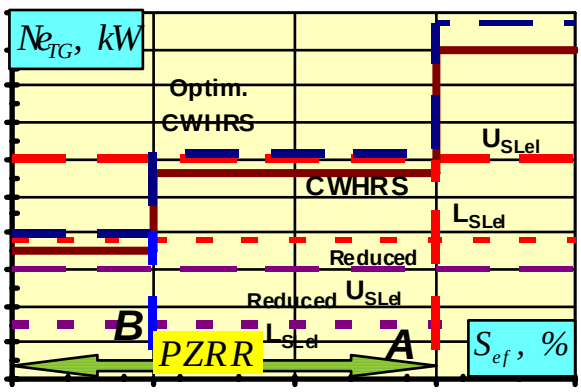

Fig.5.35 Electrical power plant and CWRHRS safe set up, adjustment diagram.

1. *HARDWARE*:
   a. the correct and optimal choice of additional energy sources (see above);
   b. alarm indication installation for both safety levels U_{SLel} and L_{SLel}, when reached;
   c. blocking software and hardware incorporation in electrical plant control unit, which does not allow some dedicated consumer start-up without additional preparation;
   d. as already considered in region of variable efficiency (see Fig.5.33) introduction of self-governing valve might increase produced electrical energy level (see Fig.5.35 – line *Optim.CWHRS*) and reduce sailing time in zones *A*÷*B*, i.e. PZRR.
2. *SOFTWARE (OPERATIONAL)*:

a. Ship's technical instructions for safe maintenance in zones *A÷B* (see Fig.5.35);
b. Guidance, when and which additional source of energy to be put into operation;
c. Dedicated equipment, e.g. lubricating & fuel oil separators and others, switch off for some time, especially, in zones *A÷B*, thus automatically reducing both electrical consumption and established safety levels U_{SLel} and L_{SLel} either;
d. Reduction of saturated steam consumption by switching off unnecessary consumers;
e. For items **c.** and **d.** instruction manuals shall be elaborated by ship's operator;

5.III.7. CONCLUSIONS.

1. Due to reduced thermodynamic parameters of exhaust gasses further increase in WHRS efficiency could be obtained by extensive utilization of ME cooling water heat.
2. In dependence on service conditions and economical usefulness the extent of which cooling heat part shall be recovered might differ. In ultimate version of heat recovery, i.e. *CWHRS+HTS*, when both all possible low potential heat consumers and feed water pre-heat is ensured by recovered cooling water heat only, efficiency rise is ensured up to $K_{\Delta\eta} = 20 \div 40\% \div 60\%$ (see Fig.5.21).
3. Besides efficiency gain just CWHRS ability to provide all ship's demands in electricity and heat is the main core point of the task. Therefore, possible efficient ways, how to compensate eventual electrical/heat shortage, shall be considered, when shortage levels are find out in dependence on various factors of ships' service.
4. Not only on ME rating and its load level make direct influence on *CWHRS (+HTS)* efficiency, but also ambient conditions via flue gas dates (see Fig.5.20/21). So by moving ship in warmer climate zones CWHRS ability to perform in autonomous regime becomes more certain. Nevertheless at possible MCR level below $\leq 80\%$ ship demands in electricity and heat are fully covered, when ME nominal output is above $Ne_{ME}^{crit} \geq 15 \div 18MW$, and more higher for colder regions - $Ne_{ME}^{crit} \geq 28MW$.
5. HTS efficient performance is highly dependent on both ambient temperatures and ME MCR. Therefore this upgrade possibility shall be carefully revised based on following:
   a. HTS cannot supply enough recovered cooling heat for consumers type A ##2, 3, thus slightly increasing saturated steam consumption and diminishing power gain $\Delta Ne_{TG_\xi}^{t/c} \downarrow$, when ME load level is below $\approx 72\% MCR$ at **ISO**, $\approx 76\% MCR$ at **B&W** and $\approx 83\% MCR$ at **Nordic** ambient conditions;

b. By further MCR diminution HTS cannot supply enough heat for consumers to ensure feed water preheating till designed temperature; and in a result relevant steam turbine power gain drops down $\Delta Ne_{TG_{\Delta t}}^{t/c} \downarrow$ at next critical load levels:

- $\approx 67{,}5\% MCR$ at **ISO**, but at $\approx 60\% MCR$ feed water temperature before thermostatic mixing valve will drop down till $90^o C$;
- $\approx 73\% MCR$ at **B&W** , but further reduction in ME load level is accompanied by relevant cooling water temperature decrease after HTS till $\approx 80^o C$ at $60\% MCR$ and feed water preheating temperature as well;
- $\approx 79\% MCR$ at **Nordic** ambient conditions with further cooling water temperature after HTS drop down till $\approx 70^o C$ at $68\% MCR$, when this turbocharger HTS is switched off.

6. With the reduction of design inlet gas temperature before EB t_{g_0}, i.e. different ME modification, turbocharger type, *CWHRS (+HTS)* ability to supply ships' demands in electricity and heat reduces significantly.
7. (C)WHRS Efficiency exploration for different trade lines is important to find the optimal choice for electrical/heat plant set up with the consideration of this shortage extent and duration at lowest required investments and highest reliability.

CHAPTER 6. POLLUTION COEFFICIENT DETERMINATION POSSIBILITIES FOR POWER PLANT IN OPERATION.

Pollution coefficient from gas side ε is not only an important heat transfer efficiency characteristic, but also safe and durable operational factor. Very often due to high ash deposit formation tail surfaces are exposed to heavy acid corrosion, which leads to boiler section breakdown and dramatic decrease in total efficiency of WHRS. There are a lot of investigations carried out for main boilers running on coal, meantime, quite limited explorations for EB, that are installed for ship's use. In our case pollution coefficient is proposed found indirectly via heat transfer efficiency k determination based on solution of both equations of heat balance and convective heat transfer accordingly $Q = k \times F \times \Delta t_{LOG}$.

Therefore in this part of analytic and pilot (experimental) studies we will try to establish

- How accepted meanings of pollution coefficient coincide with those determined based on experimental results;
- Certainty of obtained results;
- Possible ways for improvement of proposed approach of pilot (experimental) studies

In order to explain and understand results of experiment the nature of this phenomenon will be described applicably to EB by revising other carried out researches for main boilers.

6.1. NATURE OF POLLUTION COEFFICIENT FROM GAS SIDE.

Formation of pollution coefficient ε could be classified in accordance with gas temperature level, i.e. high temperature, when gas temperature is - $T_g > 600^o K \left(> 327^o C\right)$; and low temperature, when - $T_g \leq 600^o K \left(\leq 327^o C\right)$ [4, 47, 58, 107, 112, 125]. For EB low temperature factor will have the dominant impact, while high temperature one could be present in super-heater section for advanced GT as a ME of power plant. The main physical factors contributing ash deposit formation are as follows:

1. The effect of thermo-forese, when movement is ensured in direction from hot part of gas stream to cold surface of tube.
2. Condensation of alkali compounds on relatively "*colder*" convective surfaces plus forces of chemical reaction (process of formation sulphates and others).
3. Adhesion forces – cohesion (bonding process) of particles on steel surfaces, consisting of molecular force interaction, including electrostatic and capillary; and being intensified by sticky film of condensation (H_2O, H_2SO_4).

4. **Autoadhesion** due to molecular attractive forces between themselves.

In dependence on particle joint type and mechanical strength of a layer deposits are classified as mealy, cohesive-mealy, tough-cohesive and melted slag type. For EB it is mostly observed the appearance of the first two types, while the last type of layer deposits practically is absent; and the biggest problem is caused by cohesive-mealy ash deposits, the development of which is influenced by both chemical reaction forces and high cohesive (binding) characteristics. Ash deposit formation velocity could be presented as a sum of two processes $g = g_1 + g_2$, where g_1 - speed (intensity) of deposit formation by neutral particles; g_2 - speed of deposit formation by reactive particles, i.e. with cohesive (binding) properties. Summary fall-out of either neutral or active particles building up deposits is found in direct ratio on gas linear speed, corresponding to lines ##1, 3 respectively (see Fig.6.1), while functional dependencies ##2, 4 represent ash abrasive wastage by same particles. In a result due to these two contradictory effects it is found ash deposit formation intensity g, g_1, g_2 in dependence on gas flow linear velocity (see Fig.6.2). Particles with neutral characteristics are in majority in gas flow, especially, where EB is installed on main internal combustion engine. Therefore constituent g_1 is considerably higher than other one g_2. However, in some cases, when diesel engine is continuously running at reduced load, unburned cylinder oil might significantly contribute in the growth of deposits by reactive particles g_2; and it would result in serious deterioration of service safety factor as well (fires in EB). The highest deposit formation is achieved at speed equal to w_0^{crit}, when biggest contribution is provided by neutral ash particles (see Fig.6.2), however, being not enough resistant to wear out. Therefore with the speed increase until some critical one equal to w_1^{crit} neutral particle deposits are being rapidly self-destroyed till ash will consist of particles with cohesive (binding) characteristics only, i.e. $g = g_1 + g_2$, but, when $g_1 = 0$, then $g = g_2$. By further speed rise also this part

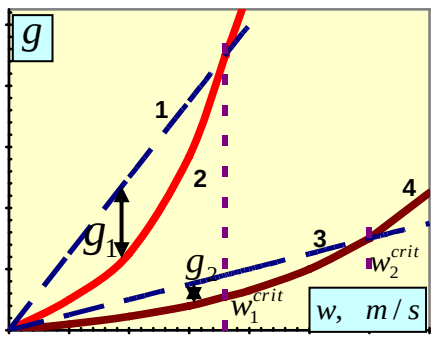

Fig.6.1. Mechanism of ash deposit formation on gas velocity.

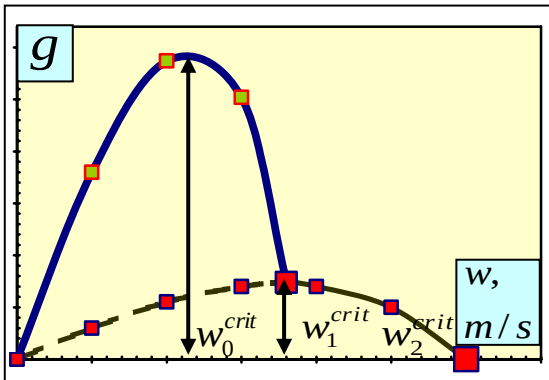

Fig.6.2. Intensity of ash deposit formation on gas velocity, critical speeds.

of deposits will be exposed to self-destruction; and by reaching gas linear velocity equal to w_2^{crit}, boiler surfaces will be free of ash formations, i.e. $g = 0$. Meantime, gas flow is full of different particles; and relevantly at speeds higher than critical one $w > w_2^{crit}$ instead of deposits on surfaces tubes will be exposed to wear-out; therefore unlimited increase in flue gas linear speed is restricted either. Since the temperature at EB inlet could vary from the lowest meaning $t_{g_0} = 250 \div 320^o C$, when advanced low speed diesels is ship ME, till the highest ones $t_{g_0} \cong 400 \div 500^o C$, when modern four stroke diesels or gas turbines are introduced, but at boiler outlet gas temperature is cooled down to $t_{g_{exh}} = 180 \div 160^o C$, consequently the nature of ash deposit formations will differ for each boiler constituent.

6.2. LIQUID FUEL OIL IMPACT ON ASH DEPOSIT FORMATION.

Despite of quite insignificant ash amount in marine heavy fuel oils $A^P = 0.04 \div 0.10\%$ till $A^P_{MAX} = 0.15\%$ in IFO-380, comparatively high both sulfur $S = 3.5 \div 5.0\%$ and other mineral fraction content pre-determines deposit formation by particles with cohesive (binding) characteristics g_2 in super-heater and evaporator parts of EB. The main constituents of mineral fraction are Na, Si, Ca, Mg, V, Fe; and in small amounts nickel Ni also is present. Meantime, quite high content of metal Na & V compounds leads to low melting temperature of ash in fuel oil, what contributes to their Na & V condensing on relatively cold tube surfaces; and in a result there is increased soot formation with cohesive characteristics, i.e. pre-determined g_2 growth. On high temperature surfaces ash pollution is a formation based on chemical compounds - Na_2O + V_2O_5 + SO_3, constituting around $60 \div 80\%$ of mineral part in fuel oil. Deposits by reactive particles are those which have the main impact on both decrease of heat transfer efficiency k_i and rise in boiler aero-resistance ΔP_{g_i}. Sensitivity of chessboard-type lay-out boiler to soot formation could be limited by increasing relative tube steps in the bundle [27, 60, 100, 104, 108, 114].

6.3. LOW TEMPERATURE IMPACT.

The largest part of EB surfaces is exposed to temperatures below 327°C, i.e. $T_g \le 600^o K$, thus pre-determining the nature of soot formation. Content of iron Fe in deposits on steel tubes is increasing (up to $\approx 38\%$) due to surface corrosion by active parts of

ashes, resulting in more thick soot layer with increased cohesive properties, especially on lateral tube parts. Deposits, which are water soluble, are mainly constituents of sulfate compounds with different metals, including condensed water, while it's insoluble part are dominantly consisting of organic components. The presence of free sulfur acid H_2SO_4 is found in all type of deposits, increasing with the surface temperature reduction. For EB with chessboard-type bundle arrangement the main soot formation is observed on rare and front part of tubes directly in way of gas current (see Fig.6.3) and in turbulent whirling zones. It results in narrowing gas channels between tubes to a great extent, especially for compact chessboard-type layout, when crest of soot deposits rapidly penetrates spacing in-between tubes. Consequently, gas flow linear speed is increasing, directly influencing on relevant boiler gas resistance value, moreover intensity of soot deposit formation might and will grow as well. Continuous tendency of resistance $\Delta P_{g_i} \uparrow$ increase, especially in low-temperature zones, results to further soot overlaying between adjacent in-line located tubes as due to on-flow gas current, so from rare side of tubes as well. The last effect finally comes to the fact that nature of gas flow is influenced in such extent, that heat exchange surface is becoming

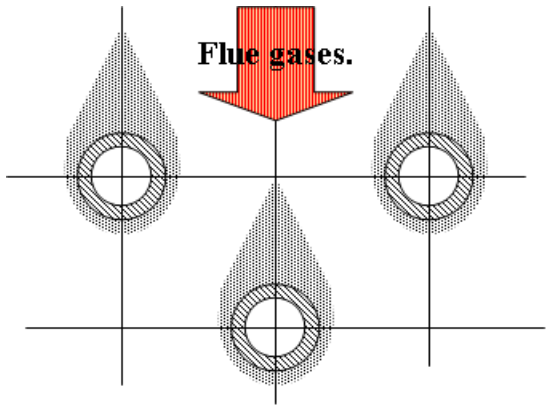

Fig.6.3. Soot formation configuration on EB tubes.

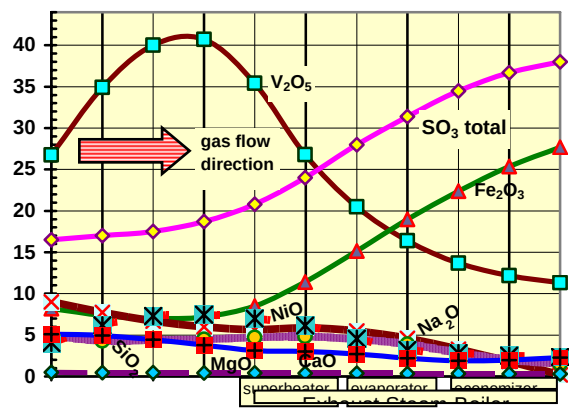

Fig.6.4. Soot constituents for main & EB.

partly excluded from heat transfer process. The distribution of soot deposit chemical compounds is influenced by both temperature and consumed fuel oil; and with some correlations it might be adapted for EB as well (see Fig.6.4). By concluding discussed above all main factors, having influence of ash deposit formation on tubes, could be presented as complex interaction between causes and consequences of this phenomenon (see Fig.6.5) [14, 62, 66, 92,94, 112, 117, 119, 123, 136, 137, 143, 145]. For fined tube surfaces generally mechanism of soot formation will be similar, however spacing between fins will be more affected for clogging also by deposits of neutral particles. In this case not only heat transfer efficiency of base tube will be adversely influenced, but also fin part. In addition ribs will be

more exposed to erosion and corrosion effect, which results in affected by increasing soot deposit formation, than plain tube bundle with similar geometrical characteristics. Finally, presented information, being revised applicably for exhaust steam boilers, reveals not only complexity of investigated phenomenon, but it is also giving ideas how and in which extent further explorations shall be carried out to determine pollution coefficient ε nature in dependence on various factors as boiler surface type, fining density, burned fuel oil types and others. Meantime, in our experimental part of the thesis we will try to find average service level of coefficient ε and also for each surface ε_i.

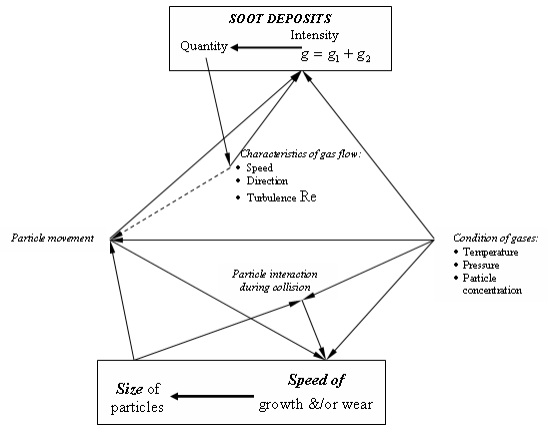

Fig.6.5. Mechanism of soot deposit formation.

6.4. PREPARATIONS FOR PRACTICAL PART OF EXPERIMENT.

Practical part was carried out onboard of one of the most interesting design is a Ro-Ro ship of type "Captain Smirnov" with speed as high as 25 knots (1974). The unique double gas-steam turbine installation COGAS type (see Fig.4.1) of 50 000 HP total power output, driving on two propeller shafts, was selected for ship's (see Fig.6.6) propulsion. Installed exhaust boiler type ***KYP-3100*** is rectangular type with round spiral type fined tubes. In our case pollution coefficient ε is proposed to find indirectly based on determination of gas-steam cycle parameters.

Fig.6.6 "Kapitan Smirnov" type Ro-Ro ship.

In order to obtain results with good trustworthiness it was chosen high precision class measuring equipment. For gas temperature detection either before t_{g_0} or after $t_{g_{exh}}$ boiler both mercury thermometers and $Cu-Ni$ type thermocouples were used. Due to uneven temperature distribution within boiler cross-section, measuring was carried out in several zones on various distances from boiler inner shell; in our case three thermocouples per each on three rods installed - 150mm, 350mm and 550mm relevantly. In dependence on range of

measurement boiler water t_{fwp}, t_{fw} and steam temperatures t_s, t_{st} were found by means of relevant mercury thermometers with absolute accuracy equal to $\pm 0.1^o C$. In order to find steam p_s, p_{st} and feed/boiler water p_s, p_e pressures deformation type manometers with precision class $0.15 \div 0.50$ and measurement range within $0 \div 15bar$, $0 \div 25bar$ have been used. In this case instrumental accuracy is around 0.03 till $0.13bar$. Exhaust gas G_g and relevant steam amounts, i.e. for ST G_{ST}, steam turbo-generator G_{STG}, low potential saturated steam consumers G_{sat}, ejector G_{eject} and total one G_{KYP}, were found indirectly, based on measured pressure drop of installed and calibrated diaphragms Pressure drop was measured either by water or mercury U-tube manometers. Measuring instrument with precision class 0.50 allows us to find flue consumption with root mean square deviation (RMSD) around $0.5 \div 1,2\%$, but at probability 0.95 RMSD constitutes $1.0 \div 2,4\%$ [50, 122, 124]. When gas amount is found this accuracy is equal to $1.3 \div 3.5\%$ at $\alpha = 0.95$ probability. In our case it was also possible to find gas amount based on turbo-compressor revolutions and ambient conditions, as thorough diagrams $G_g = f(n_{TC})$ were elaborated before by research institutes (CNIIMF and CNII named by academic Krilov in St. Petersburg). Both results have good coincidence. In order to find air excess coefficient α_{air} exhaust gas chemical composition, as following ones - CO_2, O_2, CO, was found by volumetric type gas analyzers. Measuring equipment accuracy is around $0.1 \div 0.2\%$. Fuel consumption G_f^v is found by using calibrated measure of capacity. Knowing the temperature and density mass consumption G_f^m is determined; and in a result we come to the third way how to find gas flow through boiler, as - $G_g = f\left(G_f^m,\ \alpha,\ amb.cond.\right)$.

6.5. MEASUREMENTS OF EXPERIMENT.

According described above general principles of measurements following main parameters were detected during stable performance of both HRC (see Fig.6.7) and power plant in total. Based on obtained results (see Tables #6.1, 6.2, 6.3) missing ones were acquired by joint solution of equations of both heat balance and transfer for each surface separately – economizer (3), evaporator (1) and super-heater (2) as follows - $G_g \times \Delta h_{g_i} \times 3600 = k_i \times F_i \times \Delta t_{LOG_i}$ with relevant surface sizes equal to

$F_1 = 1926m^2$, $F_2 = 268m^2$, $F_3 = 1178m^2$ as per technical passport of the boiler. Summary gas enthalpy difference recovered in boiler is determined directly based on measured temperatures $\Sigma\Delta h_{g_i} = f\left(t_{g_0} - t_{g_{exh}}\right)$, while for each surface it could be found indirectly based on next formulae solution - $\Delta h_{g_i} = \xi_i \times \Delta h_i / \eta_{al}$, where relative steam amount is found as division of relevant measured absolute against gas one $\xi_i = G_{steam_i} / G_g$. When gas enthalpy drop Δh_{g_i} in each surface is evaluated, then respective temperature meanings t_{g_i} are estimated based on relevant enthalpy $h_{g_i} = h_{g_{i+1}} - \Delta h_{g_i}$ and air excess coefficient α_{air} (see formulae ##3.1, 3.11). By substituting both directly and indirectly measured meanings gas pollution coefficient is found based on equation solution - $k_i = 1/\left(1/\left(\omega \times \alpha_{1_i}\right) + \varepsilon_i + d/d_i \times 1/\alpha_{2_i}\right) = \left(G_g \times \Delta h_{g_i}\right)/\left(F_i \times \Delta t_{LOG_i}\right)$.

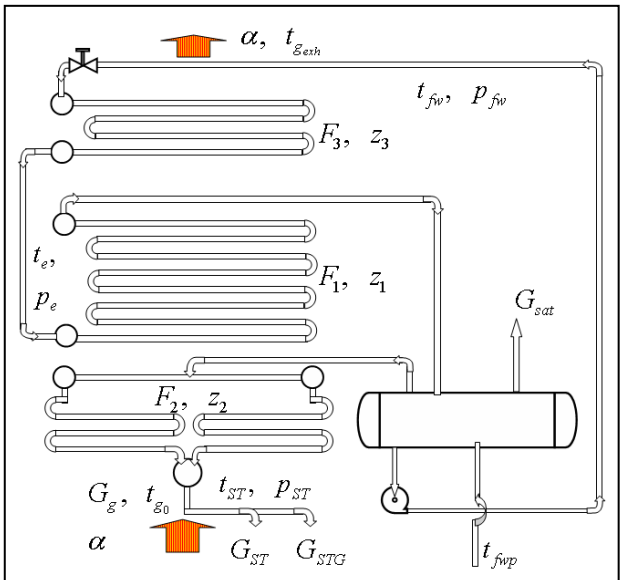

Fig.6.7. Heat Recovery Circuit on m/v "Kapitan Smirnov".

In a result following average meanings of the coefficient ε is obtained for each boiler constituent –

- Super-heater - $\varepsilon_2 = 0.884 \times 10^{-3}\ m^2 \times {}^oK/W \quad \left(0.752 \times 10^{-3}\ m^2 \times {}^oC \times hr/kcal\right)$;
- Evaporator - $\varepsilon_1 = 2.988 \times 10^{-3}\ m^2 \times {}^oK/W \quad \left(2.543 \times 10^{-3}\ m^2 \times {}^oC \times hr/kcal\right)$;
- Economizer - $\varepsilon_3 = 2.290 \times 10^{-3}\ m^2 \times {}^oK/W \quad \left(1.949 \times 10^{-3}\ m^2 \times {}^oC \times hr/kcal\right)$.

Summary average meaning of pollution coefficient for boiler KYP-3100 was found based on heat efficiency of specific surfaces, i.e. $\bar{\varepsilon}_{KYP-3100} = \sum_{i=1}^{3}\left(\Delta h_{g_i} \times \varepsilon_i\right) \Big/ \sum_{i=1}^{3} \Delta h_{g_i}$; and then we have the coefficient equal to $\bar{\varepsilon}_{KYP-3100} = 2.650 \times 10^{-3}\ m^2 \times {}^oK/W \quad \left(2.255 \times 10^{-3}\ m^2 \times {}^oC \times hr/kcal\right)$ at approximately heat efficiency of each surface as follows - $\overline{\Delta h_{g_1}} = \Delta h_{g_1} \Big/ \sum_{i=1}^{3} \Delta h_{g_i} \cong 0.7079$, $\overline{\Delta h_{g_2}} = \Delta h_{g_2} \Big/ \sum_{i=1}^{3} \Delta h_{g_i} \cong 0.09576$ and $\overline{\Delta h_{g_3}} = \Delta h_{g_3} \Big/ \sum_{i=1}^{3} \Delta h_{g_i} \cong 0.19636$. Obtained in a result of

experiment average meaning of pollution coefficient $\bar{\varepsilon}_{KYP-3100}$ slightly differs from that one accepted during the project stage $\bar{\varepsilon}_{PROJ} = 2.35 \times 10^{-3}\ m^2 \times {}^oK/W \quad \left(2.0 \times 10^{-3}\ m^2 \times {}^oC \times hr/kcal\right)$, what could be explained by the fact, that lower fuel grade marine gas-oil (MGO) was burnt instead of assumed better one DMA type.

Option.	1	2	3	4
Measurement.				
$G_{ST},\ kg/h$	15 288	15 849	16 074	21 704
$G_{STG},\ kg/h$	4 048	4 114	3 936	0
$G_{sat},\ kg/h$	2 000	2 000	1 620	2 000
$G_{eject},\ kg/h$	250	250	250	180
$G_{KYP},\ kg/h$	21 586	22 213	22 080	23 884
$p_s,\ bar$	11.3	12.1	11.8	14.6
$p_{ST},\ bar$	10.1	10.6	10.8	13.7
$p_e,\ bar$	14.3	15.0	14.0	17.8
$p_{fw},\ bar$	14.8	15.3	15.6	19.4
$t_{ST},\ {}^oC$	305.0	317.0	322.0	339.0
$t_s,\ {}^oC$	184.4	187.5	186.3	190.1
$t_e,\ {}^oC$	178.6	180.0	180.7	191.4
$\Delta t_{sp},\ {}^oC$	10.7	9.9	6.6	9.5
$t_{fw},\ {}^oC$	144.0	141.0	141.0	151.0
$t_{fwp},\ {}^oC$	32.2	33.5	32.5	40.5
$G_g,\ kg/s$	100.2	102.9	102.1	95.9
α_{air}	5.99	5.70	5.60	5.50

Table No.6.1. Heat Recovery Circuit Experimental Results.

	Option.	1	2	3	4
Flue Gas Temperature at Exhaust Boiler Outlet $t_{g_{exh}},\ {}^oC$ @ $\alpha = 0.95$	Measurement.				
	1st Rod	171.1	171.8	172.5	180.1
		170.9	170.2	172.1	181.3
		170.8	169.1	170.0	180.7
	2nd Rod	169.8	170.1	170.1	180.7
		169.0	169.0	172.0	180.0
		169.1	169.2	171.0	179.1
	3rd Rod	170.1	171.9	169.7	180.3
		168.8	170.6	171.8	180.7
		169.1	171.2	171.9	180.0
	4th Rod	170.8	173.2	174.2	183.1
		171.0	173.0	174.6	182.3
		169.9	173.1	173.9	182.2
	$\Delta S_a,\ {}^oC$	0.2561	0.4490	0.4690	0.3513
	$\Delta t_g,\ {}^oC$	0.80	1.80	1.50	1.00
	$\overline{t_{g_{exh}}},\ {}^oC$	170.0	171.0	172.0	181.0

Table No.6.2. Heat Recovery Circuit Experimental Results.

	Option.	1	2	3	4
Flue Gas Temperature at Exhaust t_{g_0}, ^oC Boiler Inlet @ $\alpha = 0.95$	Measurement.				
	1st Rod 150mm from boiler casing	343.9	354.2	360.1	379.1
	2nd Rod 350mm from boiler casing	343.7	355.0	359.5	380.0
	3rd Rod 550mm from boiler casing	341.4	352.8	357.4	377.9
	ΔS_a, ^oC	0.800	0.643	0.810	0.6069
	Δt_g, ^oC	1.40	1.10	1.40	1.00
	$\overline{t_{g_0}}$, ^oC	343.0	354.0	359.0	379.0

Table No.6.3. Heat Recovery Circuit Experimental Results.

Another interesting outcome is different values ε_i obtained for each boiler surface. The lowest meaning is noticed for super-heater due to reduced amount of impurities in consumed fuel oil such as V, Na and others, that are influencing on ash deposit formation in this temperature region (see Fig.6.4); and due to higher mean gas temperatures increased linear gas velocity in section $w_2 > w_1 > w_3$ contributes to more intensive deposit erosion (see Fig.6.1, 6.2) either. Accordingly, it looks like that economiser should be more affected to ash formation than evaporator part, i.e. $\varepsilon_3 > \varepsilon_1$, also due to sulphate and Fe_2O_3 forming (see Fig.6.4). Meantime, according results of our experiment just the evaporator part is found more polluted than economizer one, i.e. $\varepsilon_3 < \varepsilon_1$ on $25 \div 35\%$ in average. Let's try to explain our outcome. On figures Nr.6.1 and 6.2 intensity of deposit formation g_1, g_2 is dependent not only on gas speed velocity, but also on thermal, chemical and physical characteristics of ash particles (see Fig.6.5); also their concentration in gas flow is important, which in its turn has a direct impact on critical speed level w_2^{crit}. Just in evaporator section it is ensured the deepest gas cooling rate $\overline{\Delta h_{g_1}}$ equally around 70% of heat-temperature capacity, covering the main zone of particle settling (see Fig.6.4). Hence the evaporator is performing as filter, thus significantly reducing the amount of suspended particles. At evaporator outlet due to immediate and high increase of area for free passage gas flow is being slow down considerably; and due to appearing turbulence it comes to increased settlement of remaining suspended particles just before an economizer. Another factor explaining this phenomenon is that consumed fuel is considerably high quality with low sulfur content around $S \approx 0.3\%$, which is the main factor in formation of pollution coefficient level; meantime originated

sulfates are more mealy, which due to considerably high gas velocity ($w_3 \geq 20\, m/s$) are subject of intensive self blow-off. At the same time deposit structure on evaporator surfaces is more consistent due to, however minor, but still the presence of different metal oxides as V_2O_5, Na_2O and others (see Fig.6.4). These conclusions are quite interesting; however more deep investigations would be useful, especially, when low grade with high sulfur content fuels are burnt in main engines. Definitely the pollution coefficient level will be higher; and based on service experience sulfur deposit formation on economizer part might be an obstacle to ensure durable safe boiler operation. In this case based on observations ash deposit amount is tempt to be the highest one on tail parts of heat exchange surfaces; and it will come that following dissimilarity is becoming valid - $\varepsilon_2 < \varepsilon_1 < \varepsilon_3$. Reliability of obtained results is grounded by the fact that with the growth of linear gas velocity there is found a tendency in reduction of pollution coefficient $\bar{\varepsilon}_{KYP-3100} = f(w)$ (see Fig.6.8), being in good conformity with results of different other similar explorations. The next important part of our experimental part of theses is determination of measurement accuracy - $\overline{\Delta\varepsilon}_{KYP-3100}$; $\overline{\partial\varepsilon}_{KYP-3100}$,%, i.e. trustworthiness of the proposed method. Hence, the influence of each specific directly measured value by encountering its error (instrumental and occasional) level is being investigated on case by case basis; and for EB type KYP-3100 the fluctuations of main parameters are considered as below -

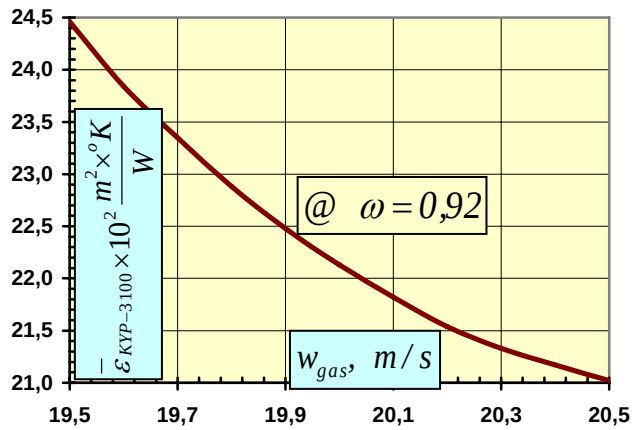

Fig.6.8. Pollution coefficient average meaning for EB type KYP-3100 on gas flow linear velocity.

$$\overline{\Delta\varepsilon}_{KYP-3100} \Big/ \Delta G_g = 2.12 \times 10^{-5} \left(m^2 \times {}^oK/W\right) \Big/ (kg/s) \quad \left(1.85 \times 10^{-5} \left(m^2 \times {}^oC \times hr/kcal\right) \Big/ (kg/s)\right);$$

$$\overline{\Delta\varepsilon}_{KYP-3100} \Big/ \Delta G_{KYP} = 4.43 \times 10^{-5} \left(m^2 \times {}^oK/W\right) \Big/ (\pm 1\% \quad deviation \quad from \quad actual) \quad ;$$

$$\left(3.77 \times 10^{-5} \left(m^2 \times {}^oC \times hr/kcal\right) \Big/ (\pm 1\% \quad deviation \quad from \quad actual)\right)$$

$$\overline{\Delta\varepsilon}_{KYP-3100} \Big/ \Delta t_e = 7.52 \times 10^{-5} \left(m^2 \times {}^oK/W\right) \Big/ ({}^oC) \quad \left(6.40 \times 10^{-5} \left(m^2 \times {}^oC \times hr/kcal\right) \Big/ ({}^oC)\right);$$

$$\overline{\Delta\varepsilon}_{KYP-3100} \Big/ \Delta t_{ST} = 3.17 \times 10^{-5} \left(m^2 \times {}^oK/W\right) \Big/ \left({}^oC\right) \left(2.70 \times 10^{-5} \left(m^2 \times {}^oC \times hr/kcal\right) \Big/ \left({}^oC\right)\right);$$

$$\overline{\Delta\varepsilon}_{KYP-3100} \Big/ \Delta t_{fw} = 2.23 \times 10^{-5} \left(m^2 \times {}^oK/W\right) \Big/ \left({}^oC\right) \left(1.90 \times 10^{-5} \left(m^2 \times {}^oC \times hr/kcal\right) \Big/ \left({}^oC\right)\right);$$

$$\overline{\Delta\varepsilon}_{KYP-3100} \Big/ \Delta t_{g_i} = 26.44 \times 10^{-5} \left(m^2 \times {}^oK/W\right) \Big/ \left({}^oC\right) \left(22.50 \times 10^{-5} \left(m^2 \times {}^oC \times hr/kcal\right) \Big/ \left({}^oC\right)\right).$$

The real influence of each measured value on the trustworthiness of acquired pollution coefficient meaning would allow us to plan the experiment method as well. Since measurement accuracy of heating media, such as water and steam, is high enough $\leq 0.1^oC$ due to even temperature distribution inside pipeline either, and then its final influence is minor one. Finding the actual meaning of gas temperature and its deflection is one of the most difficult tasks of the experiment. First of all the specific gas influence on pollution coefficient accuracy is the highest one, therefore high precision measurement equipment should be chosen. Secondly, besides measurement technique, there are also objective conditions regarding irregularity of gas temperature field within specific boiler cross section, which Δt_{g_i} might reach up to $2 \div 3^oC$. Hence following main precautions shall be observed and next one considerations might be useful in future, when gas temperatures are measured:

1) High accuracy measurement devices shall be chosen;
2) Only those results are to be considered, where the lowest irregularity of temperature field is achieved;
3) Determination of temperature gradient change within the whole cross section in order to find real average gas temperature $\overline{t_{g_i}} = \sum_{i=1}^{n} \left(F_i \times t_{g_i}\right) \Big/ \sum_{i=1}^{n} F_i$, which might probably require different method for measurement execution, e.g. infrared scanning;
4) Possibility to carry out measurements on special prototype units with installed nozzles, thus increasing gas flow turbulence in order to reduce temperature field irregularity;
5) To foresee a possibility to find some local meanings of pollution coefficient in some determined area of heat exchange surface.

The next considerable impact on measurement trustworthiness is generated by both gas ΔG_g and steam ΔG_{KYP} amount determination due to their quite high error level. The accuracy might be improved by using high precision gauges, devices, but it will lead to significant increase in costs of the experiment at doubtful outcome. Following errors of measurements

were obtained during thermotechnics experiment at proposed method - $\Delta G_g = \pm 2kg/s$; $\Delta G_{KYP} = \pm 1.3\%$; $\Delta t_{g_i} = \pm 1.0^o C$; $\Delta t_{ST} = \pm 0.1^o C$; $\Delta t_{fw} = \pm 0.1^o C$; $\Delta t_e = \pm 0.1^o C$. Based on these figures it could be estimated the lowest possible deflection of measurements from average meaning of pollution coefficient; and it will be equal to following - $\overline{\Delta\varepsilon}_{KYP-3100} = 27.22 \times 10^{-5}\ m^2 \times {}^oK/W \quad \left(23.16 \times 10^{-5}\ m^2 \times {}^oC \times hr/kcal\right)$; and its relative error equal to - $\overline{\partial\Delta\varepsilon}_{KYP-3100} = 10.3\%$. By reducing gas temperature measurement error till $\Delta t_{g_i} = \pm 0.5^o C$ trustworthiness of the experiment will be improved adequately up to - $\overline{\Delta\varepsilon}_{KYP-3100} = 14.77 \times 10^{-5}\ m^2 \times {}^oK/W \quad \left(12.52 \times 10^{-5}\ m^2 \times {}^oC \times hr/kcal\right)$ and $\overline{\partial\Delta\varepsilon}_{KYP-3100} = 5.55\%$.

6.6. CONCLUSIONS.

1. Acquired results are in good conformity with proposed ones for WHRS optimization.
2. Average meaning of pollution coefficient during power plant operation is higher on around 12% against project one due to lower grade fuel burnt in gas turbine.
3. Pollution coefficient for each boiler constituent is found and following dissimilarity elaborated - $\varepsilon_2 < \varepsilon_3 < \varepsilon_1$, what could be in a result of both higher grade fuel oil for gas turbine and evaporator performance as a filter, thus leaving more clean gases behind.
4. Trustworthiness of acquired results is supported by pollution coefficient tendency curve being dependent on linear gas velocity changes (see Fig.6.8).
5. Since pollution coefficient is found indirectly based on measurements of various parameters, then each of them accumulates the growth of experiment error. However, still the major impact is originated by flue gas temperatures, mainly due to its uneven distribution within boiler cross section.
6. Nevertheless achieved accuracy of experiment is obtained high enough till around $\overline{\partial\Delta\varepsilon}_{KYP-3100} = 10.3\%$.
7. By thorough examination of results of carried out explorations it becomes possible to optimize experiment planning in future.

MAIN CONCLUSIONS .

The object of investigations is Waste Heat Recovery System for ship power plants. Meantime, the efficiency improvement itself is not a target of or investigations, but the main core of our studies is obtained the highest net gain of the propulsion plant in the whole within limited WHRS dimensions. Since an exhaust boiler is the main and biggest constituent of the system, then its placement inside ship, especially in some high rated and specialized ones, would be a challenge at targeted efficiency. If boiler cross section is rather limited either by lowest or highest level of linear gas velocity, then just the height would be the measure value of heat exchange surface sizes; and, moreover, just the height would be that restriction for EB installation onboard some specialized ships either. Therefore our studies are targeted to ensure the highest output throughout an optimization of HRC both thermodynamic and geometrical parameters at fixed exhaust boiler dimensions, particularly its height, thus maximizing efficiency of power unit within limited its dimensions and costs as well. Meantime, based on WHRS application range the main task could be different. Despite that conclusions were presented at the end of each chapter, still some main outcomes are presented in *CONCLUSIONS*.

1. In ***Chapter 1*** main key items, why WHRS shall be chosen, are discussed. Various environmental, design, trade and other origins, that influence system efficient performance, are thoroughly revised.
2. When the idea that heat recovery would found acceptable for our ship, then its actual design choice should be substantiated, being described in ***Chapter 2***. The methodology for initial design parameter set up is elaborated, that considers not only benefits of our particular option, but also tries to reveal all threats that might occur. If some changes in initially stated principal items in Chapter 1 would take place it might possibly have definite impact on our choice made in Chapter 2.
3. Analytic method for WHRS thermic and geometrical parameter evaluation, based on initially accepted EB dimensions, particularly its height, is presented in ***Chapter 3***.
4. Based on elaborated mathematic model thorough optimization of HRC with thermostatic mixing valve is carried out in ***Chapter 4***. In order to achieve the highest output per one volume unit of EB different parameters are optimized as follows:

a. During studies the impact of each boiler constituent, i.e. an economizer, an evaporator and a super-heater, on total efficiency, their contradictory interdependence is presented; and in a result ultimate EB surface dimensions are found that ensures the highest growth of power plant in the whole with the consideration of adverse gas resistance impact on ME performance;

b. Within fixed boiler dimensions, i.e. height, steam pressure influence on WHRS efficiency is rather complex, as despite of direct dependence of Rankine cycle efficiency recovered gas heat amount is decreasing with the pressure growth; therefore balance between them shall be found. In a result two meanings of optimal steam pressure are found, at which the highest output of either ST or power plant in the whole is obtained. The second one pressure is important, when combined power plant, that jointly drives prime mover, is in place; and it p_s^{opt} is slightly reduced against the first one $p_{s_0}^{opt}$ due to encountered EB aero-resistance.

c. Within fixed boiler dimensions boiler surface internal re-distribution is important from the view point of both service reliability and efficiency. In a result an optimal mutual convective surface distribution is found within approximate limits at subsequent inlet gas temperature raise as follows – an evaporator - 70÷53%; an economizer - 18÷22%; a super-heater – 12÷25%;

d. WHRS with intermediate steam extraction is considered as an alternative versus heat recovery circuit with re-circulation, firstly, due to service reliability, that reduces boiler tube oxygen corrosion internally. Meantime, at equal boiler heights there is no any additional gain in overall efficiency; however, due to better steam cycle utilization less gas heat is required to obtain the same output. In a result gas temperature at EB outlet is slightly higher on around 12÷15°C for intermediate extraction cycle, that reduces sulfur corrosion risk in economizer part. At condition of equal gas recovery rate ST output might be increased up to 4÷5%, however, required EB surface enlargement might result into zero outcome due to adverse impact of gas resistance, especially, at rather low gas temperatures;

e. Tube fining efficiency is thoroughly studied out in dependence on various factors at two different conditions. For available in market convective surfaces the reduction in dimensional boiler height is found as high as 21 till 25% at equal WHRS net output;

and subsequent increase in power plant efficiency up to 30% is ensured at similar EB dimensions with the consideration of different pollution coefficients either for fined or smooth tube surfaces.

5. For advanced slow speed diesel power plants some specific tasks would come forward due to both significantly lowered flue gas potential and different way of recovered energy application, i.e. ST incorporation in ship's electrical plant:
   a. Since ultimate gas heat recovery is important for diesel power plants, then presented in Chapter 3 analytic method is transformed based on pre-condition, when desired cooling rate, i.e. gas temperature drop in EB, is initially fixed. In a result boiler dimensions are evaluated and required surface re-distribution is found;
   b. Steam pressure choice is another practical issue for that sort of WHRS, as desired low cooling rate and restrictions in the lowest meaning of pressure are contradictory events. Based on explorations it could be proposed that further gas cooling, when it becomes possible and beneficial, should be carried out by installation of double pressure stage WHRS;
   c. Besides the actual amount of generated steam turbo-generator output even the most important task is the effective utilization of it, especially when there is shortage in power. Therefore recognition of duration and the level of this shortage are thoroughly explored in dependence on different service conditions. Final figures could be served as guidance for one or another particular project; however at the same time the results allow us to arrange the best and optimal electrical plant set up, including eventual diesel generator exclusion or replacement by some reduced power one. Finally, besides fuel saving also initial costs could be efficiently reduced during new-building stage.
6. The impact of pollution coefficient on boiler efficiency is evident; however followed weakening in safety matters due to tail surface corrosion might be even more important. Therefore available information is thoroughly revised against their suitability for EB, what could be effectively used during boiler choice. The proposed method to estimate pollution coefficient reveals some important and interesting matters:
   a. Proposed method could serve as an effective method of indirect measurements,
   b. But combination with other approaches should be taken into account;

c. Considerable error of measurements is not only the indicator of method accuracy, but also that makes to think upon further boiler aerodynamic improvement, so that steady temperature field would be obtained by means of effective boiler both insulation and geometry arrangement.

During the studies a lot of additional considerations and thought are brought out, which could serve as further development of our exploration:

1. To ensure further effective increment in efficiency more sophisticated WHRS might be proposed for explorations such as different arrangement double pressure stage ones. Therefore existing analytic system might be developed subsequently
2. The efficiency comparison of double stage WHRS is extensive studies with regards of system, pressure and other parameter choice.
3. Also for slow speed diesel power plants double stage WHRS might be a good solution.
4. For some cases combined composite marine steam boilers with chosen water tube one could be as an effective alternative, especially for slow speed diesel power plants.
5. From the view point of sulphur corrosion safety rather tube steel temperature is important than feed water temperature. Therefore by stating the lowest steel temperature it might be possible to reduce accepted feed water temperature at higher ME load level, thus obtaining the highest WHRS efficiency during operation time.
6. Further explorations and practical heat engineering measurements to find pollution coefficient in dependence of different factors is an important task. Here different measurement techniques might be combined together as that one considered in our studies and by measuring temperature drop between steel and adjacent gas layer. Without thorough exploration of the nature of pollution coefficient origins other potentialities for surface intensification, as ribbing density increase, might be useless.
7. Just linear gas velocity is that restrictive factor for choosing boiler technical characteristics as too high meanings of it will result in inadmissible aero-resistance growth. Meantime, the velocity shall be as high as possible, to avoid pollution intensity rise from gas side; and just economizers are mostly affected by sulphur acid corrosion due to soot deposition. Therefore it might be usefully to consider boiler construction, including analytic method revision, based on constant linear velocity (see Fig.MC.1).

8. In addition due to remaining gas potential energy it might be possible to utilize it in even greater extent by ejecting air from engine room thus contributing to ventilation system efficiency increase (see Fig.MC.1). This solution might be an effective way to reduce electrical consumption, thus increasing application range for WHRS.

9. In addition by arranging air supply system with additional sea water cooling system (see Fig.MC.1) air charge might be considerably increased as well as temperature reduction in engine room. Due to these activities both crew and equipment performance would be more efficient especially in high temperature zones, when engine room temperature reaches up to 50÷60°C. Electrical consumption for air funs might be lowered either, thus even more contributing to efficient WHRS utilization for SSDE.

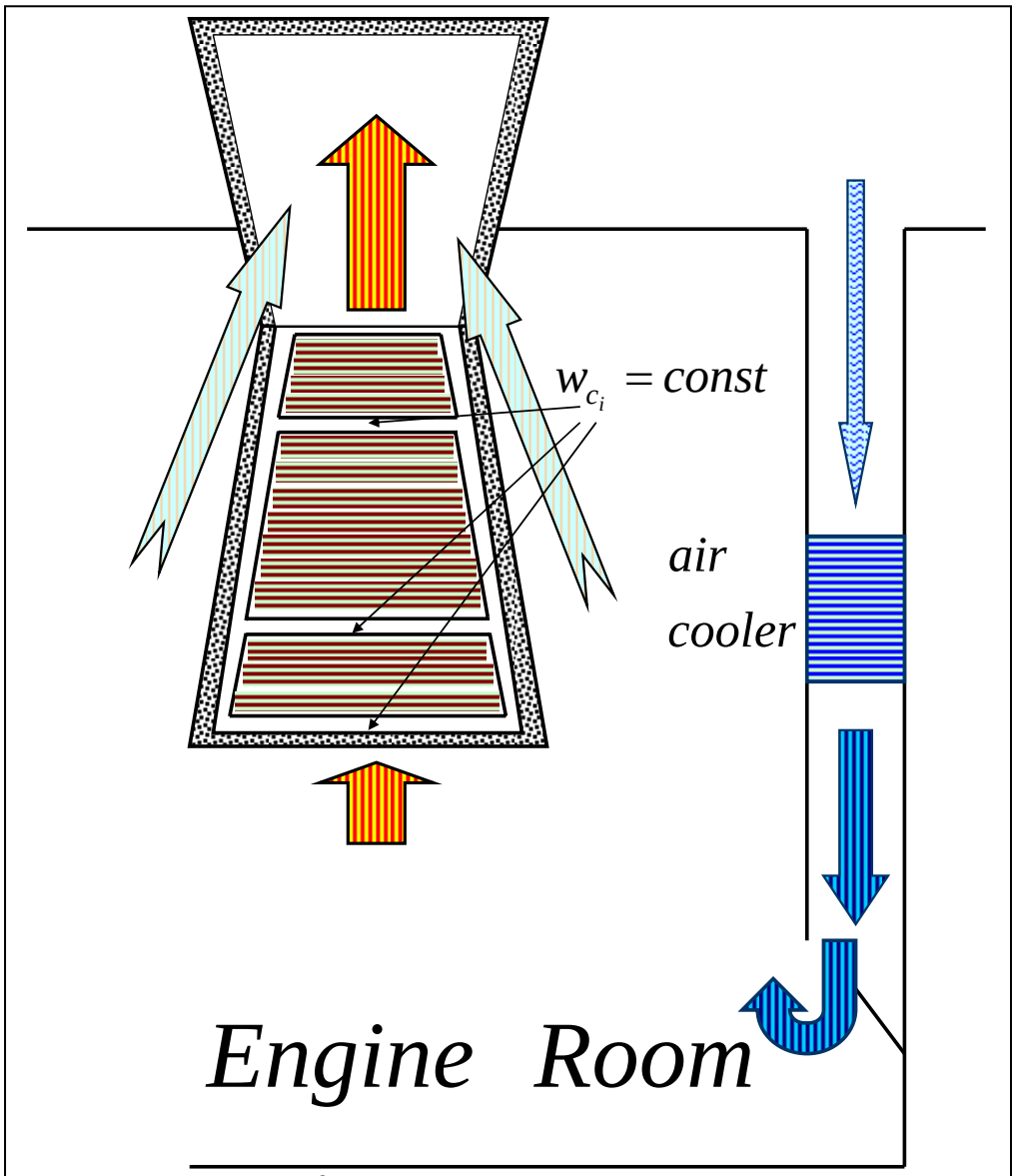

Fig.MC.1 Possible air flow arrangement in Engine Room.

REFERENCES .

1. Advanced WHR turbogenerator systems. T.A.Croxon, MER, Nov.1984, 8÷11 p.
2. Analysis and Modeling of Power Transmitting Systems for Advanced Marine Vehicles. By Leonidas M.Th.Kambanis. Massachusetts Institute of Technology 1995, p.80
3. Analysis of power plant deaerator under transient turbine loads. Trans.ASME, 1973, A95, No.3, 171-179p.
4. Ash deposits and corrosion due to impurities in combustion gasses: / Proc. of the Intern. Conference on ash deposits and corrosion from impurities in combustion gasses held at New England college, Henmiter, New Hamshire, June 26-July 1, 1977/Ed.Richard , W.Bryers-Washington; London: Hemshere publ. corp.; New York etc.: Mc.Grane-Hill corp. 1978-XII, 691.
5. ASME Steam - Properties - A CornpEter Program for Calculating the Thermal and Transport Properties of Water and Steam in SI Units, WNRE 182.
6. Baily, F.G., "Steam Turbines For Advanced Combined-Cycles," GE Power Generation Turbine Technology Reference Library Paper No. GER-3702B, 1993.
7. Brad Buecker. Basics of Boiler and HRSG Design. PennWell Publishing Company 1421 S. Sheridian Road/P.O. Box 1260, Tulsa, Oklahoma, USA, 2002, p.170
8. M. Boss. "Steam turbines for stag combined-cycle power systems". GE Power Systems Schenectady, NY, GER-3582E, 1996 GE Company, p.24
9. Boyce, Meherwan P. Turbine Engineering Handbook. 2nd Edition. Gulf Professional Publishing, Houston, Texas, USA, 2002, ISBN 0-88415-732-6, 799 p.
10. Breaux D.K. & Cdr.K.Davis. Design and service of Marine Waste Heat Boiler. Naval Engineering Journal, Vol.90, No.2 (April), 1978, 165-172 p.
11. Brooks, F.J., "GE Gas Turbine Performance Characteristics," GE Power Generation Turbine Technology Reference Library Paper No. GER-3567D, 1993.
12. Calculator method for steam turbine efficiency. R.P.Lapina. Chem.Eng. June 27, 1983, 37-42p.
13. Combined-Cycle Development Evolution and Future. David L. Chase GE Power Systems Schenectady, NY, GE Power Systems - GER-4206; 2004/01, p.18.
14. Design aspects of once through systems for heat recovery steam generators for base load and cyclic operation. M. F. Brady, Innovative Steam Technologies Ltd. 0964-3409/01/01/00035–12, 2001 Science Reviews: Materials at high temperatures 18(4), 223–229 p.
15. The design of gas turbine heat recovery systems. Precious R.W., Pasba Akber, "Intern.Power Generat.", 1984, I. N7, 38-41 p.
16. Diesel Engines and Gas Turbines in Cruise Vessel Propulsion. Horst W. Koehler, MAN B&W Diesel. Based on the author's presentation at The Institution of Diesel and Gas Turbine Engineers, London, on 17 February 2000, p.13.
17. DNV Rules For classification of ships / high speed, light craft and naval surface craft. Part 4 Chapter 7. Boilers, pressure vessels, thermal-oil installations and incinerators. Det Norske Veritas Veritasveien 1, NO-1322 Høvik, Norway, p.52.

18. Dual pressure steam cycle SC2. MER, August, 1981, 16-19 p.
19. Econosto. General Catalogue. Valves, fittings, and related equipment. Rotterdam, December 1996, p.381.
20. European Standard EN 12952-15. Water-tube boilers and auxiliary installation – Part15: Acceptance tests. September 2003, p.91.
21. Ganapathy V. Industrial Boilers and Heat Recovery Steam Generators. Design, Application and Calculations. ISBN: 0-8247-0814-8, by Marcel Dekker, Inc., NY, USA, 2003, p.648
22. Horloc J.H. Advanced Gas Turbine Cycles. Whittle Laboratory Cambridge, 044273-0 ELSEVIER SCIENCE Ltd., The Boulevard, Langford Lane, Kidlington, Oxford OX5 lGB, UK. ISBN 0-08-044273-0, 2003, p.203.
23. G.T.H. Flanagan. Marine Boilers, Third Edition (Marine Engineering Series). Butterworth-Heinemann, 25 Victoria Street, London SW1H OEX, England; 3 edition (August 14, 1990), 128 pages.
24. Frank P. Incropera, David P. DeWitt, Theodore L. Bergman, Adrienne S. Lavinev. Fundamentals of Heat and Mass Transfer, 6th Edition. ISBN: 978-0-471-45728-2, John Wiley and Sons, Inc., USA; September 2006, p.1024
25. Gas turbines established as propulsion option. by Doug Woodyard. Marine Propulsions. June, 1997, 9÷11 p.
26. Heat recovery steam generators for power generation and other industrial applications. Report No. COAL R232 DTI/Pub URN 03/804 by D Blood, S Simpson and R Harries, Powergen UK plc, D Dillon, Mitsui Babcock Energy Ltd, A Weekes, ME Engineering Ltd. Crown Copyright March, 2003, p.38.
27. Heat recovery steam generators. API recommended practice 534, Second edition, Draft 6, April 20, 2005, p.71.
28. The IAPWS Formulation 1995 for the Thermodynamic Properties of Ordinary Water Substance for General and Scientific Use. W.Wagner and A. Pruß. J. Phys. Chem. Ref. Data, Vol. 31, No. 2, 2002, p.149
29. Industrial Heat- Recovery Strategies. Copyright © May 1997, Pacific Gas and Electric Company. PG&E Energy Efficiency Information© "Industrial Heat-Recovery Strategies", p.16
30. Influence of Ambient Temperature Conditions. MAN Diesel A/S, Copenhagen, Denmark,16/03/2006, p.15.
31. INTERTANKO - Global forum for chemical tanker owners. INTERTANKO, June 2003, p.10.
32. Kehlhofer R., Bachmann R., Nielsen H., Warner J. Combined Cycle Gas & Steam Turbine Power Plants. ISBN 0-87814-736-5; by PennWell Publishing Co., Tulsa, Oklahoma, USA, 1999, 328 p.
33. Less Emissions through Waste Heat Recovery. Heinrich Schmid. Wärtsilä Switzerland Ltd, Winterthur. Wärtsilä Corporation, April 2004, p.10.
34. Maintenance Manual (Technical procedures). Published by Ship Management Latvian Shipping Company Group, Rīga, LV 1045, Latvia, p.329.

35. Marine Engineering Progress in 1996. Annual Review. Bu1letin of the M.E.S.J., Vo1. 25, No.2; October 1997, p.18-62.

36. Marine News, Wärtsilä Corporation, No.2 -2005, p.44.

37. Marine Technologies for Reduced Emissions. Heinrich Schmid and German Weisser. Wärtsilä Switzerland Ltd, Winterthur. Wärtsilä Corporation, April 2005, p.12

38. MARPOL 73/78 Consolidate edition 2006. International Maritime Organization, London, 2006, p.488

39. R.K. Matta, G.D. Mercer, R.S. Tuthill. GE Gas Turbine Performance Characteristics. GE Power Systems, GER-3567H, (10/00), p.20

40. R.K. Matta, G.D. Mercer, R.S. Tuthill. Power Systems for the 21st Century – "H" Gas Turbine Combined-Cycles. GE Power Systems, GER-3935B, (10/00), p.22.

41. Mc.Creath C.G., Conde J.F.G. A state of the art review of factors contributing to the turbine environment causing hot corrosion of gas turbines operating in a marine environment. Journal Inst.Energy, 1981, 54, No.421, 192-196p.

42. McGeorge H.David. Marine Auxiliary Machinery. 7th Edition. Butterworth Heinemann. Elsevier Science Ltd., Oxford OX2 8DP, UK, ISBN 0 7506 4398 6, 2002, p.514.

43. Michael J. Moran, Howard N. Shapiro. Fundamentals of Engineering Thermodynamics. John Wiley and Sons, Inc., USA; 5th Edition, 2004, p.896.

44. More gas turbine cruise ships at sea. MARINE LOG MAGAZINE. August 12, 2003.

45. Morton A.Y. Thermodynamics of waste Heat recovery on Motor Ships. Transactions © of the Institute of Marine engineers, 1981, vol.93, Conference No.9, 1-7; 66-67p.

46. MT30 marine gas turbine Fact Sheet. 2003 Rolls-Royce plc., www.rolls-royce.com

47. Naegeli D.W., Dodge L.G., Moses C.M. Effects of flame temperature and fuel composition on soot formation in gas turbine combustors. Journ. Combustion Sci. and technology., 1985, 35, No.1-4, 117-131 p.

48. Nickel oxide as a new inhibitor of vanadium-induced hot corrosion of super-alloys - comparison to MgO-based inhibitor. E.Rocca, L.Aranda, M. Moliere and P. Steinmetz. The Royal Society of Chemistry 2002, 12, p.3766–3772

49. Novel propulsion machinery solutions for ferries. Oskar Levander, MSc (Nav. Arch.), Wärtsilä Corporation - Ship Power, Finland, 2004, p.18.

50. Novel unsteady temperature/ heat transfer instrumentation and measurements in the presence of combustor instabilities. K.S.Chana, K.J.Syed, M.I.Wedlock, R.W.Copplestone, M.S.Cook and G.Bulat, QinetiQ, Cody Technology Park, Farnborough, Hants, GU14 0LX, UK, Siemens Industrial Turbomachinery Ltd. Waterside South. Lincoln LN5 7FD. ASME TURBO EXPO 2005, 6-9 June 2005, Reno-Tahoe, Nevada, USA. GT-2005-68433, p.8

51. Ozisik M.N. Heat Transfer: A Basic Approach. McGraw-Hill Education (ISE Editions); International Ed edition, ISBN- 0070664609, 1985, 800 p.

52. Ozisik M.N. Heat Conduction. John Wiley & Sons, New York, ISBN-10: 047105481X, 1980, 704 p.

53. Process modeling and design of shell and tube heat exchangers. John E. Edwards. UK CHEMCAD Seminar –October 2001, p.23

54. Propulsion Trends in Bulk Carriers. MAN Diesel A/S, Copenhagen, Denmark, 04/10/2007, p.17.

55. Propulsion Trends in Tankers. MAN Diesel A/S, Copenhagen, Denmark, 19/09/2005, p.15.

56. Propulsion Trends in Container Vessels. MAN Diesel A/S, Copenhagen, Denmark, 19/01/2005, p.16.

57. Research and Development of Gas Turbine for Next-Generation Marine Propulsion System (Super Marine Gas Turbine). Masashi ARAI, Takao SUGIMOTO, Kiwamu IMAI, Hiroshi MIYAJI, Kenichi NAKANISHI, and Yasuyuki HAMACHI. International Gas Turbine Congress 2003 Tokyo November 2-7, 2003, p.7

58. A review of available information on corrosion and deposits in coal and oil fired boiler and gas turbines. Report of ASME. Research committee on corrosion and deposits from combustion gasses. By Battelle Memorial Inst.: H.W.Nelson, H.H.Krause, E.W.Ungar [a.o.]. London [a.o.], Pergamon press, N.York. The Amer.Soc. of Mechanical Engineers, 1959. VIII, p.198

59. Rolf Bachmann, Henrik Nielsen, Judy Warner, Rolf Kehlhofer. Combined - Cycle Gas & Steam Turbine Power Plants. PennWell Publishing Company 1421 S. Sheridian Road/P.O. Box 1260, Tulsa, Oklahoma, USA, Aug 1999, p.288

60. Sadik Kakaç, Yaman Yener. Convective Heat Transfer, Second Edition. CRC Press LLC; 2 edition, December 16, 1994, 432 pages

61. Selection of LNG Carrier Propulsion Systems. MAN Diesel A/S, Copenhagen, Denmark, p.12

62. Shah Ramesh K. Heat exchanger basic design methods. Low. Reynolds Number Flow Heat Exchange Process. ASI Heat Transfer, Ankara, July 13-24, 1981. Washington e.a., Berlin e.a., 1983, 21-71 p.

63. Shaft Generators for the MC and ME Engines. MAN Diesel A/S, Copenhagen, Denmark, 16/03/2006 , p.27

64. Short comment - World merchant fleet 2006/2007. Christel Heideloff, www.isl.org, p.5

65. Small and medium size gas turbines. ISHIDA Katsuhiko. Kawasaki Heavy Industries, LTD. Gas Turbine Development Center. Gas Turbine Technology in Japan. Bulletin of GTSJ 2003, p.3

66. Soot Deposits and Fires in Exhaust Gas Boiler. MAN Diesel A/S, Copenhagen, Denmark, 22/04/2004, p.21.

67. Spey marine gas turbine. Fact Sheet. 2003 Rolls-Royce plc., www.rolls-royce.com

68. Standard Specification for High Frequency Electric Resistance Welded Finned Tubes. 2002 Fintube Technologies, Inc., 2002, p.7.

69. Superconductivity Web21. Superconducting Industry – Transport Equipment Technology – Prospects for Electric Propulsion Ships. Tetsuji Hoshino, Deputy Chief Researcher Nagasaki Research & Development Center Mitsubishi Heavy Industries, Ltd. Published by International Superconductivity Technology Center; July 17, 2007, p.2.

70. Sulzer RTA48T and RTA58T Diesel Engines. Engine Selection and Project Manual. Issue June 1995. 172p.

71. Turbines. PRODUCTS: LMG-20E™; LMG-30E®. High Temperature Corrosion. http://www.liquidminerals.com/turbines.htm

72. Thermo Efficiency System (TES) for Reduction of Fuel Consumption and CO2 Emission. MAN Diesel A/S, Copenhagen, Denmark, 19/07/2005, p.12

73. Warren M. Rohsenow, James P. Hartnett, Young I. Handbook of Heat Transfer. By the McGraw-Hill Companies, Inc., USA, 1998, p.911.

74. WÄRTSILA VASA 46. Really Reliable Propulsion Power. Project Guide for Marine Application. Wartsila Diesel Oy Turku Factory Stalarminkatu 45 SF-20810 TURKU FINLAND, p.133, 1994.

75. WÄRTSILA TECHNICAL JOURNAL, Issue No.1, 2007, p.52.

76. WATER WALL BOILER FOR AIR AND OXYGEN FIRED CLAUS SULPHUR RECOVERY UNITS. Mahin RAMESHNI, P.E., Technical Director, Sulphur Technology. WorleyParsons, 125 West Huntington Drive, Arcadia, California 91007, USA, p.14.

77. The World merchant fleet in 2005. Equasis statistics, p.115

78. Year Book 2005: Progress of Marine Engineering Technology in the year 2004 - Translated from Journal of the JIME Vol.40, No.4 (2005) – (Original Japanese).

79. Teaching efficacy of Web-based teaching methods in an undergraduate thermodynamics course. Jinny Rhee. San José State University, San José, United States of America. World Transactions on Engineering and Technology Education, Vol.2, No.1, 2003, p.37-40.

80. Today's Targets & Technologies for Reducing Emissions from Large Marine Diesel Engines. S. Bludszuweit, H. Jungmichel, B. Buchholz; Motoren- und Energietechnik GmbH. Motor Ship Conference 1999, March 1999, Athens, p.22.

81. Tomlinson, L.O. "Single Shaft Combined-Cycle Power Generation System," GE Power Generation Turbine Technology, Reference Library Paper No. GER-3767, 1993.

82. Агафонов В.Г., Пугачов Ю.П. Использование вторичных энергоресурсов

83. Алгоритмы численных методов. М., МИФИ, 1979; 75 с.

84. Анализ теплоотдачи к двухфазным потокам на основе оточненной двухскоростной модели течения. Прядко Н.А., Петренко В.П., Тобилевич Н.Ю., Засядко Я.И. М.: Тр.ЦКТИ, 1981, 241, с. 51-56.

85. Артемов Г.А., Бойков Б.П., Гильмунтдинов А.Г. Судовые газотурбинные установки. Л.: Судостроение, 1978, 269 с.

86. Аэродинамический расчёт котельных установок (нормативный метод) под ред. С.И.Мочана. Л., Энергия, 1977; 255 с.

87. Бажан П.И., Каневец Г.Е., Селиверстов В.М. Справочник по теплообменным аппаратам. М., Машиностроение, 1989; 365 с.

88. Беляев И.Г. Эксплуатация утилизационных установок дизельных судов. М: Транспорт, 1979, 142 с.

89. Быстров П.Г. Разработка и исследование перспективных конвективных поверхностей нагрева паровых котлов. Автореферат диссертации на соискание уч.степени к.т.н., Ленинград, 1981, 21 с.

90. ВНТО им. Акад. А.Н.Крылова. Тезисы докладов на Всесоюзной Научно-Технической конференции «Актуальные проблемы технического прогресса судовых турбинных установок». Л.: Судостроение, 1989,136 с.

91. Волков Д.И., Сударев Б.В. Судовые паровые котлы. Л.: Судостроение, 1988, 136 с.

92. Вопросы загрязнения конвективных проверхностей нагрева парогенераторов. Под общей ред. К.т.н., доц. Деринга И.С., Красноярск: Кр.П.И., 1972, ISBN: 5-7355-0041-4, 131с.

93. Вудворд Дж. Морские газотурбинные установки. Л.: Судостроение, 1979, 358 с.

94. Гаврилов А.Ф. Уменьшение вредных выбросов при очистке паровых котлов. М.: Энергоатомиздат, 1980, 240 с.

95. Гартвиг В.В., Литаврин О.Г., Плискин Г.М. Расширенные испытания ГТУ судна «Капитан Смирнов». Судостроение, №1, 1983, 14-17с.

96. Гидравлический расчет котлов. Нормативный метод. Под ред. Локшина В.А., Петерсона Д.Ф., Шварца А.Л. М.: Энергия, 1978, 256 с.

97. Григоренко В.Я., Магин Л.А., Матвеев Л.А. Результаты исследования статических характеристик энергетической установки судна типа «Капитан Смирнов». Судостроение, №8, 1983, 18-20с.

98. Гуревич А.Н., Зинин В.И., Колесниченко А.Г., Нагибин А.Я., Пильциль В.Г. Особенности утилизационного прямоточного котла для судовой комбинированной газопаротурбинной установки. Л.: Судостроение, 1984, 4, с.22-24

99. Денисенко Н.И. Основы комплексного решения проблемы повышения использования судовых котельных установок. Диссертация на соискание д.т.н., Л.: ЛВИМУ, 1986, 428 с.

100. Дементъев К.С., Романов В.А. и др. Проектирование судовых парогенераторов. Л.: Судостроение, 1986, 336 с.

101. Дикий Н.А. Судовые газопаротурбинные установки. Л.: Судостроение, 1978, 250 с.

102. Енин В.И. Судовые паровые котлы. М., Транспорт, 1984; 248 с.

103. Енин В.И., Денисенко Н.И., Ефимов Т.М. Современные утилизационные парогенераторные установкию М.: ЦРИА, МОРФЛОТ, 1979, 40с.

104. Енин В.И., Денисенко Н.И., Костылев И.И. Судовые котельные установки. - М: Транспорт, 1993, 216 с.

105. Жаров Г.Г., Венцюлис Л.С. Судовые высокотемпературные газотурбинные установки. Л.: Судостроение, 1973, 275 с.

106. В.И. Зайцев, Л.Л. Грицай, А.А.Мойсеев. Судовые паровые и газовые турбины. М.: Транспорт, 1981, 312 с.

107. Зегер К.Е. Исследование золового заноса высокотемпературных поверхностей нагрева котлов, работающих на сернистном мазуте и разработка способов его предотвращения. Автореферат дисс. На соискание уч.степени к.т.н. М: ВТИ, 1970, 24 с.

108. Иллиес К. Судовые котлы. Т.3. Расчет. Л.: Судостроение, 1964, 672 с.

109. Исследование и внедрение интенсифицированных поверхностей нагрева котлоагрега..научн.тр./ Под ред. д.т.н. Мигая В.К. и к.т.н. Назаренко В.С., НПО ЦКТИ, 1983; 80 с.

110. Камкин С.В., Возницкий И.В., Большаков В.Ф. и др. Эксплуатация судовых дизельных энергетических установок. М.: Транспорт, 1996. 432 с.

111. Кириллин В.А. Сычев В.А., Шейндлих В.А. Техническая термодинамика. М.: Энергоатомиздат, 1983, 247 с.

112. Клячко Б.И. Коррозия и загрязнение поверхностей нагрева паровых котлов при сжигании сернистных мазутов, высокотемпературная коррозия. Обзор составил к.т.н. Клячко Б.И. ред. к.т.н. Липштейн. М.: 1963, 52 с.

113. Курзон А.Г., Юдовин Б.С. Судовые комбинированные энергетические установки. Л.: Судостроение, 1981, 213 с.

114. Кутателадзе С.С. Теплопередача и гидродинамическое сопротивление. Справочное пособие. М.: Энергоатомиздат, 367 с.

115. А.М.Кутенов, Л.С.Стерман, Н.Г.Стюшин. Гидродинамика и теплообмен при парообразовании. М., Высш.Шк., 1986; 448 с.

116. Лазарев В.В., Ланда Л.Е., Литаврин О.Г., Туснаков А.М. Совершенствование эксплуатации теплоутилизационного контура энергетической установки судов типа «Капитан Смирнов». М.: Мор.Тр-т, Техн. Экспл. Флота, 23 (571), 1983, 7-16 с.

117. Г.И.Левченко, И.Д.Лисейкин, А.М.Копелиович, В.К.Мигай, В.С.Назаренко. Оребрённые поверхности нагрева паровых котлов. Энергоатомиздат, 1986; 168 с.

118. Маслов В.В. Утилизация теплоты судовых дизелей. Транспорт, 1990; 144 с.

119. Мосин Е.А. Исследование влияния температуры сжигания на интенсивность образования и свойств связанных золовых отложений. Автореферат дисс. На соискание уч.степени к.т.н. Томск, 1970, 29 с.

120. Нормативный метод гидравлического расчёта паровых котлов. Т.1. Руководящие указания . Л., ЦКТИ, ВТИ, 1973; 165 с.

121. Овсянников М.К., Петухов В.А. Эффективность топливо-использования в судовых дизельных установках. Л.: Судостроение, 1984, 96 с.

122. Петунин А.Н. Измерение параметров газового потока. М: Машиностроение, 1974, 332 с.

123. Портянко А.А., Локмин В.А., Фомина В.Н. Расчет коэффициентов загрязнения поперечно оребренных поверхностей нагрева. Конф. »Методы сжигания канско-ачинского бурового угля в крупных энергетических установках». Красноярск, 1983, с.54-59.

124. Преображенский В.П. Теплотехнические измерения и приборы. М.: Энергия, 1978, 104 с.

125. Проблемы загрязнения и очистки наружных поверхностей нагрева паровых котлов. Грузинская Республиканская конф. (1988 Батуми). Тезисы докладов республиканской конференции, 19-23 апр., 1988, Батуми: Б.и; Тбилисы: Мецнисребл., 1988, 165 с.

126. Ривкин С.Л., Александров А.А. Термодинамические свойства воды и водяного пара. Справочник. М.,Энергоатомиздат, 1984; 80 с.

127. Ривкин С.Л. Термодинамические свойства газов. Справочник. М., Энергоатомиздат, 1987; 288 с.

128. Ривкин С.Л. Термодинамические свойства воздуха и продуктов сгорания топлива. Справочник. М., Энергоатомиздат, 1984; 104 с.

129. Романов В.А. Исследования низкотемпературной коррозии в газотурбинных установках с теплоутилизационным контуром. Судостроение, 1978, 30-33с.

130. Розенберг Г.Ш. и др. Техническая эксплуатация судовых газотурбинных установок. М.: Транспорт, 1986. 222 с.

131. Семека В.А. Тепловой расчёт судовых паротурбинных установок. Транспорт, 1965; 137 с.

132. Семека В.А. Формулы , определяющие теплофизические свойства пара в области, используемой при расчётах паровых турбин. НТО им.акад. А.Н.Крылова. Л., Судостроение, 1982; с. 4¸24.

133. Справочник судового механика. Том I. Под общей редакцией к.т.н. Л.Л.Грицая. Издание второе, переработанное и дополненное. М., Транспорт, 1973. – 696 с.

134. Справочник судового механика. Том II. Под общей редакцией к.т.н. Л.Л.Грицая. Издание второе, переработанное и дополненное. М., Транспорт, 1974. – 697 с.

135. Тепловой расчет котельных агрегатов (нормативный метод). Под редакцией Н. В. Кузнецова и др. - М: . Энергия, 1973, 295 с.

136. Тепловой расчёта котельных агрегатов (Нормативный метод). Т.1. Руководящие указания. Л., ЦКТИ, ВТИ, 1973; 357 с.

137. Тепловой расчёта котельных агрегатов (Нормативный метод). Т.2. Руководящие указания. Л., ЦКТИ, ВТИ, 1975; 171 с.

138. Тепловой расчет котлов. Нормативный метод. Изд.третье переработанное и дополненноею НПО ЦКТИ. Санкт-Петербург, 1998, 256 с.

139. Теплообмен от стенки к восходящему пузырьковому течению при малых скоростях жидкой фазы. Горелин А.С., Каменский А.С., Накоряков В.Е. М.: Теплофизика высоких температур. 1989, 27, №21, с. 300-305.

140. Трусов А.С. Исследование влияния различных факторов на определение расчетного значения температуры забортной воды для судов паротурбиннох установок. Диссертация на соискание к.т.н., Л.: ЛВИМУ, 1973, 167 с.

141. Турчак Л.И. Основы Численных методов. М., Наука, 1987; 320 с.

142. Тушманов Н.С., Промыслов А.Л. Экспериментальные исследования аэрации и деаэрации конденсата в конденсаторе ПТУ. М: энергомашиностроение, 1977, №12, с.36-38.

143. Урунбаев М.А. Исследование некоторых особенностей процессов коррозии и загрязнения низкотемпературных поверхностей нагрева при сжигании жидких и газообразных сернистных топлив. Автореферат дисс. на соискание уч.степени к.т.н. Алма-Ата, 1975, 18с.

144. Фраас А., Оцисик М. Расчет и конструирование теплообменников. М: Атомиздат, 1971, 380 с.

145. Хавин А.А. Исследование теплоотдачи и сопротивления пучков труб с приварным спиралбно-ленточным оребрением и результаты внедрения. Автореферат дисс. на соискание уч.степени к.т.н. Киев, 1975, 31 с.

146. Хряпченков А. С. Судовые вспомогательные и утилизационные котлы. - Л.: Судостроение, 1988., 296 с.

147. ЦНИИМФ, ЛВИМУ. Комплексные системы глубокой утилизации тепла на судах ММФ с двигателями с постянным давлением наддуваю Технико-эксплуатационное требования. РД 31.27.28-82, Л.: ММФ, 1983. 17 с.

148. ЦНИИМФ, Лен.ЦП-КБ, ЛВИМУ. Технико-эксплуатационные требования по оптимальной комплектации электростанций морских транспортных судов. РД 31.03.41-84. Л.: 1985, 131 с.

149. ЦНИИМФ, ММФ. Извещение об изменений №1 РД 31.03.41-84. Технико-эксплуатационные требования по оптимальной комплектации электростанций морских транспортных судов. Л.: 1988, 99 с.

150. Чебулаев В.В., Локшин В.А., Вуколова А.И. Расчет тепловой разверки в ступенях пароперегревателей паровых котлов при наличии разницы температур пара во входных коллекторах. Теплоэнергетика, 1983, №11, с.50-53.

151. Шиняев Е.Н. Состояние и пути улучшения утилизации тепла судовых энергетических установок. М: Мор.Тр-т серия ТЭФ 1(18) 1980, 40с.